Novel roles of plasma membrane K_{ATP} channels in the heart

by

Nermeen Hosny Ibrahim Youssef

A thesis submitted in partial fulfillment of the requirements for the degree of

Doctor of Philosophy

Department of Pharmacology

University of Alberta

ABSTRACT

Plasma membrane ATP-sensitive potassium (K_{ATP}) channels are found in many excitable cell types where they couple cellular metabolism and membrane excitability. . Studies on K_{ATP} deficient mice show that parameters of cardiac mechanical function are similar to those of wild-type mice under basal aerobic conditions. However, in the setting of ischemia-reperfusion injury hearts of mice lacking K_{ATP} channels were shown to recover poorly after the insult and exhibit larger infarct sizes than in wild-type mice. Absence of K_{ATP} channels was also shown to abolish the protective effects of ischemic and pharmacological preconditioning against ischemia-reperfusion injury.

Recent evidence suggests that genetic ablation of the channel causes changes in global metabolism. Furthermore, a previous proteomic study has shown that genetic ablation of the K_{ATP} channels is associated with a noticeable change in cardiac metabolic proteins. In that regard, efficient energy utilization is one of the means by which the heart can recover functionally after ischemia. Therefore, if cardiac metabolism is suboptimal under basal aerobic conditions, it is likely that the heart becomes more susceptible to damage if subjected to an ischemic insult. In this thesis, the author investigates whether K_{ATP} channels regulate cardiac metabolism. If so, how would those changes in metabolic profile contribute to the pronounced cardiac damage observed during ischemia in K_{ATP}-deficient mice?

In this regard, K_{ATP} channels were shown to possess Mg-ATPase activity in addition to their well-identified electrical activity. This Mg-ATPase activity allows the channel to alter the nucleotide concentration in its microenvironment which directly

affects channel activity. Therefore, we sought to study the molecular determinants that regulate this enzymatic property. It is plausible that commonly used pharmacological agents that target K_{ATP} channels such as diazoxide and sulfonylureas may not only be affecting K_{ATP} electrical activity but Mg-ATPase activity as well. The functional consequences of these effects are unknown thus far, however, elucidation of these effects provides insight into the manifestation of side effects that may occur due to the use of such pharmacological agents. Due to the close association between K_{ATP} channels and several nucleotide-sensitive enzymes known to modulate metabolism, most notably AMP-activated protein kinase (AMPK), we investigated whether K_{ATP} channel openers and inhibitors affected activity of this enzyme. We also examined the effect of diazoxide, glibenclamide and gliclazide on Mg-ATPase activity of the channel in an effort to correlate the enzymatic activity of the channel and activity of AMPK.

Overall, the findings in this thesis highlight the importance of the presence of an intact plasma membrane K_{ATP} channel metabolome in the regulation of cardiac metabolism via modulation of AMPK activity. Moreover, we show that alteration of Mg-ATPase activity can directly affect pharmacological sensitivity of K_{ATP} channels to drugs that are designed to modulate their electrical activity. Understanding the functional consequences of the alteration of non-electrical properties of K_{ATP} channels provides clues to aid the development of more specific pharmacological agents with less prominent adverse effects.

To the memory of my father whose loving heart could not survive the attack.

To my mother for sharing with me the limitless love and strength in hers.

ACKNOWLEDGEMENTS

First and foremost, I would like to thank my PhD supervisor and mentor, Dr. Peter Light, for taking a chance on me and accepting me into his lab. I have been extremely lucky to have such a patient and involved supervisor. He has offered me invaluable advice, support and numerous development opportunities that I will always be grateful to him for. I am certain that he will remain a person that I will continue to aspire to be like.

I am greatly indebted to my PhD supervisory committee members, Dr. Jason Dyck and Dr. John Seubert, for sharing their expertise and offering positive guidance and advice throughout my program. Jason and John have provided me with very insightful discussions and useful suggestions regarding my project. I also thank the members of the Dyck and Seubert labs who have assisted me in technical troubleshooting and were always open to brainstorm ideas with me.

I would also like to thank Dr. Alexander Clanachan and Dr. Manoj Gandhi for helping advancing the project with their expertise in cardiac metabolism and working heart perfusions.

Many thanks to my Light lab family; Dr. Mohammad Fatehi, Dr. Chris Carter, Dr. Yi Yu, Dr. Wei Yang, Beth Hunter, Shaheen Rahman, Amy Barr, Scott Campbell, Katarina Ondrusova and Zosia Czarnecka. Each of them has provided me with support, care, technical assistance, training and on-demand entertainment when necessary. I will forever cherish their friendship and camaraderie.

I would like to thank the Department of Pharmacology, especially Dr. Elena Posse de Chaves and the late Dr. Susan Dunn for being instrumental in the continuation of my degree at the University of Alberta. I would also like to extend my gratitude to Dr. Andy Holt for his continuous support and Dr. Frances Plane for all her help during my candidacy examination process.

Many thanks to all the administrative staff of the Departments of Pharmacology, the Alberta Diabetes Institute and the Cardiovascular Research Centre who have made applications, forms and events appear seamless despite all the behind-the-scenes effort and time they put into them.

Many thanks to the funding agencies who have made this research project possible: Canadian Institutes for Health Research, the Mazankowski Alberta Heart Institute, the Alberta Diabetes Institute, TransAlta Life Canada, the Faculty of Graduate Studies and Research and the Faculty of Medicine and Dentistry.

Lastly, thanks to my mother, Dr. Samira Abdelkarim, for always encouraging me to follow my dreams and to stay true to myself. Thanks for being my inspiration and my rock. Thanks to my siblings, Kamal and Amal, for always having my back, for their weird sense of humor and unconditional love. Thanks to all the friends I made in Edmonton who have been there for me in good times and gloomier days. Thanks to my friends in Egypt who have shared memories with me through Skype conference calls, virtual birthdays and for including me in their major life events via often unstable internet connections.

TABLE OF CONTENTS

LIST OF TABLES

LIST OF FIGURES

LIST OF ABBREVIATIONS

ACC	**Acetyl CoA carboxylase**
ADP	**Adenosine diphosphate**
Akt	**Protein Kinase B**
AMP	**Adenosine monophosphate**
AMPK	**5'-AMP activated protein kinase**
ATGL	**Adipose triglyceride lipase**
ATP	**Adenosine triphosphate**
CoA	**Coenzyme A**
CPT	**Carnitine palmitoyl transferase**
CS	**Citrate synthase**
DEND	**Developmental delay, epilepsy, and neonatal diabetes**
EETs	**Epoxyeicosatrienoic acids**
FACS	**Fatty acyl CoA synthase**
FATP1	**Fatty acids transporter protein 1**
GDP	**Guanosine diphosphate**
GLUT	**Glucose transporter**
GTP	**Guanosine triphosphate**
HK	**Hexokinase**
HSL	**Hormone sensitive lipase**
K_{ATP}	**ATP-sensitive potassium channels**
KCO	**K_{ATP} channel opener**
Kir	**Inward rectifier subunit**
LKB1	**Liver kinase B1**

LV	**Left Ventricle**
mTOR	**Mammalian target of rapamycin**
NAD+/NADH	**Nicotinamide adenine dinucleotide**
NBD	**Nucleotide binding domain**
ND	**Neonatal diabetes**
P70S6K	**Ribosomal Protein S6 Kinase**
PDH	**Pyruvate Dehydrogenase**
PDK	**Pyruvate Dehydrogenase Kinase**
PGC1α	**Peroxisome proliferator-activated receptor gamma coactivator 1 alpha**
PI3K	**Phosphatidylinositol-4,5-bisphosphate 3-kinase**
PKC	**Protein Kinase C**
PPAR	**Peroxisome Proliferator Activated Receptors**
SU	**Sulfonylurea**
SuDH	**Succinate dehydrogenase**
SUR	**Sulfonylurea receptor**
T2D	**Type 2 diabetes**
VDAC	**Voltage-dependent anion channel**
WT	**Wild-type**

Chapter 1
Introduction

Excerpts from this chapter have been published in *Current Diabetes Reports*

The molecular genetics of sulfonylurea receptors in the pathogenesis and treatment of insulin secretory disorders and type 2 diabetes - Veronica Lang, Nermeen Youssef, Peter E. Light.

2011 Dec;11(6):543-51

1.1. Introduction

Cardiovascular diseases are the leading cause of death and have claimed over 17.1 million lives worldwide in 2004 alone[1]. By 2030, this number is projected to be 23.6 million, with more people adopting the Western diet and following a more sedentary lifestyle. Ischemic heart disease accounts for a significant proportion of cardiovascular diseases and results in significant morbidity and mortality[1]. Consequently, a thorough understanding of the pathophysiology that underlies ischemic heart disease is not only essential to ease the strain on the already taxed health care system, but also to reduce the number of lives lost. The heart possesses multiple endogenous protective mechanisms to reduce the damage that may result from such ischemic episodes and to aid in cardiac recovery. Among these mechanisms is the opening of ATP-sensitive potassium ($K_{ATP)}$ channels. For over thirty years, K_{ATP} channels have been known as an important class of potassium channels that couple cellular excitability to metabolic status. While it is an undisputed fact that they regulate cellular excitability, there is recent evidence to suggest that they may play a key role in regulating cellular metabolism.

1.2. The discovery of K_{ATP} channels

In 1983, K_{ATP} channels were first identified when Akinori Noma reported an outward current in cardiac cells that increased upon treatment with cyanide and during hypoxia but was blunted upon intracellular injection of ATP[2]. One year later, Francis Ashcroft reported that K^+ channels in the pancreas were regulated by changes in glucose which suggested that K_{ATP} channels could be the link between changes in glucose metabolism and insulin secretion in the pancreas[3].

Ashcroft's discovery was of great importance because it identified the K_{ATP} channel as a key physiological regulator of insulin secretion. This meant that studying K_{ATP} channels could help identify irregularities in the insulin secretion mechanism thereby enabling the development of drugs to fix them. However, it was not until the early nineties that the molecular structure of the channels was identified. Aguilar-Bryan and Inagaki et al. were able to clone the different subunits of K_{ATP} channels to finally describe the topology of K_{ATP} channels to give us further insight into their function[4].

1.3. K_{ATP} structure

K_{ATP} channels are hetero-octameric channels[5] (Figure 1.1.A), composed of four subunits belonging to the inward rectifying potassium channel family, Kir6.x which exhibits fairly weak inward rectification. Kir6.x subunits have been molecularly identified as Kir6.1 or Kir6.2 and are encoded by *KCNJ8* and *KCNJ11* genes respectively[6]. The Kir6.x subunit of K_{ATP} channel is comprised of an intracellular N-terminus, two transmembrane domains (M1 and M2) connected by an extracellular pore region. In most K^+ channels the pore region determines K^+ ion selectivity through a highly conserved glycine-tyrosine-glycine sequence, which is substituted by a glycine-phenylalanine-glycine motif in Kir6.x subfamily subunits. Both N- and C-termini of Kir6.x are located inside the cell. The outer portion of the channel surrounding the pore is composed of four sulfonylurea receptor (SUR) subunits belonging to the ATP Binding Cassette (ABC) protein family. The first isoform of the SUR subunits to be identified was SUR1; cloned from hamster insulinoma cells and is encoded by the *ABCC8* gene[7]. The other SUR isoform, SUR2, was cloned by Inagaki et al.[8] from the rat brain and is encoded by the *ABCC9* gene. A splice variant of the SUR2 isoform that only differs from SUR2 in the last 42 amino acids in the C-terminus (C42) was identified by Isomoto et al. and

was designated SUR2B as the original isoform was renamed SUR2A[9]. Another splice variant of SUR2A with a yet unknown function has been cloned recently[10] and named SUR2C[11]. The SURx subunit possesses 17 transmembrane helices (TMs 1–17) grouped in three domains (TMD0, TMD1 and TMD2), which contains five, six and six helices, respectively. Each of the TMDs is linked to a large intracellular nucleotide binding domains (NBDs), namely NBD1 and NBD2, by intracellular coupling domains which are helical extensions of the TMDs themselves. Two consensus nucleotide binding sequences, Walker A and Walker B motifs, for MgATP-binding and catalytic Mg-ATPase activity have been identified on each of the NBDs[6,12,13]. (Figure 1.1.B)

1.4. K_{ATP} channel distribution

Different isoforms of Kir6.x and SUR subunits form different combinations of K_{ATP} channels in the various excitable cell types where they are expressed. This gives rise to channels with distinct pharmacological properties and adenine nucleotide sensitivities[8–10,14–20]. Co-expression of the Kir6.2 K^+ channel and the sulfonylurea subunit resulted in a recombinant channel with identical properties to the native channel[4]. Studies thus far have confirmed that the pancreatic β-cell K_{ATP} channels are composed of Kir6.2 and SUR1[14,15]. Cardiac and skeletal muscle K_{ATP} channels were shown to be composed mostly of Kir6.2 and SUR2A[8,10,15,18,19]. The majority of smooth muscle K_{ATP} channels are comprised of the Kir6.1/SUR2B combination[21,22], although the presence of Kir6.2 has also been reported[9,10]. In neurons, K_{ATP} channels are composed of Kir6.2/SUR1 subunits[23–25] however, the subunit combination Kir6.2/SUR2B was also detected[16]. (Figure 1.2.)

The cardiac and skeletal muscle K_{ATP} channels are thought to be solely composed of Kir6.2/SUR2A subunits. However, a new study demonstrated that there may be chamber

specific expression of different K_{ATP} channel isoforms, with SUR1 being expressed in the murine atria[26], nevertheless, this remains to be confirmed in human atria. Due to the distinct biophysical and pharmacological characteristics of K_{ATP} channels containing SUR1 or SUR2A as will be reviewed later, this observation is of potential importance in elucidating the precise role of K_{ATP} channels in different chambers of the heart. Moreover, a recent study suggested that SUR1Δ2 which is a truncated splice variant of SUR1 is present in both the pancreas and heart[27]. This may potentially be the reason why probing for the full length SUR1 has not been successful in the heart. However, this is yet to be confirmed; if the same expression pattern holds true in human atria and ventricles, it will provide important clues in terms of the action of different clinically used K_{ATP}-targeting drugs and may explain some of their observed side effects.

1.5. Regulation

Physiological regulation

K_{ATP} channels are primarily regulated by adenine nucleotides[28] and the key determinant of channel activity relies on the fine balance in nucleotide concentrations in the channel's microenvironment. In response to a decrease in the ATP to ADP ratio, K_{ATP} channels are activated, leading to K^+ efflux from the cell, membrane hyperpolarization, and suppression of electrical activity[29].

The concentration at which ATP inhibits K_{ATP} channels differs according to the cell type they are expressed in and accordingly to subunit combination. For example, in native pancreatic β-cells and reconstituted Kir6.2/SUR1 K_{ATP} channels, the IC50 value for inhibition ranges between 5 and 10 μM[4]. On the other hand, in native cardiomyocytes the IC50 ranges from 8 to more than 500 μM and 20 to more than 100 μM for reconstituted

Kir6.2/SUR2A channels[8,19]. K_{ATP} inhibition by the free-acid form of ATP ($ATP4^-$) or its Mg^{++}-bound form (Mg-ATP) can occur, whichever is more potent appears to be tissue-specific. In cardiac K_{ATP} channels, both the free and the bound forms are equipotent with a half-maximal inhibition at 20–30 μM[30]. In contrast, $ATP4^-$ is more potent in pancreatic K_{ATP} with and IC50 of 4 μM compared to 26 μM for Mg-ATP[31]. In the rat portal vein, Mg-ATP appears not have exert any inhibitory effect on K_{ATP} channels while half-maximal inhibition can be achieved by 29 μM $ATP4^-$[22]. Noting that the intracellular ATP concentration in cardiac tissue is kept at a concentration of approximately 10 mM[32], one would expect that all K_{ATP} channels would be in the closed state. That being said, it has been suggested that some action potential shortening could still occur at millimolar levels of ATP. Termed "The spare channel hypothesis" by Cook et al., this theory suggests that given that since the membrane density of K_{ATP} channels is estimated to be as high as 3000-5000 channels per cardiomyocyte, and that single-channel conductance of approximately 20 pS, the $k_{i\ ATP}$ for channel inhibition in the range of 20-100 μM will mean that [ATP] changes in the millimolar range can significantly affect action potential duration[33]. A similar description of K_{ATP} channel activity regulation at physiological levels of ATP has been proposed by Nichols et al. in ventricular cardiomyocytes[34].

K_{ATP} channels as enzymes

As previously mentioned, ATP-inhibition at Kir6.2 is counteracted by Mg-ADP activation at the NBDs resulting in channel opening[29,35,36]. The current understanding is that Mg^{++}-dependent ATP hydrolysis at the SUR NBD dimer is essential in counteracting the ATP inhibitory effect[37,38]. Using radio-labelled ATP, it was confirmed that the NBD dimer possessed hydrolytic properties[39–41]. The dimer acts as a Mg-ADP sensor and the catalytic

site for the channel's intrinsic Mg-ATPase activity which enables the channel to convert Mg-ATP present in its local environment to Mg-ADP. This was proposed to stabilize ATP binding at NBD1 and drive dimerization of the NBDs leading to channel opening at Kir6.2[42–45]. Interestingly, it has recently been shown that NBD2 of SUR1 subunit exhibits higher intrinsic Mg-*ATPase* activity than NBD2 of the SUR2A subunit[46], suggesting that this difference in metabolic sensing may contribute to the tissue specific function of the SUR isoforms.

With respect to factors that can influence the local nucleotide concentration at the vicinity of the channel, an important link has been made between K_{ATP} channels and the phosphotransfer shuttle system. The phosphotransfer system in the cell composed of adenylate kinase and creatine kinase has been proposed to play an important role in controlling the nucleotide pool in the vicinity of K_{ATP} channels[47–49]. Adenylate kinase 1 (AK1) mediates phosphotransfer reversibly between ADP and ATP in the presence of AMP and its role in modulating processes related to ATP utilization has been well described previously[50–52]. AK1 can couple ATP- producing or sensing processes that occur remotely in the cell to the K_{ATP} channel microenvironment via the phosphotransfer system[53,54] and in conjunction with creatine kinase it works to propagate cellular metabolic flux[53,55]. In this regard, it is worth mentioning that in the presence of high intracellular ATP concentration, reversal of the ATP-liganded state via AK in the vicinity of K_{ATP} can occur[47,53,56]. Thus, ADP concentration in the K_{ATP} channel microenvironment would be an important determinant of channel activity since besides it being an activator of the channel, it can be utilized by AK1 on site to produce ATP and AMP[53]. Other enzymes involved in phosphotransfer reactions

include glycolytic enzymes which interestingly have previously been shown to have the ability regulate K_{ATP} activity[47,57,58].

K_{ATP} channels were also shown to be regulated by membrane phospholipids, particularly phosphoinositol-4,5-bisphosphate which upon binding to Kir6.2 markedly increases channel activity[59] and decreases ATP-sensitivity[60,61]. Similarly, long chain acyl CoAs were found to activate K_{ATP} channels by interacting with the Kir6.2 subunit[62] and the degree of activation by acyl-CoA is directly proportional to side-chain length. Moreover, protein kinases were shown to be involved in K_{ATP} channel regulation.

Protein Kinase A (PKA) was shown to regulate the channels expressed in the pancreatic β-cells and in smooth muscles by phosphorylation of certain moieties on the Kir6.2 subunit and increasing the open probability of the channel[63–65]. Currently no evidence shows that PKA regulates activity of Kir6.2/SUR2A combination. On the other hand, Light et al. have demonstrated that PKC has dual actions on the channel complex activity where the channel is inhibited at low concentrations of ATP and activated at high concentrations[66]. Modulation of K_{ATP} channel activity was also associated with protein kinase C (PKC)[67] and cGMP-dependent protein kinase (PKG)[68]. Another link between K_{ATP} activity and phosphorylation was established by Lazarenko et al. who have shown that activation of K_{ATP} channels is dependent on protein phosphatase C in MIN6 cells[69]. Moreover, Light et al. have also shown that inhibitory phosphorylation of K_{ATP} by PKC is dependent on the activity of membrane-bound protein phosphatase 2A[70].

Another potential regulator of K_{ATP} channel activity is mechanical stress. The mechanosensitivity of K_{ATP} channels was first recorded by Van Wagoner as evident by

stretching atrial cardiomyocytes using negative pressure on isolated cell membrane patches then measuring changes in K_{ATP} current[71]. The same group showed that K_{ATP} channel current was activated by hypotonic stimulation of atrial myocytes[72]. Nakaya's group has also demonstrated that the atrium and isolated atrial cells from Kir6.2 knockout mice produced a larger amount of atrial natriuretic peptide (ANP) in response to stretch than those of the wild-type suggesting that K_{ATP} channels could be a negative regulator of stretch-induced ANP secretion[73]. Additionally, Wang's group has shown that K_{ATP} channels are involved in the regulatory volume decrease in rat ventricular myocytes[74]. Work from Rodrigues et al. has recently shown that activation of the cellular fuel sensor, 5'-AMP activated protein kinase (AMPK) is more significant in hearts perfused in the working mode where it pumps against an afterload as opposed to Langendorff mode where no pressure or volume work is involved[75]. In this regard, Mosca et al. showed that stretch-induced cardioprotection against ischemia-reperfusion injury is lost upon pharmacological inhibition of K_{ATP} channels[76] suggesting that the channels are activated downstream of mechanically-activated upstream effectors or they themselves are mechanosensitive. The effects of mechanical stress on the channel's Mg-ATPase activity have not been studied and it is unclear at this point whether the increase in channel current observed is due to electrical activity or is regulated in part via the channel's enzymatic activity. In chapter 4, the author investigates if the effects of stretch on cardiac K_{ATP} channels are solely through changes in channel gating or due to changes in K_{ATP}-Mg-ATPase activity.

K_{ATP} channel expression was also found to be regulated by 17 β-estradiol in H9C2 cells[77]. Additionally, Davies et al. have reported the regulation of vascular K_{ATP} channel gating via the action of the caveolae-associated protein, caveolin-1[78]. Hydrogen sulfide has

also been shown as an activator of K_{ATP} channels in pancreatic β-cells as well as cardiomyocytes[79,80] and vascular smooth muscles[81–83]. This effect was partially blocked by glibenclamide, a classical sulfonylurea K_{ATP} channel blocker[84]. It is worth mentioning that hydrogen sulfide is a well studied cardioprotective agent[85]. Moreover, epoxyeicosatrienoic acids (EETs) which are products of arachidonic acid metabolism by CytP450[86] were also shown to activate K_{ATP} channels in rat ventricular myocytes and in the vasculature[87]. Additionally, it has been suggested that EETs exert their cardioprotective effect by activating the PI3K/Akt pathway upstream of K_{ATP} channels[88]. The same mechanism of protection by the EET-PI3K-K_{ATP} pathway was also suggested in cerebral ischemia[89]. Cellular pH has also been shown to directly affect the activity of K_{ATP} channels where low intracellular pH was shown to activate channel activity in frog skeletal muscle[90], ventricular myocytes[91] and insulin secreting cells[92]. Another physiological regulator of K_{ATP} channels is nitric oxide where it has been shown to activate the channels under normoxic as well as hypoxic conditions in rabbit ventricular myocytes[93], Purkinje fibres[94] and in sensory neurons[95].

Pharmacological regulation

K_{ATP} channels have very rich and well-documented pharmacology. In the present time, both K_{ATP} channel openers (KCOs) and inhibitors are currently being used in the clinical setting.

Diazoxide (DZX) which was initially used as a diuretic has been shown to be associated with the occurrence of hypotension at the beginning of the 1960s, the first demonstrated evidence of its interaction with K_{ATP} channels followed more than two decades later. In a study by Trube et al., DZX was applied to patches from pancreatic β-cells causing a significant increase in the activity of the channels[96]. Later, evidence for the hypotensive

effect of different KCOs was found to involve increased K^+ permeability of cells and was established using nicorandil[97], DZX[98] and cromakalim[99]. In cardiomyocytes, single-channel recordings later showed that the other newer KCOs like cromakalim[100] and pinacidil[101] also increased K^+ efflux through K_{ATP} channels. DZX, pinacidil, cromakalim and nicorandil, were also shown to activate the channels in smooth muscle K_{ATP} channels leading to hyperpolarization of the plasma membrane and reduced electrical activity[102]. Interestingly, Bienengraber et al. have also shown that pinacidil increases the rate of hydrolysis of ATP at NBD2 and promotes channel opening by maintaining it in the Mg-nucleotide bound state[103].

Although, DZX was initially thought to have no effect on the cardiac SUR2A/Kir6.2 channels, its cardioprotective action was therefore proposed to be via its action on mitochondrial K_{ATP} channels[104]. This explanation was based on the assumption that mitochondrial K_{ATP} channel would be composed of a different K_{ATP} channel subunit combination compared to cardiac sarcolemmal K_{ATP} channels, and would be sensitive to DZX. Therefore, these mitoK_{ATP} channels would open in response to ischemia to protect the myocardial tissue from I/R injury[105] . To date, despite the presence of numerous publications in the literature attributing cardioprotection to mitoK_{ATP}, it remains a subject of debate and the presence of mitoK_{ATP} channels remains unequivocally supported[106] and the detailed composition and architecture of mitoK_{ATP} remain unsolved[107–111].

The DZX molecular site of action in the heart was resolved when it was shown that native and recombinant cardiac K_{ATP} channels can in fact be activated by DZX but only under the condition that ADP concentration is raised above 10 μM which may occur during ischemia[112]. Not only was the action of DZX found to be dependent on the concentration of ADP but the drug itself was shown increase the potency of ADP to promote channel

opening[113]. [^{3}H]glibenclamide and [^{3}H]P-1075 binding displacement assays demonstrated the presence of a functional binding site for DZX in all SUR isoforms with K_d = 140 μM at SUR1, K_d = 18 μM at SUR2B and K_d = 76 μM at SUR2A[114].

An intriguing aspect of DZX pharmacology is that in absence of ADP, it is still able to activate vascular SUR2B/Kir6.2 channels but hardly exerts an effect on cardiac SUR2A/Kir6.2 channel. For example, as indicated previously, DZX was found to activate Kir6.2/SUR1 and Kir6.2/SUR2B channels more strongly than Kir6.2/SUR2A[26,115], however, it was shown in the presence of MgADP, Kir6.2/SUR2A become comparably sensitive to DZX as Kir6.2/SUR1[112]. This suggested that the last C-terminal 42 amino acids (C42) which are the difference between the SUR2B and SUR2A splice variants were responsible for this differential pharmacology. The importance of C42 was therefore thought to be through the interaction between its charged residues with Walker A motif on NBD2[113,116]. Though chimeric approaches to determine the exact binding site of DZX were thus far inconclusive, Dabrowski et al. used a DZX derivative (NNC 55-9216) to map its site of action in SUR1 and their data so far suggest that helices 8–11 most likely are a part of the binding site for DZX[117].

Inhibitors of K_{ATP} channels are an established class of oral antidiabetics. The sulfonylureas (SUs), along with metformin they are the most prescribed type 2 diabetes drugs globally[118]. Their hypoglycemic properties were first discovered by accident when they were used in the 1940s as antibiotic sulfonamides to treat typhoid fever. The noticeable hypoglycemia observed in patients made their glucose-lowering effect hard to ignore[119,120]. K_{ATP} channels were later identified as the primary molecular targets of SUs[121]. First generation SUs such as tolbutamide, chlorpropamide were designed after altering the initial

sulfonamide structure and used clinically for the specific purpose of lowering blood glucose[122]. More potent second generation SUs such as glibenclamide, gliclazide, glipizide were developed later[123] but because SUs are not specific to K_{ATP} channels in pancreatic β-cells, they were associated with an increased risk of cardiovascular disease. Inhibition of cardiac K_{ATP} channels appeared to impair endogenous cardioprotective mechanisms such as ischemic preconditioning and may increase susceptibility to cardiac arrhythmias as evident by altered ST segment and T wave configuration on the rest electrocardiogram (ECG) during acute myocardial ischemia[124]. This led to the development of third generation SUs that are more SUR1 selective such as gliclazide and newer agents, such as the insulin-sensitizing thiazolidinediones and the biguanide compounds that would appear to have less detrimental cardiac effects.

SUs can also be classified according to their SUR1 site of action. Two drug binding pockets have been identified; the A and B-sites. SUs can act at either site such as gliclazide which is an A-site SU, or even both sites such as glibenclamide which is an AB-site SU (Figure 1.3.A, B). The A-site of SUR lies within the transmembrane helices 14 and 15 close to NBF2, while the B-site lies at the cytoplasmic loop between TMD0 and TMD1 and the N-terminus of Kir6.2[125,126]. The exact mechanism by which SUs exert their inhibitory effects on K_{ATP} channels is not fully understood, however it is suggested that SUs may interfere with Mg-ATPase activity of SUR1, the A-site ligands in particular, or through interfering with Kir6.2 gating and therefore affecting K^+ conduction[39,127,128]. SUs do not only conduct their inhibitory effects at SUR1, they also inhibit the cardiac SUR2A receptor which may account for the potential cardiotoxic effects of some SUs with similar SUR1 and SUR2A affinities[129,130].

Other K_{ATP} inhibitors include HMR1098 which is thought to be a Kir6.2/SUR1 specific inhibitor[131] however that was later refuted by Zhang et al. who showed that inhibition of Kir6.2/SUR2A currents occurs by using HMR1098 as well but at a higher concentration[132]. 5-hydroxydecanoic acid (5-HD) is another K_{ATP} inhibitor that was shown to abolish ischemic preconditioning and cardioprotection induced by other K_{ATP} channel openers by preventing the channels from opening which would lead to intracellular calcium accumulation[133]. Marban's group reported that in the presence of 5-HD (500 μM), the mitoK_{ATP} channel opening effect of pinacidil failed to increase flavoprotein oxidation suggesting that 5-HD was a selective inhibitor of mitoK_{ATP} channels without affecting plasma membrane K_{ATP} channels[134]. However, Li et al. showed that 5-HD was also an inhibitor of plasma membrane K_{ATP} as evident in inside-out patches excised from rat ventricular myocytes at IC_{50} 30 μM[135].

A summary of physiological and pharmacological activators and inhibitors of K_{ATP} channels is presented in Figure 1.4.

1.6. The controversy of SU cardiotoxicity

Drug-associated cardiotoxicity has been defined as a toxicity that suppresses cardiac mechanical or electrical function[136]. This definition includes direct effects of drug on the heart and takes into account indirect effects due to enhancement of haemodynamic flow alterations or due to thrombotic events[137]. The cardiotoxic effects of SUs have been a subject of prolonged controversy. Though the literature is rich with studies that investigate their toxicity, groups studying the topic are unequivocal when it comes to conclusively agreeing upon the cardiac safety of SUs in the clinical setting. This controversy has put not only SUs

under considerable scrutiny but other antidiabetic drugs such as the thiazolidinediones are under constant monitoring for cardiovascular effects.

The debate started in 1970, where a multicentre, randomized, placebo-controlled trial contrasting the effects of tolbutamide, insulin and diet alone on blood glucose, the University Group Diabetes Program (UGDP) trial, was prematurely terminated[138]. The reason being that compared to placebo's 4.9%, cardiac deaths in the tolbutamide-treated group had reached 12.7% suggesting that the SU in the study was accounting for the increase in cardiac deaths[138]. Despite several weaknesses in the methodology of the UGDP trial[139], all SU drugs were required to come with a warning stating potential cardiovascular risks[140].

The mechanism by which SUs may cause cardiotoxicity has been difficult to pinpoint. However, knowing that SUs are inhibitors of K_{ATP} channels, it is safe to say that at least the first generation SUs would be expected to inhibit K_{ATP} channels in every organ that expresses them. While inhibition of K_{ATP} channels in the pancreas stimulates insulin secretion[141], this same inhibition would be detrimental to the heart. During a physiological stress or an ischemic insult, opening of cardiac K_{ATP} channels shortens the action potential duration and reduces workload, where opening of vascular K_{ATP} channels leads to muscle relaxation and subsequent vasodilatation. Together these endogenous protective mechanisms reduce potential tissue damage caused by these stresses[142,143]. Therefore, it is plausible that inhibition of cardiac and vascular K_{ATP} by the action of SUs may compromise the channel's ability to exert its protective function in the heart.

Thus the question of SU tissue-selectivity is of importance in the development of their proposed cardiovascular side effects. Different SUs when administered at therapeutic doses exhibit distinct tissue-specific binding affinities as reviewed by Abdelmoneim et al.[144].

For example, gliclazide and glipizide are more selective for the pancreatic SUR1 isoform, whereas glibenclamide is non-selective and binds to pancreatic SUR1 and cardiovascular SUR2A/B isoforms[144,145]. The differences in the pharmacological properties are supported by animal studies whereby glibenclamide, but not gliclazide, was shown to abolish ischemic preconditioning, resulting in a larger infarct size and worse deterioration in left ventricular function. In animal models, the differential pharmacology of glibenclamide was demonstrated in the form of loss cardiac ischemic preconditioning, with larger infarct sizes and poorer functional recovery[146–152]. Similar effects of abolished cardiac preconditioning were observed in patients undergoing one-vessel coronary angioplasty[153] as well as in isolated human atrial trabeculae[154]. Despite this observed loss of cardioprotection caused by glibenclamide, the exact mechanisms by which it disrupts endogenous protection have not been fully established.

In chapter 5, the author contrasts the effects of glibenclamide, the non-selective SU and gliclazide, the pancreas-selective SU, on the myocardium's protective mechanisms in an effort to understand the means by which glibenclamide possesses potential cardiotoxicity.

1.7. Rare monogenic K_{ATP} channel mutations

Given the crucial role that K_{ATP} channels play in regulating insulin secretion, genetic mutations that alter appropriate β-cell K_{ATP} channel activity can have profound effects on insulin secretion. Genetic mutations in the *KCNJ11* and *ABCC8* genes have been linked to persistent hyperinsulinemic hypoglycemia of infancy (PHHI) and neonatal diabetes (ND). K_{ATP} channel inactivity resulting from PHHI mutations leads to persistent membrane depolarization and excessive secretion that is not coupled to fluctuations in blood glucose levels. The majority of PHHI mutations identified to date have been found in

the *ABCC8* gene encoding the SUR1 subunit. Mutations can impair trafficking of functional K_{ATP} channel to the cell surface or result in functional expression of K_{ATP} channels with abnormal MgADP stimulation. In addition, several PHHI mutations have been identified in *KCNJ11* (Kir6.2) and similarly prevent trafficking of the mature K_{ATP} channel complex to the cell surface. In mutations where K_{ATP} channels remain partially functional, pharmacologic treatment with the KCO DZX may increase channel activity sufficiently to effectively reduce insulin secretion. However, in severe mutations, near-total pancreatectomy is required to reduce insulin secretion and relieve the hypoglycemia[155].

In contrast to mutations that result in loss of K_{ATP} channel activity, ND mutations in pancreatic K_{ATP} channel subunits lead to varying increases in K_{ATP} channel activity, resulting in clinical phenotypes ranging from the most severe developmental delay, epilepsy, and neonatal diabetes (DEND) syndrome and permanent neonatal diabetes mellitus to the less severe transient neonatal diabetes mellitus phenotype. In general, K_{ATP} channel mutations that cause the greatest increase in channel activity also precipitate a deleterious extrapancreatic phenotype resulting in the symptoms of DEND syndrome[156]. The developmental delay associated with the DEND syndrome is thought to result from persistent activation of K_{ATP} channels in the central nervous system (CNS) encoded by the *ABCC8* and *KCNJ11* genes. The majority of ND mutations identified to date are found in the *KCNJ11* gene that encodes the Kir6.2 subunit, leading to increases in channel open probability by altering channel gating or reduce ATP inhibitory effect on Kir6.2 subunits by impairing ATP binding affinity[157]. However, several ND mutations (R1380L and R1380C) were recently discovered in *ABCC8* (SUR1) that increase the SUR1 NBD1/2 intrinsic Mg-ATPase activity[158]. Increased Mg-ATPase activity of the K_{ATP} channel complex is thought to

cause elevation of the MgADP levels in the localized environment of the ADP-sensing region of NBD2, resulting in excessive activation of the K_{ATP} channel that is poorly coupled to metabolic status of the β cell. It is therefore likely that more ND mutations in *ABCC8* will be discovered in the future.

In direct contrast to rare monogenic mutations that result in overt insulin secretory disorders, common genetic variants in the *KCNJ11* and *ABCC8* genes may not manifest a clinical phenotype but are associated with an increased risk for diabetes. For example, the K23 single nucleotide variant (E23K, rs5219) within the *KCNJ11*gene (Figure 1.5.) is associated with impaired glucose-stimulated insulin secretion in approximately 20% of the Caucasian T2D population[159,160]. Moreover, the K23 variant has also been shown to be associated with T2D in almost every ethnic group examined[161–164]. As an estimated 10% of the world's population possesses two copies of K23, they may be at increased risk of developing T2D. Despite intense research on the K23 variant, the molecular mechanism(s) that increases T2D susceptibility have not been conclusively established, suggesting perhaps a more complex process underlies K23's association with T2D. In this regard, it is important to note that the *ABCC8* A1369 variant (rs757110) is tightly associated with the K23 variant, forming a T2D risk haplotype (K/A), such that greater than 95% of people with two copies of K23 also possess two copies of A1369[165]. It should also be noted that the *ABCC8* and *KCNJ11* genes are located adjacent to each other on the same chromosomal position (11p15.1), further supporting a tight inheritable risk haplotype that may alter the properties of the K_{ATP} channel complex. Our laboratory has recently performed mechanistic studies on human K_{ATP} channels containing both variants to characterize the contributions of each variant to the intrinsic properties and pharmacology of the K_{ATP} channel complex[166].

Several rare heterozygous mutations in *ABCC8* that cause overt ND (R1380L and R1380C) act by increasing Mg-ATPase activity[158]. Interestingly, the SUR1 S1369 residue is located in close proximity to the Mg-ATPase catalytic site and residue R1380 in the SUR1 nucleotide-binding fold 2[45]. Work from our laboratory has now confirmed that the Mg-ATPase activity of the K_{ATP} channel complex is increased in the presence of the A1369 variant[167], providing a mechanistic explanation as to why carriers of the variant are more prone to develop T2D.

In contrast to the detailed identification and description of pancreatic K_{ATP} channel genetic variants, very little is known about the few identified mutations in cardiac K_{ATP} channels. In the human heart, an ABCC9 mutation that increases the risk of atrial fibrillation originating from the vein of Marshall has been identified[168]. Electrical instability caused by K_{ATP} channels has been demonstrated in atrial fibrillation patients who have altered mRNA transcription that includes downregulation of the K_{ATP} channel pore and the subsequent associated current[169,170]. Additionally, heterozygous mutations in ABCC9 have been associated with dilated cardiomyopathy with tachycardia[103]. Moreover, the relationship between the common Kir6.2 polymorphism and heart disease has been studied in heart failure patients interestingly showing that there was higher frequency of the K23 allele amongst heart failure patients. That, along with the high mortality risk in heart failure patients of the blunted heart rate response during exercise suggest that the E23K polymorphism could highlight the role of K_{ATP} channels in cardiac pathophysiology[171].

1.8. Role of K_{ATP} in the heart

The bulk of studies in the cardiac K_{ATP} literature refer to their protective role during stress episodes and their important role in transduction of cellular metabolic signals into membrane potential changes and regulation of critical cellular functions such as

cytoprotection[172,173,174.] However, it is essential to understand what their role is in normal physiology before discussing how they protect the myocardium during stress.

It is generally considered that K_{ATP} channels in the heart are predominantly closed under resting aerobic conditions[175]. Studies on Kir6.2-/- mice showed that the action potential duration and contractile function in wild-type and Kir6.2-/- hearts are similar[176]. Therefore it is has been suggested that cardiac K_{ATP} channels play little or no role in regulating cardiac excitability in the basal aerobic state. On the other hand, in the case of metabolic strain such as during an ischemic insult, cardiac K_{ATP} channels open, leading to K^+ efflux, membrane repolarization and shortening of the action potential duration as well as blunted contraction[177,178]. This is also accompanied by reduction in Ca^{++} influx, preventing intracellular accumulation and preserving cellular energy rather than it being directed towards ionic homeostasis[179] (Figure 1.6.). This protective function of K_{ATP} channels in the heart is lost in Kir6.2-/- mice which exhibit larger infarct sizes in ischemia-reperfusion models and poorer functional recovery post-insult[180–182].

Several studies have previously described the antiarrhythmic effects of cardiac K_{ATP} inhibition in the setting of ischemia-reperfusion using in vitro[183–187] and in vivo models [188–195]. Some clinical studies have also demonstrated antiarrhythmic effects of SUs[196–198], and in spite of KCOs showing proarrhythmic effects in certain animal models, clinically, that was not the case[199–202], on the contrary, some studies have demonstrated the antiarrhythmic effect of KCOs but under different experimental conditions[188,189,203–205].

A recent study by Bao et al. demonstrated the presence of an intracellular endosomal K_{ATP} reservoir pool which during stress conditions can alter K_{ATP} surface density[206]

emphasizing the crucial role of K_{ATP} during ischemia. In that regard, Du et al. have demonstrated that the overexpression of SUR2A in cardiac tissue leads to a phenotype that appears to be resistant to ischemia[207]. However, pharmacological inhibition using glibenclamide and tolbutamide[178] as well as genetic ablation of K_{ATP} leads to loss of the protective effects of K_{ATP} channel opening[208]. On the other hand, Baczko et al. have demonstrated that the activation of K_{ATP} channels using pinacidil and P-1075 aided in preventing Ca^{++} overload resulting from chemically-induced hypoxia/reoxygenation via a mechanism that is dependent on hyperpolarization of diastolic membrane potential[209]. The same group proposed that this protection was due to reductions in abnormal diastolic Ca^{++} homeostasis mediated by reverse-mode Na^{+}/Ca^{++} exchange[210]. Moreover, the use of the K_{ATP} opener, pinacidil, significantly reduced action potential duration during ischemia and preserved ATP levels[211]. This was also confirmed by Suzuki et al. using Kir6.2-/- mice where they showed that during ischemia cardiac contraction was longer than in wild-type mice and action potential duration was unaffected[180]. Additionally, repeated exercise known for its cardioprotective effects through preconditoning (see Frasier et al.[212] for review) was shown to increase K_{ATP} expression by almost 40% in murine ventricles leading to action potential shortening in response to higher heart rates, and this effect was lost when transgenic mice that expressed non-functional K_{ATP} channels were used[213]. Additionally, the same group has previously shown that Kir6.2-/- mice exhibit less ability to perform high-intensity exercise and are more vulnerable to catecholamine cardiotoxicity[181]. Similarly, it was previously demonstrated by Ton et al. that mice with cardiac specific overexpression of a dominant negative Kir6.2 subunit exhibited a proarrhythmic phenotype and poor tolerance to exercise[214].

Ischemic preconditioning is another protective mechanism that is compromised in the absence of K_{ATP} channels. In 1986, Charles Murray described the protective effects of preconditioning hearts by subjecting them to four short ischemic occlusions preceding prolonged ischemia in dogs. Ischemic preconditioning limited infarct size to 25% of that seen in the control group[215]. In the absence of K_{ATP} channels, the protective effect of ischemic preconditioning is lost and functional recovery was worse than in wild-type mice[180,106,216]. Since it is difficult to predict when a heart attack will occur exactly, many groups attempted to study pharmacological agents that could mimic ischemic preconditioning that could potentially used prophylactically in predisposed individuals. One of those agents is the KCO, DZX. Likewise, a study by Nakaya's group demonstrated that the preconditioning effect of DZX was also lost in Kir6.2-/- mice[106].

Additionally, the effect of another cardioprotective agent; resveratrol[217], was found to be lost in the absence of K_{ATP} channels[218]. It is unclear if resveratrol has a direct K_{ATP} channel opening effect, however it has been established that one of the ways that resveratrol exerts its cardioprotective action is through activation of the central energy sensor in the cell; AMPK[219–222].

1.9. Cardioprotection and metabolism

In order for the heart to function normally, an intricate process for the production of ATP has to complement its tremendous work load. The heart itself has a relatively limited ATP content which is metabolised very quickly resulting in a complete cardiac ATP pool turnover every 10 seconds[223]. Therefore the heart meets this continuous ATP demand by hydrolyzing ATP through utilizing fatty acids and glucose and translating it into mechanical energy via the actin-myosin mechanism[224]. Cardiac contractility alone consumes

approximately 60-70% of myocardial ATP hydrolysis is while the other 30-40% is directed to maintain ionic homeostasis[225]. Under basal aerobic conditions, mitochondrial oxidative phosphorylation produces almost 95% of total ATP[223]. Under basal aerobic conditions, between 60% and 90% of the acetyl CoA that enters the tricarboxylic acid cycle is derived from β-oxidation of fatty acids and the remainder comes from oxidation of pyruvate that is either produced through glycolysis or lactate oxidation[226–228]. Below is a brief overview of the main pathways of the intricate and complex process that is cardiac metabolism.

Fatty acid oxidation

Cardiomyocytes utilize either circulating free fatty acids bound to albumin or those released by lipoprotein lipase on the cell surface from triacyl glycerol in very low density lipoproteins or chylomicrons[229–231]. The fatty acids are then transported into the cell via transporters such as CD36/FAT, fatty acid transport proteins (FATP) and plasma membrane fatty acid binding protein (FABPpm)[232–234]. Triacyl glycerols are catabolyzed in a lipolytic series mediated by adipose triglyceride lipase[235], hormone-sensitive lipase and monoglyceride lipase[236]. Fatty acyl CoA synthetase 1 esterifies free fatty acids into fatty acyl CoA esters[237]. To transport the fatty acids into the mitochondria, the acyl CoA moiety is converted to acyl carnitine. The rate limiting enzyme for mitochondria fatty acid transport is carnitine palmitoyl transferase - 1 (CPT-1)[238,239]. The allosteric inhibitor of CPT-1, malonyl CoA, is produced by carboxylation of acetyl CoA by acetyl coA carboxylase (ACC)[240–242]. The predominant form of ACC in the heart is ACC2 and its activity is under the control of AMPK[243–245]. AMPK is the cellular energy sensor that among its other roles up-regulates fatty acid β-oxidation during times of increased energy demand via phosphorylation and

decrease of ACC activity leading to less conversion of acetyl CoA to malonyl coA thus allowing fatty acids to be transported into the mitochondria for β-oxidation[244,246,247].

In fatty acid β-oxidation, the enzymes involved in the process are under a precise control by transcription factors. The most well-studied transcriptional regulators of fatty acid β-oxidation are peroxisome proliferator-activated receptors (PPARs) and a transcription factor coactivator peroxisome proliferator-activated receptor gamma coactivator 1-alpha (PGC-1α)[248]. PPAR-α is the predominant PPAR isoform that is expressed in highly metabolic tissues such as the heart, skeletal muscle and the liver[249–251]. PGC-1α binds to and increases the activity of PPARs[252,253] resulting in upregulation of the expression of enzymes involved in fatty acid uptake and oxidation[248,254,255].

Glycolysis and glucose oxidation

Glucose utilized by cardiomyocytes is either derived from endogenous glycogen stores, or is transported from the blood stream into the cell via glucose transporters (GLUT), specifically isoforms 1 and 4. GLUT1 is constitutively active being responsible for maintaining basal glucose uptake, while GLUT4 translocates to the plasma membrane in response to increased workload and insulin signalling[233,256–258]. Inside the cardiomyocyte, glucose undergoes aerobic glycolysis (Figure 1.7.) where it is initially phosphorylated by hexokinase into glucose-6-phosphate and following a series of enzymatic reactions it is converted into two pyruvate molecules[226,259]. Phosphofructokinase 1 is the rate limiting enzyme of glycolysis which catalyzes the conversion of fructose-6 phosphate to fructose 1,6-bisphosphate. Phosphofructokinase 1 is activated by the nucleotides AMP and ADP and is inhibited by ATP and citrate[260,261]. PFK1 can also be stimulated allosterically by fructose-2,6-bisphosphate generated by the enzyme PFK2[262–264]. Fructose 1,6-bisphosphate is

converted by aldolase into two triose sugars; glyceraldehyde 3-phosphate and dihydroxyacetone phosphate, which is then interconverted into glyceraldehyde-3-phosphate by triosephosphate isomerase. That is followed by dehydrogenation by glyceraldehyde 3-phosphate dehydrogenase forming 1,3-bisphosphoglycerate. One phosphate group is then transferred from 1,3-bisphosphoglycerate to ADP by phosphoglycerate kinase, producing ATP and 3-bisphosphoglycerate. Phosphoglycerate mutase then converts 3-bisphosphoglycerate to 2-bisphosphoglycerate and by the action of enolase is converted to phosphoenolpyruvate. The final step of glycolysis is catalyzed by pyruvate kinase which phosphorylates phosphoenolpyruvate producing ATP and pyruvate[226,259]. In ischemic conditions, glycolysis-produced pyruvate can be converted to lactate by lactate dehydrogense[229,265]. In times of cardiac stress, lactate and protons produced by anaerobic glycolysis can accumulate and compromise cardiac work and efficiency[266,267].

Oxidation of glycolysis- or lactate-derived pyruvate accounts for the majority of carbohydrate-derived ATP[237,268,269] and is transported into mitochondria through the mitochondrial pyruvate carrier[270–272]. The rate limiting step in glucose oxidation is oxidation of pyruvate to acetyl CoA by the pyruvate dehydrogenase (PDH) complex which consists of PDH, PDH kinase (PDK), and PDH phosphatase (PDHP) enzymes[273]. PDH is regulated both by substrate/product ratios and by covalent modifications. Covalent modifications that regulate PDH activity include phosphorylation and acetylation. Dephosphorylation of PDH increases PDH activity, while phosphorylation of PDH decreases its activity resulting in reduced oxidation of pyruvate. Increased PDK protein expression, which results in increased PDH phosphorylation, is a key mechanism involved in reduced PDH flux and glucose oxidation[274,275].

The Randle Cycle

The balance between fatty acid oxidation and glucose oxidation is described as the glucose/fatty acid cycle or more commonly, the Randle cycle[276]. An increase in fatty acid oxidation is associated with increased mitochondrial acetyl CoA:free CoA and NADH:NAD^+ ratios. This enhances the activity of pyruvate dehydrogenase kinase leading to downstream phosphorylation and inhibition of pyruvate dehydrogenase. Inhibition of pyruvate dehydrogenase prevents the conversion of pyruvate to acetyl coA which eventually results in halting of glucose oxidation[223]. Furthermore, high fatty acid oxidation inhibits phosphofructoinase 1 by the action of citrate and accordingly limits flux through glycolysis. The resulting inhibition of glucose oxidation however is greater than that of glycolysis, leading to uncoupling between the two processes and resulting in accumulation of lactate and H^+[277]. On the other hand, stimulation of glucose oxidation reduces the rate of fatty acid oxidation[278] via accumulation of malonyl coA resulting in CPT-1 inhibition[240].

Regarding the uncoupling between glycolysis and glucose oxidation mentioned above, it appears to be more accelerated during ischemia[279] Intracellular acidosis reduces the myofibrillar Ca^{++} sensitivity, leading to weaker contraction[280]. Intracellular acidosis stimulates Na^+/H^+ exchange through activation of reverse mode Na^+/H^+ antiporter leading to accumulation of intracellular Na^+[281–283]. Additionally, the drop in ATP leads to inhibition of Na-K-ATPase which extrudes three Na^+ and introduces two K^+ ions into the cell[284] leading to further gradual accumulation of Na^+[285–287]. Subsequently, this elevation in Na^+ leads to increased reverse mode Na/Ca exchanger activity leading to further accumulation of Ca^{++} inside the cytoplasm of the myocytes[287–289]. The significant drop in ATP also leads to disruption of the sarcolemmal and sarcoplasmic reticulum Ca^{++}-ATPase leading to more

accumulation of intracellular Ca^{++}[284]. Accumulation of calcium leads to hypercontraction, reduced relaxation of the contractile machinery and activation of Ca^{++}-dependent proteases, caspases, the apoptotic pathway and the necrotic pathway ultimately leading to cellular demise[286,287,289].

1.10. AMPK

Expression of AMPK in heart tissue was demonstrated in the early 1990s[290] despite being discovered in the liver almost in 1973. where it was shown to function as a fatty acid and cholesterol biosynthesis regulator[291,292]. AMPK is now known as the key cellular energy sensor as during times of energetic stress. AMPK is activated to promote ATP-producing catabolic pathways and halting ATP-consuming anabolic processes[293].

AMPK is a hetero-trimeric serine/threonine protein kinase composed of a catalytic subunit, the α subunit and regulatory β and γ subunits. AMPK is activated by phosphorylation of the Thr172 residue in the N-terminus of the catalytic subunit[294]. Its role as a cellular energy sensor based on its sensitivity to changes in the ratio of AMP to ATP. AMP binds to and activates the γ regulatory subunit of AMPK allosterically or through promotion of phosphorylation of Thr172 on the α catalytic subunit by upstream kinases such as AMPKK or by hindering Thr172 dephosphorylation by phosphatases[295]. These various mechanisms by which AMP regulates AMPK activity make it sensitive to small changes in free AMP concentration[295]. Most of intracellular AMP exists in the protein-bound form, therefore changes in AMPK phosphorylation and hence activation may be a result of small changes in free AMP concentration while total AMP concentration remains the same[296]. Similar to AMP, ADP has been reported to regulate AMPK activity as well via hindering Thr172 dephosphorylation but not through allosteric activation[297,298].

The upstream AMPKKs identified so far include LKB1, Ca^{++}/Calmodulin dependent kinase kinase β (CaMKKβ) and transforming growth factor-β-activated protein kinase-1 (TAK1)[299–307]. Dephosphorylation of the Thr172 residue of AMPK by protein phosphatases, namely PP2A and PP2C reduces its activity[308]. In that regard, AMP binding to the γ-subunit of AMPK impairs PP2C from dephosphorylating AMPK[308]. Since it is hard to pigeonhole the role of AMPK into regulation of a single process in the cell, the author will focus in this thesis on its role as a metabolic sensor.

The role of AMPK in fatty acid metabolism

Fatty acid uptake into the cardiomyocyte can be increased via AMPK by several mechanisms. Firstly, AMPK can increase recruitment of LPL to the coronary lumen[75] which increases the availability of free fatty acids for cardiomyocytes to utilize. Free fatty acid uptake is directly proportional to fatty acid supply [237]. Secondly, activation of AMPK increases expression and translocation of CD36 to the cell membrane[309]. Thirdly, AMPK also is directly involved in fatty acid oxidation as it phosphorylates ACC and inhibits it.[310,311,312]. ACC as mentioned previously leads to the production of malonyl coA which is an inhibitor of fatty acid uptake into the mitochondria and leads to subsequent β-oxidation. Studies have pointed to the strong link between increased AMPK activity and inhibition of ACC and increased fatty acid oxidation rates. Though this is not the case in all studies [313,314]. Fourth, AMPK has been associated with the activation of MCD in skeletal muscle and H9C2 cells but the occurence of this in the heart is controversial[315,316]. Finally, AMPK activates PGC-1α by phosphorylating PGC-1α on threonine and serine residues[254]. It was suggested that AMPK increases PGC-1α mRNA levels by regulating the binding of transcription factors to specific sequences located in the PGC-1α gene promoter[248,254,237].

The role of AMPK in glucose oxidation

AMPK can increase glucose uptake in various ways, for example, its activation increases translocation of glucose transporter GLUT4 to the plasma membrane[317,318,319]. AMPK may also regulate glucose uptake in a manner that is dependent on glycogen content as evident from research from the Clanachan group showing that activation of AMPK does not affect glucose uptake in glycogen replete hearts[320]. The same group has also shown that under basal conditions AMPK activation does not stimulate glucose uptake but shifts it towards glycolysis rather than glycogen synthesis[313]. The AMPK activator AICAR has been shown to activate and inhibit glycogen synthesis in skeletal muscle. AICAR has also been shown to increase glycogen breakdown in the heart in the absence of changes in glycogen synthase activity. Moreover, mutations in AMPK lead to significant accumulation in glycogen in both myocardial and skeletal tissue. AMPK can also regulate glycolysis via phosphorylation and thereby activation of phosphofructokinase 2 in the heart. This increases the production of fructose 2,6 bisphosphate[321] which in turn activates phosphofructokinase 1.

1.11. AMPK in cardioprotection

As many studies have established, in the event of myocardial ischemia, AMPK is rapidly activated[322–324]. Activation of AMPK leads to downstream changes in cellular metabolism in order to reduce ATP utilization and increase its production during the oxygen and nutrient deprivation experienced during I/R. The literature has been unequivocal when it comes to AMPK activation during I/R. For example, several studies have demonstrated that the heart is protected against I/R when AMPK is activated pharmacologically during ischemia[325,326]. In AMPK α2 kinase-dead mice, I/R was found to be more damaging than in wild-type mice[327,323]. Other studies have also shown that activating AMPK using AICAR,

adiponectin, metformin as well as caloric restriction is protective in I/R injury[328–331]. Interestingly, Kim and colleagues have also shown that stretch-induced protection against ischemia-reperfusion injury is mediated by AMPK[332]. On the other hand, studies have also shown that in a transgenic mouse model with suppressed AMPK activation, (dominant-negative α2-subunit) cardiac metabolism was not compromised and in fact exhibited improved functional recovery post I/R[333].

1.12. The interplay between K_{ATP} and AMPK

Since both K_{ATP} and AMPK are important in cardioprotection and preconditioning, the question of whether they interacted with one another remained to be examined. In that regard, Coetzee and his group have shown using immunoprecipitation that AMPK physically associates with K_{ATP} , specifically on the Kir6.2 subunit using immunoprecipitation[334]. Additionally, the same group has suggested that cardiac K_{ATP} channel activation is directly regulated by AMPK in an AMP-dependent manner in isolated ventricular rat cardiomyocytes[334]. Moreover, Lim et al. have described how AMPK activation influences K_{ATP} channel trafficking in events of glucose deprivation in pancreatic β-cells[335]. Shyng's group has also shown that AMPK-regulated K_{ATP} trafficking is influenced by leptin levels[336]. Park et al. also demonstrated that this trafficking of K_{ATP} occurs via PTEN inhibition in pancreatic islets[337]. The studies mentioned suggest that AMPK activation in β-cells increases K_{ATP} trafficking to the cell membrane, leading to hyperpolarization of the membrane which would prevent insulin release. Should the same mechanism occur in the heart, membrane hyperpolarization would also prevent opening of voltage-gated calcium channels and prevent calcium accumulation during stress, however this has not been investigated yet.

1.13. K_{ATP} channels and metabolism

When an electrical channel possesses an enzymatic ability by which it can produce its own regulators, many questions regarding the implications of this property are expected to rise. Therefore, it is important to understand what possible outcomes may arise in light of our current understanding of the proteins that interact with K_{ATP} channels.

Due to the clear role of pancreatic K_{ATP} channels in glucose homeostasis, K_{ATP} channels have become key players in energy sensing. That being said, whole body energy governance, from food intake to nutrient metabolism and energy homeostasis, is regulated through the gut-brain-liver axis[338–343]. Interestingly, the K_{ATP} channel composition in the hypothalamus is the same as that in pancreatic β-cells, Kir6.2/SUR1. The central mediation of hepatic gluconeogenesis by hypothalamic K_{ATP} channels has been previously established[344, 345]. Moreover, as previously indicated, PKC has the ability to phosphorylate and activate Kir6.2/SUR1 channels[66] and following up on that, Ross et al. have shown that PKC mediated regulation of glucose production requires the presence of hypothalamic Kir6.2/SUR1 K_{ATP} channels[346]. Additionally, Abraham et al. have shown that the inhibitory effect of hypothalamic glucagon on glucose production is mediated through K_{ATP} channels[347].

As previously mentioned, K_{ATP} channels were shown to associate with glycolytic enzymes and the Terzic group has suggested that this association might facilitate channel regulation, particularly inhibition. In that regard, Weiss and Lamp have suggested that cardiac K_{ATP} channels are preferentially regulated by glycolysis-derived ATP in close proximity of the channels suggesting that glycolytic enzymes could be positioned in the vicinity of the plasma membrane[58]. This was further confirmed in a study on enterocytes

isolated from the Necturus aquatic salamander showing that K_{ATP} channels were inhibited by ATP produced by pyruvate kinase[348]. The physical association between K_{ATP} channel subunits and glycolytic enzymes, namely GAPDH, triosephosphate isomerase and pyruvate kinase was finally demonstrated by Coetzee et al.. Moreover, in that same study they showed that the functional enzymes are able to modulate K_{ATP} channel activity[349]. Following the same lead, Jovanovic et al. have also confirmed the interaction between K_{ATP} and GAPDH in 2005[350]. Additionally, K_{ATP} was found to associate to several glycolytic enzymes such as aldolase A, enolase 1, fructose-6-phosphate kinase and hexokinase 1 through mass spectroscopy, confocal microscopy and immunoprecipitation[351] (Figure 1.7.).

The physically associated glycolytic enzymes, adenylate kinase and creatine kinase are therefore capable of regulating the nucleotide concentration in the microenvironment of the channel. That change in nucleotide concentration has already been shown to open or close the channel and thereby changes membrane potential, however, it is important to understand that the Mg-ATPase activity of the channel allows it to hydrolyse Mg-ATP in its vicinity resulting in channel activation. The regulators of the ATPase activity of K_{ATP} channels are currently unknown. Despite the scarcity of information regarding the functional implications of those physical associations, it remains intriguing that a classical electrical channel would have metabolic proteins that are activated or modulated by nucleotides in what seems as a complex metabolome. Most notably, AMPK which responds to changes in metabolism and greatly contributes to energy homeostasis as previously reviewed[352], that is ultrasensitive to AMP and that is a direct regulator of cellular metabolism is associated with a stress-activated channel. Therefore, it is logical to ask the question: Is K_{ATP} an regulator of

cellular metabolism rather than just a responder? Our proposed K_{ATP} pathway for cardioprotection that is independent on electrical activity is represented in Figure 1.8.

In an effort to address this conundrum, Terzic's group executed a proteomic analysis to measure changes in protein levels in a global K_{ATP} knockout mouse model. The resulting data showed that almost 60% of the proteins whose expression was affected by genetic ablation of K_{ATP} were proteins involved in cellular metabolism. Based on that, Alekseev et al. compared whole body metabolism in wild-type and Kir6.2-/- mice revealing higher energy expenditure in Kir6.2-/- mice and a lean phenotype resistant to obesity even when fed a high fat diet. When subjected to high intensity exercise, the compromised energetics of the Kir6.2-/- mice could not support the increased workload[353]. Additionally, a recent study by Fahrenbach et al. demonstrated that genetic deletion of ABCC9 which encodes SUR2A in neonatal cardiomyocytes, the cells could not shift from a fetal metabolic profile that is reliant on glycolysis to mitochondrial oxidative metabolism[354]. To this date, the relationship between K_{ATP} channels and fatty acid metabolism is unclear.

As demonstrated, the K_{ATP} channels are complex electrical channels and at this point in time we're only scratching the surface of understanding what roles they play in the myocardium. In hopes to understand the link between the K_{ATP} channel, an extensively studied classical electrical channel, and cardiac metabolism, which is instrumental in the process of cardioprotection.

1.14. Summary of hypotheses and aims for the thesis

Overarching hypothesis

K_{ATP} channels do not only respond to changes in metabolism by changing membrane excitability. Loss of cardioprotection in the absence of K_{ATP} channels is attributed to loss of electrical homeostasis in addition to alterations in cardiac metabolism. Absence of K_{ATP} channels in the heart metabolically compromises it and sets it up for failure when exposed to a stress episode, be it physiological or pathological. The K_{ATP}-induced regulation of cardiac metabolism is directly related to the Mg-ATPase activity of the channel. Subtle changes in Mg-ATPase activity directly affect AMPK signaling which translates to changes in metabolism.

Specific hypotheses

Hypothesis I - Chapter 3

K_{ATP} channels are direct regulators of cardiac metabolism through their action on the central cellular energy sensor AMPK.

Specific aims

- To examine the direct effect of genetic ablation of K_{ATP} channels in the heart on different cardiac metabolic pathways.

- To investigate changes in protein expression of metabolic markers in the absence of cardiac K_{ATP} channels.

Hypothesis II - Chapter 4

The activity of Mg-ATPase is determined by residue-residue interactions in the nucleotide binding domain of the sulfonylurea subunit.

Specific aims

- To identify protein residues in nucleotide binding domain 2 of the K_{ATP} channel that determine Mg-ATPase activity.

- To examine whether residue differences between the splice variants SUR1 and SUR2A dictate their differential sensitivity to diazoxide.

- To test whether mechanical stress is a regulator of Mg-ATPase activity.

Hypothesis III - Chapter 5

Sulfonylurea toxicity occurs through direct inhibition of the Mg-ATPase activity of cardiac K_{ATP} channels.

Specific aim

- To compare the effects of glibenclamide and gliclazide on Mg-ATPase activity and the survival kinases in cardiac tissue.

Figure 1.1. Molecular composition of K_{ATP} channels. (A) K_{ATP} channels are hetero-octameric complexes where 4 Kir6.x subunits form the pore and are surrounded by 4 SUR regulatory subunits. (B) Membrane topology of SURx and Kir6.x subunits of the K_{ATP} channel. ATP binds to the Kir6.x subunit inhibiting K_{ATP} channels. Hydrolysis of MgATP within the SURx subunit nucleotide-binding domains (NBDs) leads to generation of stimulatory MgADP.

A.

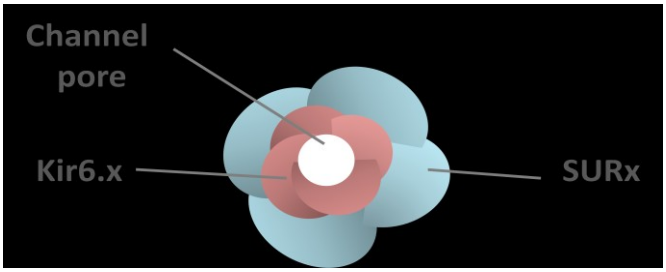
Channel
pore
Kir6.x
SURx

B.

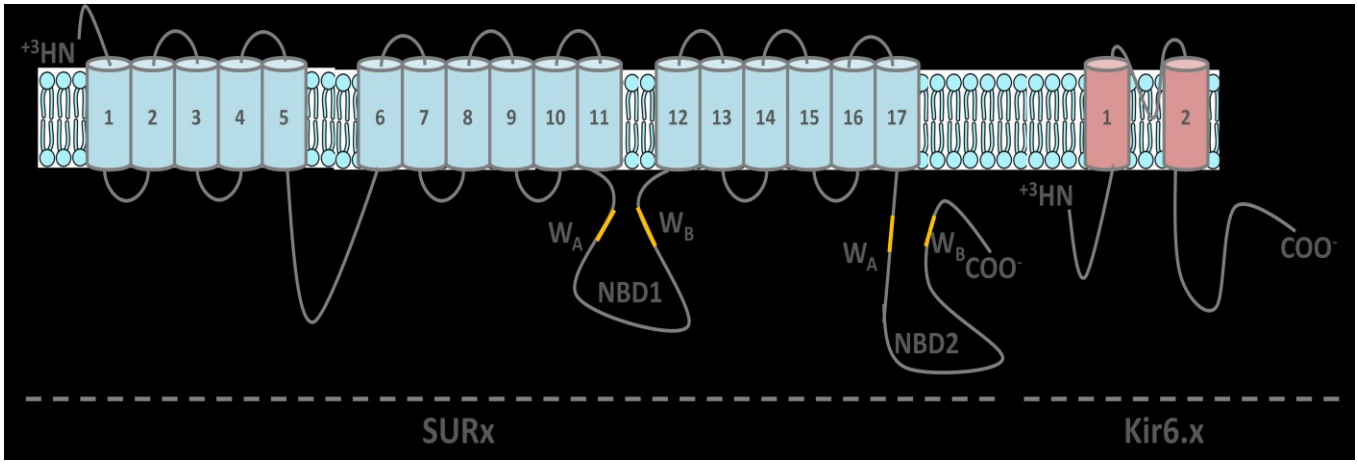
+3HN
1
2
3
4
5
6
7
8
9
10
11
12
13
14
15
16
17
1
2
+3HN
COO-
WA
WB
NBD1
WA
WB
COO-
NBD2
SURx
Kir6.x

Figure 1.2. Different K_{ATP} channel subunit isoforms and tissue-specific expression. In the brain and pancreas the channels are composed of the Kir6.2/SUR1 combination. In heart ventricles and smooth muscle, the Kir6.2/SUR2A is the combination expressed. In smooth muscle, the Kir6.1/SUR2B is the combination expressed.

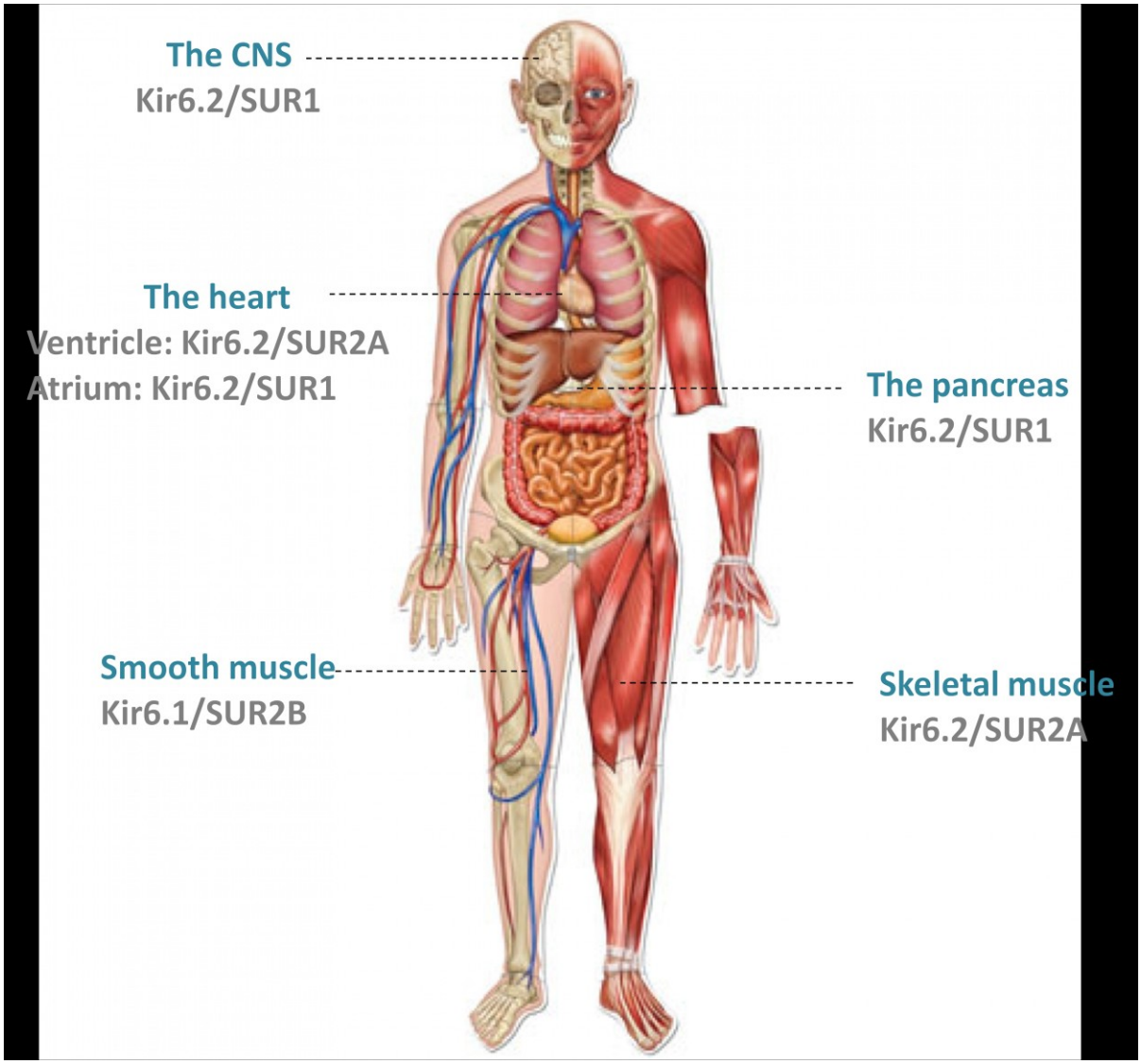
The CNS
Kir6.2/SUR1
The heart
Ventricle: Kir6.2/SUR2A
Atrium: Kir6.2/SUR1
The pancreas
Kir6.2/SUR1
Smooth muscle
Kir6.1/SUR2B
Skeletal muscle
Kir6.2/SUR2A

Figure 1.3. Drug binding sites on K_{ATP} channels. (A) General membrane topology of K_{ATP} channels with marked A-/ B- drug binding sites. (B) Chemical structures and binding-site classification of the sulfonylureas and glinides.

A.

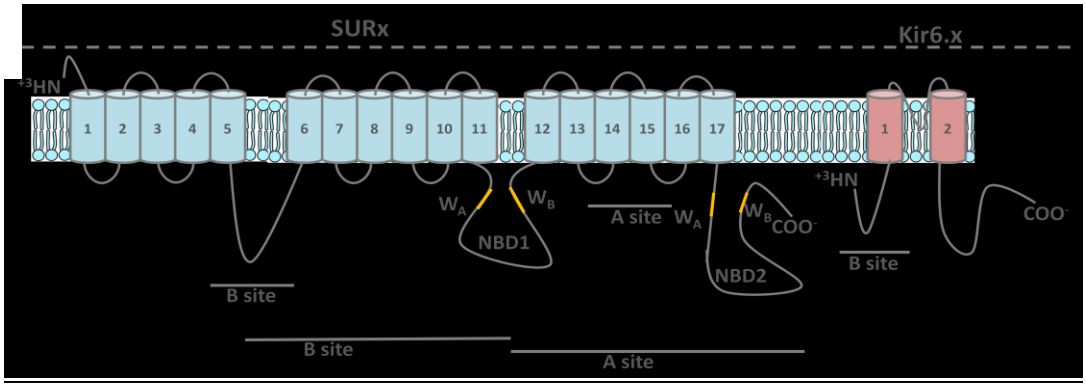
SURx
Kir6.x
+3HN
1
2
3
4
5
6
7
8
9
10
11
12
13
14
15
16
17
1
2
WA
WB
NBD1
A site
WA
WB
COO-
NBD2
+3HN
COO-
B site
B site
B site
A site

B.

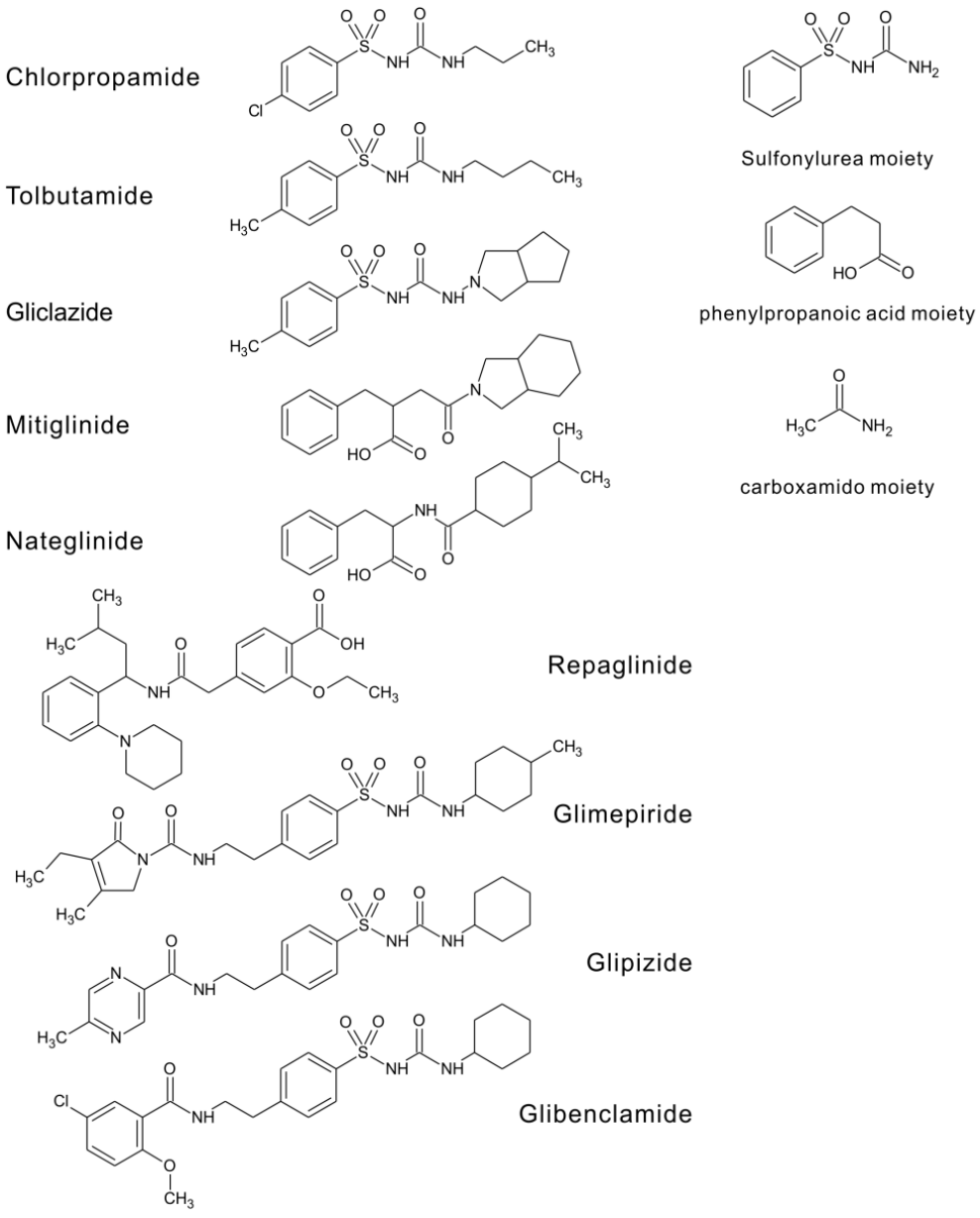
Chlorpropamide
Tolbutamide
Gliclazide
Mitiglinide
Nateglinide
Repaglinide
Glimepiride
Glipizide
Glibenclamide
Sulfonylurea moiety
phenylpropanoic acid moiety
carboxamido moiety

Figure 1.4. Physiological and pharmacological activators and inhibitors of K_{ATP} channels. (A) Activators of K_{ATP} channels, physiological activators are listed in grey and pharmacological activators are listed in green. (B) Inhibitors of K_{ATP} channels; physiological inhibitors are listed in grey and pharmacological inhibitors are listed in red.

A.

B.

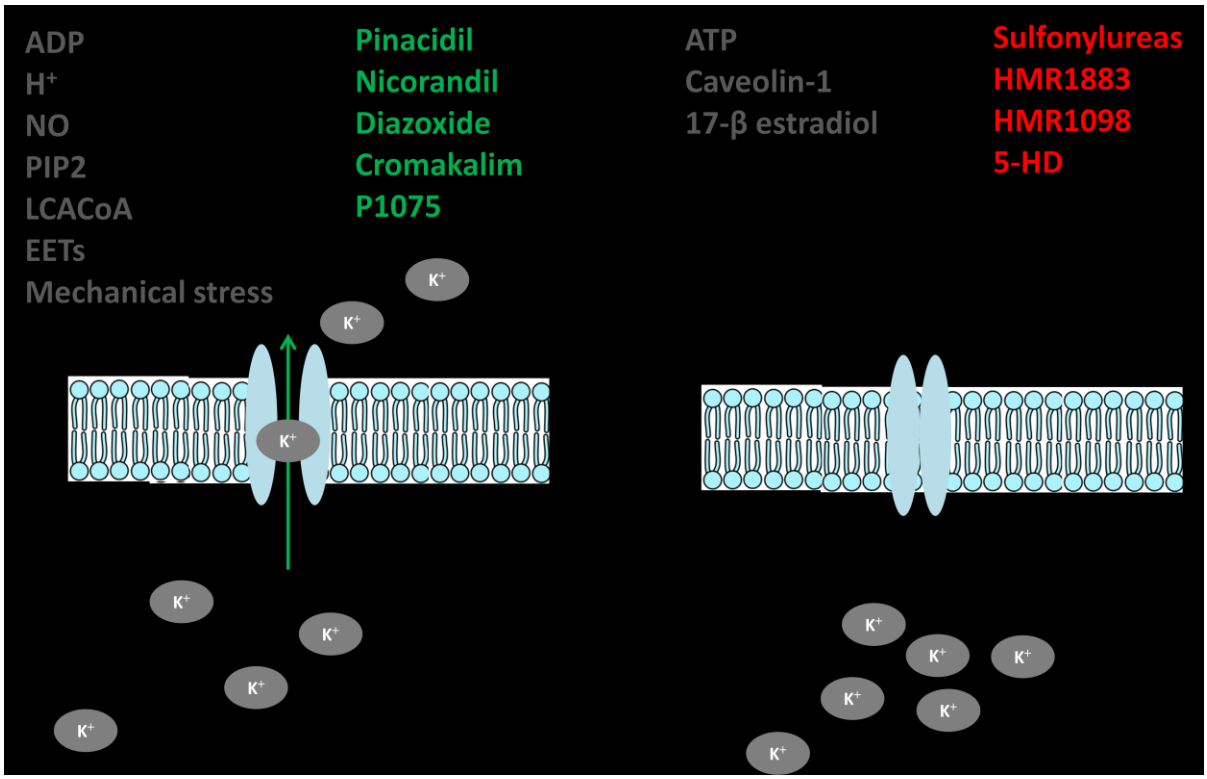
ADP
H+
NO
PIP2
LCACoA
EETs
Mechanical stress
Pinacidil
Nicorandil
Diazoxide
Cromakalim
P1075
ATP
Caveolin-1
17-β estradiol
Sulfonylureas
HMR1883
HMR1098
5-HD
K+

Figure 1.5. Common genetic variants of K_{ATP} channels. Nucleotide-binding domains (NBDs) 1 and 2 as well as the A- and B-binding sites for pharmacologic inhibitors are indicated. The location of common variants S1369A and E23K and the neonatal diabetes mutations R1380L/C (in SUR1 NBD2) and V59M (in Kir6.2) are indicated. (Figure published in Current Diabetes Reports - The molecular genetics of sulfonylurea receptors in the pathogenesis and treatment of insulin secretory disorders and type 2 diabetes - Veronica Lang, Nermeen Youssef, Peter E. Light. 2011 Dec;11(6):543-51)

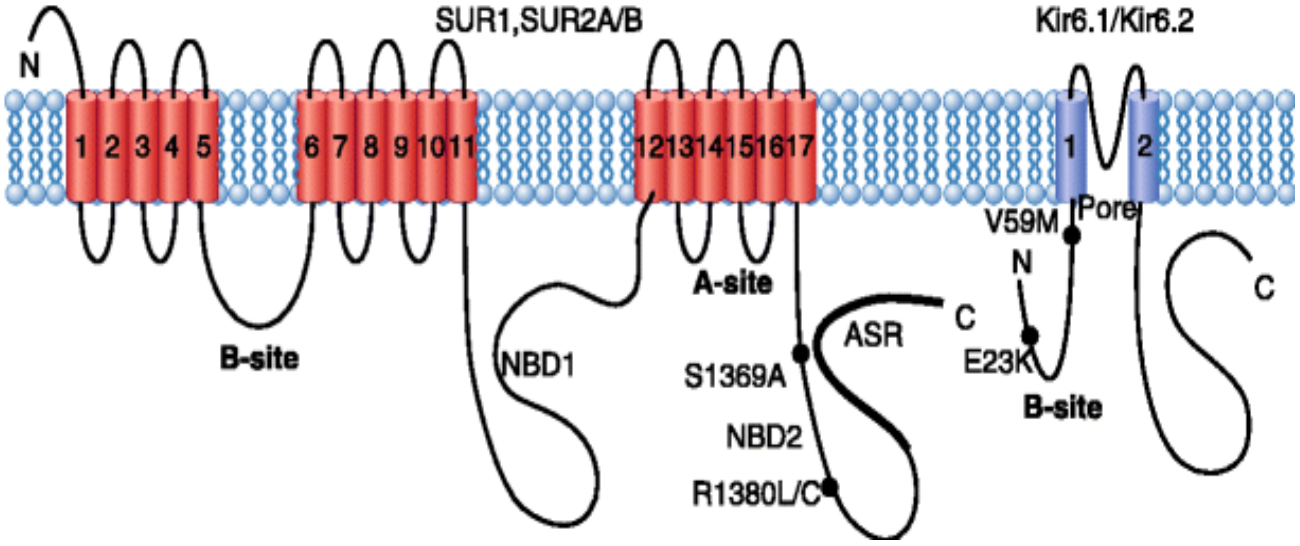
SUR1,SUR2A/B
Kir6.1/Kir6.2
N
1 2 3 4 5
6 7 8 9 10 11
12 13 14 15 16 17
1
2
V59M
Pore
N
C
C
A-site
ASR
B-site
NBD1
S1369A
E23K
B-site
NBD2
R1380L/C

Figure 1.6. Classical mechanism of K_{ATP} channel activation in the heart. (1) During physiological stress e.g. exercise or a pathophysiological stress e.g. an ischemic attack, (2) the ATP:ADP ratio decreases leading to (3) channel opening. (4) The resulting K^+ efflux leads to (5) membrane repolarization and (6) action potential (AP) shortening and (7) maintenance of ionic homeostasis.

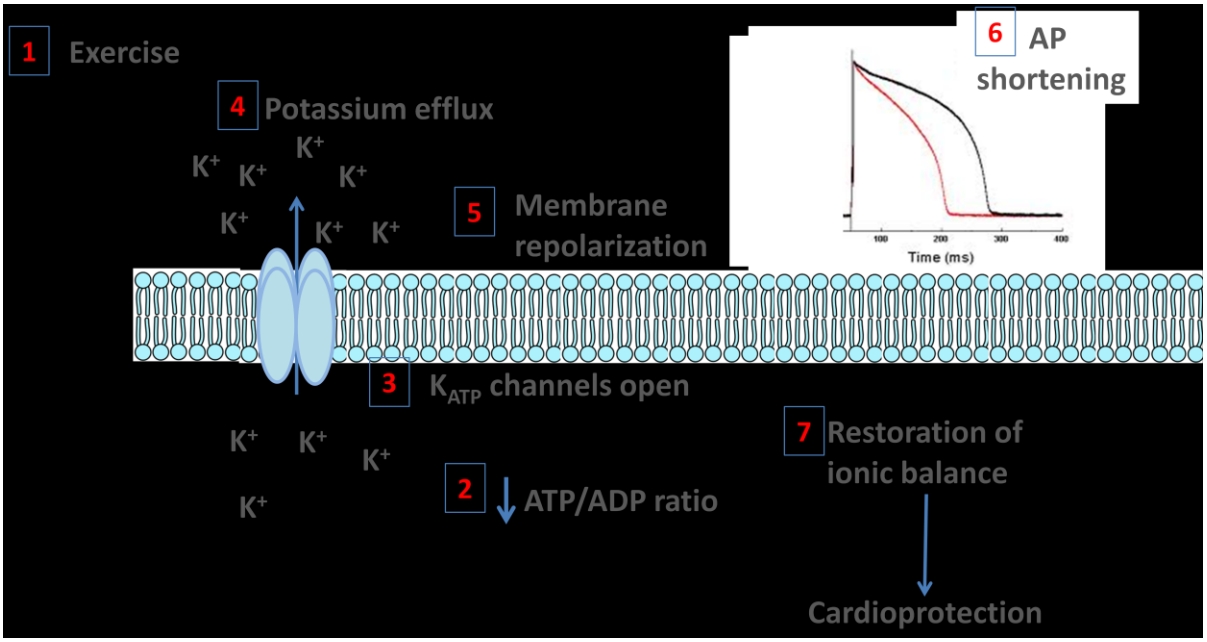
1 Exercise
4 Potassium efflux
K+
5 Membrane repolarization
6 AP shortening
Time (ms)
3 K_{ATP} channels open
2 ↓ ATP/ADP ratio
7 Restoration of ionic balance
Cardioprotection

Figure 1.7. The glycolytic pathway. Simplified illustration showing the steps of conversion of glucose to pyruvate. Enzymes marked in red have been shown to physically associate with K_{ATP} channels. GAPDH-Glyceraldehyde-3-phosphate dehydrogenase.

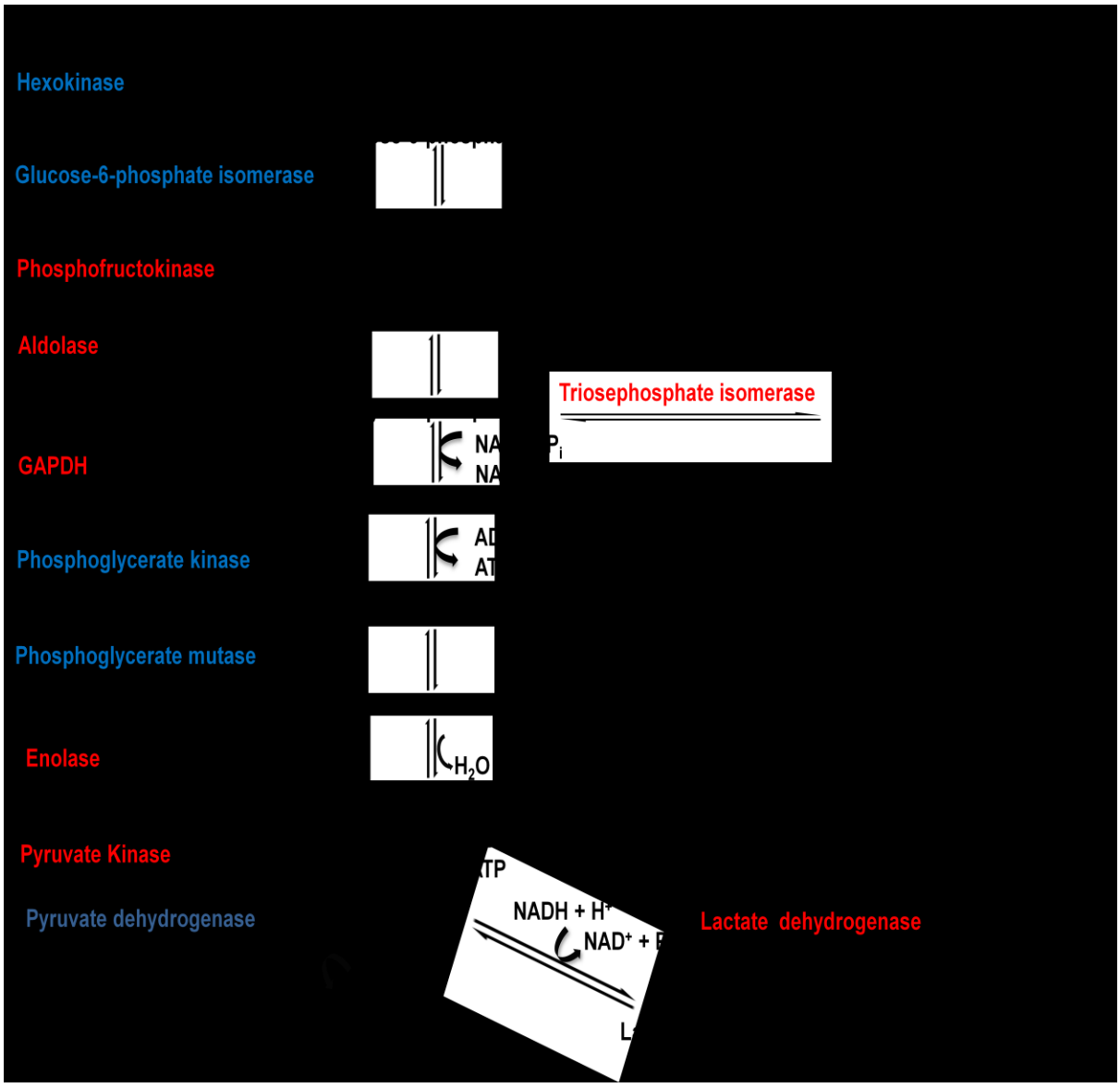
Hexokinase
Glucose-6-phosphate isomerase
Phosphofructokinase
Aldolase
Triosephosphate isomerase
GAPDH
Phosphoglycerate kinase
Phosphoglycerate mutase
Enolase
H_2O
Pyruvate Kinase
Pyruvate dehydrogenase
NADH + H^+
NAD^+
Lactate dehydrogenase

Figure 1.8. Proposed mechanism for K_{ATP} non-electrical cardioprotection. Activators of the Mg-ATPase activity possessed by the channel (possibly K_{ATP} channel openers (KCOs) or mechanical stress) cause hydrolysis of Mg-ATP into Mg-ADP. This process could be reversed due to the physical association of the channel to creatine kinase (CK). The increase in local Mg-ADP concentration causes adenylate kinase (AK) 1 which is also associated to the channel to convert Mg-ADP to ATP and AMP. AMP allosterically binds to AMPK which is bound to the channel and makes it more susceptible to phosphorylation by its upstream kinase LKB1. Activation of AMPK leads to promotion of ATP-producing pathways which are important in episodes of metabolic deficiency.

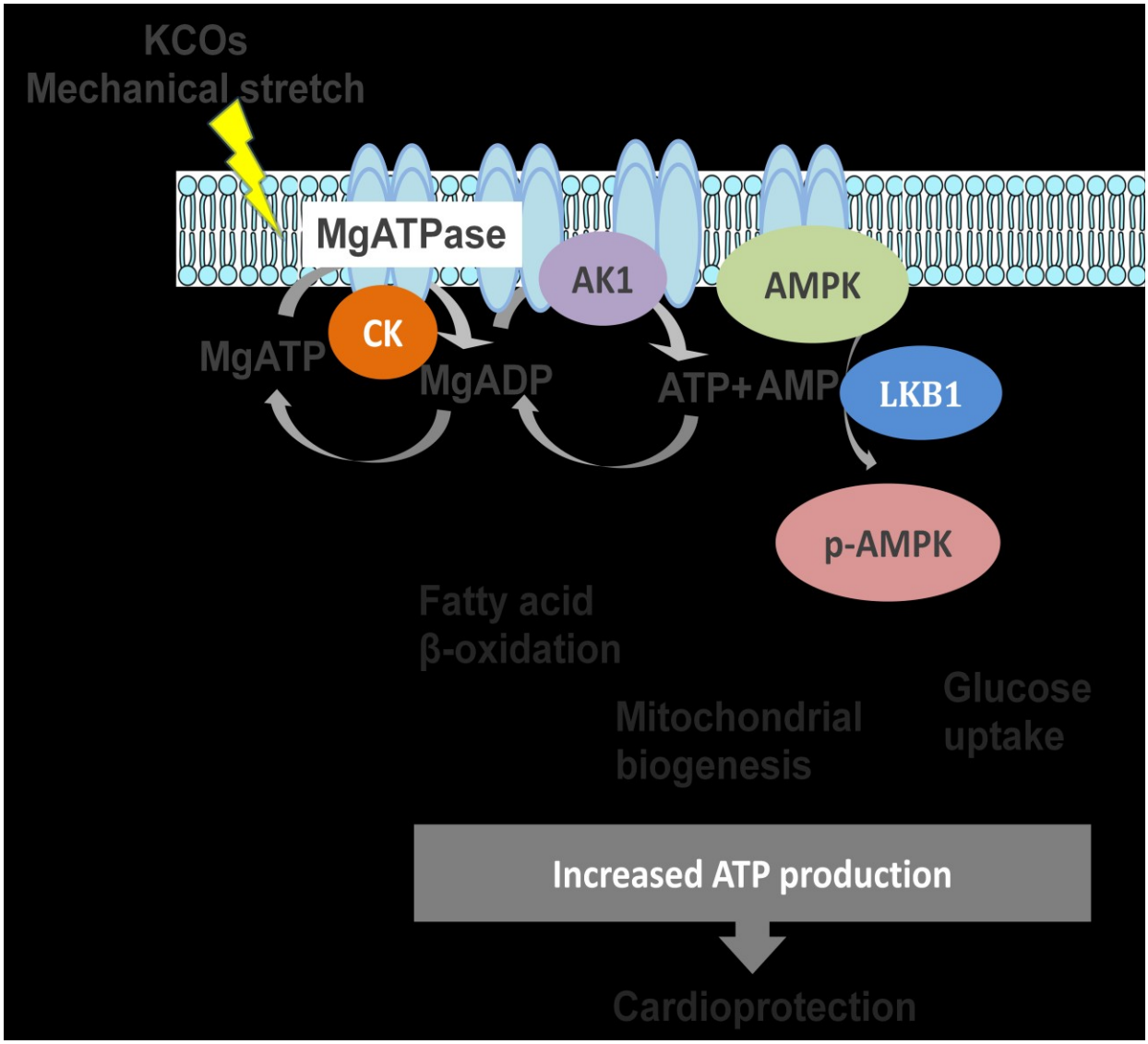
KCOs
Mechanical stretch
MgATPase
AK1
AMPK
CK
MgATP
MgADP
ATP+AMP
LKB1
p-AMPK
Fatty acid
β-oxidation
Mitochondrial
biogenesis
Glucose
uptake
Increased ATP production
Cardioprotection

Chapter 2
Materials and methods

2.1. Materials

Monoclonal and polyclonal antibodies for total AMP-activated protein kinase (AMPK) and phospho-AMPK (Thr172), total LKB1 and phospho-LKB1 (Ser428), voltage-dependent anion channel (VDAC), citrate synthase (CS), succinate dehydrogenase (SDH), PPAR-α, total Akt and phospho-Akt (Ser 473), total glycogen synthase kinase (GSK)-3β and phospho-GSK-3β (Ser 9), total mammalian target of rapamycin (mTOR) and phospho-mTOR (Ser2481), total P70S6K and phospho-P70S6K (Thr389), total acetyl CoA carboxylase (ACC) and phospho-ACC (Ser 79), total pyruvate dehydrogenase (PDH) and phospho-PDH(E1-α subunit Ser293), phospho- hormone sensitive lipase (HSL) (Ser563), acyl CoA synthetase long-chain family member 1 (ACSL1), fatty acid transport protein 1 (FATP1) and fatty acid translocase/Cluster of differentiation 36 (FAT/CD36) were purchased from Cell Signaling Technology (Danvers, Massachusetts). Primary antibodies to Kir6.2, tubulin, actin and peroxidase-conjugated goat anti-rabbit and goat anti-mouse secondary antibodies were purchased from Santa Cruz Biotechnology (Santa Cruz, California). Protease inhibitor cocktail was obtained from Bio Basic Inc. (Markham, Ontario). Phosphatase inhibitor cocktail was obtained from Calbiochem (Darmstadt, Germany). Immobilon-P PVDF transfer membranes (0.45μm) were purchased from Thermo Scientific. Carnation brand non-fat dry milk was purchased from the University of Alberta Biochemistry stores. Precision plus protein Kaleidoscope molecular weight marker, and Mini-Protean III gel electrophoresis system were purchased from Bio-Rad Laboratories, Inc. (Hercules, California). Amersham ECL Prime Western blotting detection system was purchased from GE Healthcare (Buckinghamshire, UK). Fuji medical X-ray films (Super RX) were from FUJIFILM Europe Gmbh (Düsseldorf,

Germany). BeF_2, Mg-ATP, Mg-ADP, Na^+ salts of GTP and GDP were purchased from Sigma-Aldrich (St. Louis, Missouri). All other chemicals were purchased from either Sigma-Aldrich or BioRad.. Free fatty acid free bovine serum albumin was purchased from Sigma-Aldrich (St. Louis, Missouri). Insulin (Novo Nordisk, Mississauga, Ontario) was obtained through the University of Alberta Hospital stores. For working heart metabolic measurements [U-14C]glucose, D-[5-3H]glucose and [9,10-^{3}H]palmitic acid were purchased from Perkin Elmer (Boston, Massachusetts). Ecolite™ and Cytoscint™ Aqueous Counting cintillation fluids were obtained from MP Biomedicals (Solon, Ohio). Hyamine hydroxide (1 M in methanol solution) was purchased from J.T. Baker (Phillipsburg, New Jersey). AG® 1-X4 anion exchange resin, chloride form, 4% crosslinkage, 200–400 dry mesh size was obtained from Bio-Rad Laboratories, Inc. (Hercules, California).

2.2. Methods

Cellular experiments

Neonatal rat ventricular cardiomyocytes isolation and culture

Isolation and culture of neonatal rat ventricular cardiomyocytes was performed as previously described by Kovacic et al. [355]. Briefly, hearts from two day old neonatal rat pups were removed and placed in ice-cold 1 × phosphate-buffered saline. After thorough rinsing, the ventricles were separated and cut into smaller pieces with scissors. The minced tissue was washed again in ice-cold phosphate-buffered saline solution and then placed in tissue culture flask containing ice-cold phosphate-buffered saline, (0.025%) DNAase (w/v), (0.10%) collagenase (w/v), and (0.05%) trypsin (w/v). The tissue was digested on rotator at 37 °C for 20 minutes. After digestion the tissue was centrifuged at 114 × *g* for 1 minute at 4 °C in 20 ml of DF20 media, 20% fetal bovine serum, and 50 μg/ml gentamicin. The supernatant was discarded, and the pellet was added to a buffer containing DNAase, collagenase and trypsin to be digested at 37 °C for 20 minutes. Following this digestion, the tissue was transferred into a falcon tube containing DF20 media and centrifuged at 114 × *g* for 1 minute at 4 °C. After repetition of this past step twice, the supernatants were pooled and centrifuged at 300 × *g* for 7 minutes at 4 °C. The pellet was then resuspended in 10 ml of plating media (DF20 media, 5% fetal bovine serum, 10% horse serum, 50 μg/ml gentamicin) and incubated at 37 °C for 60 minutes. After the incubation, the supernatant was placed in another tissue culture flask for 60 more minutes. After repetition of the previous steps again, the resulting pellet was resuspended in plating media. The cells were then plated on primeria dishes (Falcon) at a density of 1.8–2.0 × 10^6cells/plate.

Adult cardiomyocyte isolation

Adult C57Bl6 mice were heparinized then sacrificed with pentobarbital (60 mg/kg, i.p.) according to the University of Alberta Animal Policy and Welfare Committee and the Canadian Council on Animal Care (CCAC) Guidelines. The heart was rapidly removed, the aorta was cannulated on a Langendorff apparatus, and perfused retrogradely (at 37 °C, 70 cm H_2O pressure) through the coronary arteries was established. A Ca^{++}-containing solution was used (for 2-3 min) to rinse out remaining blood. This solution consisted of 121 mM NaCl, 5 mM KCl, 28 mM sodium acetate, 1 mM Na_2HPO_4, 1 mM Ca^{++}, 1 mM $MgCl_2$, 24 mM $NaHCO_3$, 5.5 mM glucose (equilibrated with 95% O_2-5% CO_2, giving a pH of 7.4). This was followed by a 5 min perfusion with the same solution containing only 5 M $CaCl_2$, and then by perfusion with a low Ca^{++} solution containing 0.02 mg/mg collagenase B and D (Roche, Basel, Switzerland), 0.01 mg/ml Type XIV protease, 20 mM taurine, and 40 μM Ca^{++}, for 4-6 min. The left ventricle was then removed cut into smaller pieces and placed in separate Falcon tubes which contained the low Ca^{++} solution, with 0.2 mg/ml collagenase B and D, 0.1 mg/ml Type XIV protease, 20 mM taurine, 10 mg ml/l albumin and 100 μM Ca^{++}. The tubes were agitated in a shaker bath at 37 °C. Aliquots of the supernatant which contained single myocytes were removed sequentially and placed into a storage solution (a low Ca^{++} solution with no enzymes, 20 mm taurine, 10 mg ml-' albumin and 0.1 mM $CaCl_2$). Enzymatic digestion proceeded for 15-60 min, at 37 ºC. Quiescent, rod-shaped cells with regular cross-striations were selected for cell shortening, mechanical stress or electrophysiology experiments[356].

Adult murine and human islet culture

Mouse islets were isolated by hand-picking after collagenase digestion of the pancreas as described [357], and maintained overnight in RPMI-640 supplemented with 10% (wt/vol.) FBS, 100 U/ml penicillin–streptomycin and 11 mmol/l glucose. Human islets from adult donors were isolated by The Alberta Diabetes Institute IsletCore or the Clinical Islet Laboratory at the University of Alberta as previously described[358]. Islets were cultured in low glucose (1 g/L) DMEM with L-glutamine, 110-mg/L sodium pyruvate, 10% fetal bovine serum, and 100-U/mL penicillin/streptomycin (Invitrogen, Carlsbad, California) at 37°C and 5% CO_2 for 24–48 hours, handpicked and incubated with the appropriate drug according to the experiment conducted. This was followed by processing of the islets for immunoblotting.

Cardiomyocte shortening

To measure differences in contractility between isolated wild-type and kir6.2-/- adult cardiomyocytes, freshly isolated cardiomyocytes were superfused in a continuous manner at 1 ml/min with Krebs-Henseleit buffer containing 2 mM Ca^{++} and paced by field stimulation at 1 Hz. Single cardiomyocyte contractility was measured using a video edge detector (Crescent Electronics, Salt Lake City, UT), and data were recorded and analyzed using pClamp 8.0 software. Cell shortening was expressed as percentage of fractional shortening, i.e. [(resting myocyte length − contracted myocyte length)/resting myocyte length] × 100. All experiments were performed at 21°C[359].

tsA201 cells

tsA201 cells were selected for our functional expression experiments. They are SV40-transformed variant of the HEK293 human embryonic kidney cell line. Passage number 30 was our cut off for cell splitting, after which a new aliquot was used for reseeding and further cell culture. The cells were maintained in Dulbecco's modified Eagle's medium supplemented with 10 mM glucose, 2 mM L-glutamine, 10% fetal calf serum and 0.1% penicillin/streptomycin. The flasks containing the cells were kept in an incubator at 37°C with 10% CO_2.

Plasmid transfection

Human and rabbit Kir6.2, SUR1 and SUR2A subunit clones were kindly provided by Dr. J. Bryan (Pacific Northwest Diabetes Research Institute, Seattle, WA). As previously indicated, we used tsA201 cells in functional expression. Transfection of the different plasmids was done using the calcium phosphate precipitation technique[360]. All mutants used in this thesis were generated using site-directed mutagenesis (QuickChange, Stratagene) and subsequently confirmed by sequence analysis.

Electrophysiological recordings

Transfected cells were identified by co-expression of a green fluorescent protein plasmid (Life Technologies, Gaithersburg, MD). Macroscopic K_{ATP} channel currents were recorded (pCLAMP 10.2, Axon Instruments) 48-72 hours after transfection, using the excised inside-out patch-clamp technique as described previously[361] . Pipettes were back-filled with solution containing the following components: 134 mmol/l KCl, 10 mmol/l HEPES, 1.4 mmol/l $MgCl_2$, 1 mmol/l EGTA, 6 mmol/l KOH, and 10 mmol/l glucose. The

pH of the pipette solution was adjusted to 7.4 with KOH. Rupture of membrane patches from transfected cells were performed in the bath solution containing: 140 mmol/l NaCl, 10 mmol/l HEPES, 1 mmol/l $CaCl_2$, 1.4 mmol/l $MgCl_2$, 5 mmol/l KCl and 10 mmol/l glucose. The pH of the bath solution was adjusted to 7.4 with NaOH. drugs indicated in the context, were directly applied to the cytosolic side of the cell membrane patches using a rapid exchange multi-input perfusion pipette.

Mg-ATPase activity assay

Four 681-bp long fragments of NBD2 (encoding amino acids1301–1528), containing either wild-type SUR1 (Ser1369), wild-type SUR2A (Lys1337) or the mutants SUR1 (Lys1369) and SUR2A (Ser1337) were sub-cloned into pGEX-4T-1 GST fusion protein expression vectors. The recombinant plasmids were sequenced and then transformed into BL21 (DE3) cells for protein expression. The GST–NBD2 fusion proteins were detected with a monoclonal anti-GST-tag antibody (1:5000 dilution, Santa Cruz Biotechnology). Following purification, proteins (50 μg) were incubated at 40 ◦C for 30 min followed by 1 h incubation at 4◦C to allow homogeneous dimerization ofNBD2 monomers. All experiments were performed in an ATPase activity buffer at 37 ◦C using ADP-free ATP (ATP-Gold DiscoverX) as a substrate. Mg-ATPase activities of NBD2 dimers were determined by monitoring ADP formation via coupling to production of the fluorescent product resorufin (ADP Quest, DiscoverX). Resorufin formation was monitored continuously (λex = 560 nm, λem = 591 nm) in black 96-well plates in a SPECTRAmax Gemini XPS microplate spectrofluorometer (Molecular Devices). Initial rates of resorufin formation were plotted compared with ATP concentration and data were fitted to a rectangular hyperbola with the Michaelis–Menten equation (GraphPad Prism 6.0f) to obtain *V*max and *K*M values[362].

Animal experiments

- Ethics approval

All animals used for my research were included in our animal study protocol that was approved by the University of Alberta Health Sciences Animal Policy and Welfare Committee. Animal care followed the guidelines of the Canadian Council on Animal Care.

- Kir6.2-/- mice

The kir6.2-/- mice were a kind gift from Dr. Susumo Seino who initially generated the mice in the following manner: The Kir6.2 gene was cloned using its cDNA probe from a 129/Sv mouse genomic DNA library (Stratagene). A targeting vector was constructed by inserting the neomycin-resistance gene at the *Xho*I site in Kir6.2 and the herpes simplex virus thymidine kinase gene was inserted downstream. The targeting vector was introduced into E14 embryonic stem (ES) cells by electroporation and after neomycin selection, the knockout stem cells were inserted into blastocysts and subsequently implanted into the uterus of a female C57Bl6 mouse. The heterozygous offspring produced is interbred for at least 6 generations. In this thesis, experiments utilize age -matched male C57Bl6 wild-type and their kir6.2-/- littermates that were backcrossed 6 generations to the C57Bl6 background for comparison[363]. DNA for genotyping was extracted from ear-punches utilizing the DNeasy Blood & Tissue Kit (Qiagen)/Genomic DNA Mini Kit (Geneaid). Genotyping was performed via PCR and gel-electrophoresis (2% TAE-agarosegels) using the following set of primers: Forward: TAG GCC AAG CCA GTG TAG TG, Reverse-Knockout: GGA GGA GTA GAA GTG GCG C, Reverse-wild-type: GCC CTG CTC TCG AAT GTT CT.

For homozygote Kir6.2 KO mice, a PCR band of 386bp was amplified, for Kir6.2 WT, PCR product was 222bp, for heterozygote mice both PCR amplificates were derived from genomic DNA (See figure below). PCR was carried out in 25µl reactions in a PCR thermocycler using about 100 ng of genomic DNA as template, 125pmol each primer, DreamTaq Green PCR Master Mix. PCR conditions: 95°C for 3min, followed by 30 cycles: 95°C for 30s, 55°C for 30s, 72°C for 60s, final extension 72°C for 7min.

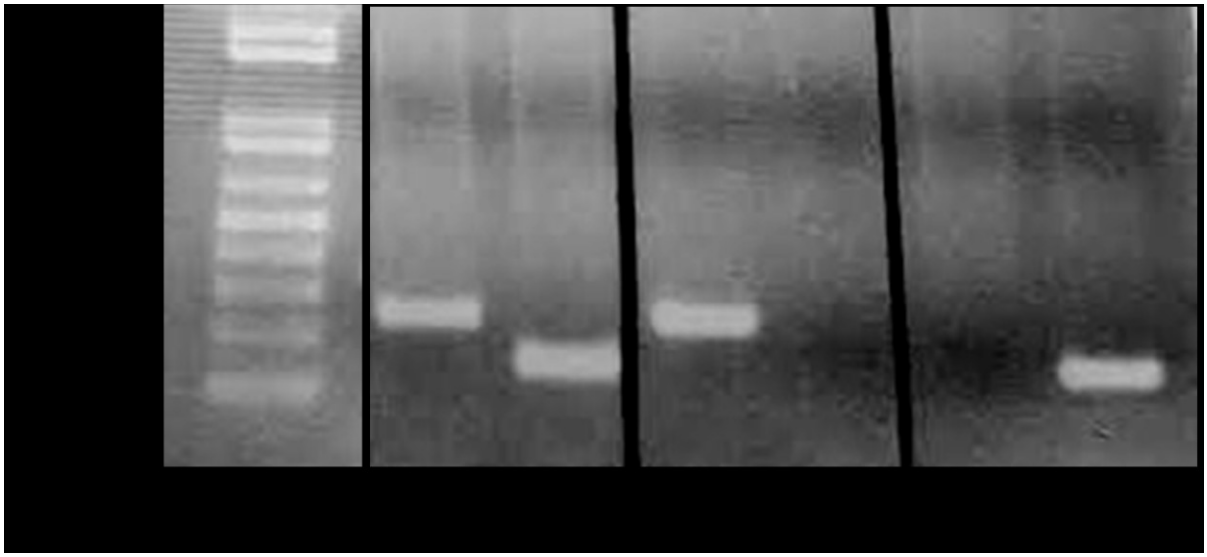

- Langendorff mouse heart perfusion

Briefly, mice were anaesthetized using 60 mg/kg sodium pentobarbital injected intraperitoneally, with 100 U of heparin. After mid-sternal incision, the heart was removed and placed in (37 ± 1 °C), modified Tyrode solution of the following composition: 128.2 mM NaCl, 4.7 mM KCl, 1.19 NaH_2PO_4, 1.05 mM $MgCl_2$, 1.3 mM $CaCl_2$, 20 mM $NaHCO_3$, and 11.1 mM glucose (pH 7.4). While bathed in the same solution, lung, thymus, and fat tissue were dissected and removed. A short section of aorta was attached to a 21-gauge cannula. After cannulation, the heart was retrogradely perfused with modified Krebs-Henseleit

solution passed through the 5-µm filter (Millipore, Billerica) and warmed (37 °C) using a water jacket and circulator (ThermoNESLAB EX7, Newtown)[364]. Perfusion was performed for 30 minutes using a peristaltic pump and heart ventricles were clamp-frozen and used for biochemical analysis.

- Isolated working mouse heart perfusion

Hearts were cannulated for isolated working mode perfusion as previously described by Lopaschuk et al.[365]. Mice were anesthetized using pentobarbital sodium and each heart was excised and placed in ice-cold Krebs-Henseleit solution followed by immediate aortic cannulation and perfusion in Langendorff mode for 10 minutes. Hearts were then switched to working mode by opening the left atrial and the aortic outflow lines and clamping off the aortic inflow line. The hearts were perfused at 37 °C at a constant workload of 11.5 mmHg left atrial preload and 80 mmHg aortic afterload . All hearts were paced at 500 beats/min. The perfusate consisted of a modified Krebs-Henseleit solution containing 118 mM NaCl, 4.7 mM KCl, 1.2 mM KH_2PO_4, 1.2 mM $MgSO_4$, 25 mM $NaHCO_3$, 2.5 mM free Ca^{++} along with 100mU/l insulin and both 1.2 mM palmitate prebound to 3% BSA and 11 mM glucose as energy substrates. The perfusate was gassed with Carbogen to maintain constant pH and O_2 saturation. At the end of each perfusion protocol, hearts were rapidly snap frozen in liquid nitrogen. Frozen tissues were powdered at the temperature of liquid nitrogen, and the resulting powders were stored at -80 ºC for future use or processed immediately for Western blotting.

- Measurement of left ventricular function

While the heart was being perfused in working mode, systolic and diastolic aortic pressures were measured using a Gould P21 pressure transducer attached to the aortic outflow line. An ultrasonic flow probes placed in the left atrial inflow line was used to measure cardiac output (ml/min) and other flow probe in the aortic outflow line was used to measure aortic flow (ml/min). Coronary flow was calculated as: cardiac output - aortic flow. Left ventricular (LV) work (Joules/min/g dry wt) was used as an index of mechanical function and was calculated as: cardiac output x LV developed pressure (systolic pressure – preload pressure) and then normalized to the heart dry weight.

- Measurement of the rates of glycolysis, glucose and fatty acid oxidation

Steady state rates of glycolysis and glucose oxidation were measured by perfusing hearts with [5-^{3}H/U-^{14}C] glucose while rates of palmitate oxidation were measured by perfusing hearts with [9,10-^{3}H]palmitate as previously described by Barr et al.[366]. The radiolabelled substrates were included in the circulating perfusate. Two separate series of experiments were performed for glycolysis and fatty acid and glucose oxidation, one with [5-^{3}H/U-^{14}C]glucose and the other with [U-^{14}C]glucose and [9,10-^{3}H]palmitate. Rates of glycolysis were determined by the quantitative determination of $^{3}H_2O$ liberated from [5-^{3}H]glucose at the enolase step of glycolysis. $^{3}H_2O$ was separated from the perfusate by passing 100 μL of perfusate samples through AG® 1-X 4 anion exchange resin columns as described previously[367]. This was followed by washing the columns with water and the eluted water was collected in scintillation vials and scintillation fluid was added (Ecolite, ICN) followed by counting the vials in a liquid scintillation counter. Rates of glucose oxidation were determined by the quantitative determination of $^{14}CO_2$ liberated from [^{14}C]glucose at

the level of pyruvate dehydrogenase and in the TCA cycle. Both $^{14}CO_2$ gas released (captured in a hyamine hydroxide trap) as well as [^{14}C]bicarbonate retained in the perfusate (measured through reaction with 9N H_2SO_4) were accounted for. Rates of palmitate oxidation were measured by the quantitative measurement of $3H_2O$ liberated from [9,10-^{3}H]palmitate. Liberated ^3H_2O was separated from the perfusate by a vapor transfer method as described by Folmes et al.[368].

- Calculation of metabolically-derived ATP production

Full oxidation of glucose yields 32 ATP molecules per molecule of glucose. Glycolysis utilizes 2 ATP molecules to produce 4, therefore the net yield from glycolysis is 2 ATP molecules. Pyruvate dehydrogenation produces 1 molecule of $NADH_2$, which produces 2.5 ATP molecules and a single full turn of acetyl-CoA through the TCA cycle produces 9.75 molecules of $NADH_2$, which produces a total of 12.25 ATP per molecule of pyruvate. On the other hand, palmitate oxidation yields 105 ATP molecules. Fatty acid oxidation initially consumes 2 high energy phosphates from ATP per molecule of fatty acid in the process of fatty acid activation. In the fatty acid oxidation of the palmitate, seven full turns of the β-fatty acid oxidation spiral produces 7 molecules of $NADH_2$ relating to 17.5 molecules of ATP, and 7 molecules of FADH relating to 10.5 molecules of ATP. Palmitate derived 8 acetyl-CoA *via* TCA cycle will produce additional 78 molecules of ATP as 9.75 ATP is produced per acetyl-CoA per one turn of TCA cycle. This results in the overall yield of 105 ATP per 1 palmitate molecule[369].

- Determination of cardiac glycogen content

Histology

Ventricles were harvested from kir6.2+/+ and kir6.2-/- mice and immediately fixed using buffered aqueous zinc formalin (Z-fix) for 6 hours. The ventricles were then placed in small perforated cassettes and infiltrated with molten paraffin wax then allowed to set as the paraffin solidified. Each wax "block" containing the embedded ventricle sliced using an automated rotary microtome into 3-5 μm slices and placed on slides. Each slide was then stained with Periodic Acid Schiff (PAS). The Periodic Acid oxidizes the vicinal diols in glycogen generating a pair of aldehydes at the two free tips of each broken monosaccharide ring. These aldehydes then react with the Schiff reagent to give a purple-magenta color. Micrographs were taken by an Olympus Q color 3 digital camera with an Olympus IX51 inverted microscope and glycogen particles were counted using ImageJ software (National Institutes of Health, Bethesda, MD) (n= 15 images/heart).

Colorimetric assay

Total ventricular glycogen was also assessed colourimetrically using a commercially available kit (AbCam, Cambridge, UK). Briefly, 10 mg of cardiac ventricles from each heart from both kir6.2+/+ and kir6.2-/- groups were washed in ice-cold PBS. The tissues were resuspended in H_2O, boiled to deactivate enzymes then centrifuged. The supernatant was used in the assay as instructed in the manufacturer's manual. The principle of the assay is that glucoamylase in the kit hydrolyzes tissue glycogen to glucose which is then oxidized to produce a product that reacts with the OxiRed probe provided in the kit to generate color that could be measured at 570 nm using a spectrophotometric microplate reader.

- Transmission electron microscopy to determine mitochondrial density

Ventricles were harvested from 2-3 month old kir6.2+/+ and kir6.2-/- mice (n=6), rapidly immersed in a fixing buffer (2.5% glutaraldehyde, 1% parafermaldehyde in PBS, Bio-Rad, Mississauga, ON) and incubated at 4°C overnight. The ventricles were then washed 3 times in 0.1 M HEPES and subsequently suspended in 1.0% osmium tetroxide for 4 h. Thereafter, the ventricles were washed 3 times in 100 mM HEPES and suspended in 2% uranyl acetate for 3 h, washed 3 times in 0.1% HEPES, and dehydrated by incubating in 25, 50, 75, 95 and finally twice in 100% ethanol. Tissue was infiltrated with resin by suspending in 50/50 ethanol/resin for 4 hours on a rotator, and later suspended in 100% resin for 4 h on a rotator. Tissue was then placed in an embedding capsule containing 100% resin, and incubated overnight in an oven set at 60°C to polymerize. Ventricles were then sliced into 100 nm slices and placed onto 200 mesh formvar–carbon copper grids and then stained with 2% uranyl acetate and Reynold's lead citrate. Each grid consisted of at least 4 sections. At least 20 images were obtained per group in a randomized systematic order at including 12 at 64,000×, 10,500×, 5800× magnifications. Samples were viewed on a Hitachi H-7650 transmission electron microscope (Tokyo, Japan). Mitochondrial density and size were counted using Zen software (Carl Zeiss MicroImaging, Thornwood, NY, USA) as previously described by Holloway et al.[370].

Immunoblotting

- Heart tissue processing

At the end of both Langendorff and working heart perfusions, the hearts were immediately flash frozen in liquid nitrogen. Cryogenic tissue grinding using a mortar and pestle was used to pulverize the each sample. This was followed by homogenization for 30

seconds using a Polytron homogenizer while in ice-cold RIPA homogenization buffer containing 20 mM Tris.HCl, 50 mM NaCl, 50 mM NaF, 5 mM sodium pyrophosphate, 250 mM sucrose, 1 mM DTT and freshly added protease and phosphatase inhibitors (Calbiochem, San Diego, USA). The homogenized tissue was then centrifuged at 1000 g for 15 minutes to separate the supernatant homogenate. 10 µl of each sample supernatant was set aside to be used for bicinchoninic acid protein assay. Aliquots of the supernatant were stored at -80 ºC for further biochemical analysis.

- Bicinchoninic acid protein assay

To determine the protein content of each sample, I used a commercially available bicinchoninic acid protein assay kit (Pierce, Thermo-Fisher Scientific, Waltham, USA). This colorimetric assay depends on the reduction of Cu^{++} to Cu^{+} by protein in an alkaline medium , also known as the biuret reaction. Two molecules of bicinchoninic acid selectively chelate one Cu+ ion generating a purple-colored product which can be measured at 562nm using a microplate reader. 10 µl of each sample supernatant was diluted with 90 µl RIPA buffer, 10 µl of this mixture was pipetted in triplicates in a 96 well microplate and allowed to react with 200 µl of the $CuSO_4$/bicinchoninic acid mixture for 30 minutes at 37 ºC and protein concentration values were determined by comparison to a standard curve.

- Sample preparation for immunoblotting

After determination of protein content, the sample supernatants were diluted with double distilled H_2O to yield either 8 µg, 15 µg, 20 µg or 25 µg of total protein per sample, depending on the experiment and protein under investigation. One part reducing SDS-sample buffer containing 0.375M Tris pH 6.8, 12% SDS, 60% glycerol, 0.6M DTT, 0.06%

bromophenol blue, was then added to 6 parts of each diluted sample, mixed well and then boiled for 5 minutes at 95ºC. Following sample boiling, each tube was centrifuged at a low speed and either stored at -20 ºC for future use or loaded onto an SDS-PAGE gel immediately.

- Sodium dodecyl- polyacrylamide gel electrophoresis (SDS-PAGE)

Cardiac homogenates prepared as described above were resolved according to size using sodium dodecyl- polyacrylamide gel electrophoresis, known as SDS-PAGE at room temperature under denaturing conditions. An equal volume of each sample was loaded on either 6%, 8%, 10% or 15% gels according to the weight of the protein under investigation. A prestained protein marker was loaded on each gel, in this case I used 10 µl Bio-Rad's precision plus Kaleidoscope marker. The running buffer used was composed of 250 mM Tris, 1.92 M glycine and 1% SDS at pH 8.3. The gel was run at constant voltage (100 V) for 1 hour 30 minutes or until the blue dye in the sample buffer reached the bottom of the gel.

- Protein transfer onto polyvinylidene fluoride

After completion of the SDS-PAGE run, the separating gel was incubated in cold transfer buffer consisting of 25 mM Tris, 0192 M glycine, and 20% methanol for 10 minutes. Meanwhile, a polyvinylidene fluoride (Immobilon-P, Millipore) membrane was cut to the appropriate size and equilibrated in methanol for 5 minutes at room temperature. The gel was placed against the equilibrated membrane and sandwiched between two thick filter papers while making sure that there were no air bubbles between the gel and the membrane. The transfer "sandwich" was placed in a Tran-Blot module then into the Mini-Protean 3 (Bio-Rad) cell apparatus which contained an ice pack. The transfer was run at a constant voltage

of 100V for 1 hour at room temperature or 30 V overnight in the 4 ºC cold room. Upon completion of the run, the membrane was stained using the reversible Ponceau stain to indicate whether the proteins have been efficiently transferred. The stain was then thoroughly washed off with TBS.

- Western blot procedure

PVDF membranes were then blocked for 1 hour at room temperature in 20 ml 5% (w/v) milk dissolved in Tris-buffered saline containing 0.1% (v/v) Tween-20 (TBST). This was followed by incubation at 4 ºC overnight with a primary antibody diluted in 5% (w/v) BSA in TBST. After extensive washing in TTBS, membranes were incubated with a peroxidase-conjugated goat anti-rabbit secondary antibody (1:2000 dilution) for 1 hour at room temperature. After further washing in TTBS, antibodies were visualized using the Amersham ECL Prime Western blotting detection system. X-ray films (Fujifilm, Tokyo, Japan) were scanned using the Brother DCP-7030 scanner and densitometric analysis of protein bands was performed using ImageJ software (National Institute of Health, Bethesda, Maryland).

Human atrial appendages

Appendages were isolated from the right atria of patients undergoing coronary artery bypass graft surgery at the Mazankowski Alberta Heart Institute and the University of Alberta Hospital on the day of the operation. Appendages were transported in ice cold phosphate buffered saline between the operating room and the laboratory. Each appendage was weighed and cut into two (1 cm x 0.5 cm) pieces serving as test and control appendage for each patient. The appendage halves were then each incubated for one hour in Carbogen

(95% CO_2-5% O_2)-gassed modified Krebs-Henseleit buffer containing: 118 mM NaCl, 4.7 mM KCl, 1.2 mM $MgSO_4$, 1.25 mM $CaCl_2$, 1.2 mM KH_2PO_4, 25 mM $NaHCO_3$ and 11 mM glucose. The appendages were incubated for 1 hour with a drug or vehicle according to the experiment and upon completion of the incubation, the appendages were washed in PBS three times, snap frozen in liquid nitrogen and processed for immunoblotting.

Statistical analyses

All data are represented as the mean SEM. Statistical analysis was performed using GraphPad Prism version 5.04 for Windows (GraphPad Software, San Diego California USA). The specific statistical test used is described in each chapter. Values of $P<0.05$ were considered significant.

Chapter 3
Genetic ablation of plasma membrane K_{ATP} channels alters the cardiac metabolic profile under basal aerobic conditions

Cardiac metabolic measurements were performed by Dr. Manoj Gandhi, isoproterenol working heart perfusions were performed by Grant Masson. Ventricular slides for histological analysis were prepared by the ADI Histology core. Cell shortening were performed by Beth Hunter. The author contributed to cardiomyocyte isolation and performed Langendorff heart perfusions, immunoblotting, electron microscopy, experimental design and statistical analysis.

A version of this chapter is currently being submitted to the *Journal of Molecular and Cellular Cardiology* - Genetic ablation of plasma membrane K_{ATP} channels alters the cardiac metabolic profile under basal aerobic conditions.

Nermeen Youssef, Manoj Gandhi, Beth Hunter, Vernon Dolisnky,Grant Mason, Jason Dyck, Alexander Clanachan, Peter Light.

August 2015

3.1. Introduction

Three decades ago, ATP-sensitive potassium (K_{ATP}) channels were discovered by Noma in cardiac tissue[2]. Classically they are known for their role in coupling cellular excitability to stress-induced upstream changes in metabolism, more precisely, changes in concentrations of nucleotides ATP and ADP which are regulators of channel activity[371]. For example, during physiological stress such as exercise or pathological stress as observed in a myocardial infarction, the concentration of ATP drops while ADP and AMP concentrations increase leading to K_{ATP} channel opening which results in potassium efflux out of the cardiomyocyte thereby shortening action potential duration[372,142]. In turn, this efflux of potassium ions eventually leads to expulsion of intracellular calcium, protecting the myocardium against its accumulation. Accumulation of calcium leads to hypercontraction, reduced relaxation of the contractile machinery and activation of Ca^{++}-dependent proteases, caspases, the apoptotic pathway and the necrotic pathway ultimately leading to cellular demise[182,286,287,289,373,374]. It is generally considered that K_{ATP} channels in the heart are predominantly closed under resting aerobic conditions[175]. Studies on Kir6.2-/- mice showed that the action potential duration and contractile function in wild-type and Kir6.2-/- hearts are similar[176]. Under basal resting conditions, genetic ablation of cardiac K_{ATP} channels does not appear to affect cardiac function in terms of heart rate, coronary flow and work load[176]. Therefore it is has been suggested that cardiac K_{ATP} channels play little or no role in regulating cardiac excitability in the basal aerobic state. However, previous studies have shown following ischemia-reperfusion (I/R), that mice lacking K_{ATP} channels exhibit poorer cardiac functional recovery and worse myocardial ischemic damage as evident by larger infarct sizes[182,375]. Additionally, cardioprotective mechanisms against I/R injury such as

ischemic preconditioning are lost upon pharmacological blockade as well as genetic ablation of K_{ATP} channels[376,216]. Similarly, protective pharmacological preconditioning of hearts using agents such as diazoxide which is a K_{ATP} channel opener is markedly reduced in the absence of K_{ATP} channels [377]. There is no denying that increased intracellular calcium accumulation in the absence of K_{ATP} channels is detrimental, and is a very plausible explanation for why cardiac function and tissue damage is worse post-I/R, but is it the only explanation? We ask this question because a growing body of literature demonstrates new K_{ATP} channel properties, mainly its possession of intrinsic catalytic Mg-ATPase activity[42,378,379] as well as the unexpected link of the channel to global metabolism.

In the heart, optimal metabolism is required to meet its constant high energy demands. Since the myocardium has limited energy stores, continuous uptake and oxidation of energy substrates; fatty acids, glucose and lactate, has to take place to maintain normal function. Most of the cardiac ATP is derived from fatty acid oxidation (60-80%), while the rest of the ATP requirements is supplied by carbohydrate and ketone body oxidation[246,380,381]. Perturbations in cardiac metabolism were shown to compromise mechanical functional recovery after a myocardial infarction[382]. Therefore, efficient energy substrate utilization and expenditure in the heart is key to function at rest and during stress conditions.

An interesting link of K_{ATP} channels to metabolism and energy expenditure has been highlighted by Alekseev et al. who have shown that upon feeding mice deficient in K_{ATP} a high fat diet, they remained lean compared to their wild type counterparts suggesting that the absence of the channel leads to global changes in metabolism[353]. The same group followed up on this finding with an elegant proteomic analysis revealing that over 60% of the proteins whose genomic expression was affected by the absence of K_{ATP} channels were proteins

involved in metabolism and bioenergetics[383]. In that regard, a central regulator of cellular metabolism and cardioprotection is 5'-AMP-activated protein kinase (AMPK). AMPK is activated upon increased metabolic demand signalled by the rise in intracellular AMP levels[384]. Activation of AMPK via phosphorylation by upstream kinases leads to subsequent activation of metabolic pathways that lead to ATP production such as glucose uptake and fatty acid oxidation while temporarily suspending ATP-consuming pathways such as protein synthesis[384]. Similar to K_{ATP} channels, AMPK activation is essential in ischemic preconditioning[385]. Interestingly, AMPK was also shown to physically associate to the Kir6.2 subunit of plasma membrane K_{ATP} channels[386]. Moreover, physical association of both adenylate kinase 1[49] and creatine kinase[387] which are important enzymes in the phosphotransfer cascade in the cell has been established. Moreover, glycolytic enzymes such as glyceraldehyde-3-phosphate dehydrogenase, aldolase, triose phosphate isomerase and pyruvate kinase have also previously been shown to bind physically to plasma membrane K_{ATP} channels[349,351].

Given evidence of alteration of the normal global metabolic profile upon genetic ablation of plasma membrane K_{ATP} channels and their physical association with various important metabolic enzymes, it is plausible that K_{ATP} channels may be part of a complex metabolome that is upstream of AMPK signalling. Loss of the integrity of this metabolome by removal of one of its components, K_{ATP} channels in this case, leads to disrupted downstream signalling and compromised myocardial stress-coping mechanisms, particularly efficient cardiac metabolism. In this study, we investigated whether cardiac metabolic changes occur in the absence of K_{ATP} channels under resting conditions setting the heart up for failure when subjected to stress. Our results demonstrate for the first time the direct effect

of the absence of plasma membrane K_{ATP} channels on cardiac metabolism. We also provide evidence that plasma membrane K_{ATP} channels, contrary to the current theory, may be capable of regulating AMPK signaling.

3.2. Methods

Experimental animals

All experiments were performed according to protocols approved by the University of Alberta Institutional Animal Care and Use Committee. Data was obtained from adult (11-20 weeks) male C57BL/6 Kir6.2+/+ and Kir6.2 -/- mice. The generation of Kir6.2-/- mice by targeted Kir6.2 gene disruption has been previously described in detail by Miki et al.[388] and were obtained from the Seino laboratory. Mice were housed on a 12-h light and 12-h dark cycle with ad libitum access to chow diet and water. Genotyping of the mice was performed as described on page 60 in Chapter 2.

Isolated heart preparations

Langendorff perfusions

Briefly, mice were anesthetized using 60 mg/kg 7pentobarbital, with 100 U of heparin. After mid-sternal incision, the heart was removed and placed in (37 ± 1 °C), modified Tyrode solution of the following composition: 128.2 mM NaCl, 4.7 mM KCl, 1.19 NaH_2PO_4, 1.05 mM $MgCl_2$, 1.3 mM $CaCl_2$, 20 mM $NaHCO_3$, and 11.1 mM glucose (pH = 7.35 ± 0.05). While bathed in the same solution, lung, thymus, and fat tissue were dissected and removed. A short section of aorta was attached to a 21-gauge cannula. After cannulation, the heart was retrogradely perfused with modified Krebs-Henseleit solution passed through the 5-μm filter (Millipore, Billerica) and warmed (37 °C) using a water jacket

and circulator (ThermoNESLAB EX7, Newtown). Perfusion was performed for 30 minutes using a peristaltic pump and heart ventricles were clamp-frozen and used for biochemical analysis.

Working heart perfusions

Mouse hearts were aerobically perfused in the working mode at a constant workload of 11.5 mmHg preload and 50 mmHg or 80 mmHg afterload with modified Krebs-Henseleit buffer containing 1.2 mmol/L palmitate prebound to 3% fat-free bovine serum albumin, 5 mmol/L glucose, and 100 μU/mL insulin as described previously[359,389]. Left-ventricular (LV) work (in J min^{-1} g dry wt^{-1}) was used as a measure of left ventricular mechanical function.

Cardiomyocyte isolation and cell shortening

Ventricular cardiomyocytes were isolated from adult Kir6.2+/+ and Kir6.2-/- mice as described previously[210]. For cell shortening studies, freshly isolated cardiomyocytes were continuously superfused at 1 ml/min with Krebs-Henseleit buffer containing 2 mmol/liter Ca^{2+} and electrically paced at 1 Hz by field stimulation. Single cardiomyocyte contractility was measured using a video edge detector (Crescent Electronics, Salt Lake City, UT), and data were recorded and analyzed using pClamp 8.0 software. Cell shortening was expressed as percentage of fractional shortening, i.e., [(resting myocyte length − contracted myocyte length)/resting myocyte length] × 100. Experiments were performed at 21°C.

Western blot analysis

Ventricular tissue was snap-frozen after Langendorff perfusion and homogenized by cryogenic grinding then diluted with RIPA homogenization buffer containing phosphatase and protease inhibitors. After a BCA protein assay (Pierce, Thermo Scientific, USA), equal

amounts of protein were resolved by SDS-PAGE, and were transferred onto a PVDF membrane. Target proteins were identified using the primary antibodies: anti-AMPK phospho and total, anti-ACC phospho and total, anti-LKB1 phospho and total, anti-Akt phospho and total, anti-GSK-3β phospho and total, phospho HSL, anti-PDH phosoho and total, FAT/CD36, FATP1, ATGL, ACSL1, VDAC, citrate synthase, succinate dehydrogenase, PPAR-α and PGC1-α. Tubulin was used as a loading control. Immunoblots were developed using the Amersham ECL Prime Western blotting detection reagents. Densitometric analysis was performed using ImageJ software (National Institutes of Health).

Metabolic measurements

Glycolysis, glucose oxidation and palmitate oxidation were measured as described previously[390]. Briefly, hearts were perfused with [5-^{3}H] or [U-^{14}C]glucose or [9,10-^{3}H]palmitate. Total $^{3}H_2O$ production and $^{14}CO_2$ production were determined at 10 min intervals during the perfusion. To measure the rates of glycolysis and palmitate oxidation, $^{3}H_2O$ in perfusate samples was separated from [^{3}H]glucose or [^{3}H]palmitate using the dowex method. Oxidation rates for glucose were determined by quantitative measurement of $^{14}CO_2$ production[390]. Rates of acetyl CoA, ATP, and proton production were calculated as described previously[391].

Glycogen content measurement

Cardiac ventricle samples were harvested from Kir6.2+/+ and Kir6.2-/- mice, immediately fixed using Z-fix, sliced and then stained with periodic acid Schiff (PAS). Micrographs were taken using an Olympus Q color 3 digital camera with an Olympus IX51 inverted microscope and glycogen particles were counted using ImageJ software (National

Institutes of Health, Bethesda, MD) (n= 15 images/heart). Colourimetric measurement of glycogen content in both hearts was performed using a commercially available glycogen assay kit (AbCam, Cambridge, UK) as per manufacturers' instructions.

Transmission Electron Microscopy

Heart ventricles were harvested from 2 month old Kir6.2+/+ and Kir6.2-/- mice and immediately fixed in PBS with 2.5% gluteraldehyde. The tissue was then postfixed in 1% osmium tetroxide for 1 h at 4 °C, rinsed, dehydrated in a graded ethanol series, and embedded in EMbed-812. Embedded tissue was polymerized then sectioned and stained with 1% uranyl acetate, followed by lead citrate. Tissue sections were then photographed with Hitachi H-7650 transmission electron microscope. Mitochondria were counted and their length was measured using Zen software (Carl Zeiss MicroImaging, Thornwood, NY, USA).

Statistical analyses

Results are expressed as means ± SEM of *n* observations. The significance of the differences was estimated by the unpaired Student's *t*-test and One-way analysis of variance. Significance between groups was determined using the Bonferroni posthoc test. Differences were considered statistically significant when $p < 0.05$.

3.3. Results

Higher fatty acid oxidation levels and suppressed glycolysis in Kir6.2 -/- mice

In order to investigate if the cardiac metabolic profile was changed under resting aerobic conditions as a result of the absence of cardiac plasma membrane K_{ATP} channels compared to that of Kir6.2+/+ hearts, we measured fatty acid, glucose oxidation rates and glycolysis by perfusing [U-^{14}C/^{3}H]glucose and [9,10-^{3}H]palmitate into a working heart

system. Our metabolic measurements clearly demonstrate that in Kir6.2-/- hearts, the rate of glycolysis is 45% lower (Figure 3.1.A), fatty acid oxidation is 102% higher (Figure 3.1.C) than in Kir6.2+/+ hearts. Since we observed a markedly higher rate of fatty acid oxidation, we expected to see a lower rate of glucose oxidation, however, the rate of glucose oxidation was not changed in response to enhanced fatty acid oxidation (Figure 3.1.B). Similarly, ATP derived from fatty acid oxidation was higher in Kir6.2-/- hearts compared to Kir6.2+/+ (Figure 3.2.C and 3.2.D). Proton production was approximately 42% less in Kir6.2-/- hearts (Figure 3.2.A). Acetyl CoA production was approximately 55% higher in Kir6.2-/- compared to Kir6.2+/+ as well (Figure 3.2.B).

Similar cardiac function on both single cell and whole heart level

To examine whether differences in cardiac metabolism observed in the previous experiment affected cardiac mechanical function in Kir6.2+/+ and Kir6.2-/- hearts, we chose to measure fractional shortening in isolated cardiomyocytes from both groups to test if contractility was affected on a single cell level. Our results show that there were no differences between both groups on single cardiomyocyte contractility (Figure 3.3.A). At the whole organ level, coronary flow (Figure 3.4.A) and left ventricular work (Figure 3.4.B) were measured in Kir6.2+/+ and Kir6.2-/- hearts perfused in working mode. Similarly, no significant differences were seen between both groups. Cardiac efficiency calculated as LV work/acetyl CoA (Figure 3.4.C) or LV work/ATP (Figure 3.4.D) was slightly but not significantly lower in Kir6.2-/-.

Basal AMPK activation levels are higher in Kir6.2-/- hearts

Since physical interaction between AMPK and the K_{ATP} channel has been demonstrated previously[386], we investigated whether basal AMPK activity is affected by the absence of the channel. Changes in AMPK activity lead to changes in cardiac metabolism as previously described. To detect changes in AMPK activity, we used Western blotting to probe for differences in phosphorylated protein expression. Our data show that phospho-AMPK normalized to total-AMPK in mice deficient in Kir6.2 subunit is significantly higher compared to their wild-type counterparts perfused in Langendorff mode (*, p= 0.0197) (Figure 3.5.A). Similarly, the upstream activator of AMPK, LKB1, was phosphorylated to a greater extent in Kir6.2-/- hearts compared to Kir6.2+/+ (Figure 3.5.B).

AMPK activation is disrupted during stress in Kir6.2-/- hearts

Since we have established that AMPK signalling is elevated under basal conditions, we decided to test whether AMPK is also changed in Kir6.2-/- hearts in response to stress. Considering that activation of AMPK through β-agonist stimulation has been previously established[75], we used 100 nM isoproterenol (Iso) due to its positive inotropic and chronotropic effects as our stressor to be infused through hearts from Kir6.2+/+ and Kir6.2-/- hearts while they were being perfused in working mode. As expected, phosphorylation of AMPK was significantly increased upon perfusion of Iso in Kir6.2+/+ hearts, however a similar activation was not observed in Kir6.2-/- hearts (Figure 3.5.C). Additionally, a similar uncoupling of AMPK signalling was observed upon blotting for phosphorylation of acetyl CoA carboxylase (ACC) which is downstream of AMPK activation (Figure 3.5.D).

Fatty acid metabolism markers are increased in Kir6.2-/- hearts

Since AMPK was more activated in Kir6.2-/- mice and fatty acid oxidation was almost doubled, we decided to look at fatty acid metabolism markers that are downstream of AMPK activation. Expression of Adipose triglyceride lipase (ATGL) which catalyzes the rate limiting hydrolysis step of triglycerides in the triacylglycerol lipolysis cascade was not significantly increased (Figure 3.6.A). Acyl-CoA synthetase long-chain family member 1 (ACSL1) which leads to acylation of fatty acids, the step preceding their oxidation, was higher (*, p=0.0142). in hearts lacking K_{ATP} channels (Figure 3.6.B). PPAR-α which is a transcription factor that regulates fatty acid metabolism was significantly higher (*, p=0.0292) in Kir6.2-/- hearts (Figure 3.6.F). To examine whether fatty acid transport markers are increased in Kir6.2-/- hearts, we measured FAT/CD36 that upon AMPK activation is expressed more densely on the plasma membrane[392]. FAT/CD36 expression was significantly higher (*, p=0.0145) in Kir6.2-/- compared to Kir6.2+/+ hearts (Figure 3.6.C). We also measured the expression of fatty acid transport protein (FATP1), which appeared to be significantly lower (*, p=0.0291) in Kir6.2-/- hearts. Phosphorylation of hormone sensitive lipase (HSL) was also higher (*, p=0.0295) in Kir6.2-/- hearts. (Figure 3.6.E)

Higher basal Akt activation and glycogen deposition in Kir6.2-/- hearts

Since we observed suppressed glycolysis, we investigated whether this was due to decreased glycogen stores or increased glycogen. Basal phospho-Akt levels were significantly higher (*, p=0.0102) in Kir6.2-/- ventricular homogenates as measured by Western blotting (Figure 3.7.A). The downstream target of Akt, GSK-3β, was more phosphorylated at Ser-9 (***, p=0.0007) which inhibits its activity in Kir6.2-/- hearts as well

leading to increased glycogen synthesis (Figure 3.7.B). We used both histology and biochemical analysis to measure glycogen content in Kir6.2+/+ and Kir6.2-/- ventricular tissue. Ventricular slices stained with Periodic acid-Schiff stain, which stains glycogen particles purple (Figure 3.7.C), showed a higher number of glycogen particles in Kir6.2-/- hearts (***, p=0.0004) (Figure 3.7.D). Colourimetric analysis of glycogen content in naive hearts from Kir6.2+/+ and Kir6.2-/- also confirms higher glycogen content in the absence of the channel. (*, p=0.0485) (Figure 3.7.E). Since pyruvate dehydrogenase activity is an important determinant of glycolysis, we measured its phosphorylation which indicates its inhibition in Kir6.2+/+ and Kir6.2-/- hearts. Our data show that phosphorylation of PDH is slightly higher in Kir6.2-/- mouse hearts compared to Kir6.2+/+ hearts (2.220 ± 0.7997 and 1.649 ± 0.1634 respectively) however statistical significance was not reached (n=3, p>0.05) (Figure 3.7.F).

Mitochondrial density

The transcriptional coactivator PGC-1α plays a key role in mitochondrial biogenesis and is downstream of AMPK activation[393]. Since our basal AMPK activation was higher in Kir6.2-/- hearts we measured if expression of PGC-1α was changed accordingly. In agreement with our AMPK data, we found that PGC-1α expression was significantly higher (***, p=0.0004) in Kir6.2-/- hearts (Figure 3.8.A). Succinate dehydrogenase, an inner mitochondrial matrix protein that constitutes respiratory complex II in the citric acid cycle, was not significantly different in both groups (Figure 3.8.B). Additionally, voltage-dependent anion channel, which is an outer mitochondrial matrix marker, was significantly lower (*, p=0.0392) in Kir6.2-/- ventricles than in Kir6.2+/+ ventricles (Figure 3.8.C) and the expression of citrate synthase which converts acetyl CoA to citric acid in the citric acid cycle,

was not significantly changed (Figure 3.8.D). Quantitative analysis of transmission electron micrographs (Figure 3.8.E) indicate that the number of mitochondria in Kir6.2-/- ventricular tissue is lower than in Kir6.2+/+ tissue (Figure 3.8.F).

3.4. Discussion

As electrical channels, K_{ATP} channels have classically been thought to act downstream of changes in metabolism and to couple them to membrane excitability. The necessity of K_{ATP} channel presence in cardioprotection has already been well established, whether in pharmacological[377] or ischemic preconditioning using the K_{ATP} knockout mouse model[216]. Most of the reports on the subject attributed that protection to more efficient calcium homeostasis conferred by K_{ATP} channel activity which prevents intracellular calcium accumulation during stress. However, a study by Grover et al. demonstrated that even when K_{ATP} action potential duration shortening is prevented, hearts are still protected after I/R[394]. This suggests that shortening of the action potential is not the only mechanism behind K_{ATP}-provided cardioprotection, but that the physical presence of K_{ATP} channels on the membrane surface is necessary for cardioprotection. In that regard, it is important to note that proteomic analysis revealed that over 60% of the proteins whose genomic expression was affected by the absence of K_{ATP} channels were proteins involved in metabolism and bioenergetics[383]. The involvement of K_{ATP} channels in energy expenditure has also been demonstrated by Alekseev et al. showing that absence of K_{ATP} channels increases global fatty acid oxidation manifested as a lean phenotype compared to Kir6.2+/+ after being fed a high-fat diet[353]).

We decided to investigate cardiac metabolism in the absence of K_{ATP} channels bearing in mind that efficient cardiac metabolism is key in myocardial functional recovery after I/R injury[395]. Our data shows for the first time that cardiac metabolism in hearts lacking

K_{ATP} channels is shifted towards fatty acid metabolism (two fold increase), this is in concert with suppressed glycolysis. Despite the discrepancy about whether fatty acid oxidation is protective or detrimental during a cardiac insult such as ischemia/reperfusion, a few elegant studies have recently demonstrated that reducing fatty acid oxidation is protective in that setting[396–401]and that has been demonstrated clinically as well[402]. However, contrary to our expectations glucose oxidation was not affected which shows that the Randle cycle has been uncoupled where an increase in fatty acid oxidation should suppress glucose oxidation via inhibition of pyruvate dehydrogenase[276]. While our data show a trend of higher phosphorylation of pyruvate dehydrogenase in hearts lacking K_{ATP} channels, we still need to increase our sample numbers to confirm this observation. However, if glucose and fatty acid oxidation are uncoupled under basal conditions, it is likely that during ischemia, with the inability to stimulate glycolysis, the myocardium becomes susceptible to more damage due to lack of efficient anaerobic oxidation. Normally, during reperfusion, the heart relies on fatty acid oxidation primarily, but it is unclear if Kir6.2-/- hearts have a similar metabolic profile and this remains a difficult subject of investigation since Kir6.2-/- hearts exhibit very poor post-ischemic recovery.

Knowing that activated AMPK is a regulator of fatty acid oxidation and since it has been shown to physically associate with the channel[386], we decided to investigate whether basal AMPK activity was affected by the absence of cardiac K_{ATP} channels. Our data shows that Kir6.2-/- hearts perfused in Langendorff mode have higher basal AMPK activity as evident by higher expression of phospho-AMPK protein. A possible contributor to that observation is that Kir6.2-/- hearts handle calcium less efficiently than in Kir6.2+/+, as previously demonstrated by Gumina et al.[182]. This increase in intracellular calcium may lead

to the activation of CaMKK which is one of the upstream kinases governing the activation of AMPK[304]. In support of our findings, a study by Hu et al., showed that K_{ATP} channels are required for the AMPK-mediated cardioprotection offered by resveratrol[218]. Recent research by several groups has linked K_{ATP} activity and trafficking to upstream AMPK activation[337,386,403], however, data from our lab suggest that K_{ATP} channels may be upstream of AMPK activation as will be described in Chapter 4. Taken together, these findings suggest a complex multi-faceted AMPK-K_{ATP}-centered metabolome with delicate interactions based on various triggers. However, it remains to be an intriguing area for future study.

We examined differences in downstream effectors of AMPK activation. A candidate target that is regulated by AMPK activation is peroxisome proliferator-activated receptor gamma coactivator (PGC)1-α[404,405]. PGC1-α is involved in mitochondrial biogenesis[406], and since we observed a significant increase in PGC1-α expression in hearts lacking K_{ATP} channels, we also decided to look at mitochondrial density. Our data demonstrate that PGC1-α expression is increased in Kir6.2-/- hearts which is in line with the increased AMPK phosphorylation observed in the same hearts. It is important to mention that our observation showing an increase in PGC1-α is in contrast to the findings of Hu et al.[407] which could be due to the difference in experimental model. Hu et al. also demonstrated that in the absence of K_{ATP} channels, PGC1-α expression in response to pressure overload was significantly lower than the sham group. If AMPK activation has already reached maximum phosphorylation in Kir6.2-/- hearts under resting conditions, it is possible that downstream activation of PGC1-α after simulated I/R would also be disrupted due to the absence of an efficient upstream stress signal.

Another target linked to PGC1-α and upregulated in response to AMPK activation is PPAR-α[408]. Upregulation of PPAR-α leads to downstream expression of proteins involved in fatty acid oxidation[409]. As we expected, PPAR-α expression was increased in Kir6.2-/- hearts. We then examined markers of different stages of fatty acid metabolism, starting with fatty acid transporters, we found that FATP1 was significantly lower in the absence of K_{ATP} however there was increased CD36/FAT expression in which may be compensatory and could be associated with increased fatty acid transport into the cell. It has been suggested that CD36 translocation to the plasma membrane and subsequently fatty acid transport into the cell is moderated by active AMPK[410]. We also observed a slight increase in expression of adipose triglyceride lipase (ATGL), a significant increase in expression of long chain fatty acyl-CoA synthetase (ACSL)1 which catalyzes the formation of fatty acyl CoAs making them available for oxidation and higher activation of hormone-sensitive lipase (HSL) which accelerates the breakdown of triacylglycerol into free fatty acids for metabolism[411]. It is worth mentioning that ACSL1 catalyzes the conversion of fatty acids to fatty acyl CoA using ATP it generates AMP which in turn can activate AMPK allostericaly[412]. It is unclear so far whether the AMPK activation we observe in our model is upstream or downstream of ACSL1 activation.

It is thought that activation of PPAR-α is beneficial in ischemia-reperfusion injury[413,414], however, in a large animal model, activation of PPAR-α was not able to provide protection against I/R[415]. Moreover, research from the Taegtmeyer group has also shown that downregulation of PPAR-α gene expression prevents lipotoxicity in an ischemic setting[416]. They have also shown that increased expression of PPAR-α in cardiomyocytes leads to

irreversible ischemic damage and is associated with increased glycogen particle deposition[416].

In agreement with their findings, we have similarly observed increased glycogen deposition. This is in line with reduced rate of glycolysis demonstrated in our working heart model. Since Akt activation is upstream to glycogen synthesis, we sought to examine differences in Akt signaling in Kir6.2+/+ and Kir6.2-/- hearts. Phospho-Akt was significantly higher in Kir6.2-/- hearts compared to Kir6.2+/+. Similarly, its downstream target GSK-3β showed higher phosphorylation at Ser-9 which is the inhibitory phosphorylation site. Akt-mediated inhibition of GSK-3β leads to glycogen synthase dephosphorylation and subsequent activation which increases glycogen synthesis as a result[417]. Since AMPK activation has been shown to inhibit glycogen synthesis, we are with the notion that the increased glycogen content in Kir6.2-/- hearts is due to suppressed glycolysis.

Taken together, while Kir6.2+/+ and Kir6.2 -/- mouse hearts appear similar in function under resting conditions, the metabolic profile in Kir6.2-/- mice may set it up for the exaggerated damage post I/R. Suppressed glycolysis observed in Kir6.2-/- hearts may be detrimental during ischemia since the only source of energy that the myocardium could rely on in that case would be anaerobic glycolysis. Although it has been previously reported that inhibition of GSK-3β is protective in I/R[418] and attenuates overload, we cannot project this on our model since it has been already established that Kir6.2-/- hearts recover poorly after I/R due to severe calcium accumulation[182]. A multitude of compensatory mechanisms could be in effect in I/R stress in our genetic knockout model, however they remain yet to be investigated.

Finally, our study shows a novel role of plasma membrane K_{ATP} channels in cardiac metabolism. This metabolic shift towards fatty acid oxidation and suppressed glycolysis takes us one step closer towards understanding why hearts lacking K_{ATP} channels may respond more poorly after I/R injury. Further experiments to examine metabolic efficiency in I/R injury are required to advance our understanding of the metabolic role of K_{ATP} channels under stress.

Figure 3.1. Cardiac metabolism is shifted towards fatty acid oxidation in Kir6.2-/- hearts. Perfusion of Kir6.2+/+ and Kir6.2-/- working hearts (n=8) with labeled glucose and palmitate to measure rates (μmol/min/g dry wt) of glycolysis (A), glucose (B) and fatty acid (C) oxidation in both groups. Values are presented as mean ± SEM, ** $p < 0.01$ compared to Kir6.2+/+)

A.

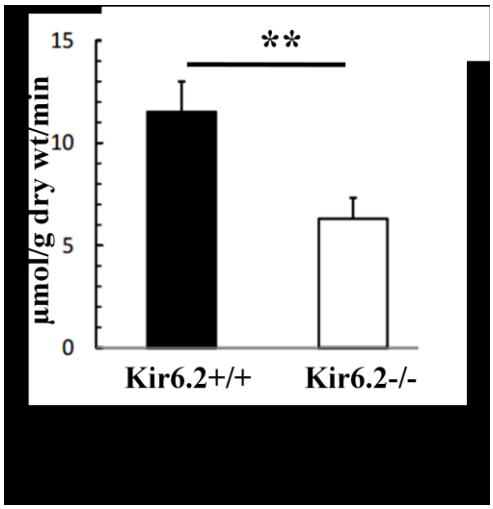
**
15
10
5
0
µmol/g dry wt/min
Kir6.2+/+
Kir6.2-/-

B.

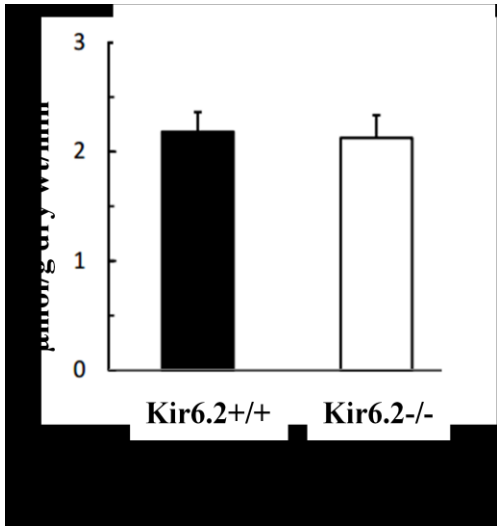
3
2
1
0
Kir6.2+/+
Kir6.2-/-

C.

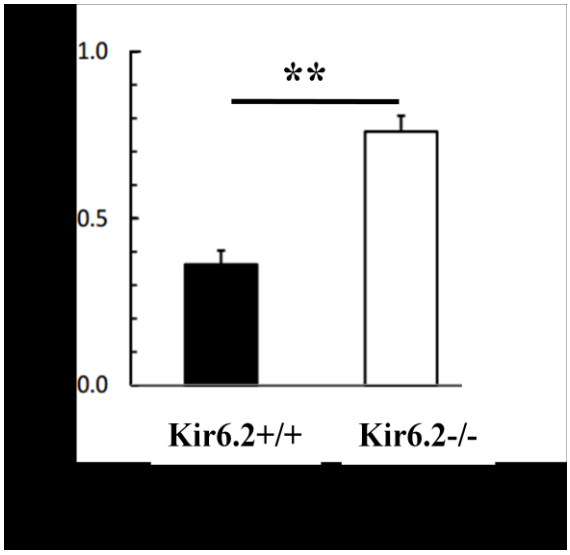
**
1.0
0.5
0.0
Kir6.2+/+
Kir6.2-/-

Figure 3.2. Comparison between proton, acetyl CoA and ATP production in Kir6.2+/+ and Kir6.2-/-. (A) Proton production (μmol/min/g dry wt) in both Kir6.2+/+ and Kir6.2-/- groups (n=8/group). (B) Acetyl CoA production (μmol/min/g dry wt) in Kir6.2-/- hearts. (C) Measurement of ATP derived from fatty acid oxidation, glycolysis and glucose oxidation represented as (μmol/min/g dry wt) or as percentages (D). Values are presented as means ±SEM, *$p<0.05$, **$p<0.01$ compared to Kir6.2+/+.

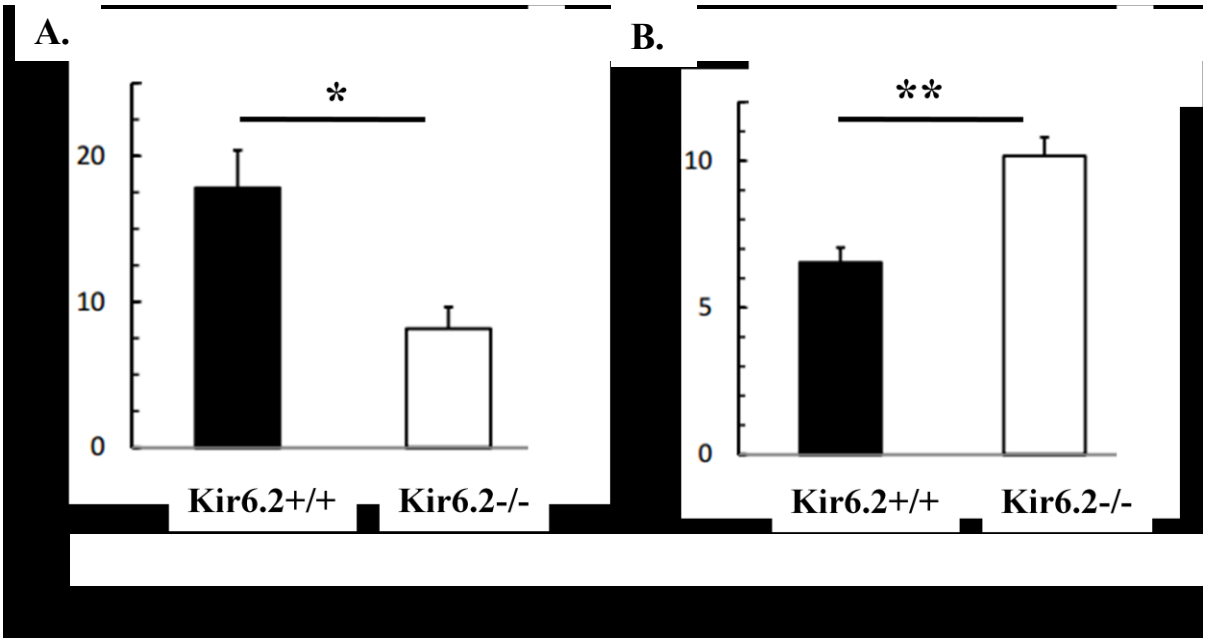
A.
*
20
10
0
Kir6.2+/+
Kir6.2-/-
B.
**
10
5
0
Kir6.2+/+
Kir6.2-/-

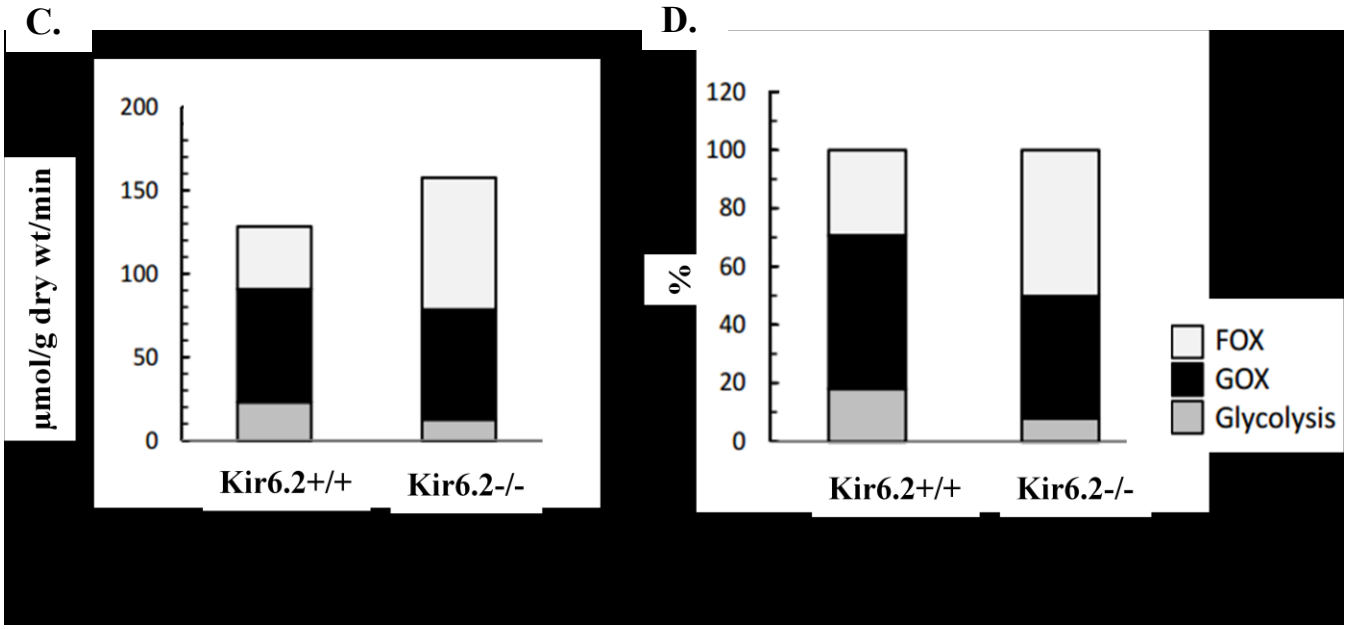
C.
µmol/g dry wt/min
200
150
100
50
0
Kir6.2+/+
Kir6.2-/-
D.
%
120
100
80
60
40
20
0
Kir6.2+/+
Kir6.2-/-
FOX
GOX
Glycolysis

Figure 3.3. Cell shortening in Kir6.2+/+ and Kir6.2-/- isolated adult ventricular cardiomyocytes. (A) Representative recordings of single cell shortening of cardiomyocytes isolated from adult Kir6.2+/+ and Kir6.2-/-. (B) Grouped data of fractional cell shortening (% of diastolic length) in Kir6.2+/+ and Kir6.2-/-. (C) Maximal rate of relengthening represented as -dL/dt. (n=15-18 cells/group)

A.


Kir6.2+/+
Kir6.2+/+
Kir6.2-/-
Kir6.2-/-

B.

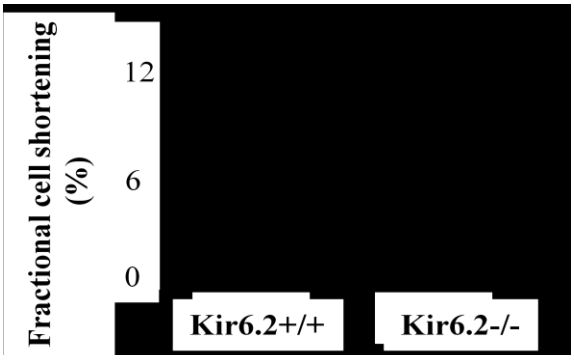
Fractional cell shortening (%)
12
6
0
Kir6.2+/+
Kir6.2-/-

C.

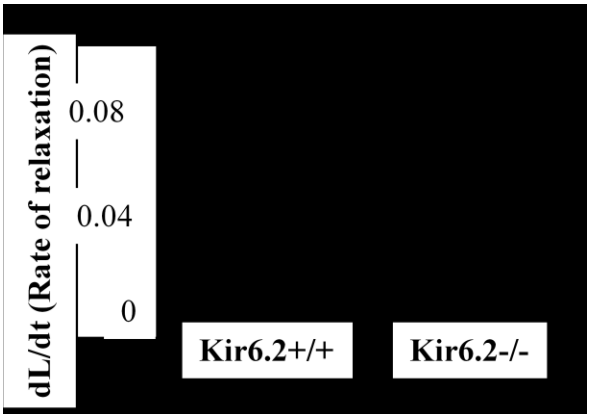
dL/dt (Rate of relaxation)
0.08
0.04
0
Kir6.2+/+
Kir6.2-/-

Figure 3.4. Cardiac function in isolated working Kir6.2+/+ and Kir6.2-/- hearts.

(A) Coronary flow (ml/min) in isolated working hearts from Kir6.2+/+ and Kir6.2-/- mice. (B) Left ventricular work(Joules/min/g dry wt). Cardiac efficiency measured as (C) LV work/acetyl CoA (Joules/µmol) produced and (D) LV work/ATP produced (Joules/µM). Values are means ± SEM. *$p<0.05$ compared with Kir6.2+/+ hearts.


A.
Kir6.2+/+
Kir6.2-/-

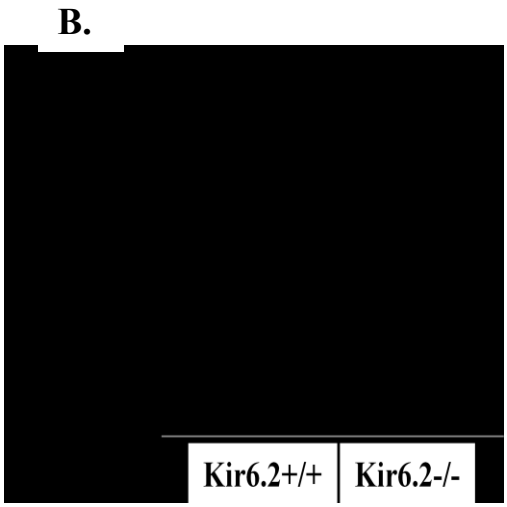
B.
Kir6.2+/+
Kir6.2-/-

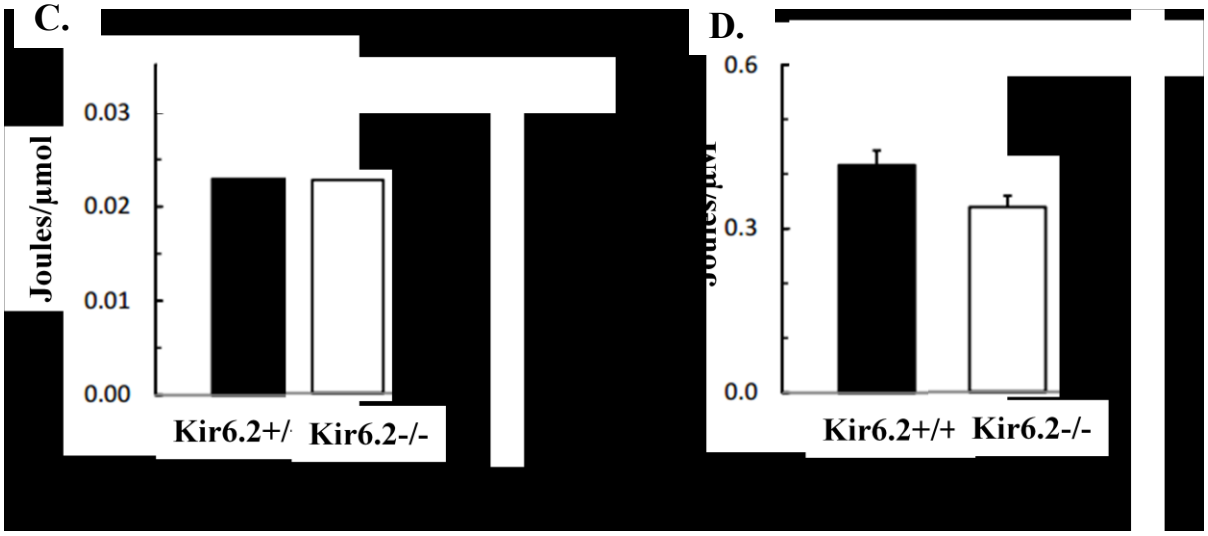
C.
Joules/µmol
0.03
0.02
0.01
0.00
Kir6.2+/
Kir6.2-/-
D.
0.6
0.3
0.0
Kir6.2+/+
Kir6.2-/-

Figure 3.5. AMPK signalling in Kir6.2-/- hearts under basal and stress conditions.

(A) AMPK and (B) LKB1 phosphorylation in Kir6.2+/+ and Kir6.2-/- hearts perfused in Langendorff mode (n=4). (C) Comparison of AMPK and (D) ACC phosphorylation in Kir6.2+/+ and Kir6.2-/- hearts (n=5) perfused in working mode with or without β-isoproterenol (iso) ACC in Kir6.2-/- was weak compared to Kir6.+/+. Values are means ± SEM. *$p<0.05$ compared with Kir6.2+/+ hearts.

A.

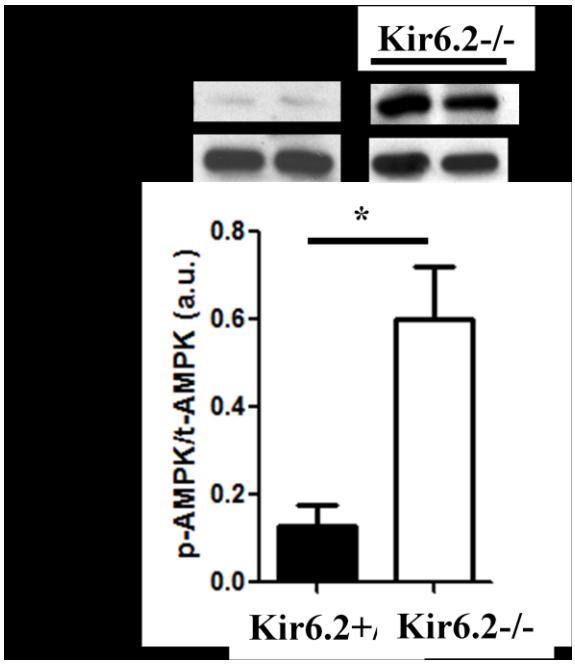
Kir6.2-/-
*
p-AMPK/t-AMPK (a.u.)
0.8
0.6
0.4
0.2
0.0
Kir6.2+/
Kir6.2-/-

B.

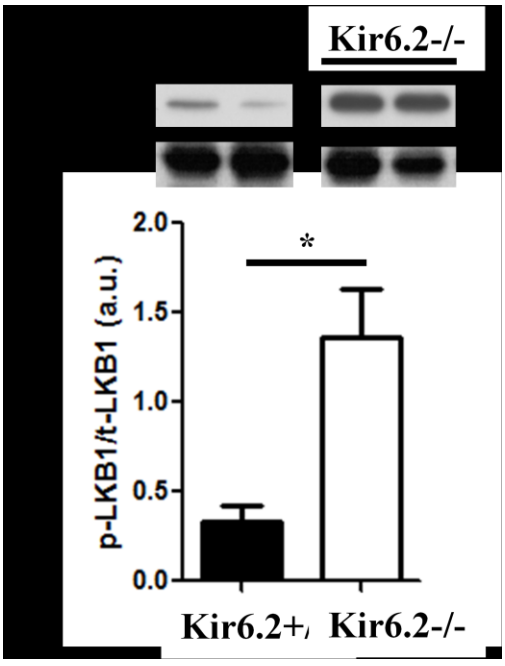
Kir6.2-/-
*
p-LKB1/t-LKB1 (a.u.)
2.0
1.5
1.0
0.5
0.0
Kir6.2+/
Kir6.2-/-

C.

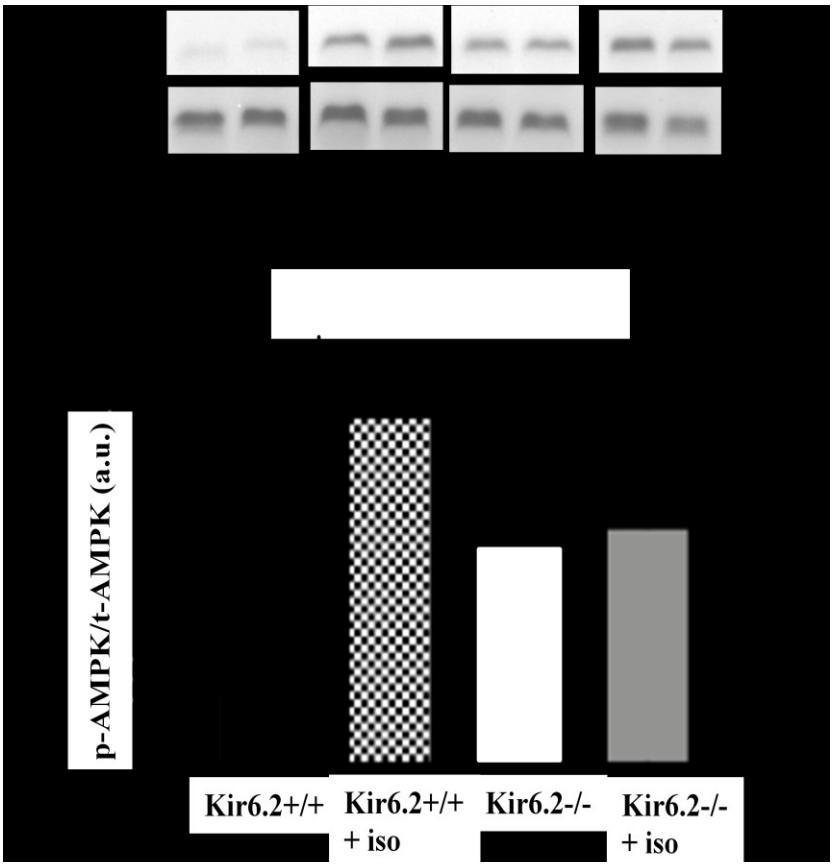
p-AMPK/t-AMPK (a.u.)
Kir6.2+/+
Kir6.2+/+ + iso
Kir6.2-/-
Kir6.2-/- + iso

D.

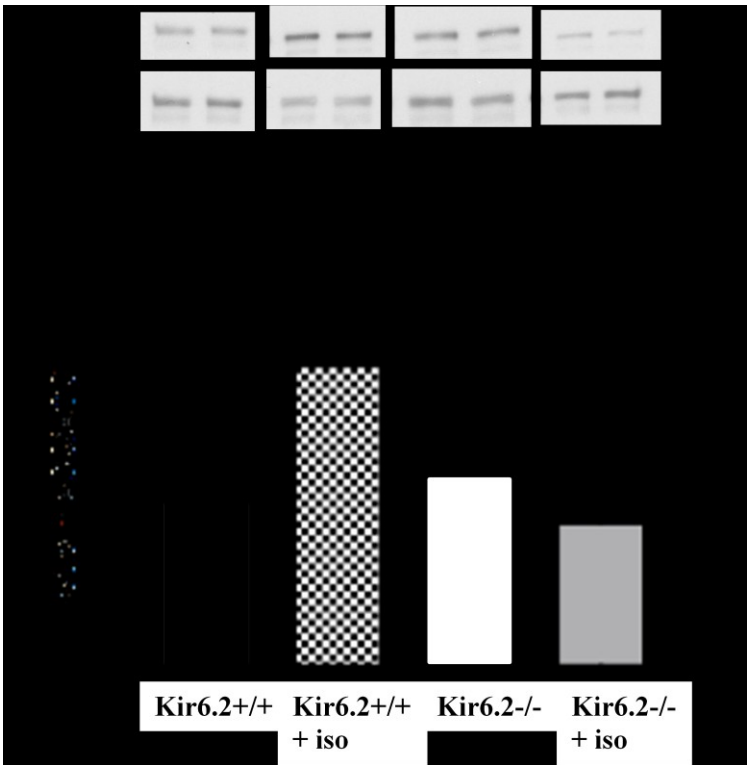
Kir6.2+/+
Kir6.2+/+ + iso
Kir6.2-/-
Kir6.2-/- + iso

Figure 3.6. Expression of fatty acid metabolism markers in Kir6.2+/+ and Kir6.2-/- hearts. Comparison of protein expression of (A) Adipose triglyceride lipase (ATGL), (B) acyl-CoA synthetase long-chain family member 1 (ACSL1), (C) CD36/FAT, (D) FATP1, (E) phosphorylated hormone sensitive lipase (p-HSL) and (F) the nuclear receptor protein Peroxisome Proliferator-Activated Receptor (PPAR) α. Histograms show results of immunoblot quantification normalized to tubulin. (n=4/group). Values are means ± SEM. *$p<0.05$ compared with Kir6.2+/+ hearts. (G) Schematic representation of the fatty acid metabolism proteins whose expression was tested in this study.

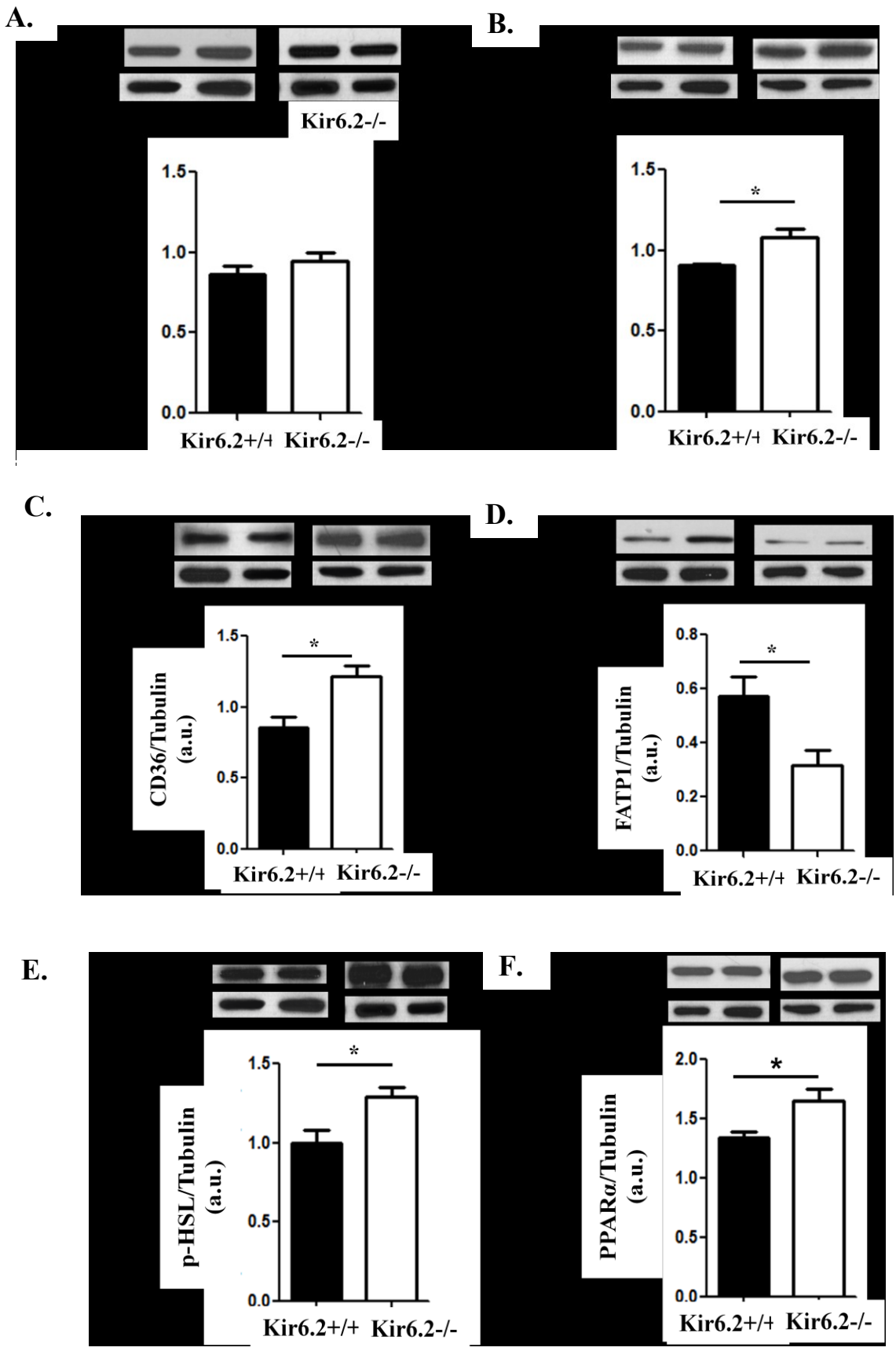
A.
Kir6.2-/-
1.5
1.0
0.5
0.0
Kir6.2+/+ Kir6.2-/-
B.
*
1.5
1.0
0.5
0.0
Kir6.2+/+ Kir6.2-/-
C.
CD36/Tubulin (a.u.)
*
1.5
1.0
0.5
0.0
Kir6.2+/+ Kir6.2-/-
D.
FATP1/Tubulin (a.u.)
*
0.8
0.6
0.4
0.2
0.0
Kir6.2+/+ Kir6.2-/-
E.
p-HSL/Tubulin (a.u.)
*
1.5
1.0
0.5
0.0
Kir6.2+/+ Kir6.2-/-
F.
PPARα/Tubulin (a.u.)
*
2.0
1.5
1.0
0.5
0.0
Kir6.2+/+ Kir6.2-/-

G.

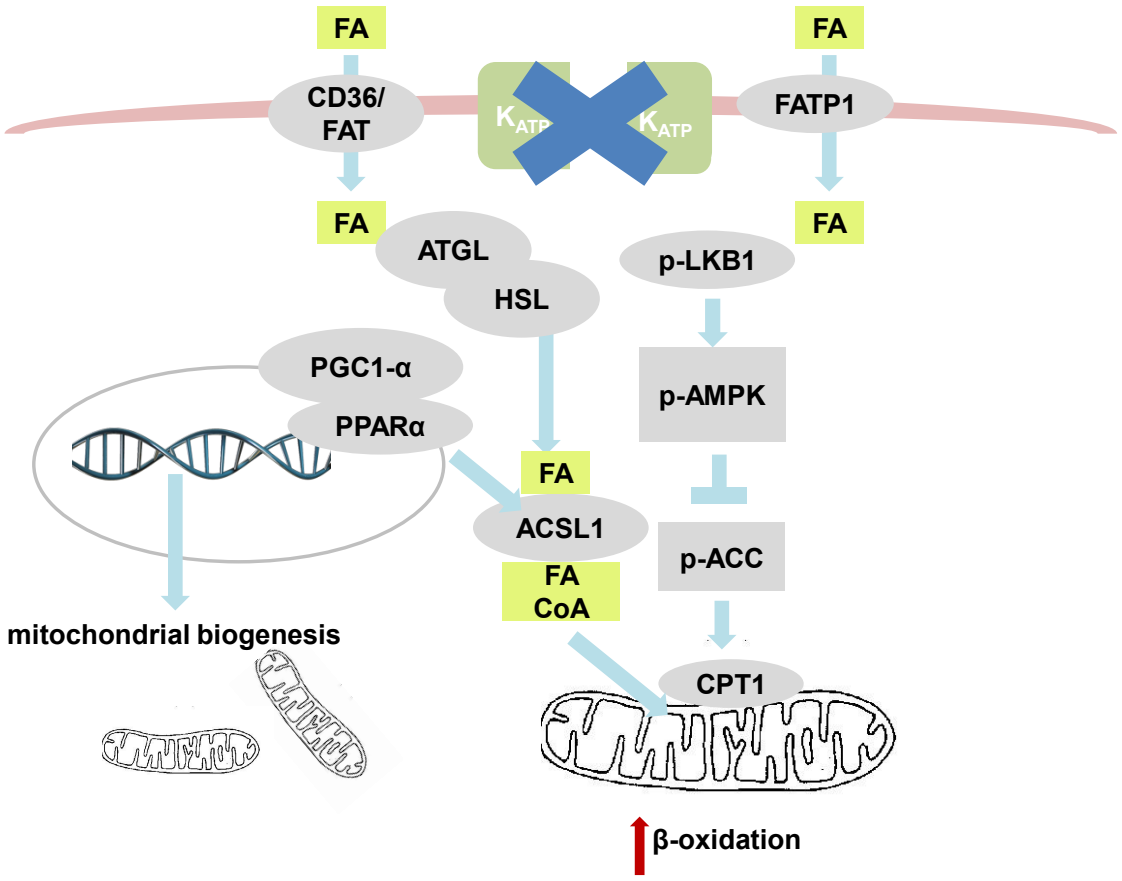
FA
FA
CD36/
FAT
K ATP
K ATP
FATP1
FA
FA
ATGL
HSL
p-LKB1
PGC1-α
PPARα
p-AMPK
FA
ACSL1
p-ACC
FA
CoA
mitochondrial biogenesis
CPT1
β-oxidation

Figure 3.7. Differences in Akt signalling and glycogen content between Kir6.2+/+ and Kir6.2-/- hearts. (A) Phosphorylation of Akt normalized to total Akt and (B) glycogen synthase kinase (GSK)-3β normalized to total GSK-3β in Langendorff perfused Kir6.2+/+ and Kir6.2-/- mouse hearts (n=4/group). (C) Representative images of a ventricular cross-section in Kir6.2+/+ and Kir6.2-/- hearts with purple particles representing Periodic Acid-Schiff stained glycogen. (D) Quantification of glycogen particles in ventricular cross sections from Kir6.2+/+ and Kir6.2-/- hearts (n=15 images/group) and (E) colourimetric analysis of glycogen content (μg/μl) in naive Kir6.2+/+ and Kir6.2-/- hearts. Values are means ± SEM. *$p<0.05$, ***$p<0.001$ compared with Kir6.2+/+ hearts. (F) Phosphorylation of the E1 α subunit of pyruvate dehydrogenase normalized to total pyruvate dehydrogenase in Langendorff perfused Kir6.2+/+ and Kir6.-/- mouse hearts (n-4/group, $p>0.05$). (G) Schematic representation of some of the proteins affecting glycogen synthesis and were investigated in this study.

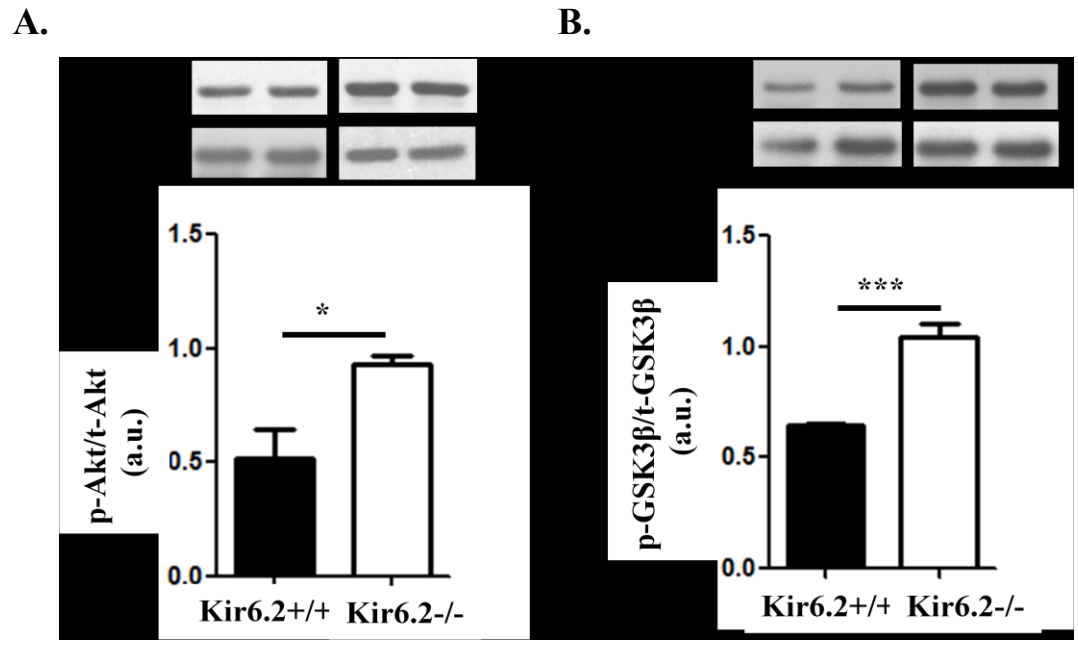
A.
B.
p-Akt/t-Akt (a.u.)
1.5
1.0
0.5
0.0
*
Kir6.2+/+
Kir6.2-/-
p-GSK3β/t-GSK3β (a.u.)
1.5
1.0
0.5
0.0
***
Kir6.2+/+
Kir6.2-/-

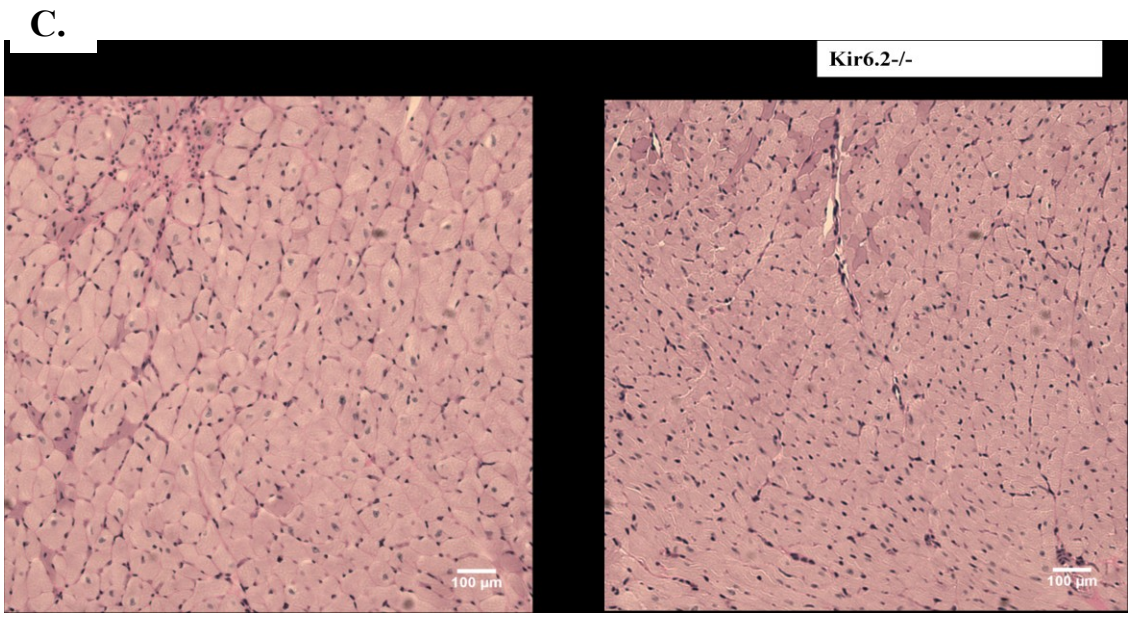
C.
Kir6.2-/-
100 µm
100 µm

D.

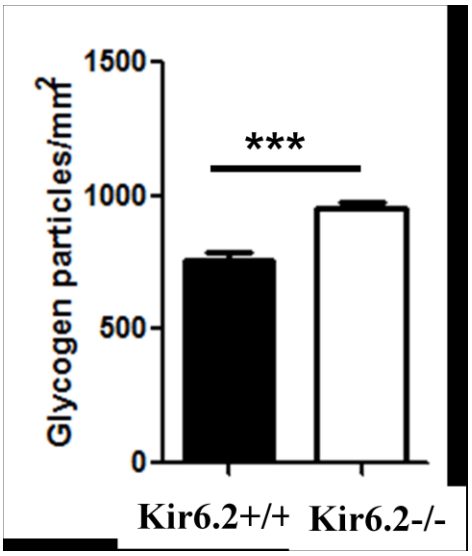
Glycogen particles/mm2
1500
1000
500
0
***
Kir6.2+/+
Kir6.2-/-

E.

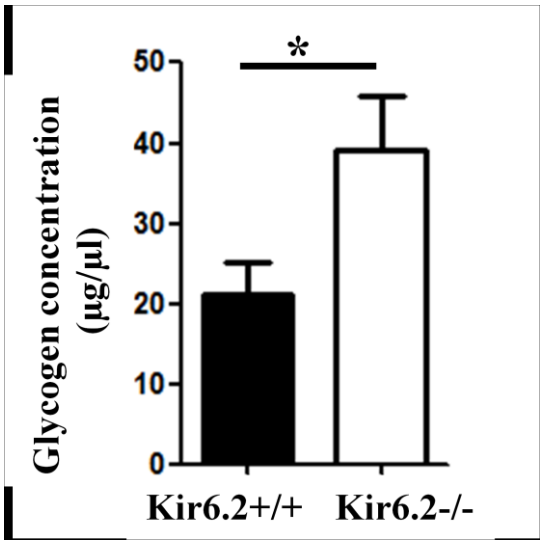
Glycogen concentration (µg/µl)
50
40
30
20
10
0
*
Kir6.2+/+
Kir6.2-/-

F.

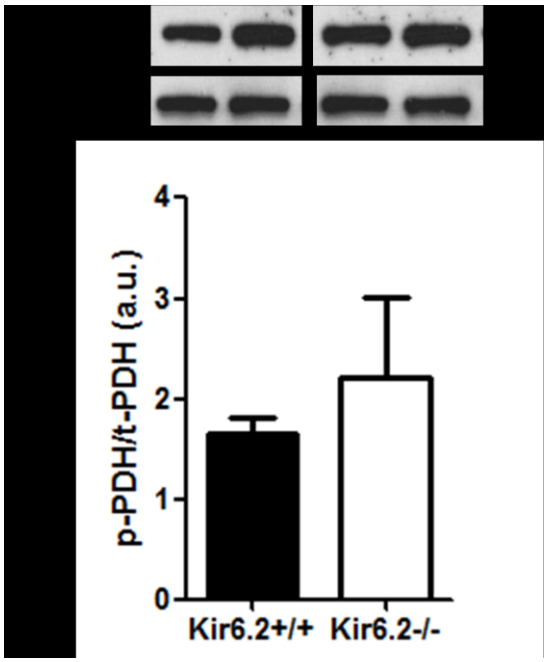
p-PDH/t-PDH (a.u.)
4
3
2
1
0
Kir6.2+/+
Kir6.2-/-

G.

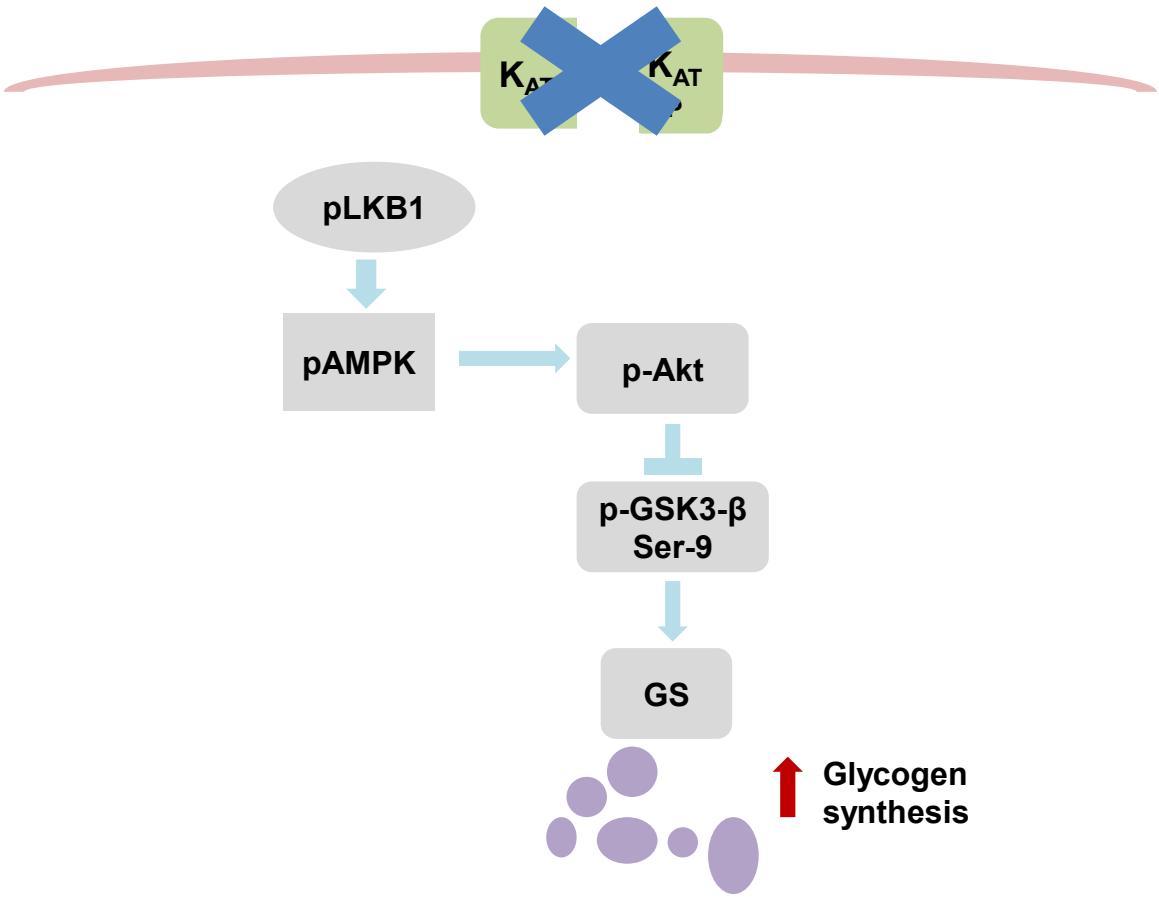

Figure 3.8. Protein expression of mitochondrial markers and mitochondrial quantification in Kir6.2+/+ and Kir6.2-/- hearts. Immunoblots of protein expression of (A) Peroxisome proliferator-activated receptor-γ coactivator (PGC)-1α, (B) succinate degydrogenase (SuDH), (C) Voltage-dependent anion channel VDAC, (D) Citrate synthase (CS) in Kir6.2+/+ and Kir6.2-/- naive hearts (n=4/group). (E) Representative transmission electron micrographs of ventricular tissue from naive Kir6.2+/+ and Kir6.2-/- hearts. (F) Quantification of mitochondria in transmission electron micrographs (n=5-6 hearts/group, 35-40 micrographs/heart). Values are means ± SEM. *$p<0.05$ compared with Kir6.2+/+ hearts.

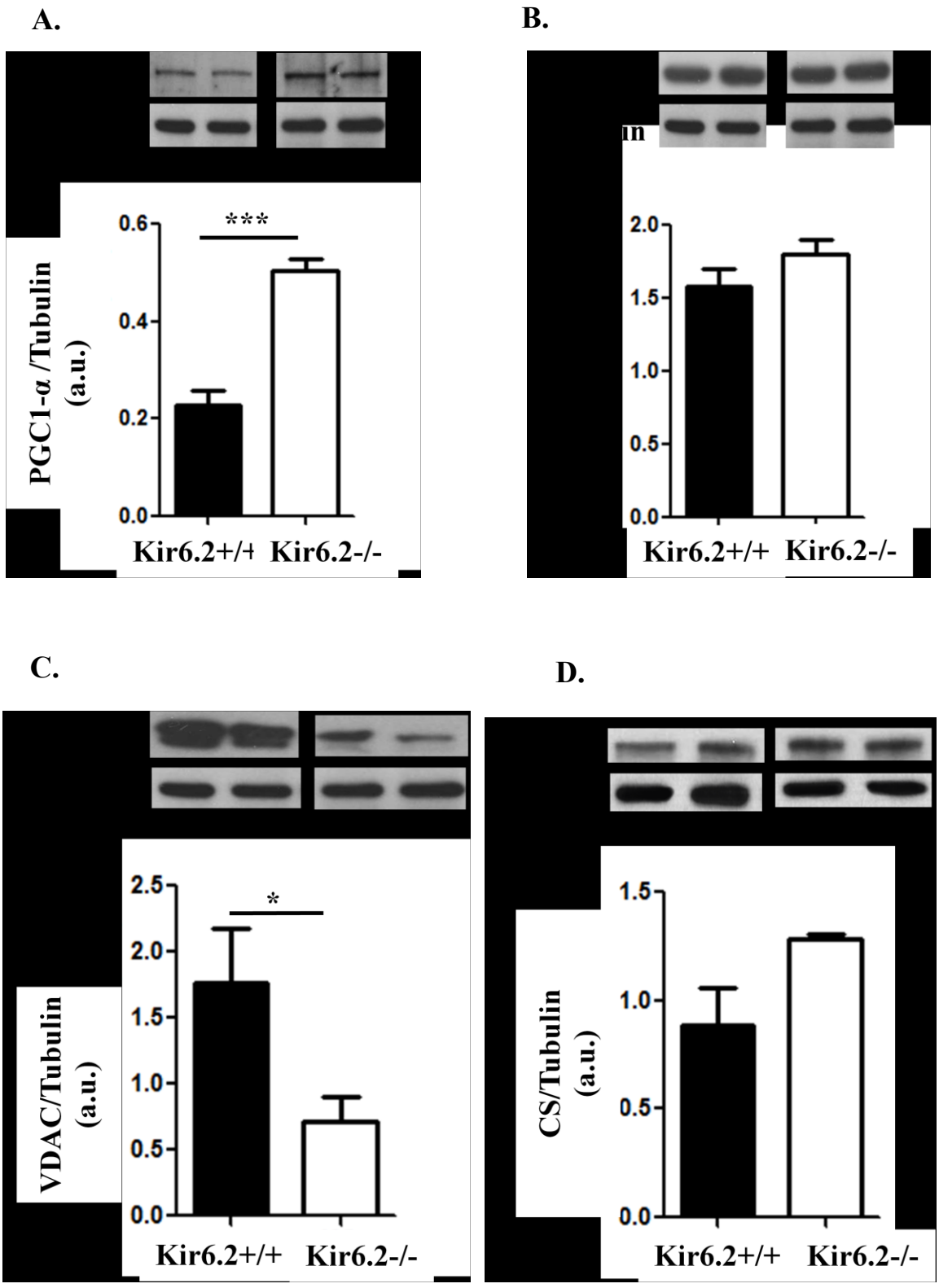
A.
B.
C.
D.
PGC1-α /Tubulin (a.u.)
***
0.6
0.4
0.2
0.0
Kir6.2+/+
Kir6.2-/-
2.0
1.5
1.0
0.5
0.0
Kir6.2+/+
Kir6.2-/-
VDAC/Tubulin (a.u.)
*
2.5
2.0
1.5
1.0
0.5
0.0
Kir6.2+/+
Kir6.2-/-
CS/Tubulin (a.u.)
1.5
1.0
0.5
0.0
Kir6.2+/+
Kir6.2-/-

E.

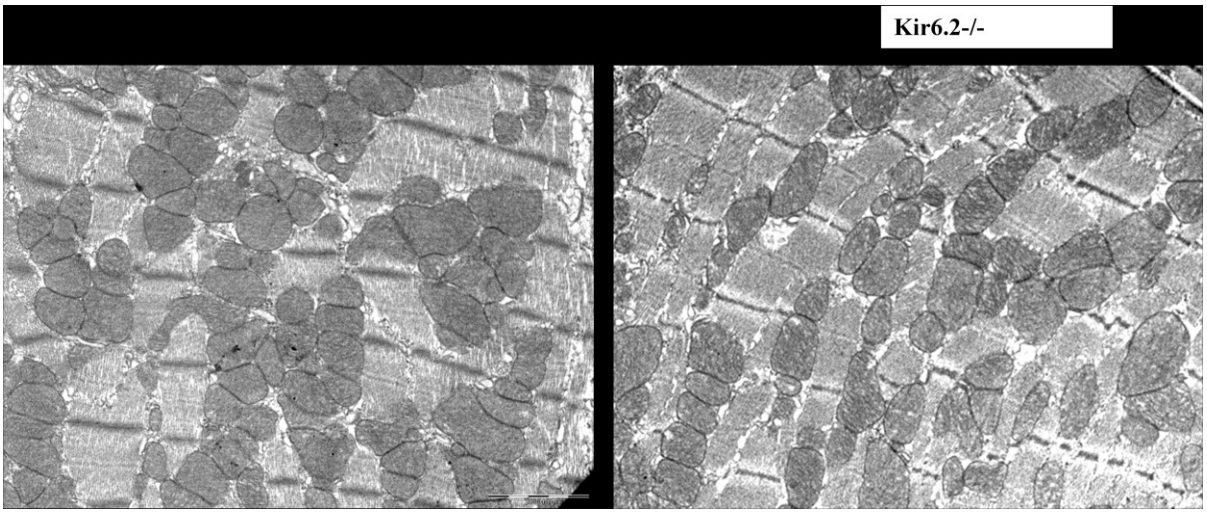

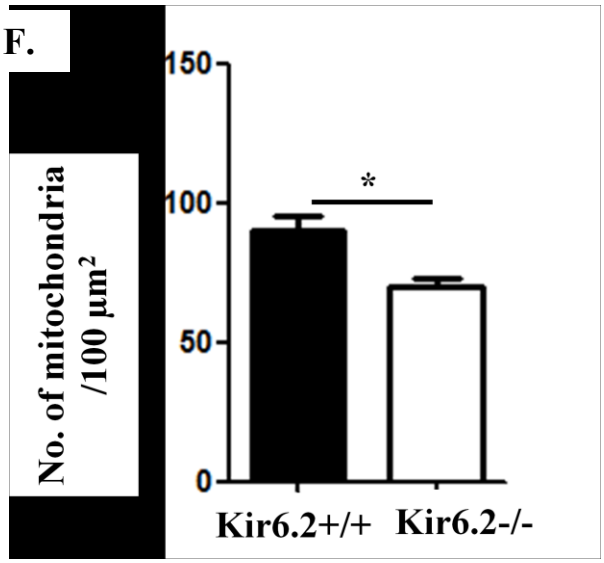

Chapter 4
Molecular and metabolic aspects of K_{ATP} channel opener pharmacology

Electrophysiological experiments were performed by Dr. Mohammad Fatehi, site-directed mutagenesis was performed by Dr. Chris Carter. The author contributed to experimental design and performed Langendorff heart perfusions, immunoblotting and statistical analysis..

A version of this Chapter has been published in *Bioscience reports*

Molecular determinants of ATP-sensitive potassium channel Mg-ATPase activity and diazoxide sensitivity- Mohammad Fatehi, Chris Carter, Nermeen Youssef, Beth Hunter, Andy Holt, Peter E. Light

2015 Jul 7. pii: BSR20150143

4.1. Introduction

K_{ATP} channels have the ability to couple cellular metabolic signals to electrical membrane excitability and therefore play important roles in many excitable tissues including the endocrine, nervous, skeletal muscle and cardiovascular systems[419]. The channels are hetero-octameric trans-membrane protein complexes comprised of four pore-forming inward rectifying potassium (Kir6.x) channel subunits surrounded by four regulatory sulfonylurea receptor (SUR) subunits that possess intrinsic catalytic Mg-ATPase activity[167,420]. Kir6.1 (*KCNJ8*), Kir6.2 (*KCNJ11*) and SUR1 (*ABCC8*) are encoded by individual genes, while SUR2A and SUR2B are splice variants of the *ABCC9* gene product. Differential subunit assembly results in distinct channel subtypes that exhibit cell/tissue specific expression patterns as well as different biophysical and pharmacological properties[6].

K_{ATP} channels function as molecular rheostats by adjusting cellular electrical excitability in response to alterations in cellular metabolism, primarily via their modulation by the intracellular nucleotides ATP and ADP. The major site for the inhibitory action of ATP is located within the pore-forming Kir6.2 subunits[421]. In contrast, ADP can release the inhibition by ATP, leading to increases in channel activity via a complex molecular interaction within the SUR subunits. The SUR subunit contains two evolutionarily conserved hydrophilic nucleotide binding domains (NBDs) with each NBD containing a Walker A and B motif that bestow intrinsic Mg-ATPase catalytic activity to the K_{ATP} channel subunit[422]. Adenine nucleotide binding and ATP hydrolysis, generating ADP, take place in the catalytic region formed between Walker motifs. It is this Mg-ATPase function that is considered important for regulating the appropriate K_{ATP} channel activity via ADP-induced K_{ATP} channel activation[35,43]. This is highlighted by the fact that human mutations in SUR1 that

increase Mg-ATPase activity underlie certain forms of rare monogenic neonatal diabetes[158]. Furthermore, our lab has previously shown that the common diabetes susceptibility variant S1369A in SUR1 results in increased Mg-ATPase activity and channel activation that may contribute to the development of type 2 diabetes by suppressing insulin secretion[167]. We speculated that the removal of the side-chain hydroxyl group in the S1369A variant results in a loss of a hydrogen bond with the side-chain of the Q1372 residue in the hairpin loop region adjacent to the catalytic Mg-ATPase site in NBD2[167]. Other determinants and regulators of Mg-ATPase activity still remain to be explored.

Diazoxide (DZX) is commonly used to treat rare monogenic hyperinsulemia resulting from certain inactivation mutations in either the *ABCC8* or *KCNJ11* genes, although the precise molecular mechanism by which DZX acts is not totally defined. K_{ATP} channels containing the SUR1 subunit are activated by the K_{ATP} channel opener DZX; while the channels containing the SUR2A subunit possesses a substantially different pharmacology[423], requiring ADP to be present[24,114]. In the heart where SUR2A is the dominant SUR subunit, DZX has shown to have protective effects in the case of ischemia-reperfusion injury where it can mimic the protection provided by ischemic preconditioning[424–428]. However, the protection provided by DZX was abolished in a K_{ATP}-deficient genetic mouse model indicating that the channels mediate this protective effect[106,425,429]. The mechanism underlying the cardioprotective effect of DZX was classically thought to be via channel opening leading to ionic homeostasis and prevention of intracellular calcium accumulation[430], or through improvement of mitochondrial metabolism[104,424,426] or through activation of the PI3K/Akt pathway[431,432]. Activation of prosurvival kinases, Akt and Erk1/2 comprise the reperfusion injury salvage kinase pathway known to mediate ischemic

preconditioning and postconditioning[433]. The effect of DZX on Mg-ATPase activity in SUR2A containing tissue and its downstream consequences have not been fully explored to date.

In this regard, DZX is thought to increase K_{ATP} channel activity via increasing the intrinsic Mg-ATPase activity of the channel complex[158,434,435]. It is noteworthy that the channel's Mg-ATPase activity is isoform dependent, where SUR1 was shown to possess higher Mg-ATPase activity than that of SUR2A[46]. It is worth mentioning that the SUR2A isoform is only sensitive to DZX in the presence of ADP[112].Therefore, DZX sensitivity may involve regions important for regulating Mg-ATPase activity such as the residues in the hairpin loop adjacent to the major Mg-ATPase catalytic site in NBD2.

4.2. Methods

Working heart perfusions, metabolic and cardiac work measurements

Briefly, Kir6.2+/+ and Kir6.2-/-mice were anesthetized using pentobarbital, with 100 U of heparin. After mid-sternal incision, the heart was removed and placed in (37 ± 1 °C), modified Tyrode solution of the following composition: 128.2 mM NaCl, 4.7 mM KCl, 1.19 NaH_2PO_4, 1.05 mM $MgCl_2$, 1.3 mM $CaCl_2$, 20 mM $NaHCO_3$, and 11.1 mM glucose (pH = 7.35 ± 0.05). While bathed in the same solution, lung, thymus, and fat tissue were dissected and removed. After cannulation, Kir6.2+/+ and Kir6.2-/- mouse hearts were aerobically perfused in the working mode at a constant workload of 11.5 mmHg preload and 80 mmHg afterload with modified Krebs-Henseleit buffer containing 1.2 mmol/L palmitate prebound to 3% fat-free bovine serum albumin, 5 mmol/L glucose, and 100 μU/mL insulin as described previously[389]. While the heart was being perfused in working mode, systolic and

diastolic aortic pressures were measured using a Gould P21 pressure transducer attached to the aortic outflow line. An ultrasonic flow probes placed in the left atrial inflow line was used to measure cardiac output (ml/min) and other flow probe in the aortic outflow line was used to measure aortic flow (ml/min). Coronary flow was calculated as: cardiac output - aortic flow. Left ventricular (LV) work (Joules/min/g dry wt) was used as an index of mechanical function and was calculated as: cardiac output x LV developed pressure (systolic pressure – preload pressure) and then normalized to the heart dry weight. Glucose oxidation and palmitate oxidation were measured as described previously[390]. Rate of acetyl CoA production was calculated as described previously[391].

Langendorff heart perfusions

Hearts from Kir6.2+/+ and Kir6.2-/- mice were separated and cannulated as described above. Cannulated hearts were then retrogradely perfused with modified Krebs-Henseleit solution passed through the 5-μm filter (Millipore, Billerica) and warmed (37 °C) using a water jacket and circulator (ThermoNESLAB EX7, Newtown). The hearts were allowed to normalize for 10 minutes and then were perfused for 30 minutes with DZX (100 μM in DMSO) or with DMSO alone. Heart ventricles were clamp-frozen and used for biochemical analysis.

Western blot analysis

Ventricular tissue from Kir6.2+/+ and Kir6.2-/- mouse hearts was snap-frozen after Langendorff perfusion and homogenized by cryogenic grinding then diluted with RIPA homogenization buffer containing phosphatase and protease inhibitors. After a BCA protein

assay (Pierce, Thermo Scientific, USA), equal amounts of protein were resolved by SDS-PAGE, and were transferred onto a PVDF membrane. Target proteins were identified using the primary antibodies: anti-AMPK phospho (Thr172) and total, anti-LKB1 phospho (Ser428) and total, anti-Akt phospho (Ser 473) and total, anti-GSK-3β phospho (Ser9), mTOR phospho (Ser2448) and total as well as anti-p70S6K phospho (Thr389) and total. (Cell Signaling Technology, Danvers, Massachusetts). Immunoblots were developed using the Amersham ECL Prime Western blotting detection reagents. Densitometric analysis was performed using ImageJ software (National Institutes of Health).

Cell Culture, Transfection and Electrophysiology

tsA201 cells, a HEK293 cell line derivative, were cultured and then transfected with the Kir6.2 and SUR1 clones using the calcium phosphate precipitation technique[436]. Transfected cells were identified using fluorescent optics in combination with co-expression of a green fluorescent protein plasmid (Life Technologies, Gaithersburg, MD). Macroscopic K_{ATP} channel recordings were then performed 48-72 hours after transfection. The excised inside-out patch clamp technique was used to measure macroscopic recombinant K_{ATP} channel currents in transfected tsA201 cells as described in detail previously[436]. Experiments were performed at room temperature (21^{o}C). The bath solution for recording in the absence of Mg^{2+} ions, contained 2 mmol/l EGTA and no $MgCl_2$ and. Beryllium fluoride (BeF_2) was dissolved in 50 mmol/l KF (33% w/v) to produce sufficient amount of the ATP γ-phosphate mimetics BeF_x (BeF^{3-} and BeF_2^{4-})[437]. In bath solutions used for experiments in the presence of BeF_x, 50 mmol/l KCl was replaced with 50 mmol/l KF. For the mechanical stress experiments, after establishing the gigaseal and moving to the inside out patch configuration,

current responses were recorded after applying GTP alone or with BeF_2 and 10 mmHg negative pressure was applied by using ALA High Speed Pressure Clamp. The insulin-secreting β-cell line INS-1 was maintained in culture with Roswell Park Memorial Institute (RPMI)-1640 medium supplemented with 11 mM glucose, 2 mM L-glutamine, 10% fetal calf serum, and 0.1% penicillin/streptomycin. Human islets from healthy donors were obtained from the Clinical Islet Laboratory at the University of Alberta. Islets were dispersed to single cells in Ca^{++}-free buffer. Islet culture was performed as described previously[438]. INS-1 cells and human islets were incubated with either DZX (100 μM in DMSO) or DMSO alone for one hour at 37º C.

Experimental compounds

BeF_2, MgATP, DZX and Na^+ salts of GTP and GDP were obtained from Sigma-Aldrich (Oakville, Canada). ATP, GTP and GDP were prepared as 10 mmol/l stock solutions in ddH_2O immediately prior to use.

Site-directed mutagenesis

The full-length human SUR1 and SUR2A DNA constructs were a generous gift from Dr. J. Bryan (Pacific Northwest Diabetes Research Institute, Seattle, WA). All mutants used in this study were generated using site-directed mutagenesis (QuickChange, Stratagene) and subsequently confirmed by sequence analysis.

In silico homology modeling

The homology model of the SUR1 NBD1 and NBD2 dimer[45], based on the prokaryotic ATP binding cassette (ABC) protein crystal structure of MJ0796 (PDB accession # 1F30) was generously provided by Dr. C.G. Nichols (Washington University, St. Louis, MO) and was used to visualize and predict the location and interactions of key regions and residues in the NBD1/2 dimer using Pymol software[45].

Biochemical Mg-ATPase assays

Four 681-bp-long fragments of NBD2 (encoding amino acids 1301–1528), containing either wild type (WT) SUR1 (S1369), WT SUR2A (K1337) or the mutants SUR1 (K1369) and SUR2A (S1337) were sub-cloned into pGEX-4T-1 GST fusion protein expression vectors. The recombinant plasmids were sequenced and then transformed into BL21 (DE3) cells for protein expression. The GST-NBD2 fusion proteins were detected with a monoclonal anti-GST-tag antibody (1:5000 dilution, Santa Cruz Biotechnology). Following purification, proteins (50 μg) were incubated at 40° C for 30 min followed by 1 hour incubation at 4° C to allow homogeneous dimerization of NBD2 monomers. All experiments were performed in an ATPase activity buffer at 37° C using ADP-free ATP (ATP-Gold DiscoverX, Fremont, CA) as a substrate. Mg-ATPase activities of NBD2 dimers were determined by monitoring ADP formation via coupling to production of the fluorescent product resorufin (ADP Quest, DiscoverX, Fremont, CA). Resorufin formation was continuously (λex 560 nm, λem 591 nm) in black 96-well plates in a SPECTRAmax Gemini XPS microplate spectrofluorometer (Molecular Devices, Sunnyvale, CA). Initial rates of resorufin formation were plotted vs. ATP concentration and data were fitted to a rectangular

hyperbola with the Michaelis-Menten equation to obtain V_{max} and K_M values. All values are given as mean ± S.E.M. Significance was calculated by unpaired two-tailed t-test.

Statistical analyses

Macroscopic K_{ATP} channel currents were normalized and expressed as changes in test current relative to control current. Macroscopic current analysis was performed using pClamp 10.0 (Axon Instruments, Foster City, CA) and Origin 6.0 software. Statistical significance was assessed using the unpaired Student's t test or one-way ANOVA with a Bonferroni post hoc test. $p<0.05$ was considered statistically significant. Data are plotted as the mean ± S.E.M.

4.3. Results

DZX stimulates glucose oxidation and suppresses fatty acid oxidation

Since AMPK is a central metabolic regulator[384] and its activation by DZX was altered in the absence of K_{ATP} channels[439], we sought to investigate how DZX altered cardiac metabolism as a result of AMPK activation and its relation to K_{ATP}. In our study, DZX increased glucose oxidation in both Kir6.2+/+ and Kir6.2-/- hearts (33% and 42% respectively, $p>0.05$) (Figure 4.1.A). It is worth mentioning that we have previously documented similar glucose oxidation rates in both groups under basal aerobic conditions. We have also previously demonstrated a 105% increase in fatty acid oxidation in Kir6.2-/- hearts, however, upon perfusion with DZX, fatty acid oxidation was suppressed by approximately 38%. In Kir6.2+/+ hearts, fatty acid oxidation was reduced by approximately 21% after DZX perfusion (Figure 4.1.B). Fatty acid oxidation-derived acetyl CoA was

reduced upon DZX-perfusion however that reduction was compensated by an increased acetyl CoA production derived from glucose oxidation. No significant difference in total acetyl coA production was observed at the end of the perfusions in both groups (Figure 4.1.C) (n=3, p>0.05).

No significant changes in LV work upon DZX treatment under basal conditions

Since DZX activates vascular K_{ATP} channels causing dilatation[98], we expected to see an increase in coronary flow in Kir6.2+/+ hearts. We did in fact observe a significant increase (98.3%) increase in coronary flow upon perfusion with DZX compared to the baseline rate, but as expected, that increase was not observed in Kir6.2-/- hearts (Figure 4.1.D).We decided to investigate whether DZX treatment was associated with positive changes in cardiac work under basal aerobic conditions. Our data show that left ventricular work was only slightly elevated upon perfusion with DZX in Kir6.2+/+ but that was not statistically significant from Kir6.2-/- (Figure 4.1. E) (n=3, p>0.05). Cardiac efficiency measured joules of LV work per μmol of acetyl coA produced per was slightly elevated in both groups upon DZX-perfusion, however, Kir6.2-/- were less efficient than Kir6.2+/+ when perfused with either vehicle or DZX (figure 4.1.F). Nevertheless, that slightly decreased efficiency exhibited by Kir6.2-/- hearts did not translate into worse poorer basal cardiac function.

AMPK activation by DZX is reduced in the absence of K_{ATP} channels

It has been previously documented that DZX-mediated preconditioning is lost in the absence of K_{ATP} channels[429]. We have previously shown that in the absence of K_{ATP} channels

basal AMPK activation is increased. Since activation of AMPK by DZX has been previously demonstrated by Kim et al.[439]. We speculated that DZX cardioprotection may be mediated via AMPK activation, therefore we decided to test whether AMPK phosphorylation was reduced in the absence of K_{ATP} channels. Our data show that in the absence of K_{ATP} channels DZX-mediated AMPK activation is approximately one sixth of that in Kir6.2+/+ hearts(Figure 4.2.A-B).(Fold change in Kir6.2+/+ and Kir6.2-/- hearts was 11.89 ± 4.241 and 1.561 ± 0.4061 respectively, p= 0.0362) (Figure 4.2.C)). We also tested the upstream kinase that phosphorylates AMPK, LKB1 and found that is followed the same activation pattern as AMPK (Figure 4.2.A-C) (Fold change in Kir6.2+/+ and Kir6.2-/- was 5.694 ± 1.594 and 0.7330 ± 0.3046 respectively, p= 0.0378) (Figure 4.2.D).

DZX activates cardiac Akt

Activation of the PI3K/Akt pathway has been suggested as the underlying preconditioning process by which DZX exerts its cardioprotective effect in neurons[431] and in heart tissue[432]. Additionally, Akt activation was shown to be mediated by AMPK[440]. Since our DZX in our hands activated AMPK in Kir6.2+/+ hearts and to a lesser extent in Kir6.2-/-, we investigated whether it would be able to exert the same activation pattern on the Akt pathway. Our results show that under basal conditions, the activation of Akt as indicated by its phosphorylation is higher in Kir6.2-/- hearts. Similar to the pattern that was observed with AMPK, activation of Akt by DZX was reduced in the absence of K_{ATP} channels (Figure 4.3.A-B), suggesting that AMPK may be controlling the activation of Akt, however, statistical significance was not reached(n=3, $p>0.05$). We examined inhibition of GSK-3β which is downstream of Akt via measuring its phosphorylation on serine 9[441,442].

Interestingly, we found that perfusion of Kir6.2+/+ hearts increased phosphorylation of GSK-3β, but even to a more significant extent in Kir6.2-/- hearts (Figure 4.3.A-C). Moreover, we examined other effectors that are downstream of Akt; mTOR and its substrate p70S6K^{443}. In our hands, we did not observe significant changes in phosphorylation of either proteins (Figure 4.4.A-C), however, it is possible that increasing the sample number could give us a clearer trend.

DZX has negligible effects on AMPK activation in SUR1 expressing cells

Since at the molecular level Mg-ATPase activity is distinct depending on SUR subunit, where it has been shown to be higher in SUR1 than in SUR2A[46], and that DZX is thought to increase Mg-ATPase activity[9,434,26], we decided to investigate whether stimulation with DZX would lead to activation of AMPK to a different extent than activation observed in the perfused hearts. We chose INS-1 cells and human pancreatic β-cells which express Kir6.2/SUR1 channels[14,15] to test DZX-mediated AMPK activation, predicting that the degree of AMPK activation would be higher in pancreatic islets. We did not see a significant difference between INS-1 cells treated with vehicle and treated with DZX (0.44 ± 0.023 and 0.47 ± 0.033 respectively) (Figure 4.5.A) nor in human pancreatic islets treated with vehicle and those treated with DZX (Figure 4.5.B) (0.73 ± 0.083 and 0.77 ± 0.054 respectively) (n=3, $p > 0.05$).

Predicted amino acid side chain interactions and their effects on Mg-ATPase activity

In an effort to probe for differential regulation of K_{ATP} channels, we decided to investigate its enzymatic Mg-ATPase properties. Our laboratory has previously shown that the side-chain of the S1369 residue may form a hydrogen bond with Q1372 and that the common genetic S1369A variant is predicted to demonstrate a loss of this interaction, leading to increases Mg-ATPase activity and K_{ATP} channel activation in pancreatic β-cells that may contribute to the observed increase in susceptibility to type 2 diabetes associated with this variant (2). These two residues are on opposite sides of a hairpin loop in the β-sheet forming the backbone of the NBD2 portion of the major catalytic Mg-ATPase site 2 in SUR1 (Figure 4.6.B). This initial work led us to speculate that the relative strength of the molecular interaction between the side chains at positions 1369 and 1372 may have an effect on the dynamic flexibility of the adjacent β-sheets and therefore influence Mg-ATPase activity in a predictive manner. Therefore, we hypothesized that an increase in the 1369-1372 side chain interaction strength would decrease flexibility and result in reduced Mg-ATPase activity, whereas a decrease in the 1369-1372 side chain interaction strength would result in increased flexibility and an increase in Mg-ATPase activity. In order to explore the effect of side chain interactions between residues 1369 and 1372, we used previously published predictions of adjacent β-sheet side chain interactions[444] to generate a panel of mutations at positions 1369 and 1372 in SUR1 (Table 4.1). We decided to generate mutations in these residues that we predicted would either 1) decrease side chain interaction and increase Mg-ATPase activity (A1369, A1372 and L1372), 2) have no effect on side-chain interaction or Mg-ATPase activity (Q1369, S1372, T1369 and Q1369/S1372) or 3) increase side chain interactions and

decrease Mg-ATPase activity (N1372, T1369/N1372 and K1369) (Table 4.1). WT or mutant SUR1 subunits were co-expressed with WT Kir6.2 subunits and the inside-out patch technique was used to measure macroscopic K_{ATP} channel currents in response to application of GTP that acts as a substrate for Mg-ATPase activity generating GDP that stimulates K_{ATP} channel activity. Therefore, an increased GTP response is a convenient way to measure Mg-ATPase activity by electrophysiology as, unlike ATP, GTP does not possess an inhibitory effect on channel function[167,434]. Based on predicted interaction values in Table 1, substitution of either residue with an alanine (A1369 or A1372) should result in a weaker interaction and a larger GTP response, indicative of increased Mg-ATPase activity. As predicted, removal of the side-chains with the A1369 and A1372 mutations each resulted in a significant increase in GTP-activated current when normalized to WT GTP-response, 163 ± 14% and 132 ± 4% respectively ($p<0.01$, Figure 4.6.B-D and F). To reduce interactions while maintaining side-chain length, we generated the L1372 mutation (Figure 4.6.E). As predicted, this mutation resulted in a significant increase in GTP-induced current (111 ± 4%) compared to WT ($p<0.01$, Figure 4.6.E, F). We then tested the effect of mutations that are predicted to possess similar side-chain interactions to WT (S1369 and Q1372) and not significantly alter the observed GTP-response (Table 1). The single mutations Q1369, S1372 and T1369 did not result in a significant change in GTP-induced K_{ATP} channel activity, 107 ± 4%, 107 ± 6% and 102 ± 3% respectively when compared to WT ($p>0.05$, Figure 4.7.A-C, E). The reversal of residues from S1369/Q1372 in WT SUR1 in the Q1369/S1372 double mutant did not produce any change in the GTP-response, 101 ± 9% ($p>0.1$, Figure 4.7.D and E). Finally, we investigated the N1372, T1369/N1372 and K1369 mutations that are predicted to increase the strength of the interaction between residues 1369 and 1372,

resulting in a decreased GTP-response. All three mutants, N1372, T1369/N1372 and K1369 resulted in a significant reduction in GTP-induced channel activity, 91 ± 3%, 89 ± 5% and 69 ± 3% respectively when compared to the WT response ($p<0.01$, Figure 4.8.A-D).

Disulfide trapping

To characterize further the side chain interactions taking place between residues in position 1369 and 1372, we employed a cysteine mutagenic strategy to evaluate the effects of reversible covalent bond formation between these two residues by generating a single SUR1 C1369 mutant (as control) and the double C1369/C1372 mutant pairing in SUR1 (Figure 4.9.). We utilized H_2O_2 (0.3%, 100 sec) as the oxidizing agent to promote disulfide bond formation between C1369 and C1372, with the disulfide-bond reducing agent DTT (10 mmol/l, 100 sec) being used to break the disulfide bond. Application of H_2O_2 did not result in a significant change in GTP-response in either WT SUR1 (S1369 and Q1372) or the single cysteine C1369 mutant SUR1 (Figure 4.9.A-B, D). However, when compared to the WT GTP-response, the GTP-response in the double cysteine mutant C1369/C1372 was significantly reduced from 176 ± 5% before H_2O_2 exposure to 130 ± 5% fold after H_2O_2 exposure ($p<0.01$, Figure 4.9.C and D). Application of DTT returned the GTP-response to values similar to those obtained prior to H_2O_2 exposure (167 ± 3%, Figure 4.9.C and D).

Mg-ATPase activity from NBD2 dimers

We decided to utilize a direct assay of Mg-ATPase activity in several selected GST-NBD2 protein dimers. Of particular interest is the large reduction in GTP-response observed in SUR1 K1369 mutant when compared to WT (S1369). Furthermore, sequence alignment of

the NBD2 catalytic region reveals that the only residue difference between SUR1 and SUR2A NBD2 is the presence of a lysine (K1337) in SUR2A at the homologous residue to S1369 in SUR1 (Figure 4.10.A). SUR1 and SUR2A containing channels also possess different properties including Mg-ATPase activity[42,445]. Therefore, we used a biochemical enzymatic assay to directly measure the Mg-ATPase activity in NBD2 dimers from WT SUR1 (S1369) and WT SUR2A (K1337) respectively, as well as from the reverse mutants SUR1 (K1369) and SUR2A (S1337) by generating the corresponding GST-NBD2 dimers. Since the relative concentrations of catalytically-active NBD2 dimers present in our assays were unknown, kinetic data from the Mg-ATPase assays could not provide useful information regarding differences in the measured V_{max} and the presence of a serine or lysine residue (Figure 4.10.B). However, the K_M values are significantly lower in NBD2 dimers containing a lysine residue such as the WT SUR2A K1337 (38 ± 6 μmol/l) and mutant SUR1 K1369 (30 ± 4 μmol/l) compared to the NBD2 dimers with a serine residue in the same position, WT SUR1 S1369 (135 ± 6 μmol/l) and the SUR2A S1337 mutant (160 ± 12 μmol/l). In order to determine what relevance these residues might play under similar conditions to those used in the electrophysiological assays, we replotted the Mg-ATPase activity observed at 0.1mmol/l ATP. These data suggest that the WT SUR1 S1369 and SUR2A S1337 NBD2s are working at rates below 50% of their V_{max} values at 0.1 mmol/l ATP (42.6 ± 0.3 % and 38.2 ± 1.8 % respectively, Figure 4.10.D), whereas, the presence of the positively charged lysine residue results in the WT SUR2A and mutant SUR1 (K1369) are functioning much closer to V_{max}, at 0.1 mmol/l ATP, 69.7 ± 1.0% and 79.0 ± 2.6 % (Figure 4.10.D).

The effect of a positively charged lysine residue at position 1369/1337 on DZX sensitivity and GTP-induced K_{ATP} channel activity

Previous work has suggested that the ability of DZX to evoke currents from the K_{ATP} channel is dependent on Mg-ATPase activity[114,435] and the SUR2A subunit is not activated by DZX unless ADP is also present[112]. Therefore, we investigated the role of the hairpin loop S1369 residue in SUR1 and its homologue, K1337 in SUR2A (Fig.ure 4.10.A) on the stimulatory effects of DZX. We observed a significantly reduced DZX-elicited K_{ATP} current in channels containing the WT K1337 SUR2A subunit ($p<0.05$, 1.28 ± 0.04) compared to the WT S1369 SUR1 subunit (2.10 ± 0.12) in our system (Figure 4.11.A-B and D,). Our data show that the introduction of a positively charged lysine residue at position 1369 (SUR1 K1369) significantly reduces the DZX-elicited K_{ATP} currents in the absence of ADP (1.41 ± 0.03), a value that is comparable to WT SUR2A K1337 (1.28 ± 0.04, Figure 4.11.A-D). Addition of 0.1 mmol/l ADP did not alter the magnitude of DZX-induced currents in WT SUR1 S1369 (Figure 4.11.A,D). However, exposure to ADP resulted in a significant increase in DZX-induced currents in both the mutant SUR1 K1369 and WT SUR2A K1337 containing K_{ATP} channels (Figure 4.11.B-D). The SUR1 K1369 single mutation appears to convert the DZX pharmacological profile of SUR1 containing K_{ATP} channels towards that of a SUR2A containing K_{ATP} channel phenotype. These results also suggest that the reduced effect of DZX and overt ADP-dependence in the SUR2A containing K_{ATP} channels may be due to the effects of the hairpin loop K1337 residue on intrinsic Mg-ATPase activity. Therefore, we investigated GTP-mediated increases in K_{ATP} channel currents and DZX sensitivity in WT SUR1 and mutant SUR1 K1369 containing K_{ATP} channels. Our results show that DZX significantly increases GTP-mediated K_{ATP} channel current in the WT SUR1

S1369 compared to GTP alone (2.83 ± 0.16 vs 1.86 ± 0.09, $p<0.01$, Figure 4.8A,D). However, introduction of the positively charged lysine residue at position 1369 (SUR1 K1369) results in a loss of this DZX-elicited increase in GTP-mediated K_{ATP} channel activity (1.36 ± 0.06 vs 1.23 ± 0.04, Figure4.8.B and D). For comparison, we also performed similar experiments in the SUR1 A1369 T2D susceptibility variant (2) and observed that DZX was still able to increase K_{ATP} current further in the presence of GTP (3.19 ± 0.10 vs 2.87 ± 0.07, $p<0.05$, Figure 4.12.C,D). Taken together, these data support the notion that Mg-ATPase activity is required for DZX-induced K_{ATP} current activation. To test this concept further, we performed DZX experiments in the absence of presence of the Mg-ATPase inhibitor BeF_x, an ATP γ–phosphate mimetic that is thought to maintain the catalytic region in its pre-hydrolytic conformation[446,447]. As expected, both WT SUR1 and WT SUR2A exhibited a significant decrease in DZX-elicited current in the presence of BeF_x (1.24 ± 0.02 vs 2.01 ± 0.08 and 1.05 ± 0.01 vs 1.27 ± 0.09 respectively, Figure 4.12.A-C). It should be noted that the overall magnitude of the decrease observed with BeF_x is substantially larger in SUR1 compared to SUR2A (Figure 4.12.E-G), indicating that SUR1 containing K_{ATP} channels possess greater intrinsic Mg-ATPase activity (compared to SUR2A).

Mg-ATPase activity is stimulated by mechanical stress

When investigating AMPK in Kir6.2+/+ and Kir6.2-/- hearts, we found that under higher afterload pressure (80 mmHg) (Figure 4.10.B), AMPK activation was similar in both groups. This is in contrast with our findings from hearts perfused in working mode at 50 mmHg afterload and hearts perfused in Langendorff mode (Figure 4.10.A). In this regard, An et al. have demonstrated that AMPK is activated to a greater extent in hearts perfused in

working mode compared to those retrogradely-perfused in Langendorff mode[75]. This led us to investigate if mechanical stress observed at higher workloads and activated AMPK was affected by Mg-ATPase activity. To test whether mechanical stress stimulated Mg-ATPase activity, we subjected transfected tsA201 cells to mechanical stress by applying vacuum in the presence of absence of BeF_2 which inhibits ATPase activity. Our results show that mechanical stress activates Mg-ATPase activity in tsA201 patches significantly compared to patches where activity was blocked by BeF_2 (Figure 4.10.C,D) (1.65 ± 0.09 and 1.20 ± 0.04 respectively, n = 9 patches, $p<0.001$).

4.4. Discussion

In the previous chapter, we have demonstrated that the absence of K_{ATP} channels increases fatty acid oxidation, which under basal conditions did not appear to pose a problem, however, in an ischemic episode would be detrimental[237]. DZX has been shown to mimic ischemic preconditioning[448,449,450], however that effect is lost in the absence of K_{ATP} channels[377] suggesting that this protection was mediated by K_{ATP} channels. Since efficient metabolism is essential in cardioprotection, and we have demonstrated that the metabolic profile is shifted towards fatty acid oxidation in Kir6.2-/- hearts (Figure 3.1.C on page 90 in Chapter 3) ,we investigated whether DZX changed cardiac metabolic rates under basal aerobic conditions. Our results show that DZX increased glucose oxidation to the same extent in Kir6.2+/+ and Kir6.2-/- hearts (Figure 4.1.A). In contrast, it modestly reduced fatty acid oxidation in Kir6.2+/+ (Figure 4.1.B) but significantly in Kir6.2-/-. Increasing glucose oxidation and reducing fatty acid oxidation is the favourable metabolic state should an ischemic insult occur since it reduces the uncoupling of glycolysis and glucose, reducing the incidence of intracellular acidosis and intracellular calcium accumulation as a result[382]. In our

study on the metabolic profile of Kir6.2-/- hearts, we attributed the increase in fatty acid oxidation to the increased basal AMPK activation observed in Kir6.2-/- hearts. In the present study, we expected to observe higher fatty acid oxidation rates as a result of further AMPK activation by DZX but contrary to our expectations, fatty acid oxidation rates were lower in groups treated with DZX and accordingly the resultant acetyl CoA derived from this process was lower. On the other hand, we did observe reduced DZX-mediated AMPK phosphorylation in Kir6.2-/- hearts compared to Kir6.2+/+ hearts, suggesting that K_{ATP} channels, contrary to the current understanding, are upstream of AMPK signaling.

The metabolic effects observed may also be K_{ATP}-independent as DZX has been shown to have several off-target effects as well[451]. DZX activation of PKCε which has been shown to subsequently reduce hypoxia-reoxygenation induced cell death in H9C2 cells[452]. PKC, as shown by Light et al. is a modulator of K_{ATP} channel activity through phosphorylation of the Kir6.2 subunit[453]. PKC has also been shown to activate Akt[454,455] which may explain why Akt phosphorylation levels were increased in DZX perfused Kir.2+/+ hearts. The phosphorylation of Akt was lost in Kir6.2-/- hearts suggesting that the presence of K_{ATP} channels is essential in its activation (Figure 4.3.A,B). Acute activation of Akt was shown to increase glucose uptake through promoting translocation of GLUT4 to the plasma membrane [456] and this may explain why glucose oxidation rates were higher upon perfusion with DZX in Kir6.2+/+. Due to reduced Akt phosphorylation in Kir6.2-/- hearts perfused with DZX, we expected to see lower glucose oxidation, however the rates were similar to those of DZX-perfused Kir6.2+/+ hearts (Figure 4.1.A).We however found that the inhibitory phosphorylation of GSK-3β which is a downstream effector of Akt was higher in Kir62-/- hearts perfused with DZX (Figure 4.3.C) indicating a high activity of Akt. Inhibition

of GSK-3β by phosphorylation at Ser 9 promotes glycogen synthesis through facilitating dephosphorylation and activation of glycogen synthase[457]. Therefore we speculate that the glycogen content in DZX-perfused Kir6.2-/- hearts would be higher as a result, however, it that was not measured in this study. It is possible that it is due to the protein phosphatase 2A (PP2A) activity which may be responsible for dephosphorylation of GSK-3β[458]. This would be an interesting target to measure since changes in PP2A activity in Kir6.2-/- mice have not been reported yet. mTOR phosphorylation and that of its substrate P70S6K was also investigated as part of the PI3K/Akt/mTOR pathway, but our data show that the phosphorylation pattern did not correlate with Akt phosphorylation. In our hands, the use of DZX increased mTOR and P70S6K phosphorylation compared to vehicle-perfused hearts and to a greater extent in Kir6.2-/- hearts (Figure 4.4.A-C) suggesting again that the effects seen by DZX may be due its action on the PI3K/Akt pathway It is worth mentioning that DZX has been shown to have direct mitochondrial effects as it inhibits succinate dehydrogenase in cardiac mitochondria[459,460] and this inhibition has been associated with cardiac preconditioning-like protection attributed to uncoupling of oxidative phosphorylation[461,462].

Since we observed disrupted DZX-AMPK phosphorylation in Kir6.2+/+ and Kir6.2-/- hearts, we decided to investigate whether DZX could activate AMPK differently in INS-1 cells and human islets which express the Kir6.2/SUR1 channel combination. We predicted that due to the higher intrinsic Mg-ATPase activity in SUR1, we would see a higher degree of AMPK activation compared to SUR2A containing cardiac tissue. Contrary to our expectation, we did not observe an increase in AMPK activation, in fact, it was comparable to that of vehicle-treated islets (Figure 4.5.A,B). Though the result still suggests distinct

signaling in SUR1 and SUR2A, it is hard to pinpoint whether AMPK was as high as in untreated islets due to reduced dephosphorylation by Ser/Thr phosphatases. The effect of DZX on the phosphatases that modulate AMPK activity has not been reported but would be an interesting area for future studies.

Aside from physically associating to AMPK, K_{ATP} channels were shown to bind to the phosphotransfer enzymes AK1 and CK, which are sensitive to subtle changes in local nucleotide concentrations[47–49]. This change in the adenine nucleotide concentration in the vicinity of the channel may occur due to the intrinsic enzymatic Mg-ATPase activity, bestowed upon the channel by the SUR subunit. Although it is an important component of the appropriate nucleotide regulation of K_{ATP} channel activity, the molecular mechanisms that govern Mg-ATPase activity are not fully understood. Molecular insights into the importance of this mechanism can be taken from a previous study on the rare heterozygous SUR1 gene (*ABCC8*) mutations R1380L and R1380C that cause neonatal diabetes via increases in Mg-ATPase activity[158]. In silico homology modeling of the catalytic Mg-ATPase regions in SUR1 places R1380 within the predicted major Mg-ATPase catalytic site in nucleotide binding domain 2 (NBD2) increasing Mg-ATPase activity and rendering the K_{ATP} channel markedly less sensitive to Mg-ATP inhibition compared with free ATP inhibition and leading to severely impaired insulin secretion in the afflicted patients[158]. Furthermore, we have recently shown that residue 1369 also regulates Mg-ATPase activity[167], providing a plausible mechanism by which the type 2 diabetes susceptibility variant S1369A in SUR1 may suppress insulin secretion in humans homozygous for the risk variant haplotype E23K/S1369A[463]. The SUR1 NBD1/2 dimer homology model[45] places residue 1369 adjacent to a hairpin loop in the β-sheet that forms the backbone of the NBD2 portion of the major

Mg-ATPase catalytic site 2 (Figure 4.7.B). Therefore, substitution of serine with an alanine at residue 1369 (S1369A) may alter the structure and/or flexibility of this region, leading to an increase in Mg-ATPase activity of the K_{ATP} channel. We further speculated that the side chain of S1369 might form a hydrogen bond with the terminal -NH_2 group on the side chain of Q1372 (Figure 4.7.B). This hydrogen bond would likely constrain the structure of the hairpin loop and the beta-sheet adjacent to the major Mg-ATPase activity in NBD2 (Figure 4.7.B). Substitution of the serine with an alanine at position 1369 (A1369) removes only the side-chain terminal hydroxyl group that would remove the ability to hydrogen-bond with Q1372 and reduce a putative structural constraint on the hairpin loop, resulting in the observed increases in Mg-ATPase activity.

Our results (Figures 4.6-4.8) provide key evidence that the interaction between the side chains of residues 1369 and 1372 is a key determinant of intrinsic K_{ATP} channel Mg-ATPase activity and that the side-chain interaction strength is inversely related to K_{ATP} channel Mg-ATPase activity, with a stronger interaction resulting in weaker enzymatic activity. Interestingly, we observed the greatest reduction in Mg-ATPase activity in K_{ATP} channels containing the SUR1 K1369 mutation (Figure 4.8.C,D). As NBD2 is the major catalytic region of the channel complex, we performed a sequence alignment of NBD2 between all SUR isoforms; SUR1, 2A and 2B (Figure 4.7.A). The only amino acid difference between these isoforms is the presence of a serine at residue 1369 in SUR1, whereas the analogous residue in SUR2A and 2B is a lysine at residue 1337. As there are documented differences in both Mg-ATPase activity and DZX sensitivity[26,464,465] we determined whether this single amino acid change from a serine to a lysine is responsible for these observed differences using a direct biochemical assay of NBD2 Mg-ATPase activity. We observed no

differences in absolute V_{max} values in any of the NBD2 constructs Figure 4.10.B), however, absolute V_{max} values are determined both by k_{cat} values and by the concentration of fully formed catalytically functional NBD2 dimers in each experimental group. As we are unable to determine the precise concentration of active dimers in our assays, the V_{max} values obtained cannot be used to compare the effects of mutations on k_{cat} values in the NBD2s tested. However, as K_M values are independent of the concentration of functional NBD2 dimers present, and since the Mg-ATPase activity meets the requirements of rapid equilibrium behavior[466], we can use this parameter to glean information on binding affinity of ATP for the Mg-ATPase active site. The observed decrease in K_M values in NBD2 dimers containing a lysine residue at 1369 (SUR1) or 1337 (SUR2A), suggests that the presence of a positively charged lysine residue results in a higher Mg-ATPase activity at lower ATP concentrations by virtue of a higher affinity for ATP as observed previously[467,468].

Our results demonstrate that the serine to lysine single amino acid switch at residue 1369 in SUR1 converts the K_{ATP} channel's DZX sensitivity over to that observed in wild-type SUR2A-containing channels that require ADP to be present in order to observe DZX stimulation (Figure 4.11.). Furthermore, our results also demonstrate that intrinsic Mg-ATPase activity is required to elicit the full DZX stimulatory response (Figure 4.12). We speculate that the positively-charged side-chain of K1337 in SUR2A may electrostatically attract the negatively-charged phosphate groups on ATP, leading to an increased local concentration of ATP within the catalytic site of NBD2 and account the observed decrease in K_M values (Figure 4.10.). Furthermore, it has been previously been suggested that the ADP-dependence of DZX actions in SUR2A-containing channels is due to the requirement for ADP-binding to lock the NBD2 region in a post-hydrolytic state rendering channels sensitive

to DZX's actions[43]. If this is indeed the case, then the requirement for ADP may result from a direct interaction between the positively charged side-chain of K1337 and the negatively charged phosphate groups on the ADP moiety. As SUR1-containing channels possess a serine at the analogous NBD2 residue in SUR1 (S1369, Figure 4.10.A), this putative electrostatic interaction is lost, resulting in the observed higher K_M values and the ADP-independent DZX stimulatory effect (Figures 4.10-4.12).

Our data also show for the first time that mechanical stress is capable of activating Mg-ATPase activity of cardiac K_{ATP} channels. This is particularly important given that the mechanical stretch has been shown to provide protection similar to ischemic preconditioning[332,469,470]. Since mechanical stress has been shown to activate AMPK[471,472], it would be interesting to test whether AMPK signaling would be altered in the absence of stretched Kir6.2-/- hearts in comparison to Kir6.2+/+ hearts.

In summary, in this study we demonstrate 1) distinct DZX-induced AMPK activation in SUR1 and SUR2A expressing K_{ATP} channels, 2) suppression of fatty acid oxidation by DZX, 3) prediction of Mg-ATPase activity of K_{ATP} channels based on the strength of the side-chain interaction between residues 1369 and 1372 in SUR1, 4) that flexibility within the hairpin-loop region proximal to the major NBD2 catalytic site is an important determinant of intrinsic Mg-ATPase activity, 5) that the different sensitivity to the clinically used drug DZX between SUR isoforms seems to be largely determined by a single amino acid in NBD2 and 6) stimulation of Mg-ATPase activity by mechanical stress. Our findings therefore provide novel mechanistic insights into the structural determinants that contribute to K_{ATP} channel activity, common genetic diabetes risk variants and pharmacology.

Figure 4.1. Effects of DZX on cardiac metabolism, work and efficiency in Kir6.2+/+ and Kir6.2-/-. Values for glucose (A) and fatty acid (B) oxidation rates measured as (μmol/g dry wt/min) in Kir6.2+/+ and Kir6.2-/- perfused with vehicle or with 100 μM DZX at minute 40 of the working heart perfusions. (C) Left ventricular (LV) work expressed as Joules normalized to dry heart weight and (D) Coronary flow expressed as ml/min. Values expressed are means ± SEM as calculated by repeated measures two-way ANOVA with Bonferroni post hoc test. Values for acetyl CoA production (E) and cardiac efficiency (F) Black bars represent baseline values and white bars represent values upon DZX treatment. (n=3/group, **, $p<0.05$)

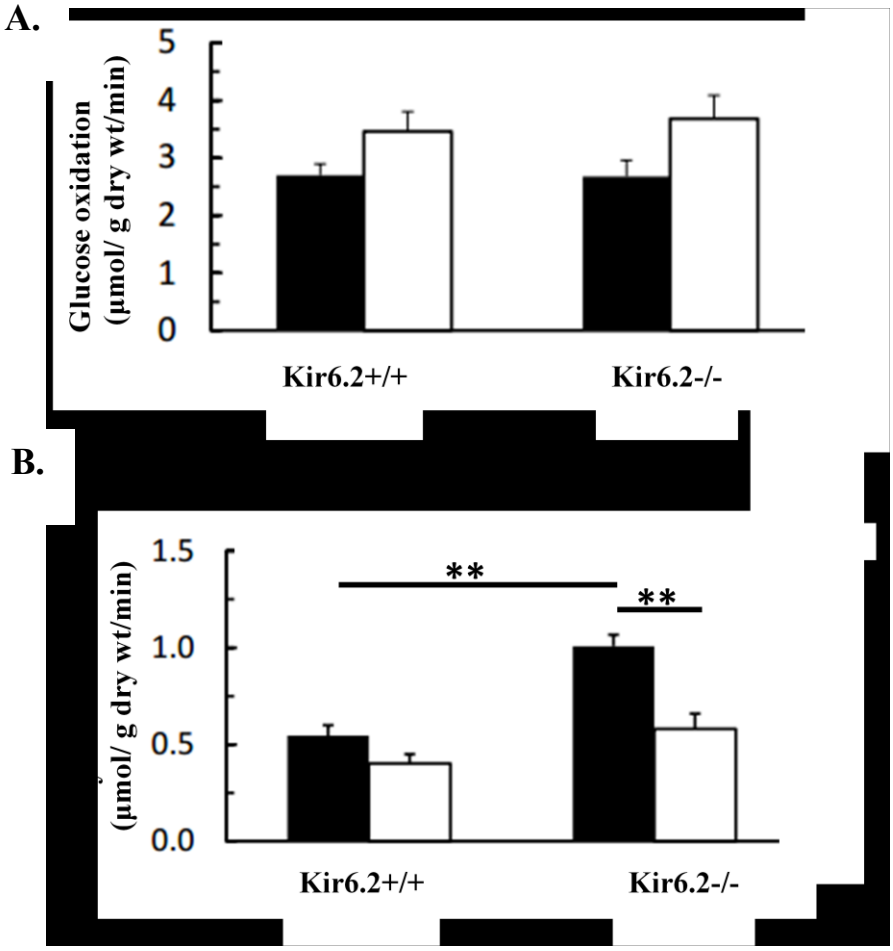
A.
Glucose oxidation (µmol/ g dry wt/min)
5
4
3
2
1
0
Kir6.2+/+
Kir6.2-/-
B.
(µmol/ g dry wt/min)
1.5
1.0
0.5
0.0
**
**
Kir6.2+/+
Kir6.2-/-

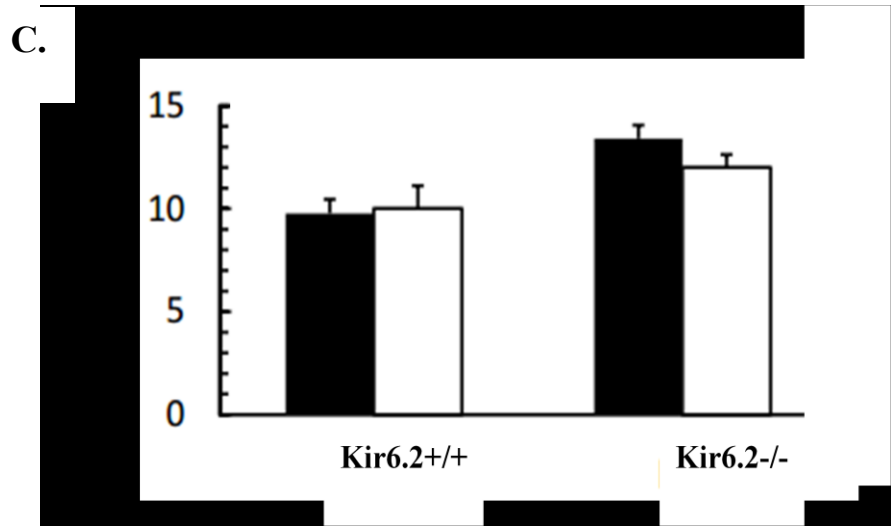
C.
15
10
5
0
Kir6.2+/+
Kir6.2-/-

D.

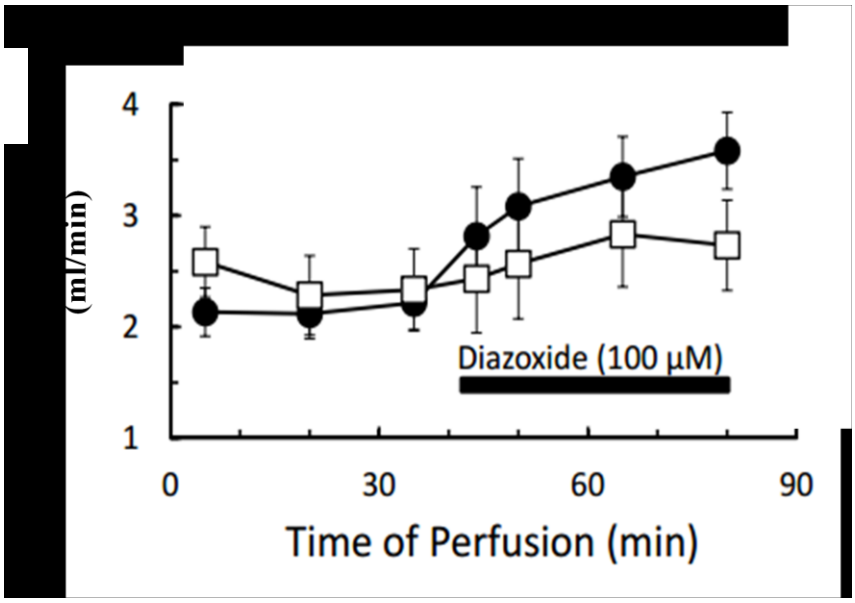
4
3
2
1
(ml/min)
Diazoxide (100 µM)
0
30
60
90
Time of Perfusion (min)

E.

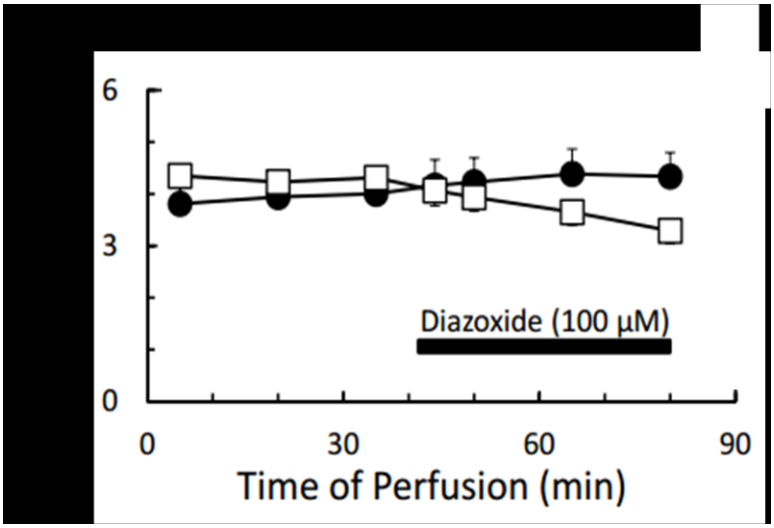
6
3
0
Diazoxide (100 µM)
0
30
60
90
Time of Perfusion (min)

F.

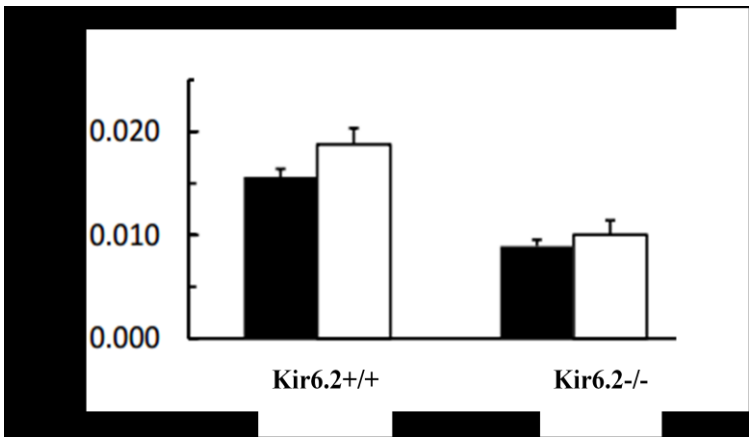
0.020
0.010
0.000
Kir6.2+/+
Kir6.2-/-

Figure 4.2. AMPK activation by DZX is impaired in the absence of K_{ATP} channels.

(A) Representative immunoblots of AMPK and LKB1 phosphorylation in Kir6.2+/+ and Kir6.2-/- hearts perfused with either vehicle or 100 uM DZX in Langendorff mode. (B) Graphical representation of phosphorylated AMPK normalized to total AMPK in Kir6.2+/+ and Kir6.2-/- hearts treated with either vehicle or 100 uM DZX. (n=3/group, * $p<0.05$, **, $p < 0.01$, ***, $p< 0.001$) (C) Graphical representation of phosphorylated LKB1 normalized to total LKB1 in Kir6.2+/+ and Kir6.2-/- hearts treated with either vehicle or 100 uM DZX. (n=3/group, * $p<0.05$) (D) Comparison of fold change in AMPK and LKB1 phosphorylation by DZX in Kir6.2+/+ and Kir6.2-/- (*, $p<0.05$)

A.

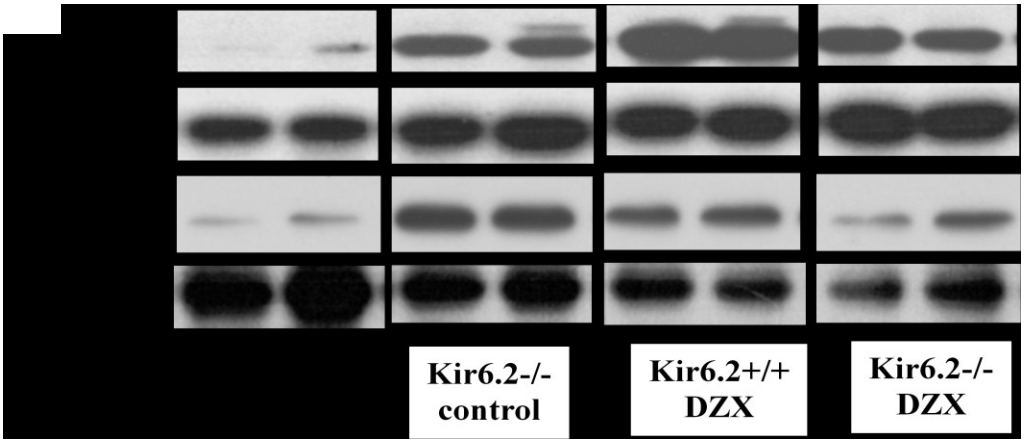
Kir6.2-/-
control
Kir6.2+/+
DZX
Kir6.2-/-
DZX

B.

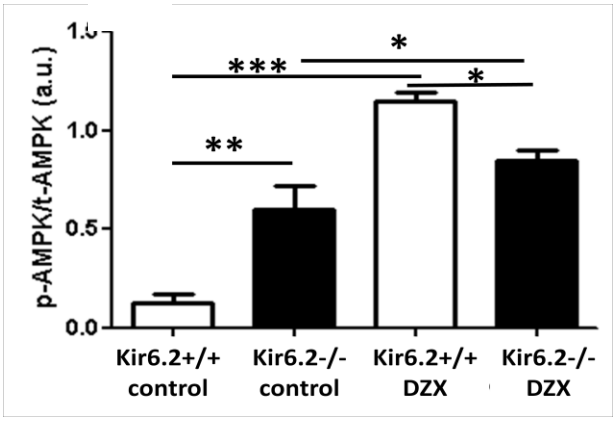
p-AMPK/t-AMPK (a.u.)
1.0
0.5
0.0
**
***
*
*
Kir6.2+/+
control
Kir6.2-/-
control
Kir6.2+/+
DZX
Kir6.2-/-
DZX

C.

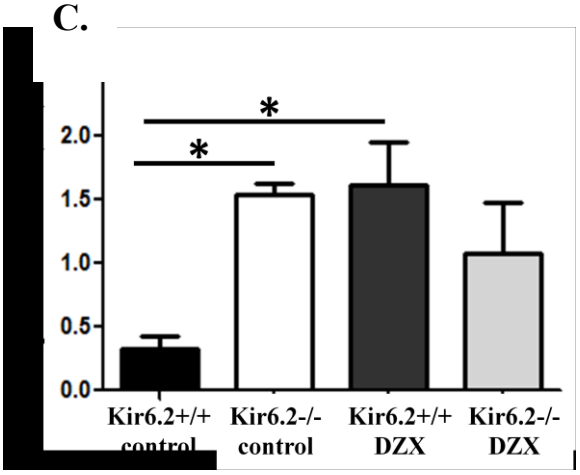
2.0
1.5
1.0
0.5
0.0
*
*
Kir6.2+/+
control
Kir6.2-/-
control
Kir6.2+/+
DZX
Kir6.2-/-
DZX

D.

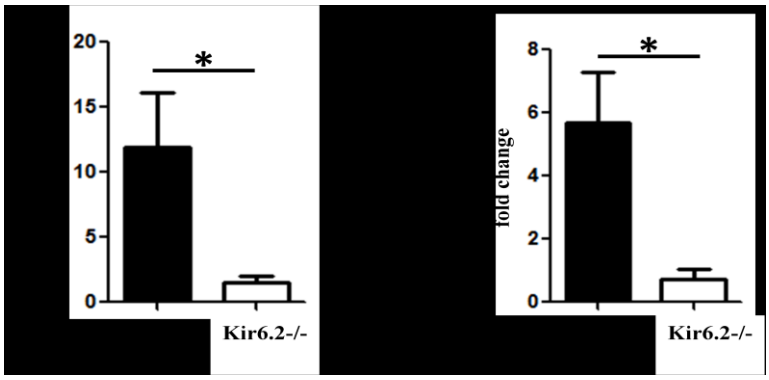
20
15
10
5
0
*
Kir6.2-/-
fold change
8
6
4
2
0
*
Kir6.2-/-

Figure 4.3. Activation of Akt and GSK-3β by DZX (A) Representative immunoblots showing phosphorylation of Akt and it downstream target glycogen synthase kinase (GSK)-3β in Kir6.2+/+ and Kir.2-/- heart ventricles treated with either vehicle or 100 uM DZX. (B) Graphical representation of phosphorylated Akt (Ser 473) normalized to total Akt showing increased basal phosphorylation in Kir6.2-/- heart ventricles and in Kir6.2+/+ hearts upon treatment with DZX but reduced phosphorylation in Kir6.2-/- heart ventricles treated with 100 uM DZX ($n=4$, $p>0.05$).. (C) Graphical representation of phosphorylated GSK-3β (Ser 9) normalized to GSK-3β also showing a significant increase in phosphorylation i.e. inhibition upon treatment with DZX in both Kir6.2+/+ and Kir6.2-/-. ($n=4$, $p<0.05$).

A.

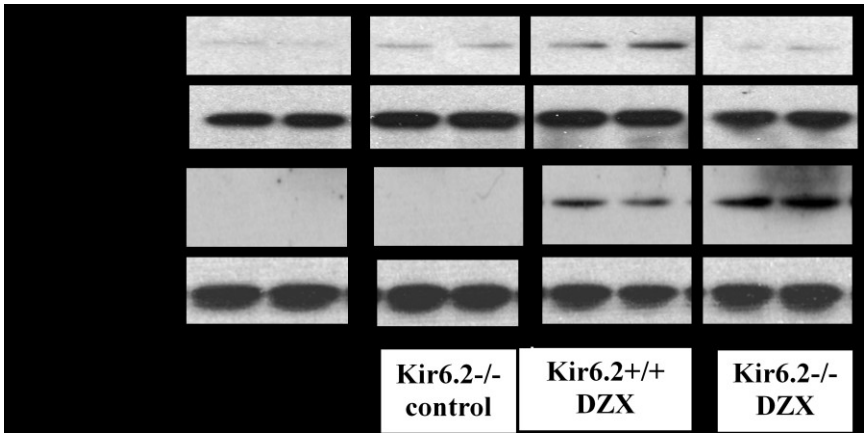
Kir6.2-/-
control
Kir6.2+/+
DZX
Kir6.2-/-
DZX

B.

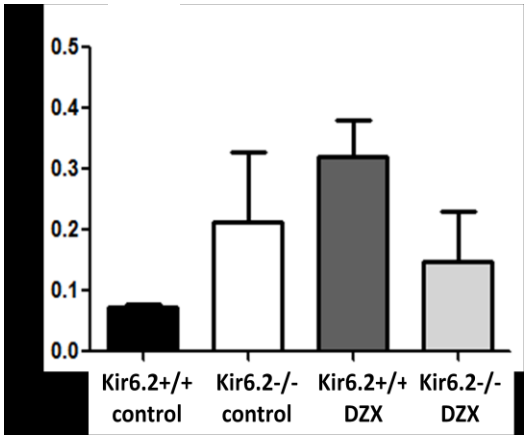
0.5
0.4
0.3
0.2
0.1
0.0
Kir6.2+/+
control
Kir6.2-/-
control
Kir6.2+/+
DZX
Kir6.2-/-
DZX

C.

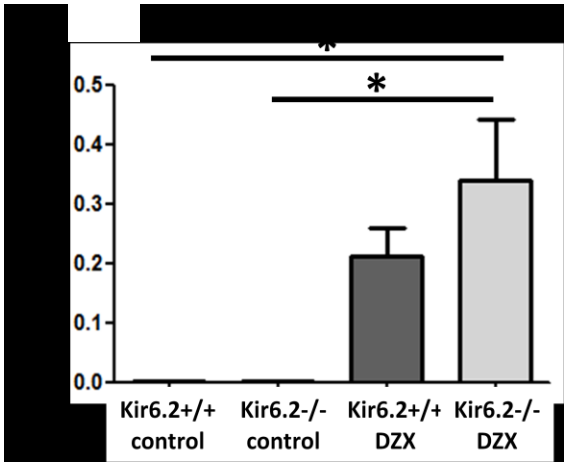
*
*
0.5
0.4
0.3
0.2
0.1
0.0
Kir6.2+/+
control
Kir6.2-/-
control
Kir6.2+/+
DZX
Kir6.2-/-
DZX

Figure 4.4. Effects of DZX on mTOR and p70S6K in Kir6.2+/+ and Kir6.2-/-hearts

(A) Representative immunoblots showing phosphorylation of mTOR and p70S6K in Kir6.2+/+ and Kir.2-/- heart ventricles treated with either vehicle or 100 uM DZX. (B) Graphical representation of phosphorylated mTOR normalized to total mTOR showing a trend towards increased phosphorylation upon treatment with DZX. (C) Graphical representation of phosphorylated p70S6K normalized to p70S6K also showing a trend towards increased phosphorylation upon treatment with DZX. ($n=4$, $p>0.05$).

A.

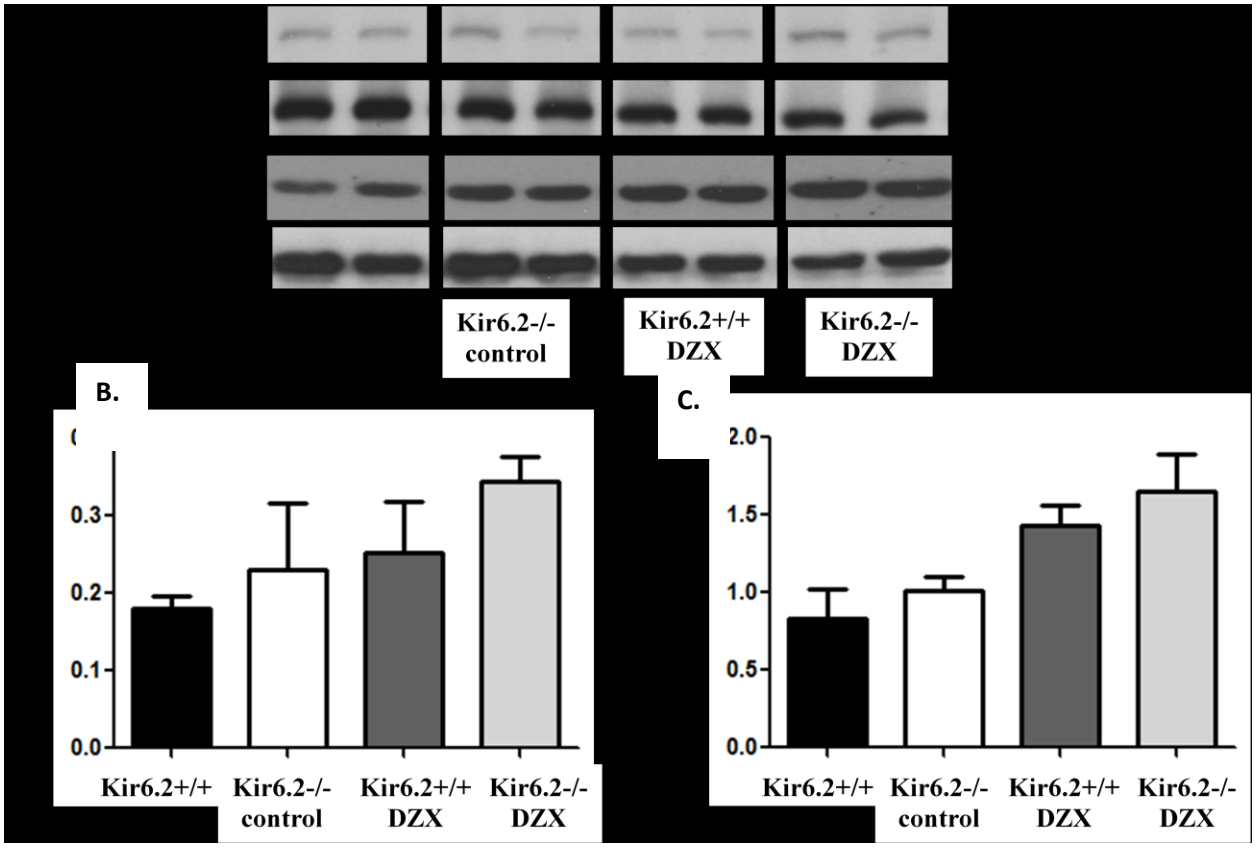
Kir6.2-/- control
Kir6.2+/+ DZX
Kir6.2-/- DZX
B.
0.3
0.2
0.1
0.0
Kir6.2+/+
Kir6.2-/- control
Kir6.2+/+ DZX
Kir6.2-/- DZX
C.
2.0
1.5
1.0
0.5
0.0
Kir6.2+/+
Kir6.2-/- control
Kir6.2+/+ DZX
Kir6.2-/- DZX

Figure 4.5. Effect of DZX on AMPK activation in INS-1 cells and human pancreatic islets (A) Representative immunoblot showing similar activation of AMPK in INS-1 cells treated with vehicle or 100uM DZX and graphical representation of phosphorylated AMPK normalized to total AMPK in both groups (n= 4/group, $p>0.05$). (B) Representative immunoblot showing similar activation of AMPK in human pancreatic islets incubated with vehicle or 100 uM DZX and graphical representation of phosphorylated AMPK normalized to total AMPK in both groups (n= 3/group, $p>0.05$).

A.

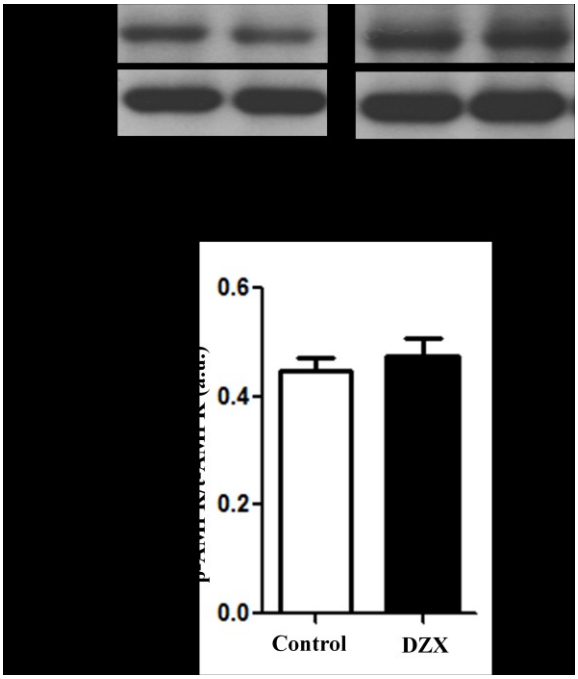

B.

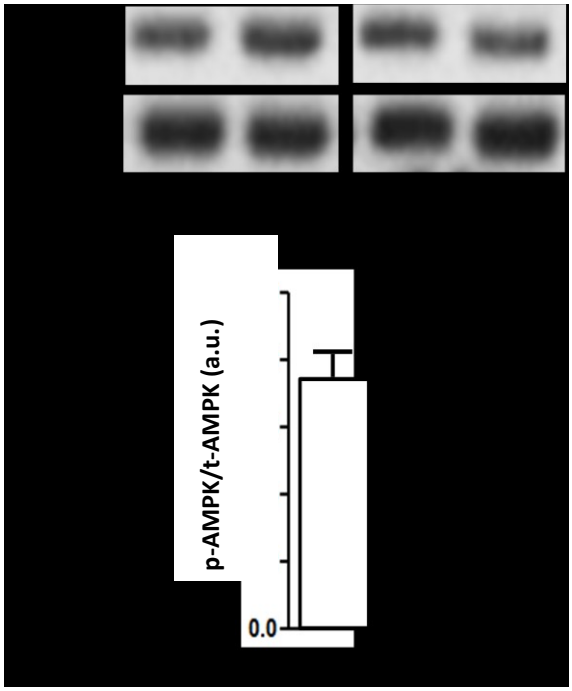

Table 4.1. Estimation of amino acid side chain interactions**.** Predicted strengths of amino acid side chain interactions. Values are based on amino acid pairing preferences in parallel β-sheets of proteins by Fooks et al.[444]

Position 1369 (side chain radii Å)	**Position 1372 (side chain radii Å)**	**Mutation(s) tested**	**Interaction value (change relative to WT)**	**Predicted change in I_{MgGTP} (relative to WT)**
(S) Serine (0.71)	(Q) Glutamine (1.86)	WT	1.5 (None)	(None)
(A) Alanine (0.00)	(Q) Glutamine (1.86)	A1369(risk)	0.9 (decrease)	Increase
(S) Serine (0.71)	(A) Alanine (0.00)	A1372	0.8 (decrease)	Increase
(S) Serine (0.71)	(L) Leucine (1.64)	L1372	0.8 (decrease)	Increase
(Q) Glutamine (1.86)	(Q) Glutamine (1.86)	Q1369	1.4 (no change)	None
(S) Serine (0.71)	(S) Serine (0.71)	S1372	1.5 (no change)	None
(T) Threonine (1.33)	(Q) Glutamine (1.86)	T1369	1.5 (no change)	None
(Q) Glutamine (1.86)	(S) Serine (0.71)	Q1369/S1372	1.5 (no change)	None
(S) Serine (0.71)	(N) Aspargine (1.59)	N1372	1.9 (increase)	Decrease
(T) Threonine (1.33)	(N) Aspargine (1.59)	T1369/N1372	3.0 (increase)	Decrease
(K) Lysine (2.27)	(Q) Glutamine (1.86)	K1369	2.2 (increase)	Decrease

Figure 4.6. Amino acid substitutions resulting in a significant increase in GTP-induced K_{ATP} channel current. (A) In silico model of the hairpin loop in the β-sheet region proximal to the Mg-ATPase activity site 2 in NBD2. The hydroxyl group on the side-chain of residue S1369 is predicted to form a hydrogen bond with the terminal NH_2 group of the side-chain on the glutamine at position 1372 (Q1372). Dotted line denotes the hydrogen bond. (B-E) stimulation of K_{ATP} channels via the application of 0.1 mmol/l ATP and 1mmol/l GTP in the WT (S1369/Q1372) and A1369, A1372 and L1372 mutant SUR1 K_{ATP} channels respectively. F, Grouped data of normalized GTP-stimulated K_{ATP} channel current. n = 10-17 patches per group, * denotes $P<0.01$.

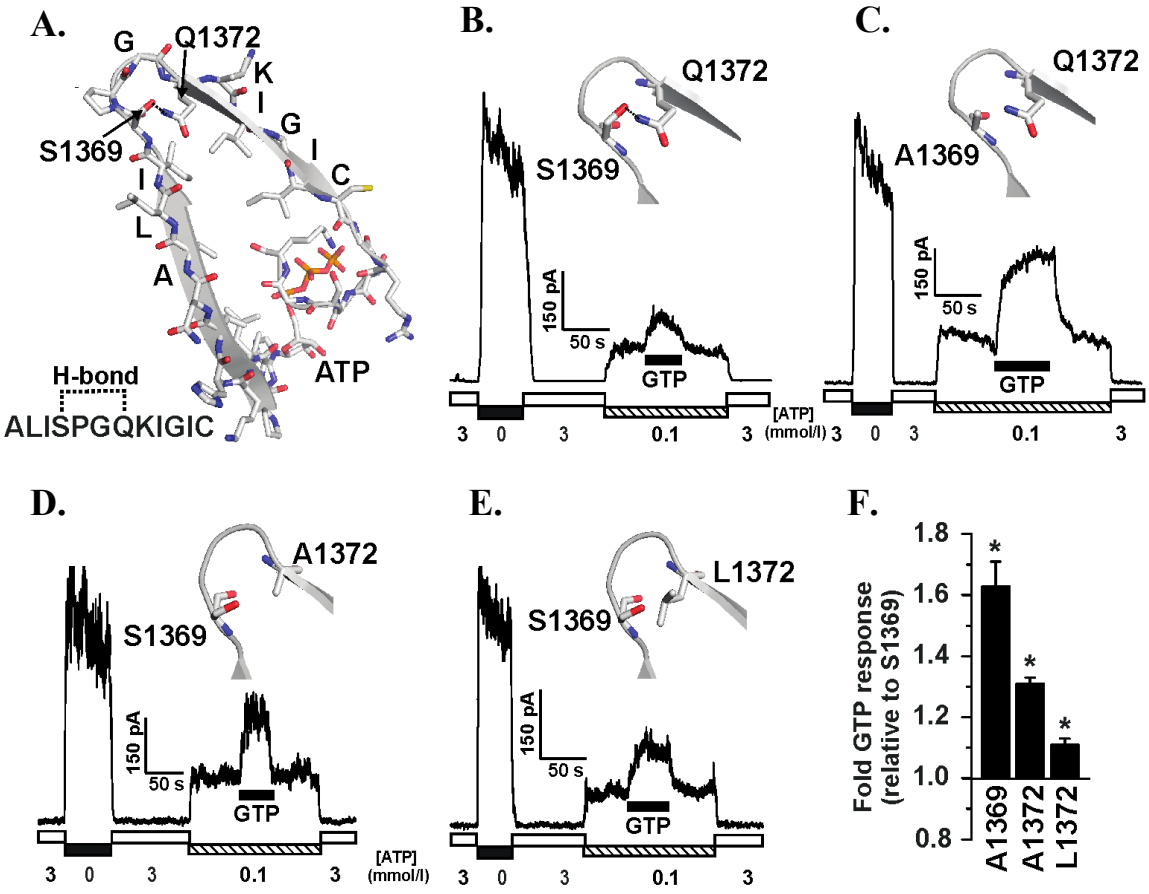
A.
G
Q1372
K
I
G
I
C
S1369
I
L
A
H-bond
ATP
ALISPGQKIGIC
B.
Q1372
S1369
150 pA
50 s
GTP
3 0 3 0.1 3
[ATP] (mmol/l)
C.
Q1372
A1369
150 pA
50 s
GTP
3 0 3 0.1 3
D.
A1372
S1369
150 pA
50 s
GTP
3 0 3 0.1 3
[ATP] (mmol/l)
E.
L1372
S1369
150 pA
50 s
GTP
3 0 3 0.1 3
F.
Fold GTP response (relative to S1369)
1.8
1.6
1.4
1.2
1.0
0.8
*
*
*
A1369
A1372
L1372

Figure 4.7. Amino acid substitutions that do not significantly alter GTP-induced K_{ATP} channel current. (A-D) stimulation of K_{ATP} channels via the application of 0.1 mmol/l ATP and 1mmol/l GTP in the Q1369/Q1372, S1369/S1372, T1369 and Q1369/S1372 mutant SUR1 K_{ATP} channels respectively. (E) Grouped data of normalized GTP-stimulated K_{ATP} channel current. (n = 5-7 patches per group).

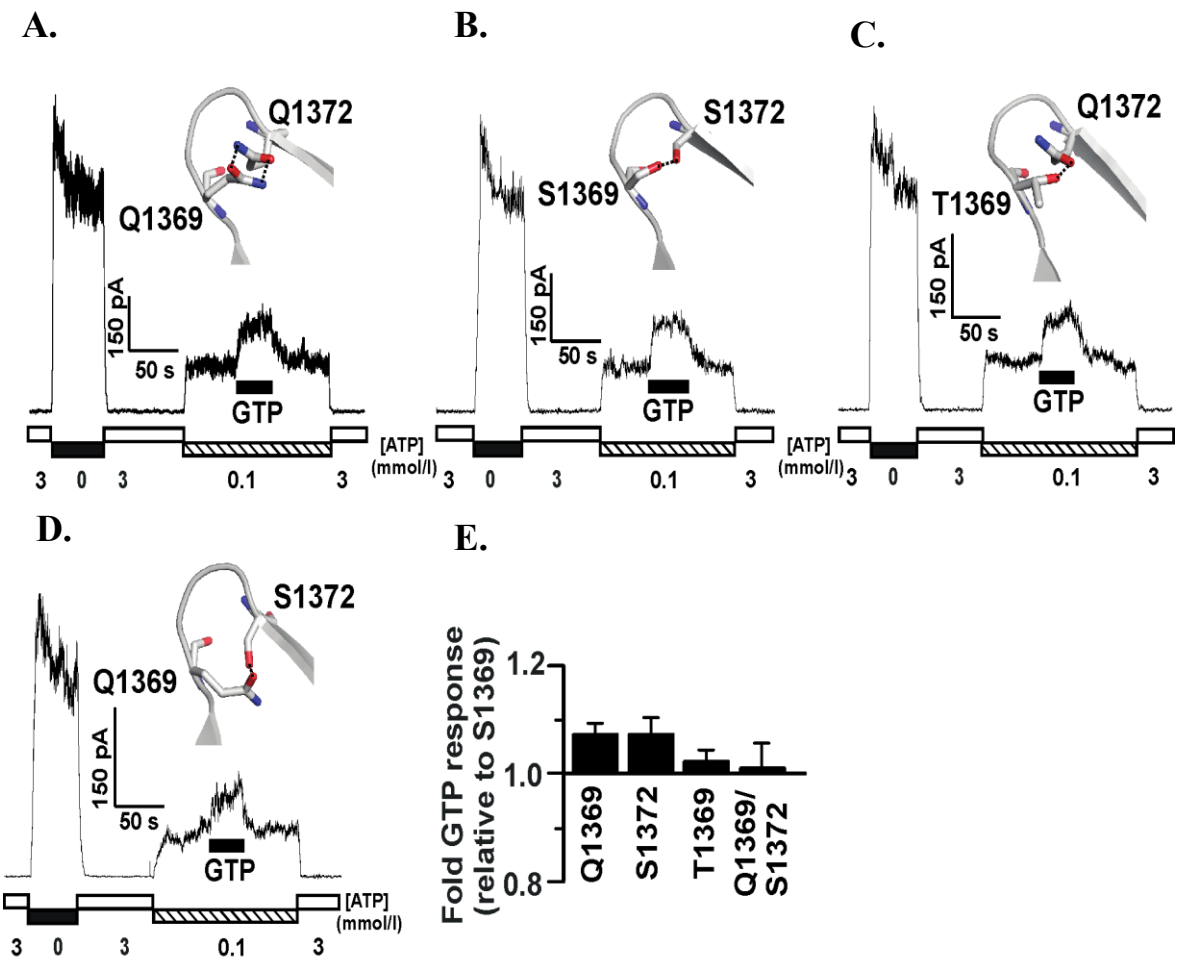
A.
Q1372
Q1369
150 pA
50 s
GTP
[ATP]
(mmol/l)
3 0 3 0.1 3
B.
S1372
S1369
150 pA
50 s
GTP
[ATP]
(mmol/l)
3 0 3 0.1 3
C.
Q1372
T1369
150 pA
50 s
GTP
[ATP]
(mmol/l)
3 0 3 0.1 3
D.
S1372
Q1369
150 pA
50 s
GTP
[ATP]
(mmol/l)
3 0 3 0.1 3
E.
Fold GTP response
(relative to S1369)
1.2
1.0
0.8
Q1369
S1372
T1369
Q1369/
S1372

Figure 4.8. Amino acid substitutions resulting in a significant decrease in GTP-induced K_{ATP} channel current**. (**A-C) Stimulation of K_{ATP} channels via the application of 0.1 mmol/l ATP and 1mmol/l GTP in the N1369, N1369/T1372 and K1369 mutant SUR1 K_{ATP} channels respectively. (D) Grouped data of normalized GTP-stimulated K_{ATP} channel current. (n = 6-14 patches per group). * denotes $P<0.01$.

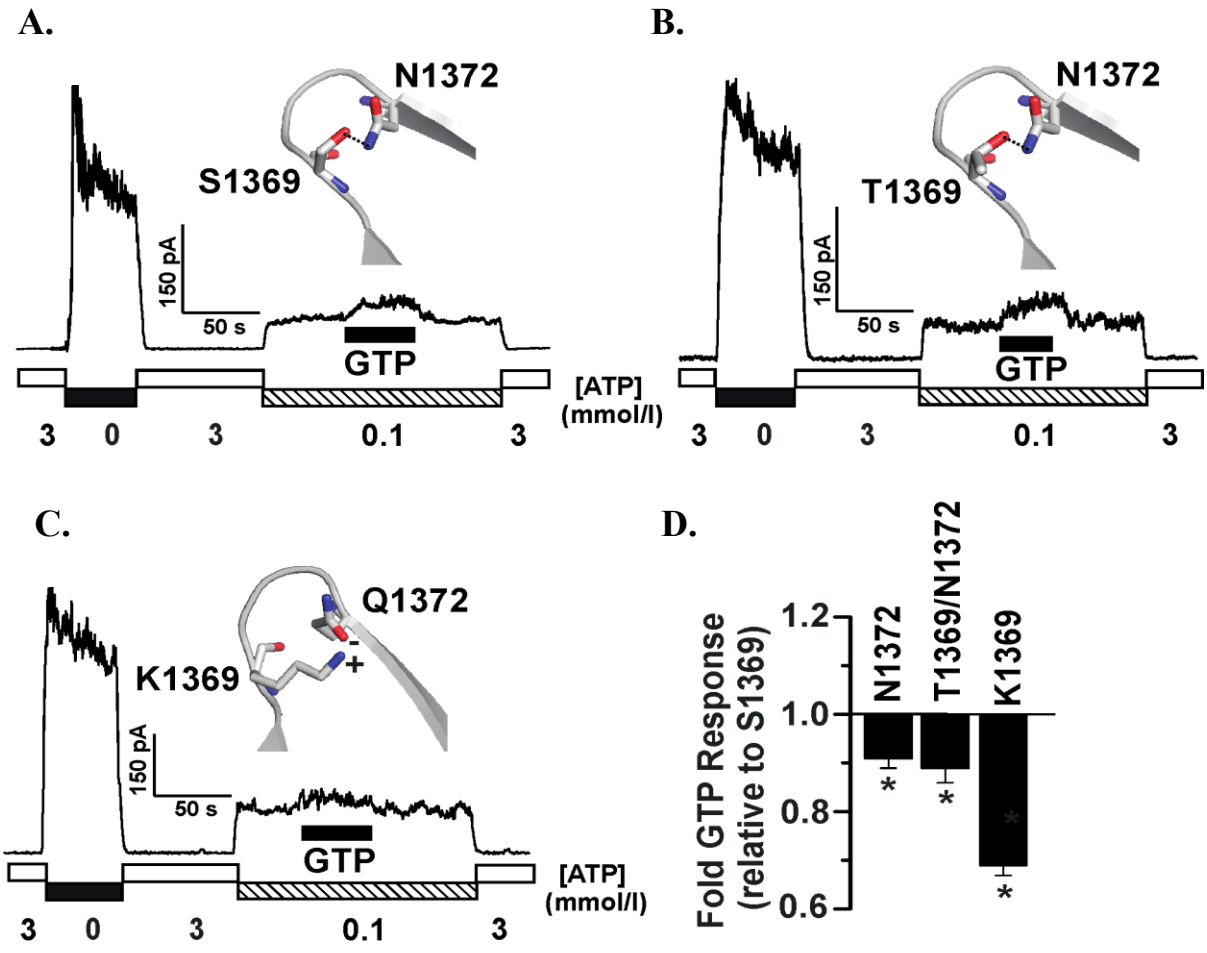
A.
N1372
S1369
150 pA
50 s
GTP
[ATP]
(mmol/l)
3 0 3 0.1 3
B.
N1372
T1369
150 pA
50 s
GTP
3 0 3 0.1 3
C.
Q1372
K1369
150 pA
50 s
GTP
[ATP]
(mmol/l)
3 0 3 0.1 3
D.
Fold GTP Response
(relative to S1369)
1.2
1.0
0.8
0.6
N1372
T1369/N1372
K1369
*
*
*

Figure 4.9. Disulfide bond formation decreases GTP-induced K_{ATP} channel function in a reversible manner. (A-B) stimulation of K_{ATP} channels via the application of 0.1 mmol/l ATP and 1mmol/l GTP in the WT S1369/Q1372 and C1369 single cysteine mutant SUR1 K_{ATP} channels respectively. Exposure to 0.3% H_2O_2 did not result in a significant change in current magnitude. (C) Exposure to 0.3% H_2O_2 significantly reduces GTP-stimulated current of the double cysteine SUR1 mutant C1369/C1372. Current is restored to previous value following application of 10 mmol/l DTT and disulfide bond reduction. (D) Grouped data of normalized GTP-stimulated K_{ATP} channel current (n = 4-9 patches per group). * denotes $P<0.01$

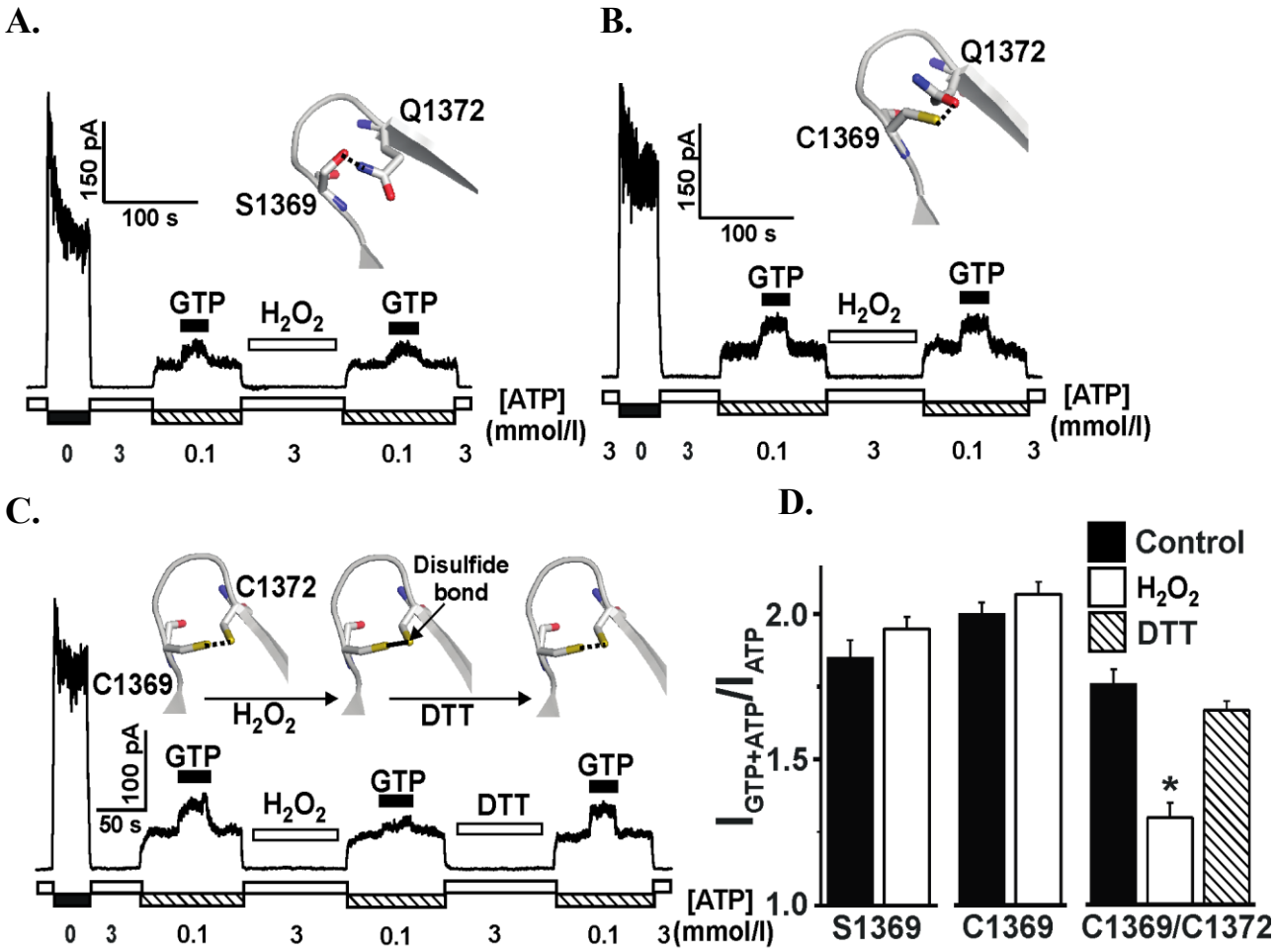
A.
150 pA
100 s
Q1372
S1369
GTP
H2O2
GTP
[ATP]
(mmol/l)
0 3 0.1 3 0.1 3
B.
Q1372
C1369
150 pA
100 s
GTP
H2O2
GTP
[ATP]
(mmol/l)
3 0 3 0.1 3 0.1 3
C.
C1372
Disulfide
bond
C1369
H2O2
DTT
100 pA
50 s
GTP
H2O2
GTP
DTT
GTP
0 3 0.1 3 0.1 3 0.1 3
[ATP]
(mmol/l)
D.
Control
H2O2
DTT
I GTP+ATP / I ATP
2.0
1.5
1.0
*
S1369
C1369
C1369/C1372

-

Figure 4.10. Direct Mg-ATPase assay of NBD2 dimers. (A) Amino acid sequence alignments of the SUR1 and SUR2A NBD2 domains. Homologous residues SUR1 S1369 and SUR2A K1337 are highlighted. (B) Hyperbolic plot of raw Mg-ATPase values. (C) Hyperbolic plot of normalized Mg-ATPase values. (D) Graphical representation of the percentage of V_{max} reached in the presence of 0.1 mmol/l ATP (n = 3-5 per group). * denotes $p<0.01$.

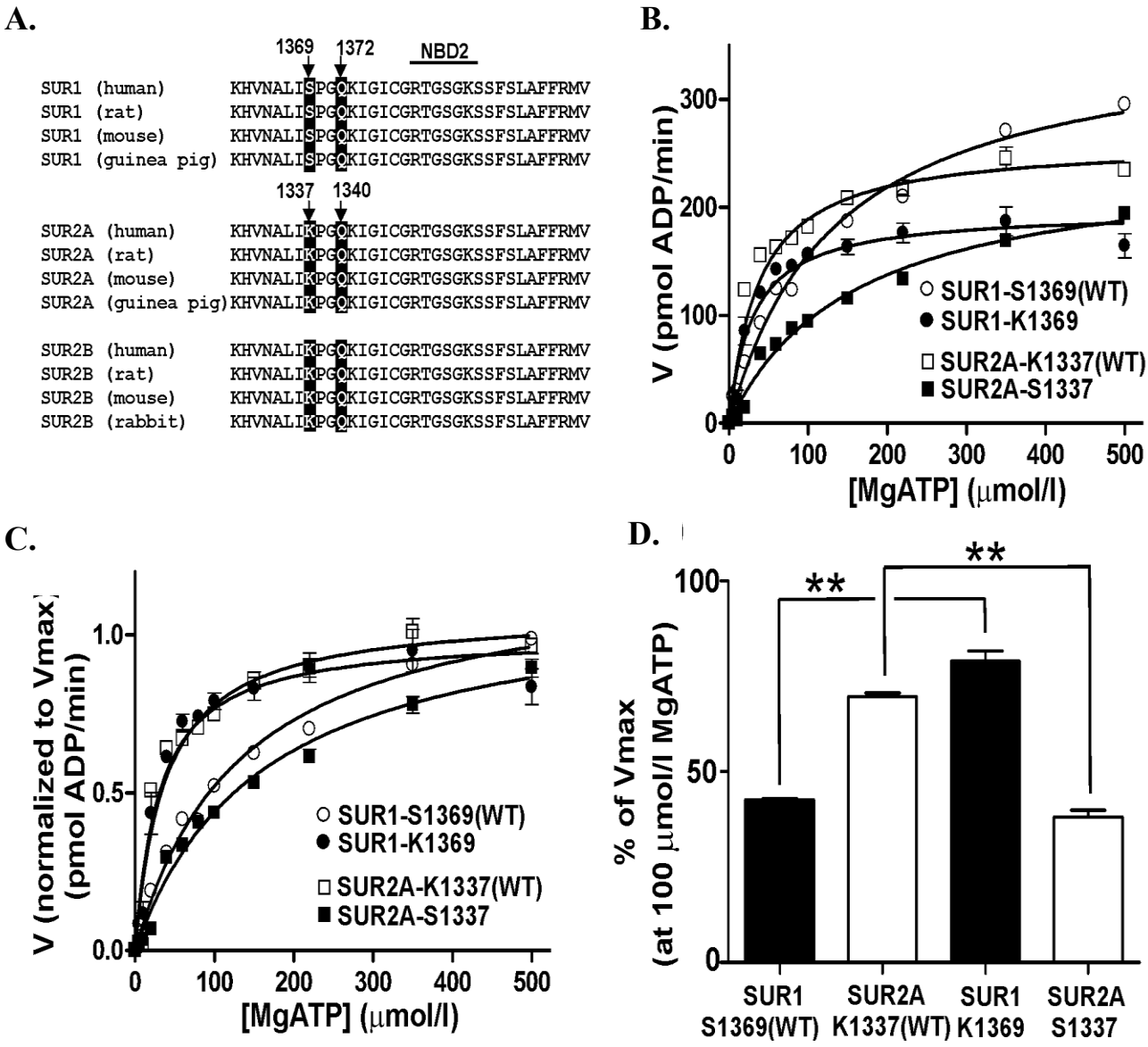
A.
1369
1372
NBD2
SUR1 (human) KHVNALISPGQKIGICGRTGSGKSSFSLAFFRMV
SUR1 (rat) KHVNALISPGQKIGICGRTGSGKSSFSLAFFRMV
SUR1 (mouse) KHVNALISPGQKIGICGRTGSGKSSFSLAFFRMV
SUR1 (guinea pig) KHVNALISPGQKIGICGRTGSGKSSFSLAFFRMV
1337
1340
SUR2A (human) KHVNALIKPGQKIGICGRTGSGKSSFSLAFFRMV
SUR2A (rat) KHVNALIKPGQKIGICGRTGSGKSSFSLAFFRMV
SUR2A (mouse) KHVNALIKPGQKIGICGRTGSGKSSFSLAFFRMV
SUR2A (guinea pig) KHVNALIKPGQKIGICGRTGSGKSSFSLAFFRMV
SUR2B (human) KHVNALIKPGQKIGICGRTGSGKSSFSLAFFRMV
SUR2B (rat) KHVNALIKPGQKIGICGRTGSGKSSFSLAFFRMV
SUR2B (mouse) KHVNALIKPGQKIGICGRTGSGKSSFSLAFFRMV
SUR2B (rabbit) KHVNALIKPGQKIGICGRTGSGKSSFSLAFFRMV
B.
V (pmol ADP/min)
300
200
100
0
0
100
200
300
400
500
[MgATP] (μmol/l)
SUR1-S1369(WT)
SUR1-K1369
SUR2A-K1337(WT)
SUR2A-S1337
C.
V (normalized to Vmax (pmol ADP/min)
1.0
0.5
0.0
0
100
200
300
400
500
[MgATP] (μmol/l)
SUR1-S1369(WT)
SUR1-K1369
SUR2A-K1337(WT)
SUR2A-S1337
D.
% of Vmax (at 100 μmol/l MgATP)
100
50
0
**
**
SUR1 S1369(WT)
SUR2A K1337(WT)
SUR1 K1369
SUR2A S1337

Figure 4.11. SUR1 amino acid residue at position 1369 determines diazoxide pharmacology of the K_{ATP} channel. (A) WT SUR1 S1369 responds in a similar manner in response to 0.1 mmol/l diazoxide in the presence or absence of 0.1 mmol/l ADP. (B-C) The presence of a positively charged lysine residue in the WT SUR2A K1337 and the mutant SUR1 K1369 K_{ATP} channels result in a significant decrease in their response to 0.1 mmol/l diazoxide in the absence of 0.1 mmol/l ADP. (D) Grouped data of normalized current. (n=4-17 patches per group) * denotes $p<0.05$.

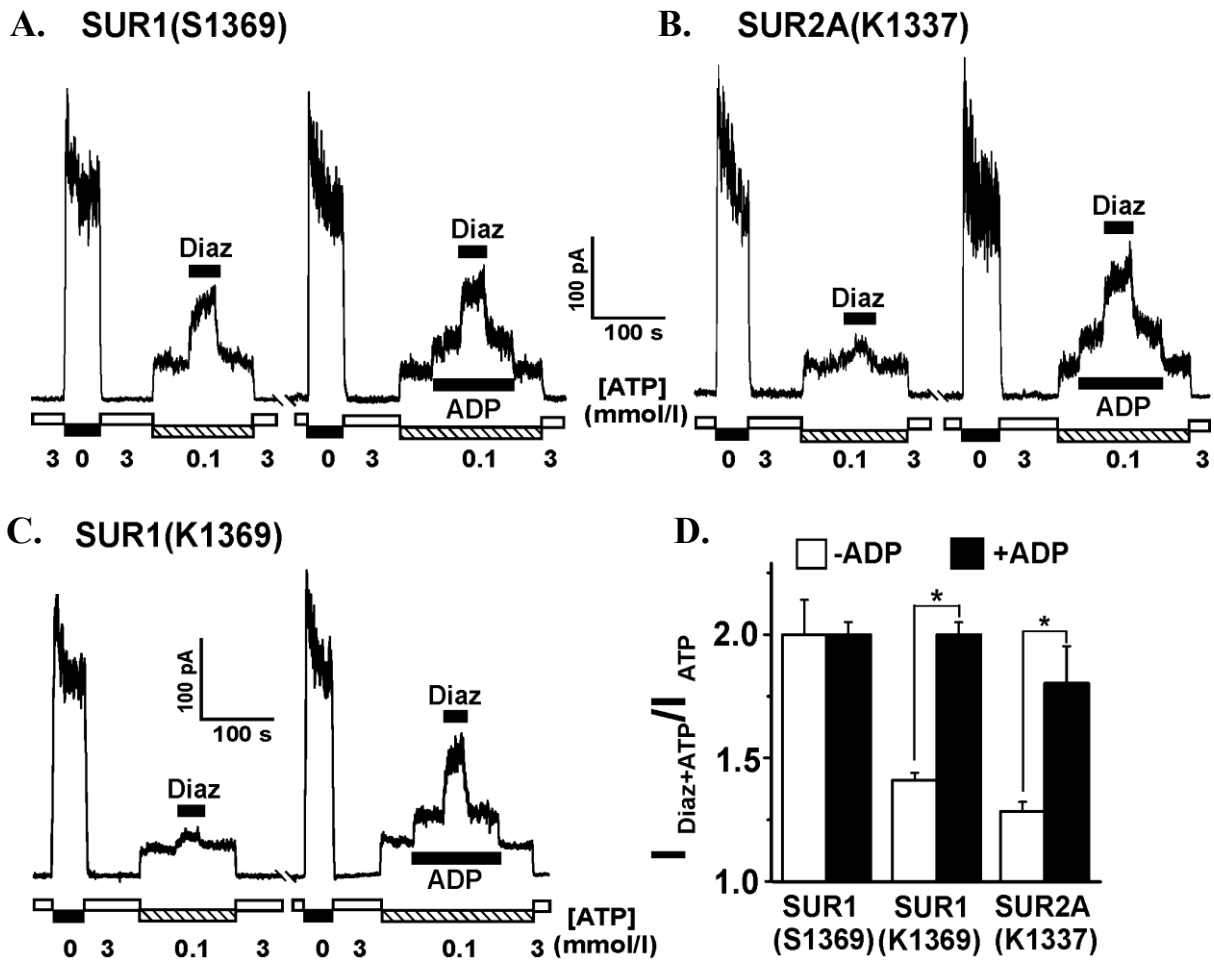
A. SUR1(S1369)
B. SUR2A(K1337)
C. SUR1(K1369)
D.
Diaz
ADP
100 pA
100 s
[ATP] (mmol/l)
3 0 3 0.1 3 0 3 0.1 3
0 3 0.1 3 0 3 0.1 3
0 3 0.1 3 0 3 0.1 3 (mmol/l)
-ADP
+ADP
I Diaz+ATP / I ATP
2.0
1.5
1.0
SUR1 (S1369)
SUR1 (K1369)
SUR2A (K1337)

Figure 4.12. The effect of DZX and the Mg-ATPase inhibitor BeFx on GTP-induced K_{ATP} channel function. (A-C) WT SUR1 S1369 and A1369 mutant channels display a significant increase in GTP-induced, Mg-ATPase-dependent channel activation while the K1369 mutant results in a decrease. (D) Graphical representation of normalized current. (E-F) WT SUR1 S1369 displays much greater inhibition of K_{ATP} channel currents elicited by 0.1 mmol/l DZX in the presence of 1 mmo/l of the Mg-ATPase inhibitor BeFx than the WT SUR2A K1337 channel. (G) Graphical representation of normalized current. (n=5-8 patches per group) * denotes $p<0.05$ and ** $p<0.01$.

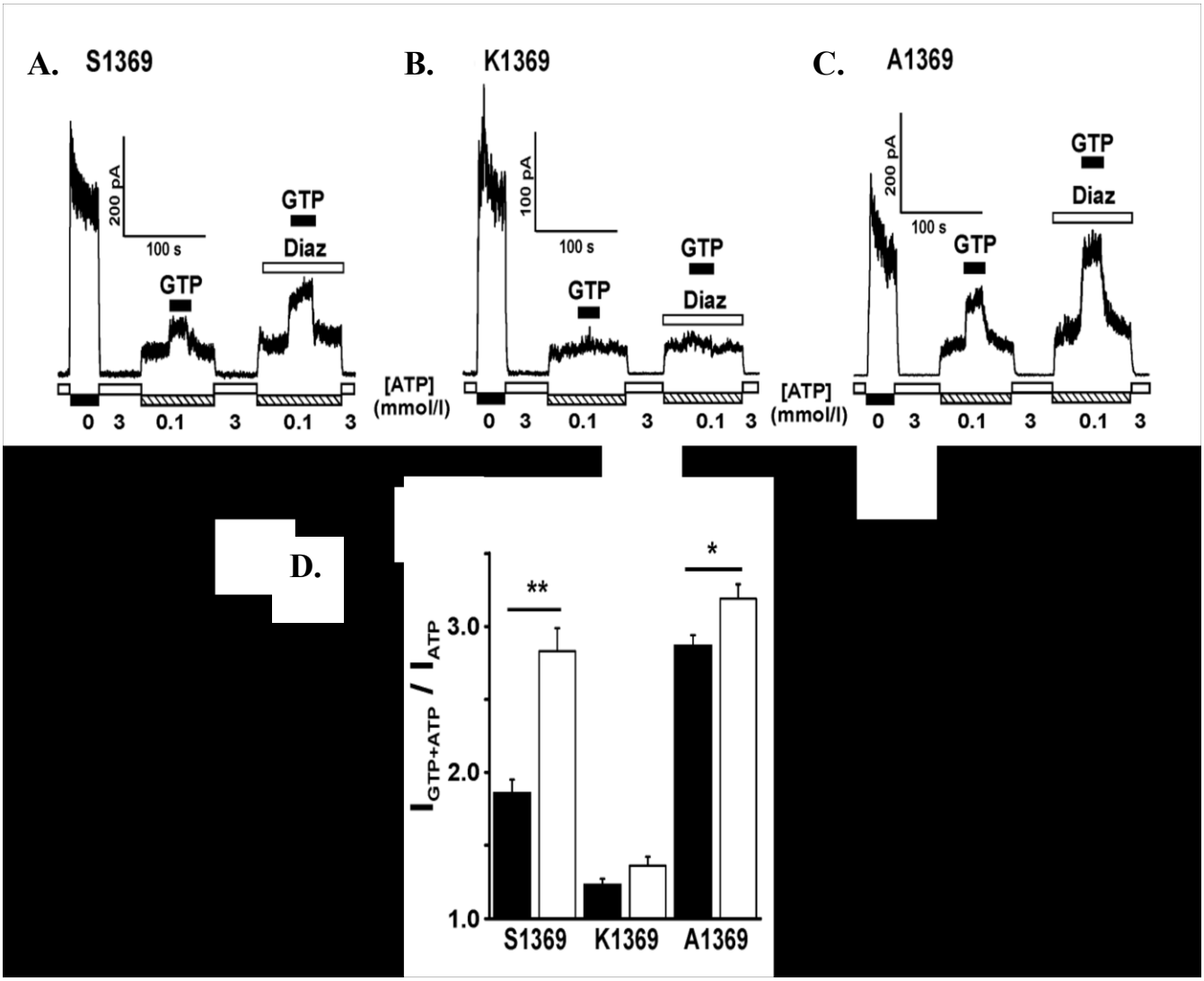
A.
S1369
200 pA
100 s
GTP
Diaz
GTP
[ATP]
(mmol/l)
0 3 0.1 3 0.1 3
B.
K1369
100 pA
100 s
GTP
GTP
Diaz
[ATP]
(mmol/l)
0 3 0.1 3 0.1 3
C.
A1369
200 pA
100 s
GTP
GTP
Diaz
[ATP]
(mmol/l)
0 3 0.1 3 0.1 3
D.
**
*
$I_{GTP+ATP} / I_{ATP}$
3.0
2.0
1.0
S1369
K1369
A1369

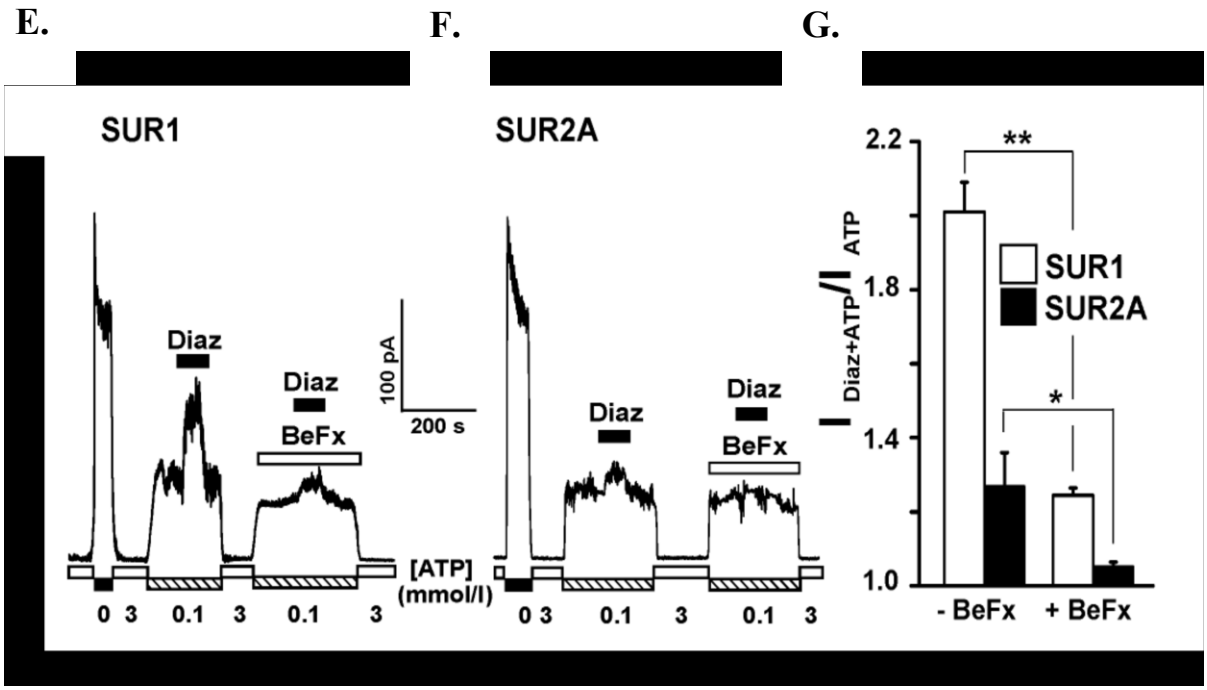
E.
F.
G.
SUR1
SUR2A
Diaz
Diaz
BeFx
100 pA
200 s
[ATP]
(mmol/l)
0 3 0.1 3 0.1 3
Diaz
Diaz
BeFx
0 3 0.1 3 0.1 3
I Diaz+ATP/I ATP
2.2
1.8
1.4
1.0
**
*
SUR1
SUR2A
- BeFx
+ BeFx

Figure 4.13. Effects of mechanical stress Mg-ATPase activity. (A) Mg-ATPase activity is stimulated by applying vacuum to patches of tsA cells transfected with Kir6.2/SUR2A. Stimulation was abolished by applying ATPase inhibitor, beryllium fluoride (BeF_2) (n= 9 patches). (B) Comparison between current (I) recorded when vacuum was applied (Istretch) normalized to current recorded from unstretched patches in patches treated with and without inhibition of ATPase activity by BeF_2 (**, $p<0.01$)

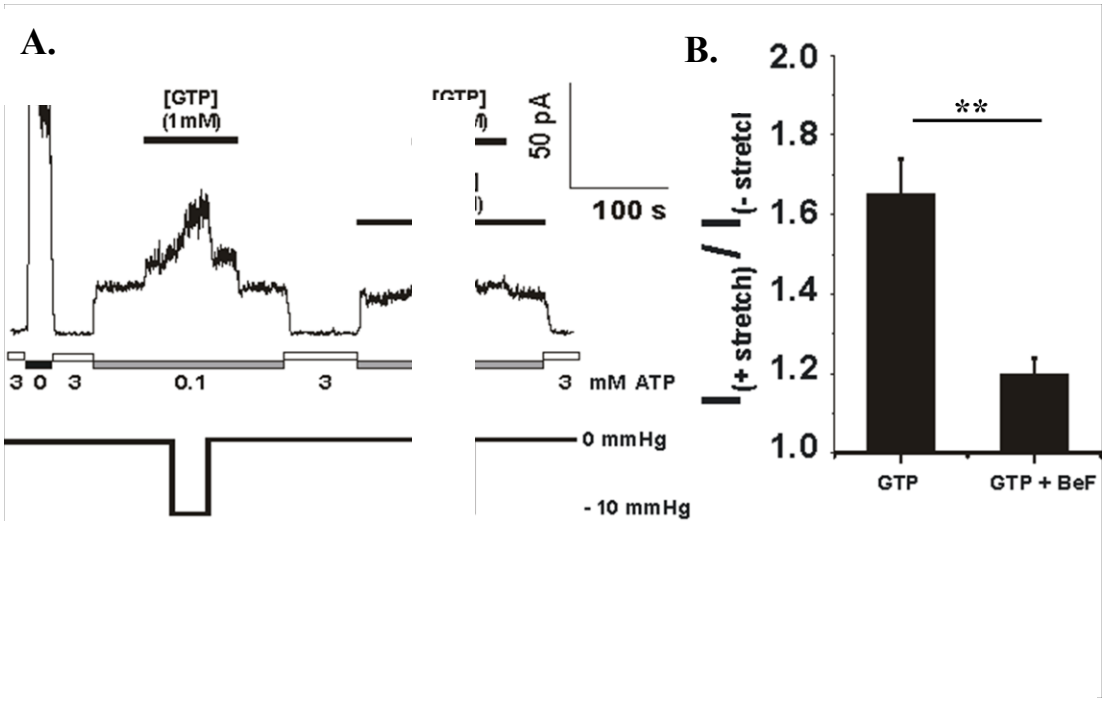
A.
[GTP]
(1mM)
50 pA
100 s
3 0 3 0.1 3
3 mM ATP
0 mmHg
- 10 mmHg
B.
2.0
1.8
1.6
1.4
1.2
1.0
**
I(+ stretch) / I(- stretch)
GTP
GTP + BeF

Chapter 5
Non-electrical effects of sulfonylureas on cardiac K_{ATP} channels and links to cardiotoxicity

Electrophysiological experiments were conducted by Dr. Mohammad Fatehi. Langendorff mouse heart perfusions were performed by Beth Hunter. Experimental design, human atria experiments, immunoblotting, statistical analysis were performed by the author.

5.1. Introduction

Sulfonylureas (SUs) are the second most-prescribed oral diabetic class of drugs used worldwide in the management of type 2 diabetes[118]. Along with metformin, they have been included in the World Health Organization's List of Essential Medicines as oral antidiabetic therapy[473]. Since the discovery of their glucose lowering effects in World War II[119,120], several generations of SUs have been developed. The first generation of SUs includes tolbutamide and chlorpropamide[122]. The second generation SUs include glibenclamide (glyburide), gliclazide and glipizide[123] and the third generation SUs include glimiperide[474].

SUs belong to a group of oral antidiabetic drugs termed secretagogues because they exert their blood glucose-lowering effects through promoting insulin secretion from pancreatic β-cells. In the pancreas, they act through inhibition of K_{ATP} channel activity which in turn leads to depolarization of the membrane potential, opening of voltage gated calcium channels causing an increase in intracellular calcium concentration and subsequently insulin vesicle secretion(Figure 5.1.)[141]. SUs can be classified according to their K_{ATP} channel binding sites as A-site, B-site, or AB-site drugs (Figure 5.2.)[125,127,475]. The A-site is located within the cytosolic loops linking trans-membrane segments 14-16 of the SUR1 subunit while the B-site, resides in the linker between the trans-membrane segments 5-6 of the SUR1 subunit and the N-terminus of the Kir6.2 subunit (Figure 5.2.)[125,127]. The A-site within SUR1 subunit interacts with the sulfonylurea moiety of the drug molecules while the B-site interacts with the non-sulfonylurea carboxamido moiety of the drug molecules.

Given that their mechanism of action is by inhibiting K_{ATP} channels, it is important to note that K_{ATP} channels are also expressed in other tissue such as the brain, skeletal

muscle, smooth muscle and the heart[28]. Therefore the question of whether inhibiting K_{ATP} channels in other tissue may give rise to undesirable off-target side effects associated with SU use becomes important to address. Moreover, it has been suggested that SUs may interfere with Mg-ATPase activity of K_{ATP} channels[39,127,128]. By virtue of this enzymatic ability, K_{ATP} channels are able to change local Mg-ATP (their inhibitor) to Mg-ADP (their activator) [42–45]. Reports of SUs interfering with SUR1, the A-site ligands in particular, or through interfering with Kir6.2 gating means that they could alter K^+ conduction[39,127,128] or potentially affect downstream signaling as we have demonstrated in Chapter 4 with diazoxide. The effect of SUs on Mg-ATPase activity in the heart remains to be investigated.

In the heart, K_{ATP} channels are mostly in the closed state under resting conditions. During physiological stress such as in exercise or a pathological stress such as in ischemia, the ADP concentration rises along with an decrease in ATP concentration leading to opening of the cardiac channels[175]. This opening of the channels leads to membrane repolarization, via potassium efflux and prevention of intracellular calcium accumulation which would activate pathways such as apoptosis that would lead to cell demise[177,178]. Therefore the ability of the channel to open during stress episodes is one of the endogenous cardioprotective means, and losing this ability compromises cardiac function should an insult occur.

In this regard, SUs have been a subject of an ongoing debate regarding their cardiovascular safety since the publication of the University Group Diabetes Program (UGDP) trial which was prematurely terminated due to the increased number of cardiac deaths in the tolbutamide-treated group compared to the placebo-treated group[138]. Several clinical studies followed after the UGDP considering the weaknesses in the methodology followed in conducting the study[139]. However, until today, there is no real consensus on

whether SUs actually pose a cardiovascular risk to patients receiving them as part of their antidiabetic regime and whether SUs that are less selective to the pancreas would produce worse cardiac outcomes[122,124,476].

Different SUs when administered at therapeutic doses exhibit distinct tissue-specific binding affinities as elegantly reviewed by Abdelmoneim et al.[144]. For example, gliclazide and glipizide are more selective for the pancreatic SUR1 isoform, whereas glibenclamide is non-selective and binds to pancreatic SUR1 and cardiovascular SUR2A/B isoforms[144,145]. The differences in the pharmacological properties are supported by animal studies whereby glibenclamide, but not gliclazide, was shown to abolish ischemic preconditioning, resulting in a larger infarct size and worse deterioration in left ventricular function. In animal models, the differential pharmacology of glibenclamide was demonstrated in the form of loss cardiac ischemic preconditioning, with larger infarct sizes and poorer functional recovery[146–152]. Similar effects of abolished cardiac preconditioning were observed in patients undergoing one-vessel coronary angioplasty[153] as well as in isolated human atrial trabeculae[154]. Despite of this observed loss of cardioprotection caused by glibenclamide, the exact mechanisms by which it disrupts endogenous protection have not been fully elucidated.

A potential mechanism for cardiotoxicity is through the inhibition of the protein kinase signalling pathway via tumour suppressor LKB1 and AMP-activated protein kinase (AMPK). AMPK is a key cellular energy sensor and regulator[384,477]. The rise in AMP:ATP and ADP:ATP ratios, intracellular calcium, and reactive oxygen and nitrogen species observed during physiological or pathological stress lead to AMPK activation. The activation mechanism consists of an allosteric component (AMP, ADP, or ATP binding to the γ-

subunit) and a covalent component (phosphorylation of Thr172 in the α-subunit controlled by upstream kinases, LKB1 or CaMKK, and phosphatases)[384,477]. Upon its activation, AMPK induces adaptation of energy metabolism through regulation of cellular signalling cascades, activity of metabolic key enzymes, and gene transcription. Activated AMPK stimulates ATP-generating processes, such as uptake and oxidation of glucose and fatty acids, and suppresses a number of ATP-consuming processes, such as protein synthesis, cellular growth, and proliferation. Interestingly, several recent studies have described a general link between a reduced LKB1–AMPK signalling and cardiac disease[478–480]. In this context, the aim of the present study was to analyse the effect of select SUs on cardiac AMPK signaling and their effects on the recently identified Mg-ATPase activity of K_{ATP} channels.

5.2. Methods

Experimental animals

All experiments were performed according to protocols approved by the University of Alberta Institutional Animal Care and Use Committee. Data was obtained from adult (11-20 weeks) male C57BL/6 wild-type and Kir6.2 -/- mice. The generation of Kir6.2-/- mice by targeted Kir6.2 gene disruption has been previously described in detail by Miki et al.[388] and were obtained from the Seino laboratory. Mice were housed on a 12-h light and 12-h dark cycle with ad libitum access to chow diet and water.

Langendorff heart perfusions

Kir6.2+/+ and Kir6.2-/-mice were anesthetized using pentobarbital, with 100 U of heparin. After mid-sternal incision, the heart was removed and placed in (37 ± 1 °C), modified Tyrode solution of the following composition: 128.2 mM NaCl, 4.7 mM KCl, 1.19

NaH_2PO_4, 1.05 mM $MgCl_2$, 1.3 mM $CaCl_2$, 20 mM $NaHCO_3$, and 11.1 mM glucose (pH = 7.35 ± 0.05). While bathed in the same solution, lung, thymus, and fat tissue were dissected and removed. After cannulation, hearts were then retrogradely perfused with modified Krebs-Henseleit solution passed through the 5-µm filter (Millipore, Billerica) and warmed (37 °C) using a water jacket and circulator (ThermoNESLAB EX7, Newtown). The hearts were allowed to normalize for 10 minutes and then were perfused for 30 minutes with either 0.228 nM or 1 µM glibenclamide 11.45 nM gliclazide, 10 µM HMR 1098, 100 µM DZX or DMSO alone as vehicle control. Heart ventricles were clamp-frozen and used for biochemical analysis.

Human atrial appendages

Appendages were isolated from the right atria of patients undergoing coronary artery bypass graft surgery at the Mazankowski Alberta Heart Institute and the University of Alberta Hospital on the day of the operation. Appendages were stored in ice cold phosphate buffered saline between the operation room and our laboratory. Each appendage was weighed and cut into two (1 cm x 0.5 cm) pieces serving as test and control for each patient. The appendage halves were then incubated for one hour in Carbogen (95% CO_2-5% O_2) gassed modified Krebs-Henseleit buffer containing 10 µM glibenclamide or 10 µM gliclazide dissolved in DMSO or DMSO only as vehicle control. After completion of the incubation, the appendages were washed in PBS three times, snap frozen in liquid nitrogen and processed for immunoblotting.

Western blot analysis

Ventricular tissue from Kir6.2+/+ and Kir6.2-/- mouse hearts was snap-frozen after Langendorff perfusion and homogenized by cryogenic grinding then diluted with RIPA homogenization buffer containing phosphatase and protease inhibitors. After a BCA protein assay (Pierce, Thermo Scientific, USA), equal amounts of protein were resolved by SDS-PAGE, and were transferred onto a PVDF membrane. Target proteins were identified using the primary antibodies: anti-AMPK phospho (Thr172) and total and anti-LKB1 phospho (Ser 428) and total. Immunoblots were developed using the Amersham ECL Prime Western blotting detection reagents. Densitometric analysis was performed using ImageJ software (National Institutes of Health).

Electrophysiology

tsA201 cells, a HEK293 cell line derivative, were cultured and then transfected with the Kir6.2 and SUR1 clones using the calcium phosphate precipitation technique[436]. Transfected cells were identified using fluorescent optics in combination with co-expression of a green fluorescent protein plasmid (Life Technologies, Gaithersburg, MD). Macroscopic K_{ATP} channel recordings were then performed 48-72 hours after transfection. The excised inside-out patch clamp technique was used to measure macroscopic recombinant K_{ATP} channel currents in transfected tsA201 cells as described in detail previously[436]. Experiments were performed at room temperature (21^{o}C). Mg-ATPase activity was measured as described previously by our group[167].

Statistical analyses

Macroscopic K_{ATP} channel currents were normalized and expressed as changes in test current relative to control current. Macroscopic current analysis was performed using pClamp 10.0 (Axon Instruments, Foster City, CA) and Origin 6.0 software. Statistical significance was assessed using the unpaired Student's t test or one-way ANOVA with a Bonferroni post hoc test. $p<0.05$ was considered statistically significant in GraphPad Prism software 5.01 for Windows. Data are plotted as the mean ± S.E.M**.**

5.3. Results

Glib activates AMPK in isolated mouse hearts

The direct effect of Glib on AMPK activation has not been demonstrated. We investigated whether Glib affected the phosphorylation of AMPK using an ex-vivo model of the Langendorff-perfused heart. We perfused age-matched C57Bl6 mouse hearts with either vehicle (DMSO) or 1 μM Glib. Our data show significant phosphorylation, thereby activation of AMPK induced by Glib compared to vehicle control (2.486 ± 0.6848 and 0.03696 ± 0.006410 respectively, n=3/group, $p<0.05$) (Figure 5.3.B). We have also contrasted the activation with DZX-induced AMPK activation previously demonstrated in Chapter 4. (Figure 5.3.A.)

Glib activation of AMPK is reduced in K_{ATP}-deficient (Kir6.2-/-) mouse hearts

Since we observed significant AMPK activation induced by Glib, we attempted to investigate whether the observed increase in AMPK phosphorylation was K_{ATP}-dependent. In order to elucidate that, we perfused wild-type C57Bl6 mice (Kir6.2+/+) and K_{ATP}-deficient mice of the same background (Kir6.2-/-). Our results show that in the absence of K_{ATP} channels, Glib-induced AMPK activation is lower (1.836 ± 0.3430) compared to Glib-

perfused Kir6.2+/+ hearts (2.282 ± 0.1420) (n=3/group, p>0.05) (Figure 5.4.A,B), suggesting that presence of K_{ATP} channels on the cell surface is necessary for the full AMPK signal to occur.

Glib inhibits Mg-ATPase activity while Glic does not affect it

Since we observed different reduced activation of AMPK in the absence of cardiac $K_{ATP,}$ we sought to investigate whether this effect was due to compromised ionic homeostasis or due to a direct effect of Glib on the channel's Mg-ATPase activity. We also investigated whether Glic had any effect on Mg-ATPase activity of the channel. Our data show that 0.5 μM Glib was able to completely abolish Mg-ATPase activity compared to control (n=5 patches, **p<0.01) while 1 μM Glic had no significant effect on Mg-ATPase activity. (Figure 5.5.A,B).

Glib further stimulates AMPK phosphorylation when perfused simultaneously with DZX

We have previously demonstrated that DZX is able to activate AMPK significantly (Figure 4.2.A on page 139 in Chapter 4). We have also shown that DZX activates Mg-ATPase activity (Figure 4.11. on page 159 in Chapter 4). We decided to investigate whether co-administration of Glib and DZX would counteract their effects on Mg-ATPase activation and how that would affect downstream AMPK activation. Our results show that Glib co-administered with DZX resulted in higher AMPK activation compared to control (0.8869 ± 0.04953) and to hearts treated with DZX alone(0.7817 ± 0.06685). (Figure 5.6.A, B). (n=3/group, * p<0.05, **, p< 0.01)

HMR 1098 does not have a significant effect on AMPK activation or Mg-ATPase activity

We then decided to test whether the cardioselective K_{ATP} inhibitor HMR 1098 [131,481] would exhibit a similar AMPK activation pattern as well as an inhibitory effect on Mg-ATPase activity as Glib. Our results show HMR 1098 caused a modest increase in AMPK phosphorylation compared to vehicle(0.3488 ± 0.1112 and 0.2654 ± 0.08913 respectively. Co-administration of DZX and HMR 1098 resulted in a further increase in AMPK phosphorylation (0.4518 ± 0.01474, n=3/group, $p>0.05$) . (Figure 5.7.A,B). HMR 1098 did not cause any changes in Mg-ATPase activity as well. (n= 5 patches, $p>0.05$) (Figure 5.8.A,B).

Glib and Glic activate AMPK in isolated mouse hearts at therapeutic doses

In order to investigate whether therapeutic doses of Glib and Glic would have an effect on AMPK activation, we perfused C57Bl6 mice with plasma steady state levels of Glib (2.280E-07 mmol/l) and Glic (1.145E-05 mmol/l)[144]. Our data show that at steady state concentration, Glib significantly increased AMPK activation in comparison to vehicle $p<0.05$). Glic was also able to significantly increase AMPK phosphorylation compared to vehicle-treated hearts, however the degree of activation was still less than in glibenclamide. ($p<0.05$) (n=3 hearts/group, **, $p<0.01$, ***, $p<0.001$). We also measured activation of LKB-1, an upstream kinase that phosphorylates AMPK, our results show that LKB-1 activation followed a similar trend of activation as AMPK where it was higher in the Glib-perfused group compared to vehicle (1.279 ± 0.1489 and 0.8796 ± 0.1736 respectively). However, the Glic-perfused group showed less activation of LKB-1 compared to vehicle

control (0.7021 ± 0.1485). No statistical significance was reached between the LKB-1 data sets. (n=3 groups, $p>0.05$)

Glibenclamide activates AMPK in human atrial tissue

To probe for whether activation of AMPK by Glib or Glic occurred in human tissue, we tested both drugs on human atrial appendages obtained from patients (4/group, age 68±13 years) undergoing coronary artery bypass graft surgery. We used each appendage as its own control and test group by cutting it in equal halves and incubating in either oxygenated modified Krebs-Henseleit containing DMSO or 10 μM Glib or 10 μM Glic. AMPK phosphorylation was consistently higher in the Glib-treated group compared to vehicle-incubated appendages in all 4 patients (Figure 5.10.A). We expected to see an increase in AMPK phosphorylation in gliclazide-treated appendages but we observed an increase in 2 patients and a decrease in the 2 other patients (Figure 5.10.B.) . Group data showed that there was a trend towards glibenclamide-induced AMPK activation in human atrial tissue

5.4. Discussion

In the previous chapter, we have shown that the K_{ATP} channel opener DZX may exert its cardioprotective effects in part through stimulation of Mg-ATPase activity and suggested that it causes downstream activation of AMPK which would potentially provide an early signal to stimulate energy conserving pathways during stress. In this chapter we attempted to address the potential cardiotoxicity attributed to the K_{ATP} channel inhibitors, the sulfonylureas (SUs) and whether it was mediated by AMPK.

In the present study we used Glib, which as an AB site SU that has been frequently associated with loss of cardioprotection in experimental settings. For example, Birnbaum's

group has shown that glibenclamide abolished the infarct size limiting effects of the oral antidiabetic pioglitazone[482]. Moreover, Gross et al. have previously shown in a canine model that cardiac preconditioning induced by left coronary circumflex artery occlusion is lost when Glib was administered[376]. Additionally, Toombs et al. have demonstrated that Glib administered 30 minutes before the induction of ischemia in preconditioned rabbits exhibited larger infarct sizes compared to the preconditioned hearts that were not treated with the drug[149]. On the other hand, Yellon's group has demonstrated that while Glib abolishes ischemic and nicorandil-induced preconditioning, administration of Glic did not abolish the protective effects of either[483]. In addition, on the clinical level, a recent study by Abdelmoneim et al. showed that Glib use was associated with a 14% higher risk of acute coronary syndrome events compared to Glic use[484].

In terms of cardiotoxicity, one would expect that mechanisms responsible for conserving cellular energy would be compromised. One of the key pathways to conserve cellular energy during stress is activation of AMPK that signals to downstream pathways to stimulate ATP-producing pathways and halting ATP-consuming ones. It has been shown previously that cardiotoxicity induced by the anti-cancer agent doxorubicin inhibited AMPK activation thus accelerating cardiomyocyte death[485]. Since the direct effects of SUs on AMPK activation have not been previously demonstrated we performed a series of experiments in an effort to understand whether SUs suppress AMPK activation leading to potential cardiotoxicity.

In this study we demonstrated that Glib activated AMPK in mouse hearts perfused in Langendorff mode significantly (Figure 5.3.B). Interestingly, activation of AMPK by the

same concentration of Glib was reduced when we perfused Kir6.2-/- mouse hearts where K_{ATP} channels are not expressed in cardiac tissue (Figure 5.4.A,B). This observation is similar to what we observed with DZX-induced activation of AMPK in Chapter 4, indicating that the presence of K_{ATP} channels on the cell membrane is essential to full AMPK phosphorylation.

Since we observed increased Mg-ATPase activation with DZX in the previous chapter, we also looked at whether Glib was affecting Mg-ATPase activity of the cardiac Kir6.2/SUR2A channel combination known to be expressed in the ventricles[6]. Our results show that in that system, Glib completely abolishes Mg-ATPase activity of the channel (Figure 5.5.A,B), thereby preventing production of Mg-ADP in the local environment of the channel. It is important to note that the local nucleotide concentration is essential in channel regulation as has been previously demonstrated[387]. The phosphotransfer-cascade enzymes adenylate kinase and creatine kinase both associate physically with the channel and they are ultrasensitive to changes in nucleotide concentration[49,54,486]. Under basal conditions, the changes in ATP, ADP and AMP may be very subtle and in our patch model, it would be helpful to test the effect of Glib and Glic in the presence different nucleotide concentrations.

We also tested co-administration of the K_{ATP} channel opener DZX along with glibenclamide as well as the cardiospecific K_{ATP} inhibitor HMR 1098 to determine whether we would still observe changes in AMPK activation. The DZX+Glib test group yielded higher AMPK activation than DZX alone indicating that Glib is exerting K_{ATP}-independent effects that are altering the cellular AMP/ATP ratio thus further phosphorylating AMPK. Under basal conditions, Yokota et al. have shown that in an ischemia-reperfusion model in

pigs administration of Glib during baseline does not alter ATP concentration, phosphocreatine content or proton production[487]. However, that is not the case during ischemia, where Glib administration has been shown to enhance ATP depletion during the beginning of regional ischemia in dogs as demonstrated by Kamigaki et al.[488]. Therefore, the effect of Glib on AMPK signaling and Mg-ATPase activity may be more pronounced in I/R where a drop in intracellular pH, decreased phosphocreatine content and ATP depletion may all contribute to worsening of cardiac function[489].

On the other hand, when we perfused C57Bl6 mouse hearts with HMR 1098, an AB site SU, on its own only modestly increased AMPK phosphorylation while having no effect on Mg-ATPase activity of the channel. (Figure 5.8.A,B). This indicates that AMPK activation in this model does not necessarily correlate with Mg-ATPase activity and AMPK phosphorylation could be a result of K_{ATP}-independent effects. Interestingly, HMR 1098 has been reported to be cardioprotective in the setting of cardiac ischemia[490,491]. This cardioprotective effect is attributed to a direct action of HMR 1098 on the mitochondria where it promotes reactive oxygen species production[492]. Moreover, Rainbow et al. have reported that during metabolic stress, HMR 1098 is unable to inhibit cardiac K_{ATP} channels fully which may explain why it does not worsen cardiac recovery in ischemia. It also suggests that its inhibition of the channel is dependent on nucleotide concentration during cellular stress[493].

Since previous studies have used concentrations of Glib and Glic that are higher than the therapeutic doses in determining the adverse effects on cardioprotective mechanisms we decided to test the effects of plasma steady state concentrations of Glib and Glic on AMPK activation. Our results show for the first time that plasma steady state concentrations of both

Glib and Glic activate AMPK in murine hearts (Figure 5.9.A, B) . This activation along with a similar pattern of activation of LKB-1 (Figure 5.9.A, C) which is an upstream kinase that activates AMPK could indicate that the heart is undergoing metabolic stress due to drug administration since that activation was not observed in vehicle treated hearts. Activation of AMPK would then lead activation of downstream energy-conserving pathways. Nevertheless, these results do not reflect how K_{ATP} channels are involved in that observed AMPK-activation, if at all. A comparison with AMPK activation induced in K_{ATP}-deficient mouse hearts would give us a clearer picture as to whether K_{ATP} channels are necessary for AMPK activation at the given concentrations.

Additionally, this study shows that Glib is able to activate AMPK in human atrial tissue compared to Glic (Figure 5.10.A, B). Since it is difficult to standardize the cardiac conditions, underlying disease, medications that the patients who were undergoing coronary artery bypass graft surgery, we opted for using the atrial appendage from each patient as the test as well as its own control to minimize error. Though our Glic-incubated group was inconsistent, our Glib-incubated appendages all demonstrated higher AMPK activation compared to their vehicle-incubated controls. The functional and mechanistic implications of that activation remain unclear and would require further investigation.

In our study, we were unable to correlate Mg-ATPase activity stimulation to AMPK phosphorylation. A more specific model that can separate electrical and enzymatic activity of the K_{ATP} channel would be more conclusive compared to genetic deletion of the entire channel. In such a model, ideally, the channel would be allowed to be expressed at the surface of the membrane and retain Mg-ATPase in the absence of electrical activity. This

model would give us clearer answers to whether the observed AMPK activation is due to direct effects on Mg-ATPase activity leading to a cascade of events mediated by the phosphotransfer enzymes leading to signal augmentation and activation of cytoplasmic AMPK. Contrary to our expectations, Glib tested at different concentrations did not inhibit AMPK activation. Nevertheless, AMPK activation could still indicate cellular stress and the effect of glibenclamide would be more pronounced to hearts subjected to I/R injury.

As a central regulator of cellular metabolism, AMPK activation would have direct effects on fatty acid and glucose oxidation as well as glycolysis. In this regard, a study by Cook et al. showed that Glib is an inhibitor of carnitine palmitoyl transferase-1 (CPT-1)[494]. CPT-1 inhibition would inhibit fatty acid oxidation by reducing fatty acid transport into the mitochondria for β-oxidation[235]. On the other hand, activation of AMPK which we have observed would lead to an increase in fatty acid oxidation. In this regard, it is important to note that the authors have used 50 μM Glib which is a significantly higher concentration than what we have used in our study. Therefore the high concentration would possibly have non-specific effects in the cell that are not solely mediated by AMPK.

Additionally, a study by Ford et al. showed that 30 uM of glibenclamide increased rates of glycolysis and proton production in an ex-vivo working heart model but did not exert a significant effect on glucose oxidation rats . The authors of that study associated increased proton production to the significantly impaired cardiac recovery of post-ischemic mechanical function[495]. On the other hand, Buffington et al. have shown that therapeutic concentrations of Glib have a direct effect on the pyruvate dehydrogenase complex in the heart leading to increased glucose oxidation. That observation however, occurred in the absence of insulin in

the perfusion system which could isolate the effects of the PI3K/Akt signaling pathway which could affect glucose uptake directly[385,496]. Therefore, there is an established link between Glib use and direct changes in cardiac metabolism. It would be interesting to compare differences in cardiometabolic rates, proton production using therapeutic concentrations of Glib and Glic and to assess cardiac recovery in the setting of I/R to understand how SUs, especially Glib, could mechanistically worsen cardiac function.

In summary, our present study shows that Glib activates AMPK at different concentrations indicating that the AMPK pro-survival pathway is not inhibited by the drug. We found that Mg-ATPase activity in this experimental model did not correlate to AMPK activity which could be addressed by more sophisticated transgenic animal models. Finally, we have demonstrated the effect of the drug on AMPK activation in the human heart. More work towards understand the metabolic effects of SUs in the heart is yet to help us elucidate the potential cardiotoxic effects of SUs.

Figure 5.1. Mechanism of action of sulfonylureas. Inhibition of K_{ATP} channels in pancreatic β-cells leads to depolarization of membrane potential causing the opening of voltage-gated calcium (Ca^{++}) channels. The resultant calcium influx stimulates insulin vesicle exocytosis.

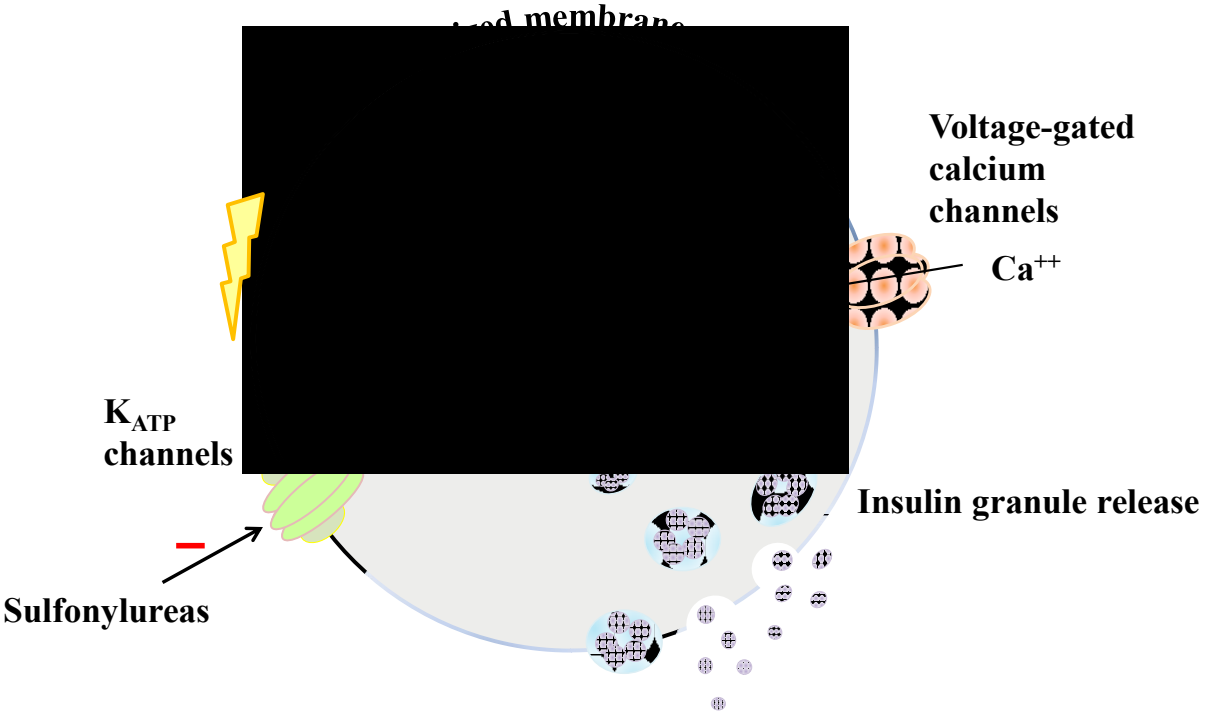
Voltage-gated
calcium
channels
Ca++
KATP
channels
Insulin granule release
Sulfonylureas

Figure 5.2. Binding sites of sulfonylureas on K_{ATP} channels. (A) General membrane topology of K_{ATP} channels with marked A-/ B- drug binding sites. (B) Chemical structures and binding-site classification of the sulfonylureas discussed in this chapter, gliclazide (Glic), glibenclamide (Glib) and HMR 1098.

A.

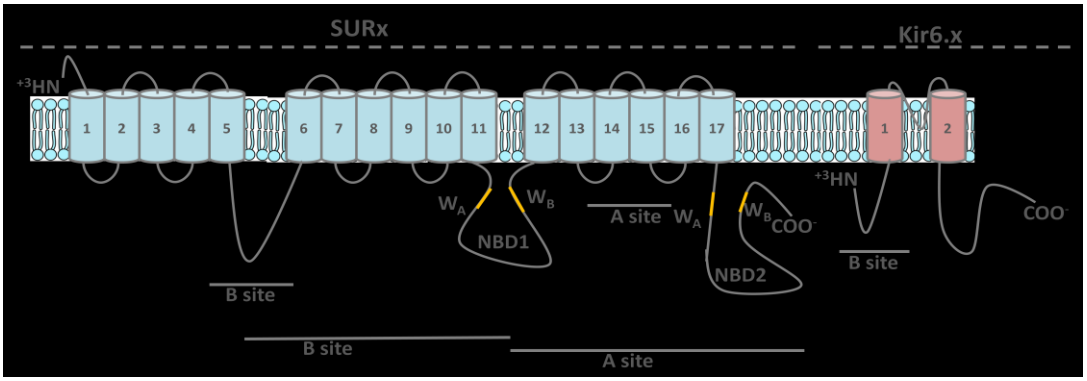

B.

Gliclazide

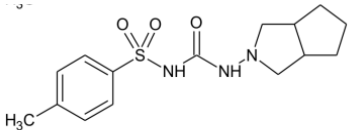

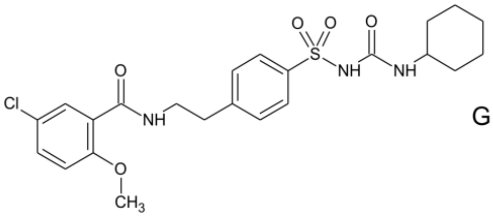

Glibenclamide

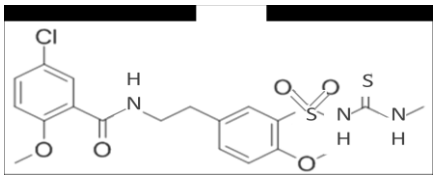

HMR 1098

Figure 5.3. AMPK activation induced by DZX and Glib in cardiac ventricles of C57Bl6 mice. (A) Phosphorylation of AMPK in murine hearts perfused with 100 μM diazoxide (DZX) and (B) 1 μM glibenclamide (Glib) in DMSO compared to vehicle (DMSO) controls. Hearts were perfused in Langendorff mode. (n=3/group, *<0.05, ***<0.001)

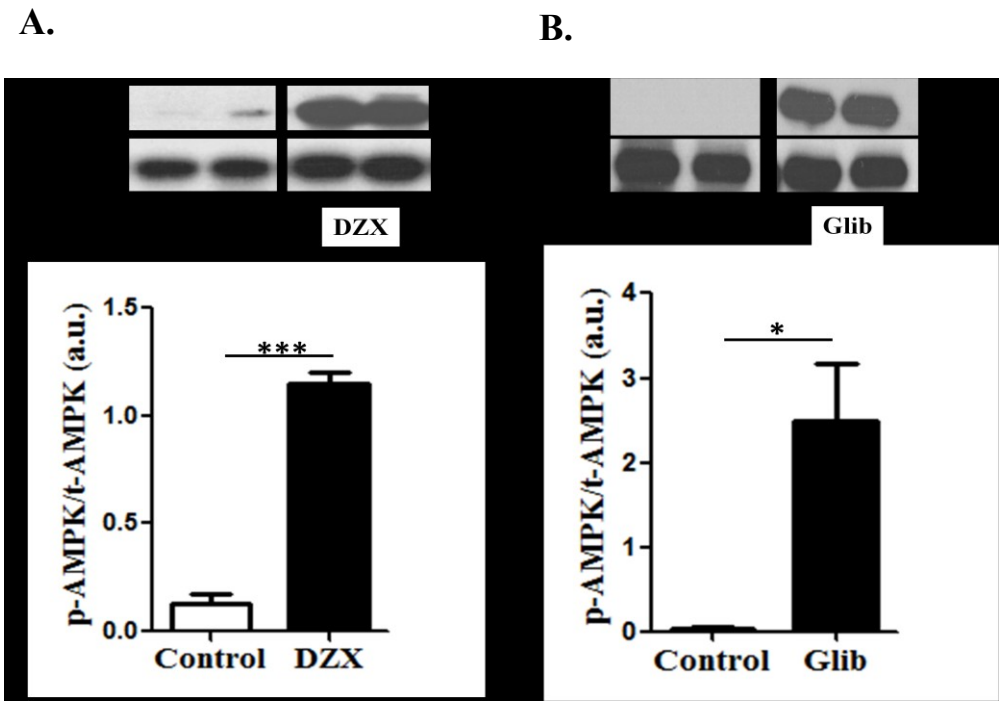
A.
B.
DZX
Glib
p-AMPK/t-AMPK (a.u.)
1.5
1.0
0.5
0.0
***
Control
DZX
p-AMPK/t-AMPK (a.u.)
4
3
2
1
0
*
Control
Glib

Figure 5.4. Glib-induced activation of AMPK in murine hearts. (A) Representative immunoblots comparing between AMPK activation in Kir6.2+/+ C57Bl6 and Kir6.2-/- C57Bl6 mouse hearts perfused in Langendorff mode with either vehicle (DMSO) or 1 μM glibenclamide (Glib). (B) Graphical representation of densitometric measurement of phosphorylated AMPK normalized to total AMPK (n=3, *, $p<0.05$)

A.

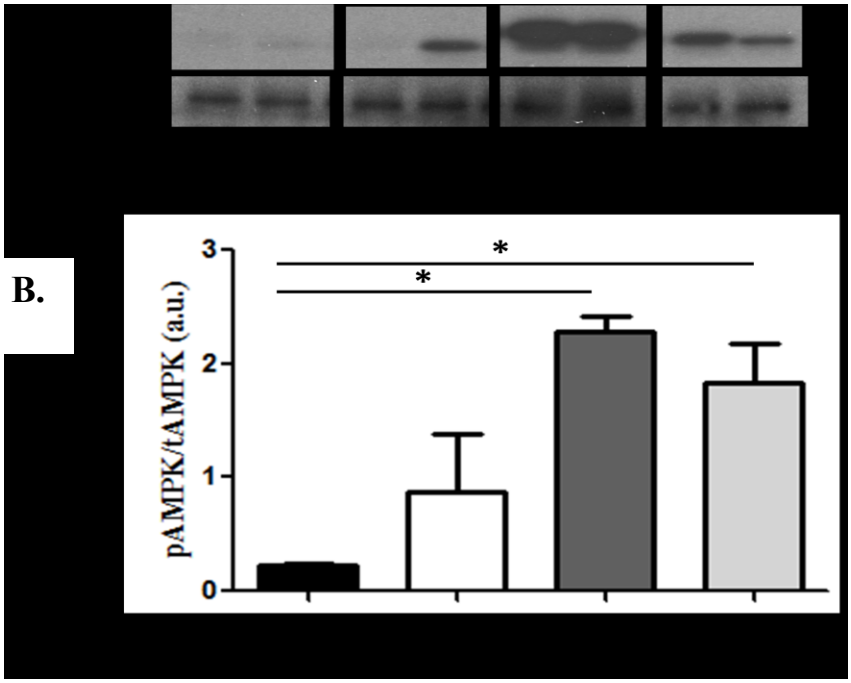

Figure 5.5. Comparison between effects of Glib and Glic on the Mg-ATPase activity of recombinant cardiac K_{ATP} channels. Representative traces of Mg-ATPase activity as measured in a system of Kir6.2/SUR2A-transfected tsA201 cells. (B) 0.5 μM glibenclamide (Glib) abolished Mg-ATPase induced increase in current (A) while 1 μM gliclazide (Glic) had no significant effect on Mg-ATPase activity (C). (D) is a graphical representation of the normalized current. (n=5 patches, **<0.01)

A.

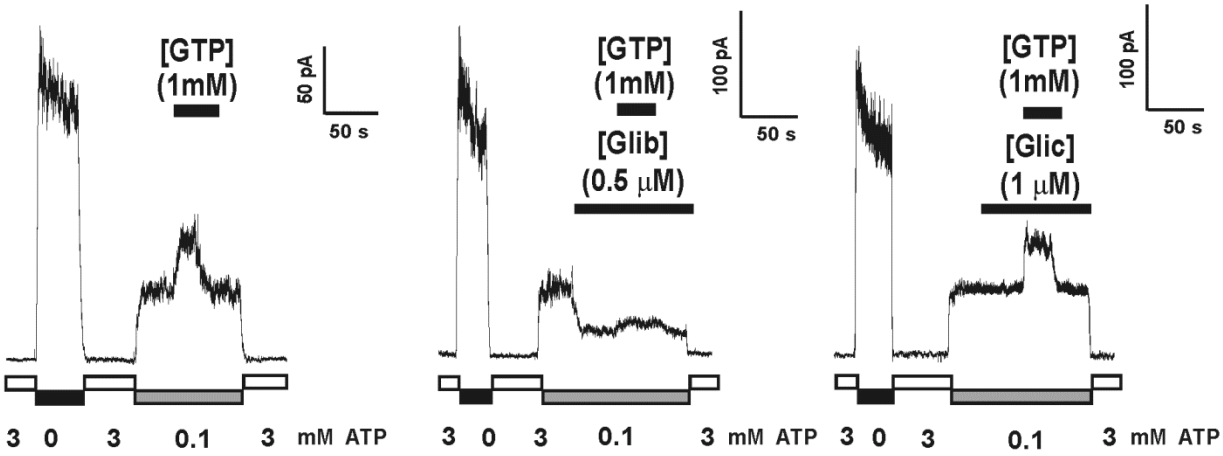
[GTP]
(1mM)
60 pA
50 s
3 0 3 0.1 3 mM ATP
[GTP]
(1mM)
[Glib]
(0.5 μM)
100 pA
50 s
3 0 3 0.1 3 mM ATP
[GTP]
(1mM)
[Glic]
(1 μM)
100 pA
50 s
3 0 3 0.1 3 mM ATP

B.

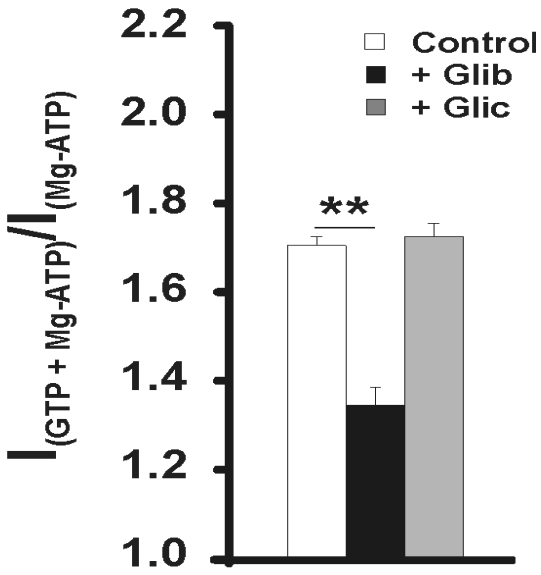
Control
+ Glib
+ Glic
**
I(GTP + Mg-ATP)/I(Mg-ATP)
2.2
2.0
1.8
1.6
1.4
1.2
1.0

Figure 5.6. Comparison between the activation of AMPK by DZX alone and by a combination of DZX and Glib. (A) Representative immunoblots comparing AMPK phosphorylation in C57Bl6 mouse hearts perfused in Langendorff mode with 100 uM diazoxide (DZX) or with 100 uM DZX and 1 uM Glibenclamide (Glib) compared to vehicle control. (B) Graphical representation of phosphorylated AMPK in the three groups normalized to total AMPK. (n=3/group, *<0.05, ** <0.01)

A.

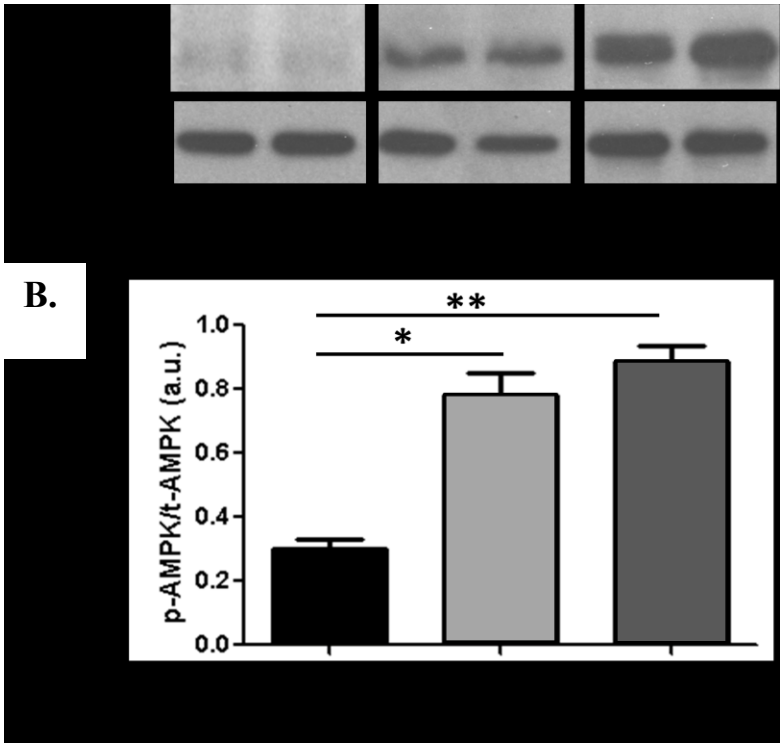

B.

<u>Figure 5.7.</u> Comparison between the activation of AMPK by HMR 1098 alone and by a combination of HMR 1098 and DZX. (A) Representative immunoblots comparing AMPK phosphorylation in C57Bl6 mouse hearts perfused in Langendorff mode with 10 μM HMR 1098 or with 10 μM HMR 1098 and 100 μM diazoxide (DZX) compared to vehicle control. (B) Graphical representation of phosphorylated AMPK in the three groups normalized to total AMPK. (n=3/group, $p>0.05$)

7

A.

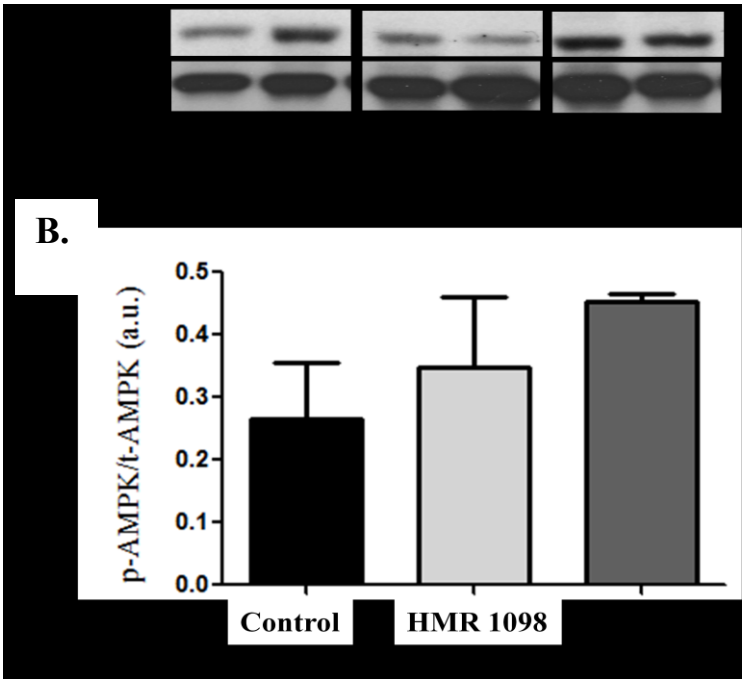

Figure 5.8. Effect of HMR 1098 on the Mg-ATPase activity of recombinant cardiac K_{ATP} channels. (A) Representative traces of Mg-ATPase activity as measured in a system of Kir6.2/SUR2A-transfected tsA201 cells showing that 10 uM of HMR 1098 has no effect on Mg-ATPase activity. (B) Graphical representation of the normalized current. (n=5 patches, $p>0.05$)

A.

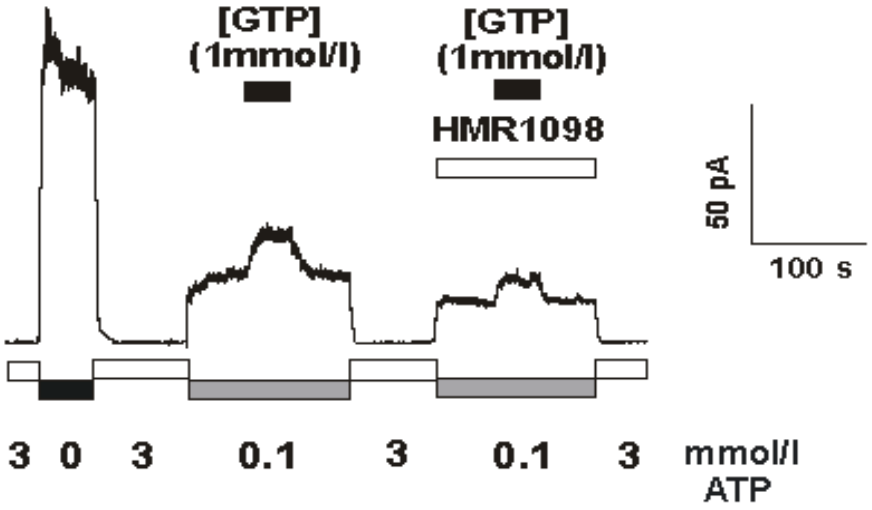
[GTP]
(1mmol/l)
[GTP]
(1mmol/l)
HMR1098
50 pA
100 s
3 0 3 0.1 3 0.1 3 mmol/l
ATP

B.

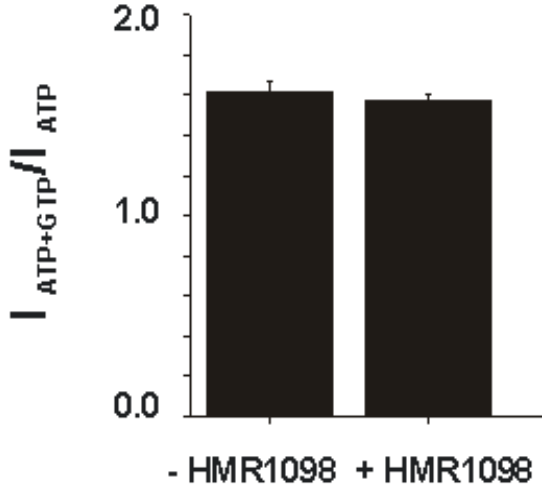
2.0
1.0
0.0
I ATP+GTP/I ATP
- HMR1098 + HMR1098

Figure 5.9. Effects of glib and glic on AMPK and LKB-1 activation in murine hearts. (A) Representative immunoblots showing phosphorylation of AMPK and its upstream activator LKB-1 perfused with steady state concentrations of glibenclamide (Glib) and gliclazde (Glic). (B) Graphical representation of phosphorylated AMPK normalized to total-AMPK in murine hearts perfused with vehicle, Glib (C_{ss}) and Glic (C_{ss}).(C) Graphical representation of phosphorylated LKB1 normalized to total-LKB1 in murine hearts perfused with vehicle, Glib (C_{ss}) and Glic (C_{ss}).

A.

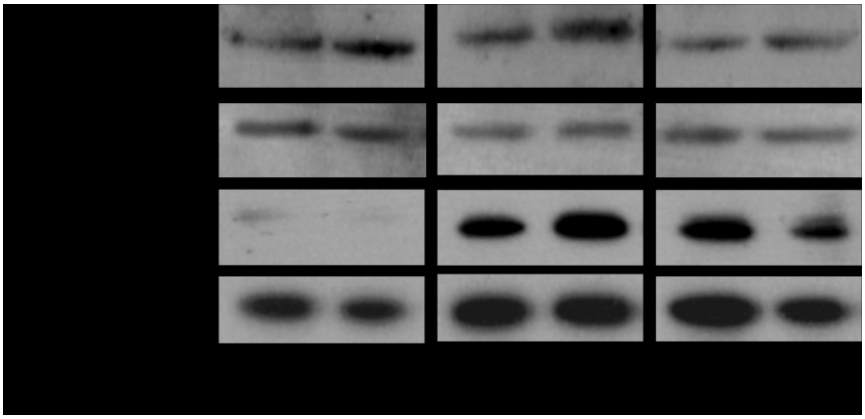

B.

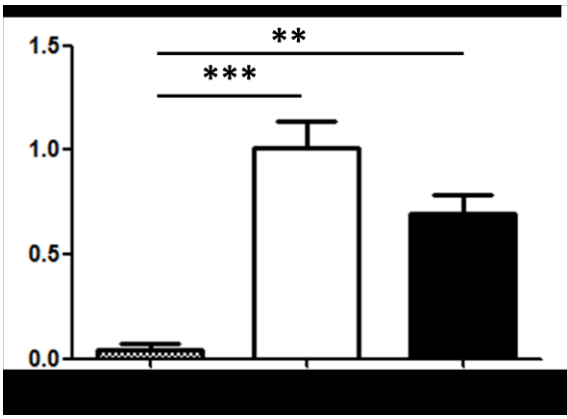

C.

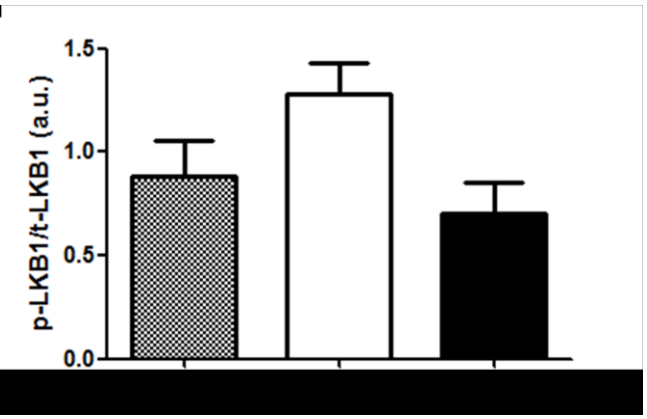

Figure 5.10. AMPK activation in individual human atrial appendages. Immunoblots and graphical representations of AMPK activation by glibenclamide (Glib) (A) and gliclazide (Glic) (B) in individual patients whose atrial appendages were isolated during undergoing coronary artery bypass graft surgery.

A.

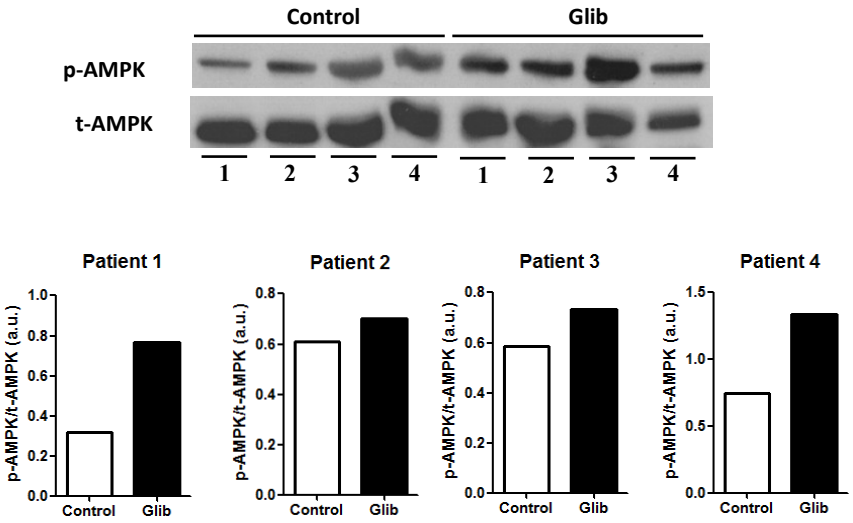
Control
Glib
p-AMPK
t-AMPK
1 2 3 4 1 2 3 4
Patient 1
Patient 2
Patient 3
Patient 4
p-AMPK/t-AMPK (a.u.)
Control
Glib

B.

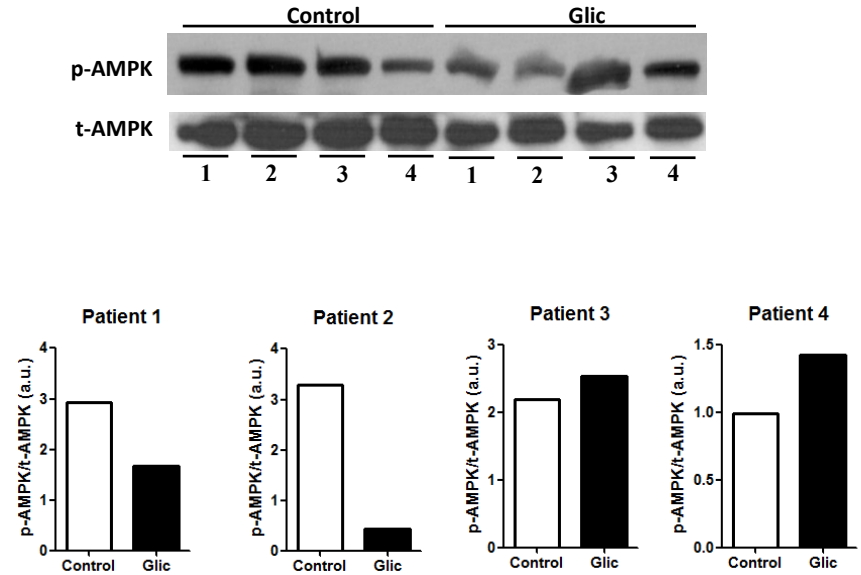
Control
Glic
p-AMPK
t-AMPK
1 2 3 4 1 2 3 4
Patient 1
Patient 2
Patient 3
Patient 4
p-AMPK/t-AMPK (a.u.)
Control
Glic

Chapter 6
General discussion and future directions

6.1. Summary

According to the World Health Organization, cardiovascular disease is the leading global cause of death and it is estimated that by the year 2030 around 23.6 million people will die of cardiovascular disease[1]. In Canada alone, a heart attack occurs every 7 minutes[497]. Development of cardiac disease may be due to several factors including genetic predisposition, unhealthy diet and a sedentary lifestyle. In order to develop treatments to guard against or limit the damage that occurs after a cardiac event, the pathways underlying the incidence of particular cardiac diseases have to be closely studied.

One of the most important pathways for maintenance of cardiac function is efficient of energy substrate utilization in the myocardium. Most (>95%) of the ATP generated in the heart is derived from oxidative phosphorylation in the mitochondria. The remaining 5% is derived mainly from glycolysis and to a lesser extent from the citric acid cycle[498,499]. The heart utilizes ≈60-70% of the ATP produced to fuel myocardial contraction and the remaining 30-40% for the different ion pumps especially the Ca^{++}-ATPase in the sarcoplasmic reticulum[225,500]. In cases such as myocardial infarction, the unavailability of oxygen and energy substrates to the myocardium severely disrupts cardiac metabolism, and upon reperfusion more damage is done due to heavy and rapid reliance on fatty acid oxidation which leads to uncoupling of glucose and glycolysis. This in turn generates protons causing cellular acidosis leading to subsequent Ca^{++} accumulation intracellularly which is ultimately detrimental to the cardiomyocyte[180,237,279].

Changes in cardiac metabolism that result in a drop in ATP concentration and increases in AMP as would be the case in an ischemic attack activate cardiac K_{ATP}

channels[430]. Despite that K_{ATP} channels have been classically known to be downstream to changes in metabolic signals, a growing body of evidence supports that K_{ATP} channels play a key role in regulating metabolism[353]. In addition to being linked to metabolism, K_{ATP} channels were shown to possess Mg-ATPase by which they can produce ADP, their activator, from Mg-ATP , their inhibitor, in their local environment[501]. Additionally, K_{ATP} channels were also shown to physically associate with several important nucleotide sensitive enzymes such as adenylate kinase 1[47,49] and creatine kinase[48], both of which are key enzymes in the phosphotransfer cascade that relays nucleotide signals between the cytoplasm and the mitochondria in case of energetic surplus or deprivation[49,502,503]. Moreover, K_{ATP} channels were shown to associate with several glycolytic enzymes[349,351] as well as the key cellular regulator of metabolism, AMPK[384]. Whether the enzymatic activity of the channel was linked to its metabolic properties had not been investigated, yet, it was plausible to speculate that the link between K_{ATP} channels and metabolism was not solely dependent on the electrical properties of the channels. As such, this thesis as a whole focused on identifying non-electrical effects of cardiac K_{ATP} channels that may contribute to changes in cellular signaling translating them potentially to changes in cardiac metabolism.

In Chapter 3, the focus was to identify whether the absence of K_{ATP} channels in the heart would alter how energy substrates would be utilized. We used Kir6.2-/- mice in order to answer that question. In our isolated working heart model, we demonstrated that absence of K_{ATP} channels in the heart leads to a significant increase in fatty acid oxidation and reduction in glycolysis under basal aerobic conditions. Additionally, we have demonstrated for the first time that active AMPK is higher in Kir6.2-/- mouse hearts under basal aerobic conditions. Moreover, under stress induced by perfusing hearts with β-isoproterenol, AMPK signaling is

compromised in the absence of K_{ATP} channels. Our data support the hypothesis that absence of K_{ATP} channels sets cardiac metabolism to a more compromised profile that hinders functional recovery should an ischemic insult occur. The increased reliance on fatty acid oxidation in the setting of ischemia-reperfusion injury has been shown to severely impede cardiac mechanical recovery[237,396], however it is yet to be investigated whether the same metabolic profile is observed under stress such as in ischemia-reperfusion injury. In line with our observation, we found that fatty acid metabolism markers are upregulated in Kir6.2-/- mice, possibly to support the reliance on fatty acid oxidation. We have also reported that naïve Kir6.2-/- mouse hearts have higher basal active Akt levels. In this regard, the interplay between the AMPK and the Akt pathway has been previously described in the heart[243]. Akt activation has been shown to inhibit AMPK activation[355], while Akt activation can also be mediated by AMPK[440]. The observed Akt activation was not as high as AMPK activation, raising the possibility that if AMPK was not as active Akt phosphorylation would be much higher. Both Akt phosphorylation in response to insulin and AMPK activation have been shown to be involved in increased glucose uptake[385,504], however, the density of surface expressed glucose transporters is not known in the Kir6.2-/- mouse and would be an interesting point for future study. It would also give us a clue as to why glucose oxidation was similar in both Kir6.2+/+ and Kir6.2-/- mouse hearts. Our results on metabolic changes in hearts may explain why other studies that utilized the Kir6.2-/- mouse model in an I/R experimental model observed worse cardiac recovery compared to Kir6.2+/+ mice. This observation however does not exclude that genetic ablation of the channel would result in loss of ionic homeostasis in an ischemic episode. As a result, the accumulation of

intracellular calcium would also contribute to the poor functional recovery as previously demonstrated[182,289].

Since we have observed changes in metabolism under basal aerobic conditions where electrical activity of K_{ATP} channels is not triggered, we speculated that our observation could be attributed to the channel's newly discovered enzymatic activity[42,379]. Nevertheless, the mechanisms that regulate Mg-ATPase activity in K_{ATP} channels have not been elucidated. In this regard, it has been previously demonstrated that human mutations in SUR1 increase Mg-ATPase activity underlie several cases of rare monogenic neonatal diabetes[158]. Furthermore, work from our lab has previously shown that the common diabetes susceptibility variant S1369A in SUR1 results in increased Mg-ATPase activity and channel activation that may contribute to the development of type 2 diabetes by suppressing insulin secretion[167]. Based on that we predicted that the removal of the side-chain hydroxyl group in the S1369A variant resulted in a loss of a hydrogen bond with the side-chain of the Q1372 residue in the hairpin loop region adjacent to the catalytic Mg-ATPase site in NBD2 leading to decreased enzymatic activity[167]. Therefore, we sought to determine potential regulators of Mg-ATPase activity of the channel in order to help us speculate what implications the difference in activity might have functionally. In Chapter 4, we showed that the strength of the interaction between amino acids in the hairpin loop adjacent to NBD2 is a direct determinant of the K_{ATP} Mg-ATPase activity. Furthermore, using site-directed mutagenesis we determined the molecular aspects that determine the sensitivity of K_{ATP} channels to understand the differential pharmacology of the K_{ATP} channel opener, DZX. We chose to study DZX because it was previously shown to possess differential effects on K_{ATP} channels expressing SUR1 and SUR2A subunits depending on the presence of ADP[179]. We were able to

demonstrate that changes in bond strengths affect the channel's sensitivity to DZX. Therefore, our results are particularly important in predicting pharmacological responsiveness to drugs such as DZX in patients carrying K_{ATP} mutations based on flexibility of the NBD2 hairpin loop which would directly affect Mg-ATPase activity. We have also shown that DZX-induced AMPK activation is disrupted in the absence of K_{ATP} channels suggesting that K_{ATP} channels are not only affected by AMPK through phosphorylation[386], but they are essential in full AMPK metabolic signal transduction. The full activation of AMPK would ensure full execution of downstream ATP-conserving and cell survival signalling which is crucial in times of metabolic stress. Moreover, we showed that applying mechanical stress on isolated patches from tsA201 cells expressing recombinant cardiac K_{ATP} channels increased Mg-ATPase activity. Whether the observed increase in enzymatic activity will be observed in the native cardiac channels is yet to be determined. If the mechanical stress-induced activation in Mg-ATPase activity is seen on the whole heart level, for example in experimental models of hypertension or hypervolemia, we would speculate that downstream signalling would be affected as a result contributing to changes in metabolism.

Following up with the possible non-electrical effects of drugs targeting K_{ATP} channels, we tested differences in AMPK activation by the frequently prescribed oral antidiabetics, the SUs. The reason we decided to study the effects of SUs is that their use has often been associated with cardiotoxity[122,484,505,506]. With the recently discovered non-electrical effects of the channel, it would be plausible that the cardiac side effects associated with SU use are mediated through K_{ATP}'s non-electrical effects. We focused in Chapter 5 on the effects of Glib since it has been extensively reported as a cardiotoxic sulfonylurea that worsens cardiac function after ischemia-reperfusion injury or leads to loss of cardiac

preconditioning[149,487,507]. Since AMPK activation in the heart is a key cellular line of defense against metabolic stress and the detrimental consequences that follow[384], it was important for us to determine whether Glib inhibited AMPK activation thereby compromising the signal propagation of survival mechanisms. At all concentrations tested, we have observed a significant increase AMPK activation caused by Glib, unlike the more pancreas-selective Glic[508]. We also measured phosphorylation of LKB-1, being the key upstream kinase that phosphorylates AMPK in the heart[509], at steady state concentrations of Glib and Glic and we have indeed demonstrated higher AMPK activation in the Glib-treated group. It is worth mentioning that LKB-1 is also regulated by deacetylation by the action of SIRT-1 particularly[510], however the effect of Glib and Glic on SIRT-1 remains to be investigated. While treatment with Glib did not inhibit AMPK signalling as expected, the increase in AMPK phosphorylation may still indicate metabolic stress induced by the drug. Keeping in mind that our treatment was acute, we need to investigate whether chronic use of Glib would affect kinase signaling. Additionally, we have shown that Glib abolishes the channel's Mg-ATPase activity while neither Glic and HMR 1098 had an effect on the channel's enzymatic activity. It is worth mentioning that previous studies have shown that Glic does not abolish protective cardiac preconditioning[152,483] and that HMR 1098 was even cardioprotective[490]. Interestingly, when we tested Mg-ATPase activity in the presence of metformin; an oral antidiabetic that has been shown to have favourable cardiac effects[511,512], we observed no change (Figure 6.1.).Whether Mg-ATPase activity was directly proportional to AMPK activation could not be established in this chapter with the current experimental model, however, a novel transgenic animal model that could address that will be discussed later in this chapter. Moreover, we also need to note that Glib is not entirely selective to K_{ATP}

channels. Glib for instance has been shown to have direct mitochondrial effects where it was shown to inhibit uncoupled respiration in both hepatic and cardiac mitochondria[513]. Additionally it has also been shown to disrupt mitochondrial membrane potential and proton gradient[514], and to lower mitochondrial ATP content in hepatic mitochondria in rats[515]. However, the exact mechanism by which Glib interferes with mitochondrial bioenergetics is not completely understood. However, disruption in mitochondrial respiration may directly increase cellular AMP:ATP ratio contributing to AMPK activation independent of K_{ATP} channel electrical inhibition or inhibition of Mg-ATPase activity.

6.2. Limitations

Due to the limited availability of our Kir6.2-/- mice, we were unable to include that group in several experiments in the thesis. For example, in Chapter 5, it would have been ideal to include Kir6.2-/- groups that are perfused with vehicle and plasma steady state concentrations of Glib and Glic to determine whether K_{ATP} channels mediated AMPK activation at therapeutic concentrations.

Since we were using a Kir6.2-/- mouse model, one could wonder if compensatory protein expression takes place. In this regard, Yang et al. have shown that expression of the Kir6.1 subunit is unchanged in Kir6.2-/- heart tissue[371]. On the other hand, Terzic's group has also shown that in the same model there is a significant increase in Na^+-K^+-ATPase expression[353], which we have confirmed as well, suggesting compensatory upregulation to maintain ionic homeostasis in these animals. Another major limitation with using this animal model for our experiments was that genetic ablation of Kir6.2 which prevented surface K_{ATP} expression. Since the absence of Kir6.2 meant that there would be no assembly with the SUR

subunit and therefore no trafficking or surface expression of the channel, that limited separating the channel's electrical activity, attributed to Kir6.2, and the enzymatic activity, attributed to SUR.

In Chapter 3, we attempted to investigate differences in cardiac metabolism between Kir6.2+/+ and Kir6.2-/- mice. We measured glycogen content in naïve hearts from both groups which would indicate differences in glycogen synthesis or utilization rates. However, since we measured metabolic rates during working heart perfusions, we could improve upon the experiment by measuring glycogen turnover in cardiac tissue at the end of the working heart perfusions (as described by Jaswal et al.[313]) which will help us understand more about the dynamics of substrate mobilization in Kir6.2-/- mouse hearts.

Additionally, we assayed Mg-ATPase activity of the channel using tsA201 cells transfected with recombinant K_{ATP} channels. Though this technique gave us important evidence regarding the direct effect of DZX, Glib and Glic on the enzymatic activity of K_{ATP} channels, it is important to note that it does not fully represent the environment that the native channel would be expressed in. For example, the attachment of glycolytic and phosphotransfer enzymes to the recombinant channel in the human kidney cell (tsA201) would be exact as would be seen in a cardiomyocyte. Therefore the subtle changes in nucleotide concentrations that may affect the channel activity would not be observed in this system. (Figure 6.2.). It would be more accurate to determine Mg-ATPase activity in native cardiomyocytes although this is complicated by spontaneous contraction which makes maintaining a gigaseal to record the current challenging.

For our cardiac perfusions, we chose the ex-vivo Langendorff-perfused heart model to administer the different drugs under investigation. Since we intended to measure the biochemical changes in cardiac tissue resulting from administration with pharmacological agents, it was fitting to the purpose of our experiments[364]. However, it is important to note that in this perfusion mode, hearts are perfused retrogradely through the aorta and do not pump against hydrostatic pressure such as the case is in normal physiology. A working heart perfusion model would be closer to a physiological setting and can enable measurement of cardiac functional parameters. Ideally, in vivo measurement of changes in cardiac function using echocardiography after drug injection and subjecting the mice to ischemia using coronary artery ligation would be a better model to address functional questions.

In this thesis, we tested the effects of several pharmacological agents on AMPK signalling. Though the concentrations we have used in our experiments are within the effective concentration range and if higher, it was for a specific experimental purpose, the drugs at these concentrations still could exert K_{ATP}-independent effects. DZX has been shown to be an inhibitor of succinate dehydrogenase which is a complex II mitochondrial protein[459,460]. Inhibition of succinate dehydrogenase has been shown to be cardioprotective[516], however, the exact mechanism is not yet established, although production of reactive oxygen species has been suggested to be one of the protective mechanisms[461,462,517]. The direct relation between inhibition of succinate dehydrogenase and AMPK activation may be through the rise in AMP in the event of uncoupling of oxidative phosphorylation that leads to direct activation of AMPK. Moreover, since we have used a Kir6.2-/- mouse model, it means that vascular K_{ATP} channels which express the Kir6.1 subunit are still expressed in the hearts we perfused, however, it is hard to speculate if

vascular K_{ATP} activation contributes to the observed AMPK activation in this experimental model. Moreover, DZX treatment has been shown to increase the production of nitric oxide[432] which in turn can contribute to AMPK activation[518].

6.3. Future directions

The findings of this thesis add another dimension to the complexity of cardiac K_{ATP} channels. Although they are generally considered to be closed in the myocardium under resting conditions, their role during physiological stress is of vast importance. Shortening of the action potential duration due to K^+ efflux through K_{ATP} channels during stress is crucial to maintain a sufficient refractory period between action potentials. This period is needed for full ionic recovery in the cardiomyocyte to sustain membrane polarization in preparation for the occurrence of the new action potential. During stress, a sufficient refractory period would minimize the generation of cardiac arrhythmias and ensures that the myocardium is working faster and harder to meet the increased workload and the accompanying increase in metabolic demands. The results in this thesis show that cardiac K_{ATP} channels directly affect the activation of AMPK, which is central in preserving cellular energy during stress. Additionally, absence of the channels markedly alters the cardiac metabolic profile. The electrical effects of K_{ATP} channels along with its presence in a plasma membrane nucleotide-sensitive metabolome may prove crucial in providing the cell with an early stress signal modulated through K_{ATP}-associated AMPK.

Although this thesis has presented novel data linking both electrical and metabolic channel properties, a significant amount of experiments needs to be performed to further characterize the non-electrical role of K_{ATP} channels. One of the important aspects that need

to be definitively tackled is whether the changes we observed in AMPK signalling and in cardiac metabolism in the absence of K_{ATP} channels were due to the loss of their electrical or enzymatic activity.

In this regard, we chose to use the Tg(CX1-eGFP-Kir6.1-AAA) mouse model, developed as previously described by the Coetzee group[519]. In that model, the conserved motif (GFG) responsible for K^+ selectivity in the Kir6.x subunit has been mutated to (AAA) which has been shown to significantly reduced K_{ATP} current[520](Figure 6.3.B). Interestingly, it does not only limit current in Kir6.1, but it reduces current in Kir6.2-expressing K_{ATP} channels by almost 75%[520]. The mutated Kir6.1 subunit would still normally co-assemble with SUR and be trafficked and expressed on the cell surface. Unlike the Kir6.2-/- model, this gives us the advantage of having the non-conducting channel normally trafficked and expressed in the plasma membrane while preserving its enzymatic activity. In order to investigate cardiac-specific effects of reducing K_{ATP} electrical conductance, we crossed the Tg(CX1-eGFP-Kir6.1-AAA) with transgenic mice that express Cre recombinase under the control of the α-MHC promoter[521]. Target mice for our future experiments would be Kir6.1AAA+/Cre+ that would not be expressing GFP in their cardiac tissue which indicates successful cardiac-specific Kir6.1AAA expression (Figure 6.3.C). Another helpful model that is currently under development is a transgenic mouse model expressing a Kir6.2AAA subunit. This transgenic mouse is being generated using Transcription activator-like effector nucleases (TALENs) which would enable genome editing by mRNA microinjection in the murine embryonic cell[522,523]. This model would have the advantage of co-assembly with SUR and expression on the cell surface, however, because the mutation is in the Kir6.2 subunit, it would abolish K_{ATP} conductance in the heart as opposed to the Kir6.1AAA mutation where

residual current by Kir6.2-expressing K_{ATP} channels can still be recorded[520]. If the metabolic changes we observed in the Kir6.2-/- mouse model were replicated in the new transgenic mouse models carrying the non-conducting AAA mutations, then the contribution Mg-ATPase activity the enzymatic property of the channel is negligible to those changes. However, if metabolism is similar to Kir6.2+/+ mice then that would imply a major role of Mg-ATPase in regulating cardiac metabolism through changing AMPK signaling. It would be imperative then to test the effects of clinically used K_{ATP}-targeting pharmacological agents to test their effects on Mg-ATPase activity in these new transgenic models under aerobic conditions and in different experimental models of I/R and heart failure. The results from these studies could shed new light on the mechanism of development of cardiovascular complications associated with sulfonylurea use.

It is important to note also that the experiments conducted used healthy mice. In reality, patients using SUs already suffer from hyperglycemia, which predisposes them to cardiac disease development[524–526]. Additionally, increased plasma glucose has been shown to may reduce cardiac K_{ATP} channels gene expression which may contribute to the poor cardiac function observed in diabetic animals[527]. Additionally, they would have a different metabolic profile than the healthy individuals. In diabetic hearts, there is a huge reliance on fatty acid oxidation at the expense of glucose oxidation[528]. In part, due to the elevated circulating free fatty acids that are a result of enhanced lipolysis in the adipose tissue due to lack of insulin which normally regulates this process[529]. Additionally, glucose uptake has been shown to be markedly reduced in diabetic hearts[530]. In fact, overexpression of GLUT4 in diabetic *db/db* mice was shown to increase glucose uptake, reduce utilization of fatty acids and to protect the heart against the development of cardiac dysfunction[530]. It would be

very informative to test the effects of SUs on diabetic Tg(Kir6.2AAA) mice to dissect the role of K_{ATP} enzymatic activity in a setting that is closer to the clinical one.

Since the subject of cardiac energy homeostasis is quite intricate and complicated, it is natural that we cannot attribute the changes we saw in Kir6.2-/- solely to AMPK activation. It would be interesting to investigate changes in the PI3K pathway since its activation would lead to increased glucose uptake through promoting the translocation of GLUT4 to the cell membrane and fatty acid uptake through the fatty acid transporters CD36 and FABPpm[531]. Further examination of how the absence of K_{ATP} channel would alter the different proteins in the cell survival reperfusion injury salvage kinase pathway, particularly MAPK/Erk since we have not probed for any of those kinases in this thesis, would give us a clearer picture on what the non-electrical aspects of K_{ATP} channels could affect cardiac recovery[532].

Another protective mechanism that has been implicated in ischemic preconditioning is cardiac autophagy[533]. Activation of AMPK leads to phosphorylation of targets upstream of mTOR in the Akt pathway as well as direct phosphorylation of mTOR complex 1 leading to its inhibition[534]. As a negative regulator of autophagy, inhibition of mTOR leads to induction of the autophagic pathway[535,536]. Since we observed an increase in activity of the Akt pathway in hearts perfused with DZX (Figure 4.3 on page 140 in Chapter 4), it would be interesting to investigate whether autophagy is still stimulated in the absence of K_{ATP} channels. A key marker of induction of autophagy is the formation of the autophagosome which in its membrane would incorporate LC3BII, a key marker of autophagosome formation[537]. Our preliminary data show that there is much less LC3BII expression in both Kir6.2+/+ and Kir6.2-/- perfused with DZX (Figure 6.4.A). This could either mean that the

rate of autophagosome formation is the same but there is increased flux of autophagosomes or that autophagosome formation is reduced due to decreased autophagy. This could be addressed by co-administration of chloroquine or NH_4Cl which have both been shown to prevent autophagosome flux leading to their accumulation thus enabling us to probe for the changes in autophagic rates[538]. This could also be tested on the cellular level using isolated cardiomyocytes from Kir6.2+/+ and Kir6.2-/- mice and transfecting them with the GFP-tagged LC3 vector construct (Figure 6.4.B,C) and inducing autophagy in the presence and absence of chloroquine to test for autophagosome formation. Electron microscopy would be the gold standard in identifying autophagosomes[538]. The link between K_{ATP} channels and autophagy has been studied in HL-1 cells where Samokhvalov et al. showed that inhibition of K_{ATP} channels resulted in the loss of the protective effects of autophagy during HL-1 cardiac cell starvation[539]. More studies need to be conducted to confirm whether this observation would be observed in the intact heart by inducing autophagy using rapamycin for example or possibly in an *in vivo* model of starvation.

Another avenue that could contribute to AMPK activation as well as Mg-ATPase activity stimulation is mechanical stress. In that regard, models of pressure overload such as transverse aortic constriction[540] could help us compare between the effects of mechanical stress in the presence and absence of K_{ATP} channels. In this case, we would use the Tg(CX1-Kir6.1AAA-eGFP) mouse as well as the Kir6.2-/- mouse models in order to separate the electrical and enzymatic activity of the K_{ATP} channel.

One more aspect that could be studied is the effect K_{ATP} channel ablation on Ser/Thr phosphatase activity. Since we observed higher phosphorylation of AMPK, LKB1, Akt and mTOR, it would help strengthen our results to examine whether the dephosphorylation

process of these proteins is normal or that the expression and activity of phosphatases such as PP1, PP2A and PP2A, shown to be involved in regulating key metabolic proteins such as AMPK and Akt[308,458,541], is lower. We can extend that investigation to the effect of the drugs we have used in our studies on expression and activity of the phosphatases since this has not been investigated as well.

6.4. Final conclusions

Overall, the presentation of the findings outlined in this thesis have confirmed the involvement of K_{ATP} channels in cellular signaling and metabolism. The results have furthered our understanding of non-electrical properties of cardiac K_{ATP} channels. Our results on Mg-ATPase activity regulation and how it may directly alter pharmacological sensitivity of the K_{ATP} channel would have direct applications in selecting appropriate therapies for patients carrying K_{ATP} channel mutations. Furthermore, we have shown that surface expression of K_{ATP} channels is essential for full stress signal transduction and the resulting cardiac metabolic profile which would be particularly important in the setting of ischemia-reperfusion injury. Moreover, we have shown that among the SUs tested, Glib was the only drug that inhibited both electrical activity Mg-ATPase activity of the K_{ATP} channel. This finding adds to the complexity of K_{ATP} channel pharmacology but could be a stepping stone towards understanding the we could further advance our knowledge of the pharmacology of SUs and their possible cardiovascular adverse effects.

Figure 6.1. Representative macroscopic inside-out patch clamp traces of recombinant expressed Kir6.2/SUR2A cardiac K_{ATP} channels. GTP causes an increase in channel activity through production of GDP by the Mg-ATPase of the channel. In the presence of metformin, no change in the GDP-induced change in current was observed.

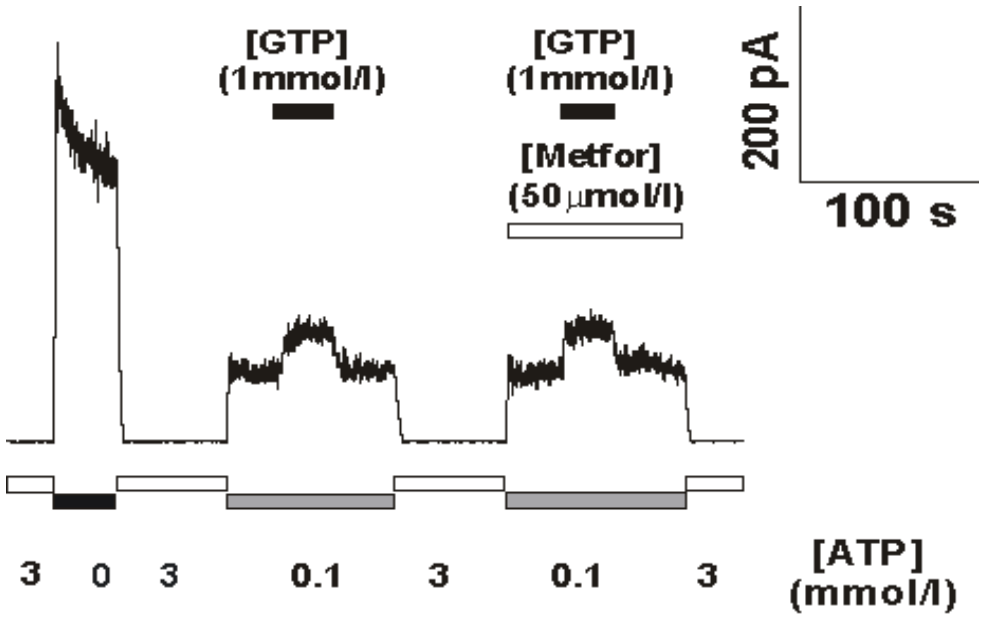
[GTP]
(1mmol/l)
[GTP]
(1mmol/l)
[Metfor]
(50 µmol/l)
200 pA
100 s
3
0
3
0.1
3
0.1
3
[ATP]
(mmol/l)

Figure 6.2. Immunoblot showing expression of adenylate kinase 1 (AK1) in (A) untransfected tsA201 cells, (B) AK1-transfected tsA201 cells, (C) tsA201 transfected with recombinant (rc) K_{ATP} channels and (D) tsA201 cells transfected with the rc cardiac K_{ATP} channels and AK1. This blot demonstrates negligible expression of AK1 which is one of the major phosphotransfer enzymes in the human embryonic kidney variant, the tsA201 cell line.

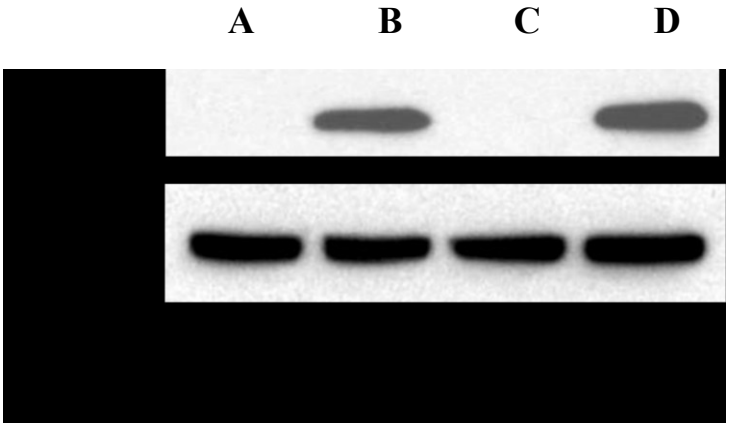
A
B
C
D

Figure 6.3. (A) Replacing the conserved (GFG) motif with AAA in the Kir6.1 and Kir6.2 subunits mutation renders the K_{ATP} channel incapable of K^+ conductance. B) The targeting construct to generate the Tg(CX1-eGFP-Kir6.1AAA) transgenic mouse. C) An isolated cardiomyocyte from our Kir6.1AAA+/Cre- offspring . (D) An isolated cardiomyocyte from our Kir6.1AAA+/Cre+ offspring . Both (C) and (D) have been photographed using a digital microscope fitted with a GFP filter.

A.

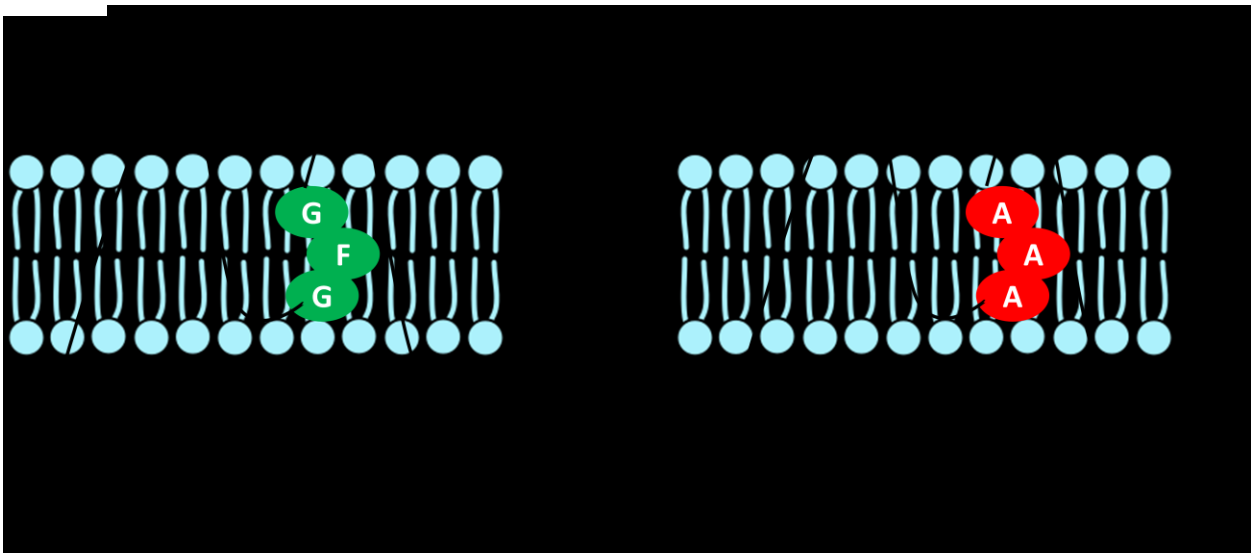

B.

C.

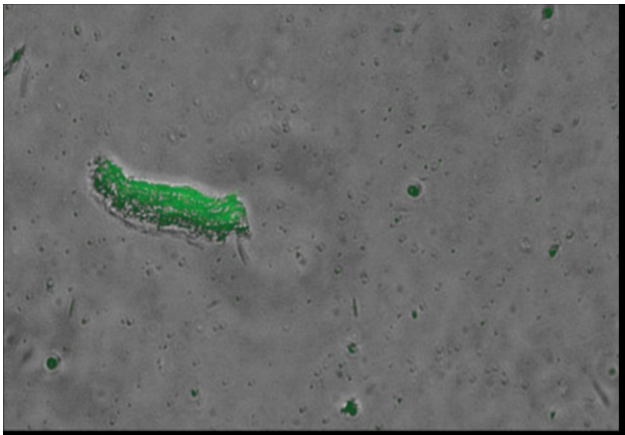

D.

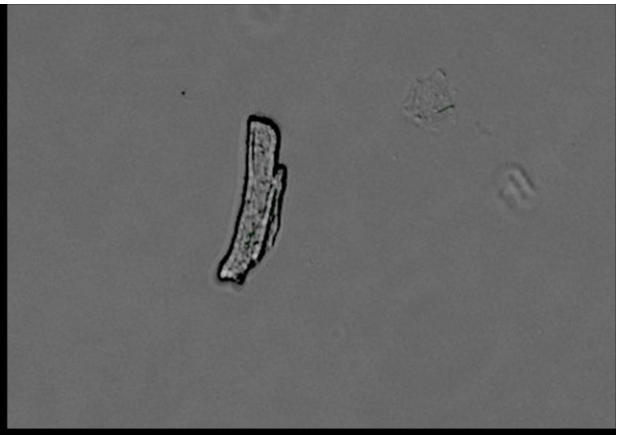

Figure 6.4. (A) Immunoblot comparing the expression of LC3BII in Kir6.2+/+ and Kir6.2-/- perfused with Krebs-Henseleit buffer containing vehicle or 100 uM DZX. (B) Spinning confocal micrographs of neonatal rat ventricular cardiomyocytes were isolated from 1-2 day old Sprague-Dawley rat pups transfected with GFP-LC3 plasmid. Upon reaching approximately 50% transfection efficiency, the cells were either (B) preserved in DMEM or (C) starved for 6 hours using Earl's Balanced Salt Solution (EBSS). The formation of puncta indicates induction of autophagy and formation of autophagosomes.

A.

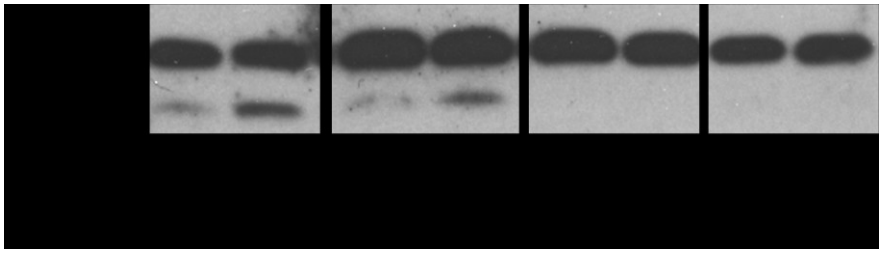

B.

C.

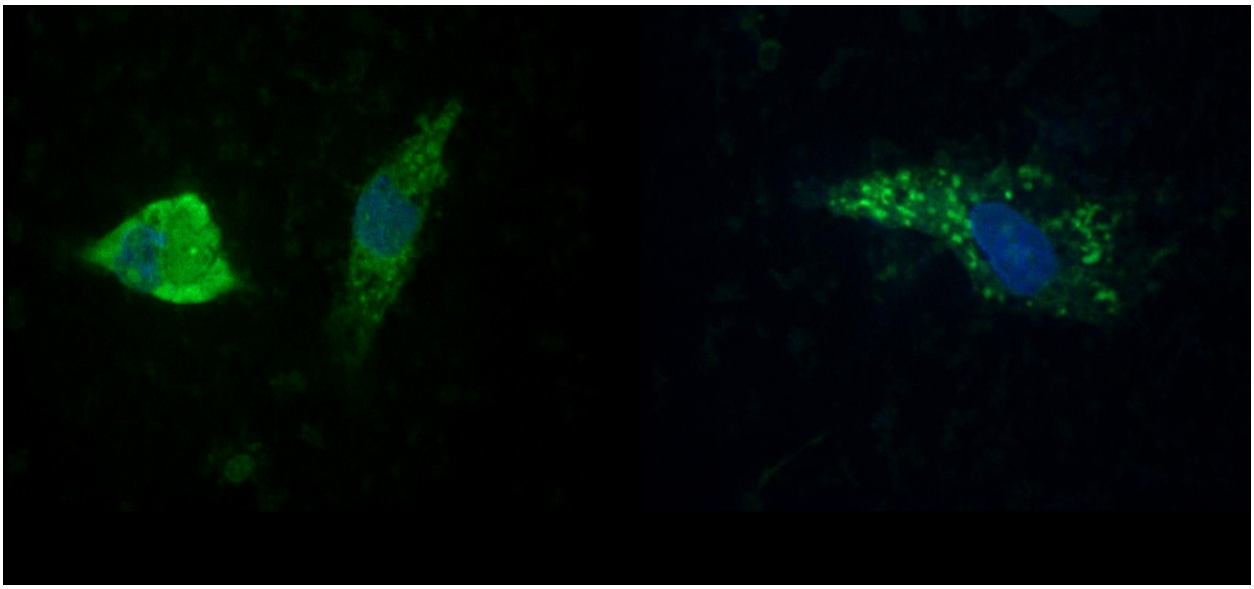

Appendices

I. Introduction

At the beginning of my PhD program, I spent one year and 3 months in the laboratory of Dr. Richard Schulz where I was studying the role of matrix metalloproteinase 2 in the heart. During my time in Dr. Schulz's laboratory, I wrote a book chapter about that topic and took part in producing a manuscript that was published in 2011. I have attached both publications in the thesis as appendices.

II. Intracellular MMP-2: Role in normal and diseased hearts

Nermeen Youssef and Richard Schulz

This chapter has been published as part of a book titled *"Molecular Defects in Cardiovascular Disease".* Editors**:** Naranjan S. Dhalla, Makoto Nagano,Bohuslav Ostadal, Springer 2011.Pages 17-28
ISBN: 978-1-4419-7129-6

Introduction

Proteases are known to be pivotal regulators of many vital physiological and pathological processes. Their activation or deactivation is a key step in preventing or effecting disease. They play key roles in cardiovascular diseases, from caspases in cardiac cell death, renin and angiotensin converting enzyme in hypertension, to matrix metalloproteinases (MMPs) in ischemic and inflammatory heart disease. Known primarily for their ability to proteolyze extracellular matrix proteins, MMPs have been extensively studied in the past fifty years following their discovery. Their proteolytic activity was later found to be central in several physiological as well as pathological processes in the human body. MMP-2 is found in almost all cells and is particularly known to be involved in cardiovascular pathologies related to enhanced oxidative stress such as ischemia-reperfusion (IR) injury. Contrary to the common idea that MMP-2 is only an extracellular protease, compelling evidence shows that there are new biological roles for it inside the cell. Acute changes in myocardial contractile function are caused by MMP-2's intracellular localization and ability to cleave specific proteins important in regulating the contractile function of the heart. In this chapter we will discuss some of the novel intracellular roles of MMP-2 that are thus far known in normal and diseased hearts.

MMPs

MMPs are a family of structurally related zinc-dependent endopeptidases. MMP activity was first discovered in 1962 by Gross and Lapiere as a collagen digesting enzyme involved in tail resorption during the morphogenesis of tadpoles into frogs[1]. This discovery opened the doors to a new field of research focusing mainly on the biological actions of these

proteases to proteolytically remodel the extracellular matrix. Such research explained how several physiological remodelling processes such as angiogenesis, embryogenesis[2], uterine involution[3], bone and connective tissue turnover, to name a few, require the extracellular matrix degrading properties of MMPs. In addition to that, MMPs have been shown to play a part in several pathologies including aortic aneurysms[4], cancer[5] and several inflammatory diseases including periodontitis[6] and arthritis[7].

MMPs are referred to numerically from MMP-1 to MMP-28. In the past they were conventionally grouped according to their substrates, primary structure or subcellular localizations into: gelatinases (MMP-2 and-9), collagenases (MMP-1, -8 and -13), stromelysins (MMP-7 and -26), matrilysins (MMP-3, -10 and -11), metalloelastases (MMP-12) and membrane-type MMPs (MMP-14-16 and MMP-23-25). MMP-4, -5, and -6 are not unique MMPs since they turned out to be either MMP-2 or MMP-3. The mammalian homologue of MMP-18 has not been found yet[8]. In cardiovascular disease, MMP-2 appears to be of greater significance compared to other MMPs, based on its elevated activity in hypertension, heart failure, ischemic and inflammatory heart diseases. We refer here to useful and extensive reviews on the intracellular[9] and extracellular[10] actions of MMPs in the heart. This chapter however will focus solely on the more recently discovered intracellular roles of MMP-2 in the heart.

MMP-2

MMP-2, previously known as gelatinase A or type IV collagenase, is expressed in almost all cell types. It proteolyzes denatured collagen (gelatin) and intact collagen type IV, both of which are core components of the basement membrane. MMP-2 is abundantly

expressed in the heart tissue, particularly in the vasculature, cardiomyocytes and fibroblasts[11-14].

Structure

MMP-2 as with other MMPs is synthesized as a 72 kDa inactive zymogen or "pro-MMP" (See Figure 9.1). At its N terminus it contains an autoinhibitory, hydrophobic propeptide domain that shields the catalytic site of the enzyme. The catalytic site contains a zinc ion that is essential for its activity. The presence of a second structural zinc ion in addition to two or three calcium ions has been suggested[15].

Regulation of MMP-2

A well studied component of the activation of pro-MMPs is the necessity to disrupt the coordination bond between the cysteine sulphydryl of the propeptide domain and the zinc ion in the catalytic domain, creating a "cysteine switch" [16]. In the case of MMP-2, this can take place through proteolytic cleavage and removal of the propeptide domain of the full length 72 kDa enzyme by action of membrane-type-1 MMP (MMP-14), in conjunction with tissue inhibitor of metalloproteinase-2 (TIMP-2), to yield an enzymatically active 64 kDa enzyme[17] (See Figure 9.1). However, far less attention has been given to what is likely a very important alternative mechanism of MMP-2 activation, independent of the proteolytic removal of the propeptide domain, by specific disruption of the cysteine-zinc bond by reactive oxygen/nitrogen species (vide infra).

The activity of MMP-2 is regulated at several different levels depending on the type of stimulus. It can be regulated through: 1) changes in gene transcription and translation, 2) post-translational modifications such as glutathiolation and phosphorylation, 3) interaction

with endogenous inhibitors known as the tissue inhibitors of metalloproteinases (TIMPs) and 4) interaction with caveolin-1 in cell membrane caveolae.

Transcription and translational changes. It was believed that MMP-2 is a constitutive enzyme; however, it is now known that its expression can be induced. The promoter region of the MMP-2 gene does not contain a TATA box, contrary to that of MMP-9, and allows for multiple transcription sites. MMP-2 transcription occurs by binding of transcription factors to a downstream GC box. The MMP-2 promoter does not contain a proximal AP-1-binding site; however, studies investigating regulation of its transcription revealed a functional AP-1 consensus binding sequence[18]. At the mRNA level, MMP-2 expression in cardiac and vascular smooth muscle cells is upregulated in response to hypoxic conditions, angiotensin II, endothelin-1, interleukin-1β or high glucose[18-21]. MMP-2 expression in human macrovascular endothelial cells was found to be notably increased upon reoxygenation following hypoxia[22], in hearts after IR injury[23] and in congestive heart failure[24]. In addition to that, protein and mRNA levels of MMP-2 are significantly increased upon signalling by pro-inflammatory cytokines[25].

Oxidative stress. Studies from our lab and others have shown that it is not necessary for the full length 72 kDa MMP-2 to lose its propeptide domain in order to become an active protease. Activation can also take place upon exposure to reactive oxygen/nitrogen species such as peroxynitrite ($ONOO^-$), an important mediator of oxidative stress injury[26]. In a reaction requiring $ONOO^-$ and glutathione, the cysteine-zinc bond in the cysteine switch is disrupted without cleavage of the propeptide domain[27-29]. Okamoto et al.[27] demonstrated that low concentrations of $ONOO^-$ caused S-glutathiolation of the cysteine residue in the PRCGVPD sequence in the MMP-1, -8 and -9 propeptide domain (highly conserved amongst

MMPs) and enhanced their enzymatic activity. Our lab found that 0.3 μ (mu)M - 10 μ (mu)M $ONOO^-$ activated 72 kDa MMP-2, whereas >100 μ (mu)M inhibited activity[29]. Fliss and Ménard showed that H_2O_2 modulated MMP-2 activity in a similar manner, whereby 4 μ (mu)M activated MMP-2 and 10–50 μ (mu)M inhibited enzyme activity. Both the responses of MMP-2 to $ONOO^-$ and H_2O_2 suggest a biphasic response to oxidative stress through different post-translational modifications of the protein and subsequent configurational changes controlling access to the catalytic zinc ion[29, 30].

Phosphorylation. Phosphorylation of serine, threonine and/or tyrosine residues is an important means to regulate the activity of some proteins. We investigated whether MMP-2 is a phosphorylated protein and if its phosphorylation status affects its enzymatic activity. Recombinant human MMP-2 and native MMP-2 secreted from HT1080 human fibrosarcoma cells were found to be phosphorylated[31]. The activity of MMP-2 after its dephosphorylation with alkaline phosphatase was enhanced whereas phosphorylation with protein kinase C in vitro reduced its activity. We identified five phosphorylation sites on residues with side chains accessible on the surface of MMP-2 (S32, S160, T250, S365 and Y271), however, the exact phosphorylation sites in vivo are yet unknown. In the setting of IR injury, isolated rat hearts perfused with okadaic acid, an inhibitor of protein phosphatase 2A, showed improved recovery following reperfusion and reduced loss of troponin I (TnI), an MMP-2 substrate (vide infra) which is an important regulator of actin-myosin interaction. This observation may be attributed to the effect of inhibiting the action of protein phosphatase 2A on MMP-2 to keep MMP-2 in a more phosphorylated and hence less active state[32]. The protein kinases and phosphatases controlling MMP-2 phosphorylation status in vivo are yet unkown. A study by Nyalendo et al. showed that MMP-14 is phosphorylated and inhibition of its

phosphorylation reduced tumor cell proliferation in mice[33]. However, the effect of MMP-14 phosphorylation on its activity is unknown.

Figure 9.2 is a diagram which shows activation pathways of MMP-2 and how this may be further modified by MMP-2 phosphorylation.

TIMPs. Tissue inhibitors of metalloproteinases (TIMPs) are endogenous inhibitors of MMP activity. The TIMP family consists of 4 known members, TIMP-1 through TIMP-4[34]. They bind to MMPs in a 1:1 stoichiometric ratio thereby inhibiting their activity. TIMPs do not show particular specificity towards various MMPs, nonetheless TIMP-2 shows some preferential inhibition of MMP-2 and TIMP-1 with MMP-9[35]. All TIMPs are constitutively expressed in the heart and vasculature[36]. TIMP-4 protein is abundant in the heart and is localized to the sarcomere within cardiac myocytes in the same subcellular compartment as MMP-2, a fact that implies TIMP-4's likely protective activity against the detrimental actions of MMP-2 in oxidative stress[37, 38] . TIMP-3 on the other hand is tightly bound to the extracellular matrix where it is exclusively localized[39]. Its level is lowered in the hearts of in mice with heart failure[40] and in aortas of patients with thoracic aortic aneurysms[41].

Caveolin-1. A recently discovered additional means to regulate MMP-2 activity is through its interaction with caveolin-1. A portion of cellular MMP-2 was found to be localized within caveolae of cardiomyocytes[13, 42] and endothelial cells[43]. Caveolae are invaginations of the cell membrane that regulate cytoplasmic signalling proteins and transport of macromolecules in and out of the cell[44]. We showed that MMP-2 co-localizes with caveolin-1 in cardiac myocytes, an integral membrane protein found within lipid rafts on the inner leaflet of the cell membrane. Hearts from caveolin-1 knockout mice show

elevated myocardial MMP-2 activity compared to wild type control hearts. A peptide containing the caveolin scaffolding domain from caveolin-1 or caveolin-3 inhibited MMP-2 activity in vitro[42]. Despite these findings we did not find impaired cardiac contractile function in isolated working hearts from young (6-8 week) mice, either in response to physiological (preload) or pharmacological (isoproterenol) challenges[45]. We speculate that the caveolin-1/MMP-2 interaction may be a means to control the activity of the portion of MMP-2 which is plasma membrane bound[42], however, more work in this area needs to be done.

Pharmacological MMP inhibitors. Most pharmacological inhibitors of MMP-2 act by chelating the zinc ion in the enzyme's catalytic site[46]. Such MMP inhibitors include batimastat, marimastat, GM-6001 (ilomastat/gelardin), *o*-phenanthroline, PD-166793[47] and ONO-4817[48]. Although these compounds selectively inhibit MMP activity in comparison to their lack of action on other protease classes, they do not preferentially inhibit a single MMP. In addition, the tetracycline class of antibiotics, dependant on their ability to chelate divalent cations, have proved to be effective inhibitors of MMPs. In investigating their structure-activity relationship, Golub and co-workers synthesized chemically modified tetracyclines which maintained their ability to inhibit MMPs but are devoid of antimicrobial activity[49]. Of the tetracyclines, the most potent MMP inhibitor belonging to this family is doxycyline[50] followed by minocycline. The latter is a more lipophilic molecule and thus exploited for its ability to cross the blood brain barrier for treatment of neurodegenerative diseases. Studies have demonstrated that doxycycline preferentially inhibits MMP-2, -9, and MMP-8 in comparison to MMP-1 and it has no effect on either MMP-3 or -7[51]. In vivo doxycycline was found to inhibit MMP activity at a plasma concentration lower than the plasma concentration

required for its antibacterial effect[52]. This led to the development of an FDA and Health Canada approved, sub-antimicrobial dose formula of doxycycline (doxycycline hyclate, 20 mg b.i.d) approved for the treatment of periodontitis (Periostat®).

Physiological roles of MMP-2 in the heart

Before discussing the role of MMP-2 in heart disease, we would like to shed light on some of its few known physiological roles in the heart. MMP-2 appears to have a crucial role in embryonic heart development[2] including angiogenesis[53], valve development and heart tube formation[54]. To exemplify the importance of MMP-2 in heart development, Linask et al. used an MMP-2 neutralizing antibody or the MMP inhibitor ilomastat to inhibit MMP-2 in developing chick embryos. This caused severe heart tube defects, cardia bifida and a disruption in the looping direction which suggested a key role of MMP-2 in cell migration and remodeling required for normal heart development[54]. MMP-2 knockout mice survive at birth and are viable as adults, however, they display significantly retarded growth in comparison to the wild-type controls[55]. These studies, however, have only focussed on the extracellular matrix degrading actions of MMP-2.

Intracellular MMP-2

In studying IR injury in perfused rat hearts, Cheung et al. found a significantly enhanced release of 72 kDa MMP-2 which peaked in the first 2-5 minutes of reperfusion[56]. This release of MMP-2 activity during reperfusion was enhanced with increasing duration of ischemia and showed a negative correlation with the recovery of contractile function during reperfusion. Addition of semipurified MMP-2 to the perfusion buffer contractile recovery of the heart following IR injury whereas a neutralizing MMP-2 antibody or the MMP inhibitors

o-phenanthroline or doxycycline improved the recovery of contractile function in reperfusion. Looking at these findings one finds compelling evidence for a role of MMP-2 in IR injury. We suggested that the release of MMP-2 from heart tissue reflects its preceding activation for example by $ONOO^-$, the biosynthesis of which peaks in the first minute of reperfusion as shown in the same rat heart model[57]. Thus MMP-2 resident within cardiomyocytes is rapidly activated by $ONOO^-$ stress and its proteolytic activity may have cleaved intracellular targets prior to its release from cells, the latter a means to reduce overall intracellular proteolytic stress. These findings[56] suggested that MMP-2 may be acting in a different way other than on extracellular matrix proteins to reduce the recovery of cardiac mechanical function as changes in the extracellular matrix were absent in a similar model of acute myocardial stunning injury[58]. A paper by Spinale's group studying the activation of MMPs in failing hearts showed the localization of MMP-2 to the sarcomere in isolated left ventricular myocytes[24]. Although the paper did not discuss this finding; it was one of the clues that led us to consider a possible and novel intracellular role of MMP-2 in cardiac myocytes independent of its actions on the extracellular matrix. In the next section we will describe the discovery of intracellular biological MMP-2 actions in the heart by its proteolysis of novel intracellular targets and discuss how this is relevant to heart pathology.

Troponin I. Although troponin I, an important regulatory protein in the contractile machinery of the heart, is known to be rapidly proteolyzed during acute IR injury, the exact protease(s) involved in this, despite some evidence for calpain, was unclear[59]. Using immunogold electron microscopy we showed that MMP-2 was localized to the sarcomere in cardiac myocytes. TnI was highly susceptible to the proteolytic action of MMP-2 in vitro, and subjecting isolated rat hearts to acute IR injury diminished myocardial TnI content, an

effect which was blocked by MMP inhibitors. We provided evidence that myocardial stunning injury is caused in part by MMP-2 mediated TnI proteolysis. This study was the first to recognize an intracellular biological role of any MMP as well as identify the first intracellular target of MMP-2 in cardiomyocytes as TnI. In hearts overexpressing a constitutively active MMP-2 in myocardial specific fashion there were marked derangements in the sarcomere, including TnI degradation and reduced contractile function[60, 61].

Other sarcomeric targets of MMP-2 beyond TnI

Myosin light chain-1. Following the same line of thought, since MMP-2 could be localized on the sarcomere, then the possibility of it targeting other sarcomeric proteins was not unlikely. Myosin light chain-1 (MLC-1) is a sarcomeric protein and a blood serum marker of the severity of myocardial infarction[62]. MLC-1 was found to be proteolytically degraded in a canine model of myocardial infarction[63] and this was confirmed in isolated rat hearts subjected to global IR injury[64], however, the enzyme responsible for its cleavage was unknown. We subjected isolated rat hearts to IR injury to test if MLC-1 degradation was due to its cleavage by MMP-2. We took a pharmacoproteomic approach to find myocardial proteins which may be cleaved by MMP activity. The hearts were treated with or without MMP inhibitors (*o*-phenanthroline or doxycycline) and 2D gel electrophoresis was performed on myocardial extracts to look at changes in protein spot density. We only considered those changes in spot density to be worthy of further analysis if they changed as a result of IR injury and were normalized in extracts from hearts treated with the MMP inhibitors. We identified spots meeting these criteria using mass spectroscopy as MLC-1 degradation products. Moreover, co-localization of MLC-1 and MMP-2 on the thick myofilaments of the sarcomere was demonstrated by immunogold electron microscopy,

immunoprecipitation experiments and isolation of purified thick myofilament fractions[65]. The loss in contractile function and MLC-1 content after IR injury was reduced in hearts treated with the MMP inhibitors. MLC-1 is thus another contractile protein element that could be protected by inhibiting MMP activity in oxidative stress injury to the heart.

Titin. It is the largest known mammalian protein (3000-4000 kDa) and is found in striated muscles, both cardiac and skeletal. It spans nearly half the length of the sarcomere, between the Z-disc to the M-line region. It consists of elastic segments in the I band region, which allows it to act as a molecular spring that helps maintain the structural and functional stability of the myocyte[66]. Titin is also the molecular superstructure on which sarcomeric proteins are assembled during sarcomerogenesis in embryonic myocytes. In cardiac muscle titin is of vast importance since it is a determinant of both diastolic and systolic function and the Frank-Starling mechanism of the heart[67]. We showed in rat and human myocardium that MMP-2 co-localizes with titin mainly near the Z-disc region of the cardiac sarcomere. Cleavage of titin in perfused rat hearts subjected to IR injury or in skinned cardiomyocytes incubated with MMP-2 was prevented with MMP inhibitors *o*-phenanthroline or ONO-4817[68]. Titin degradation in hearts was abolished in MMP-2 knockout mice subjected to IR in vivo. Thus MMP-2 plays an important role in titin homeostasis, which directly affects the contractile function of the heart at the sarcomeric level.

Cytoskeletal targets. α (alpha)-Actinin is a cytoskeletal protein found at the Z line of the sarcomere. It connects actin filaments in adjacent sarcomeres and thus serves as a pivotal protein in transmitting the force generated by the actin-myosin complex. α (alpha)-actinin was shown to activate myosin-ATPase in vitro; therefore any disturbance of α (alpha)-actinin homeostasis would directly alter the activity of the ATPase and as a result lead to contractile

dysfunction[69]. Some clues lead us to test the possibility that MMP-2 might target α (alpha)-actinin in IR: 1) myocardial levels of some cytoskeletal proteins including α (alpha)-actinin were reduced after IR injury[64, 65], and 2) immunohistochemistry and confocal microscopy for MMP-2 and α (alpha)-actinin in cardiac muscle suggested a close subcellular localization[12].

Perfused rat hearts subjected to 15 min $ONOO^-$ infusion showed a significant decline in contractile function and α (alpha)-actinin content, an effect blocked by MMP inhibitors[70]. No significant changes in the protein levels of other cytoskeletal proteins (desmin and α (alpha)II-spectrin) were observed. In vitro, α (alpha)-actinin was most susceptible to MMP-2 degradation followed by desmin, whereas α (alpha)II-spectrin was resistant[71]. A limitation of the study was the use of 64 kDa MMP-2 in the in vitro degradation experiments, and not 72 kDa MMP-2 activated by $ONOO^-$ and glutathione. Therefore the in vitro results and their interpretation may not truly reflect the exact susceptibility of cytoskeletal proteins to degradation by MMP-2 in vivo.

Nuclear targets. While investigating the subcellular localization of MMP-2 in cardiac myocytes with immunogold electron microscopy, we came across additional, unexpected findings. MMP-2 staining was not only exclusive to the sarcomere, but there was evidence of staining in mitochondria and the nuclei of cardiac myocytes as well[11]. Interestingly, the nuclear matrix has similarities to that of the extracellular matrix, and important cellular processes such as apoptosis[72] and cell cycle regulation[73] all involve proteolysis of nuclear matrix proteins. Si-Tayeb and colleagues have also shown that the truncated form of MMP-3 is localized in the nucleus, whereas the full length enzyme is cytosolic[74].

Kwan et al. showed that nuclear extracts purified from either human hearts or rat livers exhibited both MMP-2 as well as MMP-9 activity. We found that both MMP-2 and MMP-9 have a nuclear localization sequence at the C-terminal of MMP-2. Both TIMP-2 and doxycycline reduced the gelatinolytic activities seen in these nuclear extracts[75]. The study also showed that poly (ADP-ribose) polymerase, an enzyme that repairs DNA strand breaks and is present in the nuclear matrix, is susceptible to MMP-2 proteolysis in vitro. Interestingly, DNA strand breaks are caused by $ONOO^{-}$[76], which can also activate 72 kDa MMP-2[70]. When DNA damage occurs, PARP uses NAD^{+} and ATP to repair this. However, under severe $ONOO^{-}$ stress, excessive activation of PARP may cause it to deplete metabolites essential for cell survival. We speculated that MMP-2 may play dual roles in the nucleus under oxidative stress, one may be protective by reducing PARP levels to preserve cell energy requirements, and the other is detrimental whereby MMP-2 removal of PARP prevents it from repairing damaged DNA strands[75]. Much further investigation is still needed to identify the role of MMP-2 in the nucleus in both normal and stress conditions.

Other targets. Glycogen synthase kinase (GSK)-3 is a serine/threonine kinase abundantly expressed in eukaryotes and is important in regulating glycogen metabolism. One of its isoforms, GSK-3β (beta), is pivotal in regulating processes such as cell cycle, apoptosis and cell polarity[77]. GSK-3β (beta) is susceptible to proteolysis during oxidative stress and is therefore dysregulated. Work by Kandasamy et al. showed that incubation of MMP-2 with GSK-3β (beta) resulted in the time and concentration dependent cleavage of GSK-3β (beta). The cleavage product was shown to be lacking the N-terminal of the enzyme as shown by mass spectroscopy. The activity of GSK-3β (beta) was significantly enhanced upon incubation with MMP-2 and that was prevented by using MMP inhibitors GM-6001 and

ONO-4817. This study showed that GSK-3β (beta) may be a target of MMP-2, and that MMP-2 mediates its activity through cleaving the N-terminal of GSK-3β (beta) which contains the autoinhibitory phosphor-serine 9 residue. H_2O_2 stimulated GSK-3β (beta) activity in cardiomyoblasts and this was prevented with MMP inhibitors[78]. This may suggest that MMP-2 mediated cleavage and activation of GSK-3β (beta) may be an additional means whereby MMP-2 contributes to oxidative stress-induced cardiac dysfunction.

Conclusions

MMP-2 is abundant in the normal heart. In cardiomyocytes it is localized to discrete subcellular compartments including the sarcomere, nuclei, mitochondria and caveolae. It is activated within the cell as a rapid (seconds to minutes timescale) response to enhanced oxidative stress. It is in close proximity to specific proteins within the cell which it selectively proteolyses as a result of enhanced oxidative stress. Figure 9.3 gives a summary of the thus far known intracellular targets of MMP-2 in cardiomyocytes. The extensive yet incomplete body of knowledge on its activation, regulation and inhibition in both normal physiology and in disease states, has added MMP-2 to the list of proteases critical in heart disease both for in its intracellular and extracellular actions. Why MMP-2 is localized to the sarcomere at the core of the contractile apparatus, is a puzzle that needs solving. The discovery of intracellular targets of MMP-2 encourages us to further identify new biological roles of MMP-2 inside of cells as the cardiac myocyte is not the only cell where intracellular MMP-2 is found. This knowledge will help in the design of tailored pharmacological inhibitors of MMP-2 that may provide safe and effective drugs to treat cardiac diseases.

Acknowledgements

Studies from the Schulz lab have been generously supported by the Canadian Institutes for Health Research, the Heart and Stroke Foundation of Alberta, NWT and Nunavut and the Alberta Heritage Foundation for Medical Research.

Figure 9.1 Schematic structure of 72 and 64 kDa MMP-2. The figure shows the 72 kDa form of MMP-2 containing the pro-domain, the catalytic domain, the hinge region and the hemopexin/vitronectin domain. The catalytic domain contains a zinc ion that is essential for MMP-2's activity. The figure also shows the 64 kDa form of MMP-2 where the pro-domain has been removed by the action of other proteases.

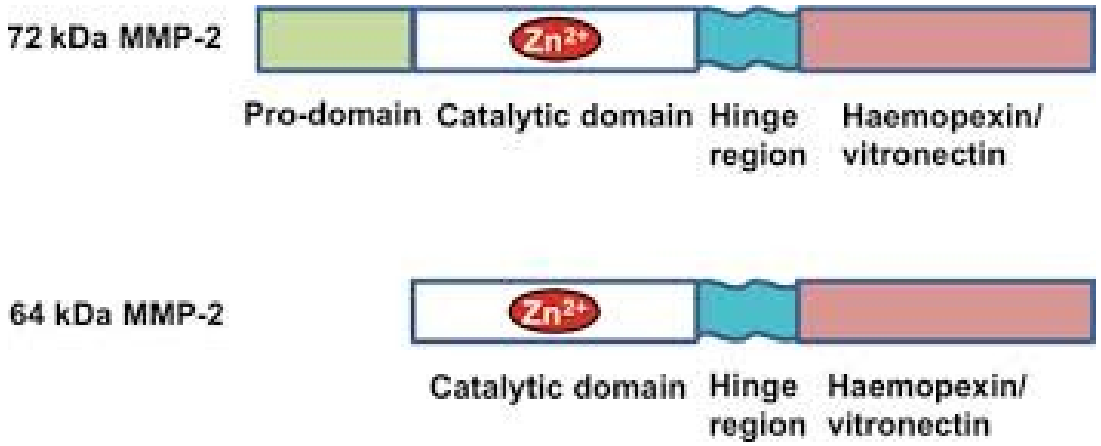
72 kDa MMP-2
Zn2+
Pro-domain
Catalytic domain
Hinge region
Haemopexin/ vitronectin
64 kDa MMP-2
Zn2+
Catalytic domain
Hinge region
Haemopexin/ vitronectin

Figure 9.2 Different modes of regulation and activation of MMP-2. The 72 kDa form of MMP-2 can be activated by MMP-14 or plasminogen via cleavage of its pro-domain to yield the 64 kDa form. 72 kDa MMP-2 can also be activated by exposure to $ONOO^-$ in the presence of cellular glutathione without losing the pro-domain. MMP-2 is also a phosphoprotein with several identified phosphorylation sites and whose activity is further modulated by its phosphorylation status[31]. However, the kinases and phosphatases involved in its in vivo regulation are unknown.

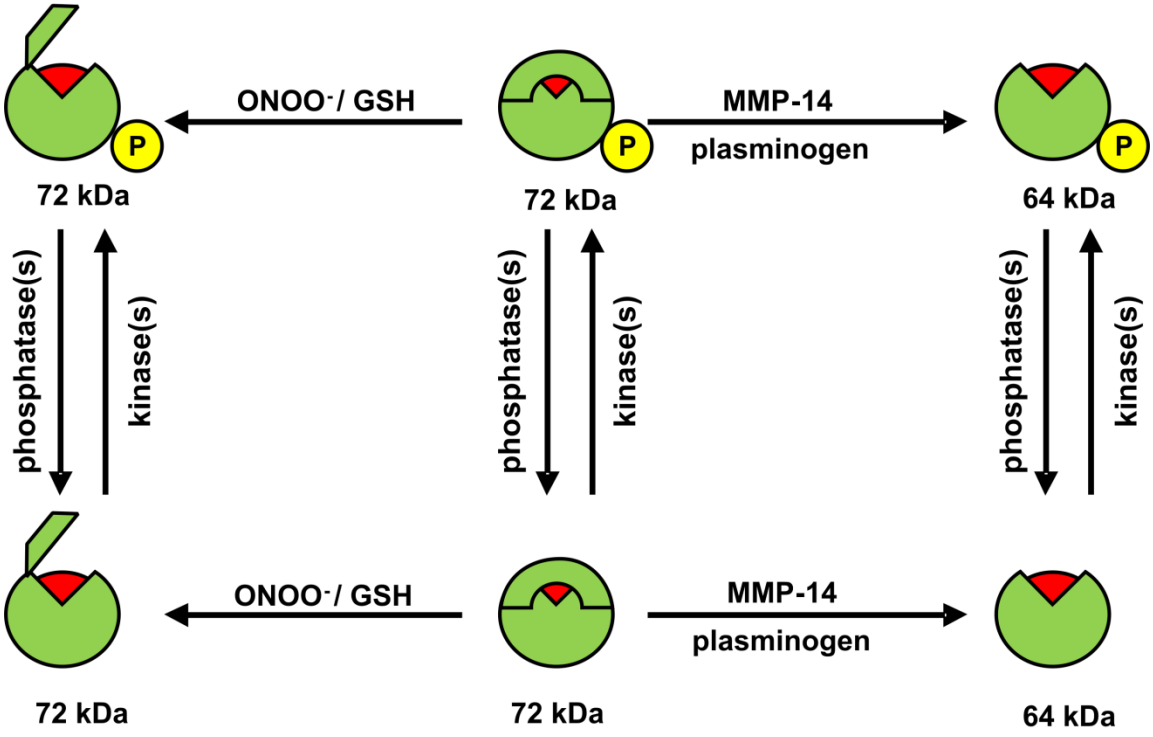
ONOO-/ GSH
MMP-14
plasminogen
P
72 kDa
64 kDa
phosphatase(s)
kinase(s)

Figure 9.3 Thus far identified intracellular targets of MMP-2 in cardiac myocytes. Shown are the: 1) sarcomeric targets of MMP-2: troponin I, titin and myosin light chain; 2) cytoskeletal targets: α (alpha)-actinin and desmin; 3) nuclear target: poly (ADP-ribose) polymerase (PARP), and 4) the cytosolic target glycogen synthase kinase (GSK)-3β (beta).

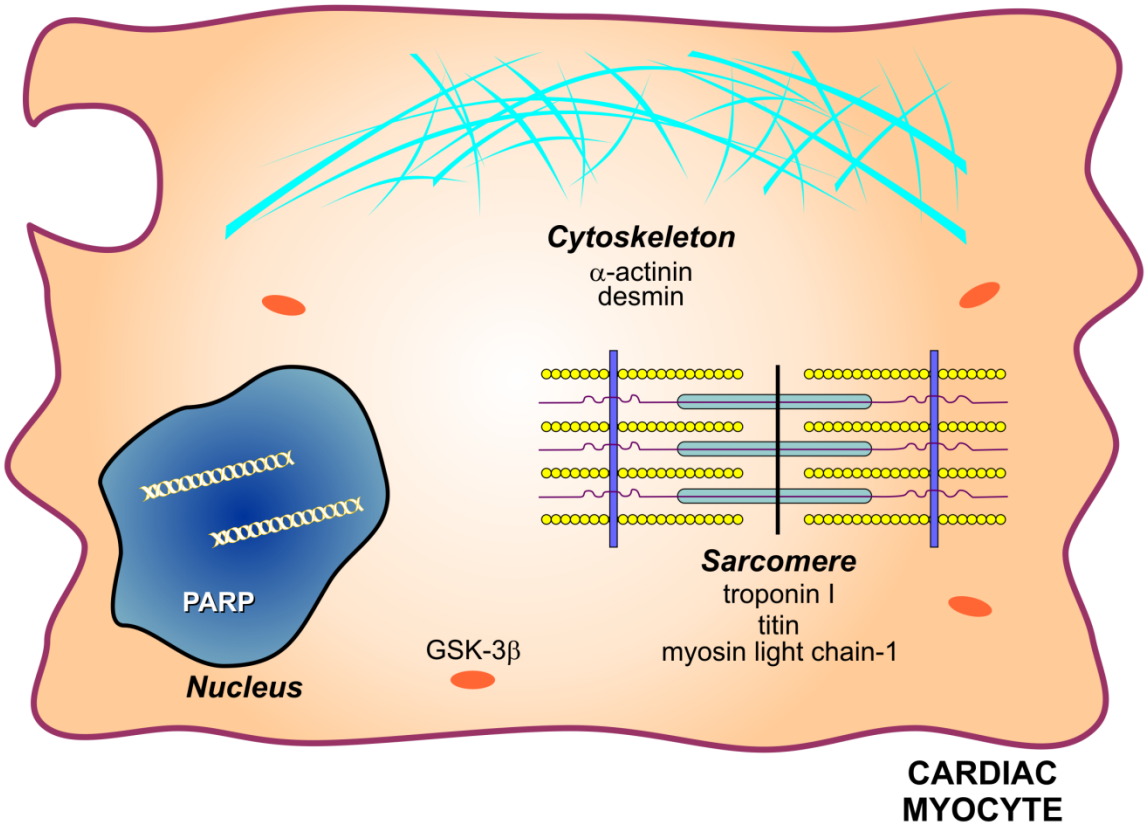
Cytoskeleton
α-actinin
desmin
PARP
Nucleus
GSK-3β
Sarcomere
troponin I
titin
myosin light chain-1
CARDIAC
MYOCYTE

References

1. Gross J, Lapiere CM. Collagenolytic activity in amphibian tissues: A tissue culture assay. *Proc Natl Acad Sci U S A*. 1962;48:1014-1022.

2. Vu TH, Werb Z. Matrix metalloproteinases: Effectors of development and normal physiology. *Genes Dev*. 2000;14:2123-2133.

3. Sellers A, Woessner JF, Jr. The extraction of a neutral metalloproteinase from the involuting rat uterus, and its action on cartilage proteoglycan. *Biochem J*. 1980;189:521-531.

4. Thompson M, Cockerill G. Matrix metalloproteinase-2: The forgotten enzyme in aneurysm pathogenesis. *Ann N Y Acad Sci*. 2006;1085:170-174.

5. Deryugina EI, Quigley JP. Matrix metalloproteinases and tumor metastasis. *Cancer Metastasis Rev*. 2006;25:9-34.

6. Beutner EH, Triftshauser C, Hazen SP. Collagenase activity of gingival tissue from patients with periodontal disease. *Proc Soc Exp Biol Med*. 1966;121:1082-1085.

7. Mohammed FF, Smookler DS, Khokha R. Metalloproteinases, inflammation, and rheumatoid arthritis. *Ann Rheum Dis*. 2003;62:ii43-7.

8. Ra HJ, Parks WC. Control of matrix metalloproteinase catalytic activity. *Matrix Biol*. 2007;26:587-596.

9. Schulz R. Intracellular targets of matrix metalloproteinase-2 in cardiac disease: Rationale and therapeutic approaches. *Annu Rev Pharmacol Toxicol*. 2007;47:211-242.

10. Spinale FG. Myocardial matrix remodeling and the matrix metalloproteinases: Influence on cardiac form and function. *Physiol Rev*. 2007;87:1285-1342.

11. Wang W, Schulze CJ, Suarez-Pinzon WL, Dyck JR, Sawicki G, Schulz R. Intracellular action of matrix metalloproteinase-2 accounts for acute myocardial ischemia and reperfusion injury. *Circulation*. 2002;106:1543-1549.

12. Coker ML, Doscher MA, Thomas CV, Galis ZS, Spinale FG. Matrix metalloproteinase synthesis and expression in isolated LV myocyte preparations. *Am J Physiol*. 1999;277:H777-87.

13. Cho WJ, Chow AK, Schulz R, Daniel EE. Matrix metalloproteinase-2, caveolins, focal adhesion kinase and c-kit in cells of the mouse myocardium. *J Cell Mol Med*. 2007;11:1069-1086.

14. Nuttall RK, Sampieri CL, Pennington CJ, Gill SE, Schultz GA, Edwards DR. Expression analysis of the entire MMP and TIMP gene families during mouse tissue development. *FEBS Lett*. 2004;563:129-134.

15. Whittaker M, Floyd CD, Brown P, Gearing AJ. Design and therapeutic application of matrix metalloproteinase inhibitors. *Chem Rev*. 1999;99:2735-2776.

16. Van Wart HE, Birkedal-Hansen H. The cysteine switch: A principle of regulation of metalloproteinase activity with potential applicability to the entire matrix metalloproteinase gene family. *Proc Natl Acad Sci U S A*. 1990;87:5578-5582.

17. Cao J, Sato H, Takino T, Seiki M. The C-terminal region of membrane type matrix metalloproteinase is a functional transmembrane domain required for pro-gelatinase A activation. *J Biol Chem*. 1995;270:801-805.

18. Bergman MR, Cheng S, Honbo N, Piacentini L, Karliner JS, Lovett DH. A functional activating protein 1 (AP-1) site regulates matrix metalloproteinase 2 (MMP-2) transcription by cardiac cells through interactions with JunB-Fra1 and JunB-FosB heterodimers. *Biochem J*. 2003;369:485-496.

19. Galis ZS, Muszynski M, Sukhova GK, Simon-Morrissey E, Libby P. Enhanced expression of vascular matrix metalloproteinases induced in vitro by cytokines and in regions of human atherosclerotic lesions. *Ann N Y Acad Sci*. 1995;748:501-507.

20. Siwik DA, Chang DL, Colucci WS. Interleukin-1beta and tumor necrosis factor-alpha decrease collagen synthesis and increase matrix metalloproteinase activity in cardiac fibroblasts in vitro. *Circ Res*. 2000;86:1259-1265.

21. Uzui H, Harpf A, Liu M, et al. Increased expression of membrane type 3-matrix metalloproteinase in human atherosclerotic plaque: Role of activated macrophages and inflammatory cytokines. *Circulation*. 2002;106:3024-3030.

22. Ben-Yosef Y, Lahat N, Shapiro S, Bitterman H, Miller A. Regulation of endothelial matrix metalloproteinase-2 by hypoxia/reoxygenation. *Circ Res*. 2002;90:784-791.

23. Alfonso-Jaume MA, Bergman MR, Mahimkar R, et al. Cardiac ischemia-reperfusion injury induces matrix metalloproteinase-2 expression through the AP-1 components FosB and JunB. *Am J Physiol Heart Circ Physiol*. 2006;291:H1838-46.

24. Spinale FG, Coker ML, Heung LJ, et al. A matrix metalloproteinase induction/activation system exists in the human left ventricular myocardium and is upregulated in heart failure. *Circulation*. 2000;102:1944-1949.

25. Mountain DJ, Singh M, Menon B, Singh K. Interleukin-1beta increases expression and activity of matrix metalloproteinase-2 in cardiac microvascular endothelial cells: Role of PKCalpha/beta1 and MAPKs. *Am J Physiol Cell Physiol*. 2007;292:C867-75.

26. Pacher P, Beckman JS, Liaudet L. Nitric oxide and peroxynitrite in health and disease. *Physiol Rev*. 2007;87:315-424.

27. Okamoto T, Akaike T, Sawa T, Miyamoto Y, van der Vliet A, Maeda H. Activation of matrix metalloproteinases by peroxynitrite-induced protein S-glutathiolation via disulfide S-oxide formation. *J Biol Chem*. 2001;276:29596-29602.

28. Okamoto T, Akaike T, Nagano T, et al. Activation of human neutrophil procollagenase by nitrogen dioxide and peroxynitrite: A novel mechanism for procollagenase activation involving nitric oxide. *Arch Biochem Biophys*. 1997;342:261-274.

29. Viappiani S, Nicolescu AC, Holt A, et al. Activation and modulation of 72kDa matrix metalloproteinase-2 by peroxynitrite and glutathione. *Biochem Pharmacol*. 2009;77:826-834.

30. Fliss H, Menard M. Oxidant-induced mobilization of zinc from metallothionein. *Arch Biochem Biophys*. 1992;293:195-199.

31. Sariahmetoglu M, Crawford BD, Leon H, et al. Regulation of matrix metalloproteinase-2 (MMP-2) activity by phosphorylation. *FASEB J*. 2007;21:2486-2495.

32. Sariahmetoglu M, Skrzypiec M, Youssef N, et al. Maintaining matrix metalloproteinase-2 in its phosphorylated form protects the heart from ischemia/reperfusion injury. *JMCC*. 2010 (under revision).

33. Nyalendo C, Sartelet H, Gingras D, Beliveau R. Inhibition of membrane-type 1 matrix metalloproteinase tyrosine phosphorylation blocks tumor progression in mice. *Anticancer Res*. 2010;30:1887-1895.

34. Baker AH, Edwards DR, Murphy G. Metalloproteinase inhibitors: Biological actions and therapeutic opportunities. *J Cell Sci*. 2002;115:3719-3727.

35. Goldberg GI, Strongin A, Collier IE, Genrich LT, Marmer BL. Interaction of 92-kDa type IV collagenase with the tissue inhibitor of metalloproteinases prevents dimerization, complex formation with interstitial collagenase, and activation of the proenzyme with stromelysin. *J Biol Chem*. 1992;267:4583-4591.

36. Nuttall RK, Sampieri CL, Pennington CJ, Gill SE, Schultz GA, Edwards DR. Expression analysis of the entire MMP and TIMP gene families during mouse tissue development. *FEBS Lett*. 2004;563:129-134.

37. Schulze CJ, Wang W, Suarez-Pinzon WL, Sawicka J, Sawicki G, Schulz R. Imbalance between tissue inhibitor of metalloproteinase-4 and matrix metalloproteinases during acute myocardial ischemia-reperfusion injury. *Circulation*. 2003;107:2487-2492.

38. Cox MJ, Hawkins UA, Hoit BD, Tyagi SC. Attenuation of oxidative stress and remodeling by cardiac inhibitor of metalloproteinase protein transfer. *Circulation*. 2004;109:2123-2128.

39. Pavloff N, Staskus PW, Kishnani NS, Hawkes SP. A new inhibitor of metalloproteinases from chicken: ChIMP-3. A third member of the TIMP family. *J Biol Chem*. 1992;267:17321-17326.

40. Fedak PW, Smookler DS, Kassiri Z, et al. TIMP-3 deficiency leads to dilated cardiomyopathy. *Circulation*. 2004;110:2401-2409.

41. Ikonomidis JS, Jones JA, Barbour JR, et al. Expression of matrix metalloproteinases and endogenous inhibitors within ascending aortic aneurysms of patients with marfan syndrome. *Circulation*. 2006;114:I365-70.

42. Chow AK, Cena J, El-Yazbi AF, et al. Caveolin-1 inhibits matrix metalloproteinase-2 activity in the heart. *J Mol Cell Cardiol*. 2007;42:896-901.

43. Puyraimond A, Fridman R, Lemesle M, Arbeille B, Menashi S. MMP-2 colocalizes with caveolae on the surface of endothelial cells. *Exp Cell Res*. 2001;262:28-36.

44. Gratton JP, Bernatchez P, Sessa WC. Caveolae and caveolins in the cardiovascular system. *Circ Res*. 2004;94:1408-1417.

45. Chow AK, Daniel EE, Schulz R. Cardiac function is not significantly diminished in hearts isolated from young caveolin-1 knockout mice. *Am J Physiol Heart Circ Physiol*. 2010.

46. Birkedal-Hansen H, Moore WG, Bodden MK, et al. Matrix metalloproteinases: A review. *Crit Rev Oral Biol Med*. 1993;4:197-250.

47. Peterson JT. Matrix metalloproteinase inhibitor development and the remodeling of drug discovery. *Heart Fail Rev*. 2004;9:63-79.

48. Yamada A, Uegaki A, Nakamura T, Ogawa K. ONO-4817, an orally active matrix metalloproteinase inhibitor, prevents lipopolysaccharide-induced proteoglycan release from the joint cartilage in guinea pigs. *Inflamm Res*. 2000;49:144-146.

49. Golub LM, McNamara TF, D'Angelo G, Greenwald RA, Ramamurthy NS. A non-antibacterial chemically-modified tetracycline inhibits mammalian collagenase activity. *J Dent Res*. 1987;66:1310-1314.

50. Lee HM, Ciancio SG, Tuter G, Ryan ME, Komaroff E, Golub LM. Subantimicrobial dose doxycycline efficacy as a matrix metalloproteinase inhibitor in chronic periodontitis patients is enhanced when combined with a non-steroidal anti-inflammatory drug. *J Periodontol*. 2004;75:453-463.

51. Smith GN,Jr, Mickler EA, Hasty KA, Brandt KD. Specificity of inhibition of matrix metalloproteinase activity by doxycycline: Relationship to structure of the enzyme. *Arthritis Rheum*. 1999;42:1140-1146.

52. Golub LM, Lee HM, Ryan ME, Giannobile WV, Payne J, Sorsa T. Tetracyclines inhibit connective tissue breakdown by multiple non-antimicrobial mechanisms. *Adv Dent Res*. 1998;12:12-26.

53. Roy R, Zhang B, Moses MA. Making the cut: Protease-mediated regulation of angiogenesis. *Exp Cell Res*. 2006;312:608-622.

54. Linask KK, Manisastry S, Han M. Cross talk between cell-cell and cell-matrix adhesion signaling pathways during heart organogenesis: Implications for cardiac birth defects. *Microsc Microanal*. 2005;11:200-208.

55. Itoh T, Ikeda T, Gomi H, Nakao S, Suzuki T, Itohara S. Unaltered secretion of beta-amyloid precursor protein in gelatinase A (matrix metalloproteinase 2)-deficient mice. *J Biol Chem*. 1997;272:22389-22392.

56. Cheung PY, Sawicki G, Wozniak M, Wang W, Radomski MW, Schulz R. Matrix metalloproteinase-2 contributes to ischemia-reperfusion injury in the heart. *Circulation*. 2000;101:1833-1839.

57. Yasmin W, Strynadka KD, Schulz R. Generation of peroxynitrite contributes to ischemia-reperfusion injury in isolated rat hearts. *Cardiovasc Res*. 1997;33:422-432.

58. Lonn E, Factor SM, Van Hoeven KH, et al. Effects of oxygen free radicals and scavengers on the cardiac extracellular collagen matrix during ischemia-reperfusion. *Can J Cardiol*. 1994;10:203-213.

59. Bolli R, Marban E. Molecular and cellular mechanisms of myocardial stunning. *Physiol Rev*. 1999;79:609-634.

60. Bergman MR, Teerlink JR, Mahimkar R, et al. Cardiac matrix metalloproteinase-2 expression independently induces marked ventricular remodeling and systolic dysfunction. *Am J Physiol Heart Circ Physiol*. 2007;292:H1847-60.

61. Wang GY, Bergman MR, Nguyen AP, et al. Cardiac transgenic matrix metalloproteinase-2 expression directly induces impaired contractility. *Cardiovasc Res*. 2006;69:688-696.

62. Yamada T, Matsumori A, Tamaki S, Sasayama S. Myosin light chain I grade: A simple marker for the severity and prognosis of patients with acute myocardial infarction. *Am Heart J*. 1998;135:329-334.

63. Tsuchida K, Kaneko K, Yamazaki R, Aihara H. Degradation of cardiac structural proteins induced by reperfusion in the infarcted myocardium. *Res Commun Chem Pathol Pharmacol*. 1986;53:195-202.

64. Van Eyk JE, Powers F, Law W, Larue C, Hodges RS, Solaro RJ. Breakdown and release of myofilament proteins during ischemia and ischemia/reperfusion in rat hearts: Identification of degradation products and effects on the pCa-force relation. *Circ Res*. 1998;82:261-271.

65. Sawicki G, Leon H, Sawicka J, et al. Degradation of myosin light chain in isolated rat hearts subjected to ischemia-reperfusion injury: A new intracellular target for matrix metalloproteinase-2. *Circulation*. 2005;112:544-552.

66. Granzier HL, Labeit S. The giant protein titin: A major player in myocardial mechanics, signaling, and disease. *Circ Res*. 2004;94:284-295.

67. Fukuda N, Granzier HL, Ishiwata S, Kurihara S. Physiological functions of the giant elastic protein titin in mammalian striated muscle. *J Physiol Sci*. 2008;58:151-159.

68. Ali M, Cho W, Hudson B, Kassiri Z, Granzier H, Schulz R. Titin is a target of MMP-2: Implications in myocardial ischemia/reperfusion injury. *Circulation*. 2010 (in press).

69. Malhotra A, Margossian SS, Slayter HS. Physico-chemical properties of rat and dog cardiac alpha-actinin. *Biochim Biophys Acta*. 1986;874:347-354.

70. Wang W, Sawicki G, Schulz R. Peroxynitrite-induced myocardial injury is mediated through matrix metalloproteinase-2. *Cardiovasc Res*. 2002;53:165-174.

71. Sung MM, Schulz CG, Wang W, Sawicki G, Bautista-Lopez NL, Schulz R. Matrix metalloproteinase-2 degrades the cytoskeletal protein alpha-actinin in peroxynitrite mediated myocardial injury. *J Mol Cell Cardiol*. 2007;43:429-436.

72. Martelli AM, Bareggi R, Bortul R, Grill V, Narducci P, Zweyer M. The nuclear matrix and apoptosis. *Histochem Cell Biol*. 1997;108:1-10.

73. Georgi AB, Stukenberg PT, Kirschner MW. Timing of events in mitosis. *Curr Biol*. 2002;12:105-114.

74. Si-Tayeb K, Monvoisin A, Mazzocco C, et al. Matrix metalloproteinase 3 is present in the cell nucleus and is involved in apoptosis. *Am J Pathol*. 2006;169:1390-1401.

75. Kwan JA, Schulze CJ, Wang W, et al. Matrix metalloproteinase-2 (MMP-2) is present in the nucleus of cardiac myocytes and is capable of cleaving poly (ADP-ribose) polymerase (PARP) in vitro. *FASEB J*. 2004;18:690-692.

76. Pacher P, Schulz R, Liaudet L, Szabo C. Nitrosative stress and pharmacological modulation of heart failure. *Trends Pharmacol Sci*. 2005;26:302-310.

77. Grimes CA, Jope RS. The multifaceted roles of glycogen synthase kinase 3beta in cellular signaling. *Prog Neurobiol*. 2001;65:391-426.

78. Kandasamy AD, Chow AK, Ali MA, Schulz R. Matrix metalloproteinase-2 and myocardial oxidative stress injury: Beyond the matrix. *Cardiovasc Res*. 2009;83:698-706

III. Phosphorylation status of matrix metalloproteinase 2 in myocardial ischaemia–reperfusion injury

Meltem Sariahmetoglu , Monika Skrzypiec-Spring, Nermeen Youssef, Anna Laura B Jacob-Ferreira, Jolanta Sawicka, Charles Holmes, Grzegorz Sawicki, Richard Schulz

This manuscript has been published in *Heart*

2012;**98**:656-662 doi:10.1136/heartjnl-2011-301250

Introduction

Ischaemia–reperfusion (IR) injury of the heart causes damage to heart muscle resulting from increased oxidative stress, which triggers a cascade of pathophysiological events including the activation of matrix metalloproteinase 2 (MMP-2)[1–4]. Activated MMP-2 does not only proteolyse extracellular matrix proteins, thereby impairing the normal structural support of cardiomyocytes,[5]but also degrades susceptible intracellular substrates, including troponin I,[6] myosin light chain 1,[7] α-actinin[8] and titin,[9] which contributes to the acute contractile dysfunction seen after IR injury and enhanced oxidative stress in the heart.

Phosphorylation of proteins is one common mechanism to regulate protein activity. The precise cellular regulation of protein phosphatase and kinase activities determines the phosphorylation status of specific cellular proteins. Protein phosphatases are responsible for phosphoprotein dephosphorylation and act as counterregulators of protein kinases. Therefore, the inhibition of phosphatase activity results in the increased phosphorylation of substrates by constitutive kinases.[10] Dephosphorylation of serine and threonine sites requires the activity of serine/threonine phosphatases such as protein phosphatase 1 (PP1) and protein phosphatase 2A (PP2A). These phosphatases are abundantly distributed in all tissues including cardiac myocytes.[11–14] We showed that MMP-2 is a serine and threonine phosphoprotein, and phosphorylation is another way to regulate its activity.[15] While dephosphorylation of native MMP-2 increases its activity, phosphorylation of MMP-2 using protein kinase C significantly inhibited its proteolytic activity.[15] Interestingly, membrane type 1 matrix metalloproteinase is tyrosine phosphorylated, whereby its phosphorylation status appears to affect tumour cell invasion and proliferation.[16,17] ATP depletion in organs during ischaemia or anoxia shifts the balance from phosphorylation towards dephosphorylation.[18] We therefore hypothesised that

changes in phosphatase activity during IR may affect myocardial MMP-2 phosphorylation status and the proteolysis of its susceptible target, troponin I. We also examined whether we can protect hearts from IR-induced injury by changing the phosphorylation status of MMP-2. Here we show that the phosphorylation status of MMP-2 affects its activity in the heart, and that inhibition of its dephosphorylation helps to protect hearts from IR-induced contractile dysfunction.

Materials and methods

Unless otherwise specified all reagents used were obtained from Sigma-Aldrich (Oakville, Ontario, Canada) or Fisher Scientific (Ottawa, Ontario, Canada). Rabbit polyclonal anti-phosphothreonine and anti-phosphoserine antibodies were obtained from Abcam (Cambridge, Massachusetts, USA). Monoclonal anti-phosphotyrosine antibody was purchased from Cell Signalling Technology (Pickering, Ontario, Canada). Rabbit polyclonal MMP-2 antibody was a gift from Dr Mieczyslaw Wozniak (Department of Clinical Chemistry, Medical University of Wroclaw, Poland). Monoclonal anti-human troponin I antibody (clone 81-7) was purchased from Spectral Diagnostics (Toronto, Ontario, Canada); 72 kDa human recombinant MMP-2 (purified from mammalian cells) was purchased from Calbiochem (Billerica, Massachusetts, USA). The RediPlate 96 EnzChek serine/threonine phosphatase assay kit was obtained from Molecular Probes (Burlington, Ontario, Canada). Goat anti-rabbit and anti-mouse IgG conjugated with horseradish peroxidase were purchased from Santa Cruz Biotechnology (Santa Cruz, California, USA). Molecular weight markers and polyvinylidene difluoride membranes were purchased from Bio-Rad (Mississauga, Ontario, Canada). Protein A and protein G-sepharose beads and ECL plus were purchased from Amersham (Little Chalfont, Buckinghamshire, UK).

Prediction of phosphorylation sites within rat MMP-2

The primary sequence of rat MMP-2 (accession number P33436) was obtained from the Swiss-Prot protein database (http://us.expasy.org/sprot/). NetPhos 2.0 (http://www.cbs.dtu.dk/services/NetPhos/) is based on a neural network method, which predicts serine, threonine and tyrosine phosphorylation sites in eukaryotic proteins.[19]

Isolated rat heart perfusions

Isolated hearts from male Sprague–Dawley rats (body weight 250–350 g) were perfused at constant pressure (60 mm Hg) using the Langendorff method with Krebs–Henseleit buffer at 37°C, as previously described.1 Coronary flow rate, heart rate and left ventricular pressure were monitored throughout the experiment. Cardiac mechanical function was expressed as the product of heart rate × left ventricular developed pressure.

After 25 min of aerobic perfusion, hearts were subjected to 20 min of global, no-flow ischaemia (at 37°C) followed by 30 min of aerobic reperfusion. Control hearts were perfused aerobically for 75 min (see figure 1A for the perfusion protocols). The serine/threonine phosphatase inhibitor, okadaic acid (OA; 10 or 100 nM, prepared as a stock solution in dimethyl sulphoxide, and used in a final dimethyl sulphoxide concentration of 0.0083% v/v) was infused into the hearts 10 min before the onset of ischaemia and for the first 10 min of reperfusion. In preliminary experiments in order to determine an appropriate concentration of OA, hearts were perfused aerobically for 15 min followed by a 40 min infusion of either 10 or 100 nM OA, after which they were frozen for analysis of protein phosphatase activity. Coronary effluent samples of equal volume (15 ml) were collected for the determination of MMP-2, PP1 and PP2A activities at 24–25, 45–47 and 74–75 min of perfusion.1 Coronary flow rates vary in constant pressure perfused hearts, thus the duration period of sampling

varied somewhat from heart to heart; however, 15 ml was always collected. The samples were concentrated using Amicon ultra (10 000 molecular weight cut-off; Millipore, Bedford, Massachusetts, USA) ultrafiltration units. Hearts were freeze-clamped in liquid nitrogen at the end of the perfusion protocol.

Preparation of heart homogenates

Hearts were crushed at liquid nitrogen temperature and then homogenised by sonication in 50 mM Tris-HCl (pH 7.4) containing 3.1 mM sucrose, 1 mM dithiothreitol, 10 μg/ml leupeptin, 10 μg/ml soybean trypsin inhibitor, 2 μg/ml aprotinin and 0.1% Triton X-100. The homogenate was centrifuged at 10 000***g*** at 4°C for 10 min, and the supernatant was collected and stored at −80°C until use. The protein content in homogenates was analysed using the Bradford protein assay (Bio-Rad) and bovine serum albumin was used as a protein standard.

Protein phosphatase activity assay

PP1 and PP2A activities in heart homogenates were measured by using the RediPlate 96 EnzChek serine/threonine phosphatase assay kit according to the vendor's instructions.

Immunoprecipitation

Heart homogenates were incubated with rabbit polyclonal anti-phosphoserine, anti-phosphothreonine, anti-MMP-2 or monoclonal anti-phosphotyrosine antibodies, or rabbit IgG serum (Sigma; immunoprecipitation control) overnight at 4°C with mixing. Protein A or G-sepharose beads (50% w/v) were added and the mixture was incubated overnight at 4°C with mixing. The beads were then washed three times at 4°C with homogenisation buffer. The immunoprecipitates were then used for both gelatin zymography and western blot.

MMP-2 activity assay

Gelatin zymography for measuring MMP activity was performed according to Sawicki [20] *et al.* Briefly, non-reduced samples were loaded onto an 8% acrylamide gel containing 2 mg/ml gelatin and electrophoresed for 60–90 min (150 V, 4°C). After washing the gels with Triton X-100 (2.5% v/v, 3×20 min) the gels were incubated at 37°C for 18–24 h, stained with 0.05% Coomassie Blue and then de-stained. Gelatinolytic activities were detected as transparent bands against the background of Coomassie Blue-stained gelatin. To quantify the activities of the detected enzymes, zymograms were processed using a GS-800 calibrated densitometer (Bio-Rad). The intensities of the separate bands were analysed using Quantity1 measurement software (Bio-Rad) and reported as such or expressed as a specific activity per milligram of protein.

Western blotting

The MMP-2 and troponin I content in myocardium were determined by western blotting. Briefly, 20 μg of protein from heart extracts was applied to 8% or 15% sodium dodecylsulphate–polyacrylamide gel electrophoresis gels under reducing conditions.21 After electrophoresis (150 V, 20°C) samples were electroblotted onto a polyvinylidene difluoride membrane (by a semi-dry technique, 25 V, 30 min; Bio-Rad). Troponin I was identified using a monoclonal anti-human troponin I antibody. The MMP-2 content in samples was identified using a polyclonal MMP-2 antibody, which specifically recognises an epitope localised in the gelatin-binding domain of MMP-2 and preferentially detects the 72 kDa form of MMP-2.6 Immunoreactive protein bands were visualised using the ECL plus detection system.

Alkaline phosphatase treatment

Homogenates prepared from hearts subjected to IR and OA treatment were incubated in dephosphorylation buffer (50 mM Tris-HCl, pH 8.5) with or without 40 units of calf intestinal alkaline phosphatase for 1 h at 37°C. The reaction was stopped by adding an equal amount of non-reducing sample loading buffer. MMP-2 activity was also analysed by gelatin zymography as described above.

Statistical analysis

Results are expressed as mean±SEM. Statistical analysis was performed using analysis of variance or the t test, as appropriate; $p<0.05$ was considered statistically significant.

Results

Theoretical prediction of rat MMP-2 phosphorylation

We previously showed that human MMP-2 is a phosphoprotein.[15] According to NetPhos 2.0, rat 72 kDa MMP-2 has 31 possible phosphorylation sites (12 for serine, 11 for threonine and eight for tyrosine; figure 2A). One putative serine and three threonine phosphorylation sites are located within the autoinhibitory propeptide domain. Three putative serine, two threonine and two tyrosine phosphorylation sites are located within collagenase-like domains 1 and 2. One threonine or tyrosine and four serine phosphorylation sites are located in the haemopexin-like domain. The other predicted phosphorylation sites (four on serine, five on threonine and five on tyrosine) are located in the collagen-binding domain. It is still unknown which phosphorylation site(s) or which domain(s) may have the greatest influence on MMP-2 activity.

Ability of OA to inhibit cardiac protein phosphatase activity

In order to determine the appropriate concentration of the serine/threonine protein kinase inhibitor OA to use in heart perfusion studies, rat hearts were perfused aerobically for 15 min, followed by a 40 min infusion of either 10 or 100 nM OA, at which time they were rapidly frozen in liquid nitrogen for analysis of protein phosphatases activity. Figure 1B shows that rat hearts have significantly more PP2A than PP1 activity ($p<0.05$, n=4) and 100 nM but not 10 nM OA significantly inhibited PP2A activity by approximately 20% ($p<0.05$ vs control, n=4). No significant inhibition of PP1 activity was observed at either concentration of OA.

OA protects hearts from IR injury

Isolated rat hearts were perfused either as aerobic control hearts (AE) for a total of 75 min or subjected to 25 min of aerobic perfusion followed by 20 min of global, no-flow ischaemia and 30 min of aerobic reperfusion (IR). Additional hearts were infused with OA (10 or 100 nM) for 10 min before and for the first 10 min following the ischaemic period (IR+OA), or for an equivalent period in the aerobically perfused hearts (AE+OA; figure 1A). IR caused a significant reduction in the recovery of mechanical function in the reperfusion period (at the end of reperfusion to 60±4% of pre-ischaemic function, n=11). Hearts perfused aerobically for 75 min had stable mechanical function (data not shown, n=5); 100 nM OA significantly improved the recovery of mechanical function to 88±6% of pre-ischaemic function ($p<0.05$ vs IR, n=8; figure 1B). The lower concentration of 10 nM OA had no significant effect on the recovery of function (n=3, data not shown); 100 nM OA itself had no significant effect on left ventricular developed pressure, heart rate, rate-pressure product or coronary flow in aerobically perfused hearts (n=11, data not shown). PP2A activity in homogenates prepared

from the IR+OA (100 nM) hearts at the end of reperfusion was significantly decreased compared with IR hearts ($p<0.05$; figure 1C).

MMP-2 in perfusates and heart homogenates

As a result of reperfusion injury following myocardial ischaemia there is a rapid and enhanced release of MMP-2 activity into the coronary effluent, which peaks within the first 2 min of reperfusion and is accompanied by a decrease in the resulting tissue activity as measured at the end of 30 min reperfusion.1 This release of MMP-2 reflects the rapid activation of MMP-2 in the myocardium, resulting in the proteolysis of troponin I.[6] Coronary effluent from aerobically perfused hearts showed weak gelatinolytic activity, the most prominent band was 72 kDa MMP-2 (figure 3A). OA (100 nM) did not alter MMP-2 release from aerobically perfused hearts. As previously shown,[1,6] IR caused a marked increase in the release of 72 kDa MMP-2 in the first 2 min of reperfusion ($p<0.05$ vs AE), which was diminished to background levels at the end of the reperfusion period. OA did not significantly alter the IR-induced release of MMP-2 activity from the heart (figure 3A). We also detected an unidentified weaker band of approximately 75 kDa gelatinase, which may be a modified form of MMP-2 or an activation product of MMP-9 by the action of neutrophil elastase (figure 3A).[1,22]

As previously shown,[1,6] homogenates prepared from AE hearts frozen at the end of the 75 min perfusion period revealed the presence of both 72 and 62 kDa activities, the former being the most predominant form (figure 3B, left panel). Western blot analysis of the AE heart homogenates showed a single band corresponding to the 72 kDa form (figure 3B, right panel). IR caused a significant loss in both 72 kDa MMP-2 activity and protein in heart tissue, both of which were attenuated by OA treatment (n=3 per group).

Alkaline phosphatase treatment enhances MMP-2 activity

We showed that human recombinant MMP-2, or that released from a human fibrosarcoma cell line, is phosphorylated and that dephosphorylation with alkaline phosphatase in vitro enhances its activity.[15] We, therefore, determined whether in-vitro treatment of rat heart homogenates with alkaline phosphatase would alter MMP-2 activity. OA, by virtue of its ability to inhibit phosphatase activities, should enhance the likelihood of MMP-2 being in a more highly phosphorylated state. Therefore, we measured the gelatinolytic activities of heart homogenates prepared from the IR+OA (100 nM) group. In-vitro treatment of the heart homogenates with 40 U alkaline phosphatase for 60 min at 37°C significantly increased 72 kDa activity from 100±10 to 117±13 arbitrary units ($p<0.05$, $n=3$), but not 62 kDa gelatinolytic activity. One plausible explanation is that MMP-2 is present, at least to some extent, as a phosphorylated enzyme in the heart and that dephosphorylation enhances its activity.

MMP-2 in heart homogenates is phosphorylated

We, therefore, determined whether MMP-2 is phosphorylated in heart tissue. Heart homogenates prepared from AE, IR and IR+OA hearts were first immunoprecipitated with anti-MMP-2 antibody, and the immunoprecipitates were then immunoblotted with either phosphoserine, phosphothreonine or phosphotyrosine antibodies. We observed that MMP-2 in the heart is phosphorylated at serine and threonine, but is less likely at tyrosine residues (data not shown). This is in accordance with MMP-2 isolated from a human fibrosarcoma cell line, which was phosphorylated in the same pattern.[15]

Homogenates from the same hearts were alternatively immunoprecipitated with either phosphoserine or phosphothreonine antibodies and the immunoprecipitates were analysed for

MMP-2 protein content by western blotting. Results showed a band corresponding to 72 kDa MMP-2 in all heart samples when anti-phosphoserine antibody was used, suggesting that some proportion of MMP-2 also exists in a phosphorylated form in the heart (figure 4A). We could not interpret the results using anti-phosphothreonine to immunoprecipitate as the unrelated IgG used as a control also resulted in a non-specific band at the molecular weight of MMP-2 (data not shown).

Inhibition of protein phosphatases prevents degradation of troponin I

As MMP-2 is localised to cardiac sarcomeres and is responsible for troponin I degradation in acute myocardial IR injury,[6] we determined whether OA would alter the degradation of troponin I in hearts. Analysis of troponin I levels in homogenates prepared from the hearts at the end of perfusion showed a marked loss of 31 kDa troponin I in comparison to aerobically perfused hearts (figure 4B). The degradation of troponin I was abolished in IR+OA (100 nM) hearts (figure 4B).

Discussion

MMP-2 is a ubiquitous protein and is abundant in several cell types. MMP-2 is also found in cardiomyocytes where it co-localises with the sarcomere, and as a consequence of enhanced oxidative stress is responsible for the proteolytic degradation of troponin I,[6] myosin light chain 1,[7] α-actinin[8] and titin,[9] which contribute to the acute contractile dysfunction following such an injury. Moreover, overexpression of a constitutively active MMP-2 in the myocardium results in severe systolic dysfunction, which is accompanied by disruption of the sarcomere, lysis of myofilaments and loss of troponin I.[23]

We have demonstrated for the first time that MMP-2 activity depends on its phosphorylation status in the heart tissue and that protein phosphatase inhibition reveals a protective effect

against contractile dysfunction induced by IR. OA (100 nM), a potent PP1 and PP2A serine/threonine phosphatase inhibitor, decreased PP2A activity in the heart without a significant reduction on PP1 activity. This was expected as in terms of its IC_{50} values, OA has approximately two orders of magnitude greater potency against PP2A than PP1.[24] Contractile dysfunction, which correlates with increased MMP-2 activity in coronary effluent at the first minute of reperfusion,[1] was significantly improved by OA treatment. IR injury results in the acute depletion of myocardial MMP-2 as a result of its activation and release into the coronary effluent.[1] Our results showed that IR caused troponin I degradation and significantly decreased the activity and protein level of MMP-2 in heart tissue, seen as indicators of the precedent activation of MMP-2 during early reperfusion. OA treatment normalised the activity and levels of MMP-2 and protected troponin I from degradation in IR hearts.

We observed no inotropic effect of 100 nM OA. A positive inotropic effect of OA has been observed in isolated papillary muscles, but this requires at least a 300-fold higher concentration than we used here.[25] At least 1 μM OA is necessary to increase the phosphorylation of phosphoproteins in cardiomyocytes such as troponin I, phospholamban and myosin light chain.[25] Our data suggest that the cardioprotective effect of OA is independent of any inotropic action but may include maintaining MMP-2 in a more phosphorylated (and thus less active) state. However, we cannot exclude effects of OA on the phosphorylation of other important regulatory cardiac phosphoproteins.

Pharmacological inhibition of PP1 and PP2A is cardioprotective in different experimental ischaemia models.[26–28] OA reduced IR-induced necrosis in hearts from both aged and young adult rats.[29] Armstrong and Ganote[26] showed that OA or calyculin A, which inhibits PP1 and

PP2A equally, reduces the rate of injury relative to the rate of ATP depletion in adult rat cardiomyocytes subjected to metabolic inhibition. They also showed similar protection with calyculin A or fostriecin, a potent and selective inhibitor of PP2A, against prolonged ischaemia in rabbit cardiomyocytes.[27] Weinbrenner *et al*[30] showed that fostriecin reduced myocardial infarct size in rabbit hearts when administered after the onset of ischaemia. Although PP1 and PP2A are both present in virtually all tissues including the heart, Ingebritsen *et al*[31] showed that PP2A activity in homogenates of rabbit hearts was approximately threefold greater than that of PP1. This is in accordance with our results, which showed that the rat heart has significantly higher PP2A activity. These results imply that the protective effect of phosphatase inhibition may be mediated by the inhibition of PP2A.

In this study we used isolated hearts perfused with crystalloid buffer devoid of cells and global ischaemia before reperfusion. This is a simple and well understood model that allows one to control physiological parameters, allows for the precise delivery of drugs, and facilitates the collection and analysis of substances released from the coronary circulation.[32] This is also the same model we used previously, which revealed MMP-2 activation[1] [6] and loss of TnI in the heart[6] in IR injury, thus allowing for direct comparison. However, this is also a limitation of the study, and extrapolation of the results to in-vivo studies requires caution especially in humans in whom myocardial ischaemia is regional and cardiomyocytes bordering the ischaemic region are likely to influence IR injury, and due to lack of blood, especially neutrophils, which play an important role in reperfusion injury by releasing pro-oxidants, proteases and inflammatory products, thereby extending the severity of tissue damage.[33]

Although these results suggest that the inhibition of endogenous phosphatases elicit cardioprotection against cell injury induced by ischaemia, the target substrate is still unclear. We postulate here that MMP-2 may also be one of the target substrates for intracellular phosphorylation/dephosphorylation reactions in the heart. Although ischaemia is a complex insult that includes acidosis, the build-up of toxic metabolites, and generation of reactive oxygen/nitrogen species, keeping MMP-2 in its less active phosphorylated state may have major implications in the design of rational drug therapies to lessen the impact of IR injury of the heart.

Figure 1

Effect of okadaic acid (OA) on myocardial contractile function and protein phosphatase 2A (PP2A) activity subsequent to ischaemia–reperfusion (IR) injury. (A) Experimental protocol for isolated heart perfusions. Rat hearts were perfused either aerobically for 75 min or subjected to 25 min of aerobic perfusion followed by 20 min of global, no-flow ischaemia and 30 min of aerobic reperfusion. In some experiments OA was infused 10 min before and for the first 10 min following the ischaemic period, or for an equivalent period in the aerobically perfused hearts. (B) Effect of OA (100 nM) on cardiac mechanical function measured as the rate-pressure product (heart rate × left ventricular developed pressure) during reperfusion after 20 min of ischaemia. *$p<0.05$ versus IR (analysis of variance, n=8–11). (C) PP2A activity in the IR hearts at the end of the perfusion period. *$p<0.05$ versus IR (t test, n=3 per group). IR+OA, ischaemia–reperfused hearts treated with 100 nM OA.

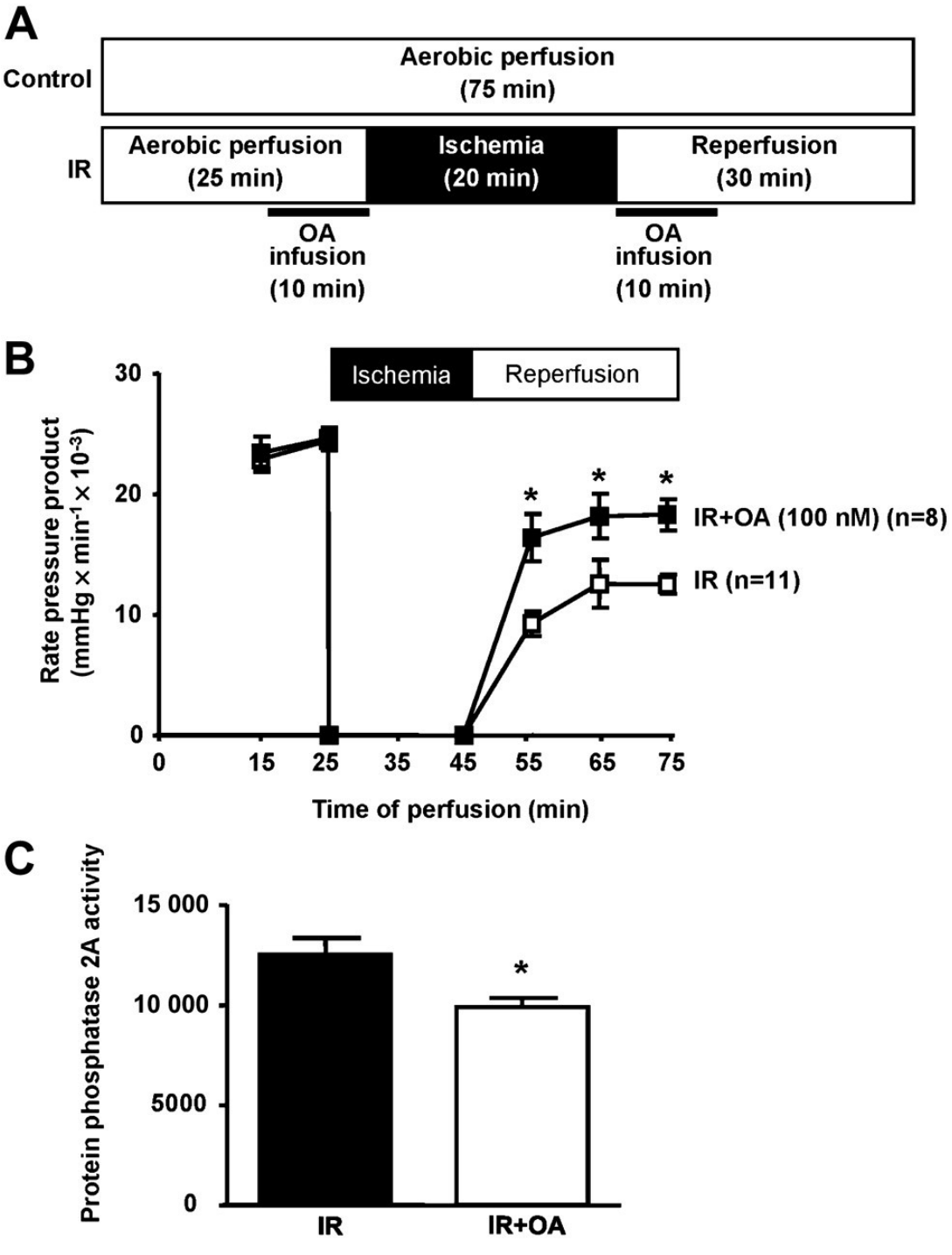
A
Control
Aerobic perfusion
(75 min)
IR
Aerobic perfusion
(25 min)
Ischemia
(20 min)
Reperfusion
(30 min)
OA
infusion
(10 min)
OA
infusion
(10 min)
B
Ischemia
Reperfusion
Rate pressure product
(mmHg × min-1 × 10-3)
30
20
10
0
0
15
25
35
45
55
65
75
Time of perfusion (min)
IR+OA (100 nM) (n=8)
IR (n=11)
C
Protein phosphatase 2A activity
15 000
10 000
5000
0
IR
IR+OA

Figure 2

(A) Domain structure and theoretical phosphorylation sites for rat matrix metalloproteinase 2 (MMP-2). Potential phosphorylation sites within rat MMP-2 were identified using the NetPhos prediction program. Vertical lines that extend above the demarcated threshold indicate putative amino acid phosphorylation targets, whether serine, threonine, or tyrosine. (B) Effect of okadaic acid (OA) on protein phosphatase 1 (PP1) and protein phosphatase 2A (PP2A) activities in homogenates from aerobically perfused hearts. Hearts were perfused aerobically for 15 min, followed by a 40 min infusion of either 10 or 100 nM OA. PP1 and PP2A activities were determined in heart homogenates prepared at the end of the perfusion. *$p<0.05$ versus control (analysis of variance, n=4 per group); †$p<0.05$ versus PP1 (t test, n=4 per group).

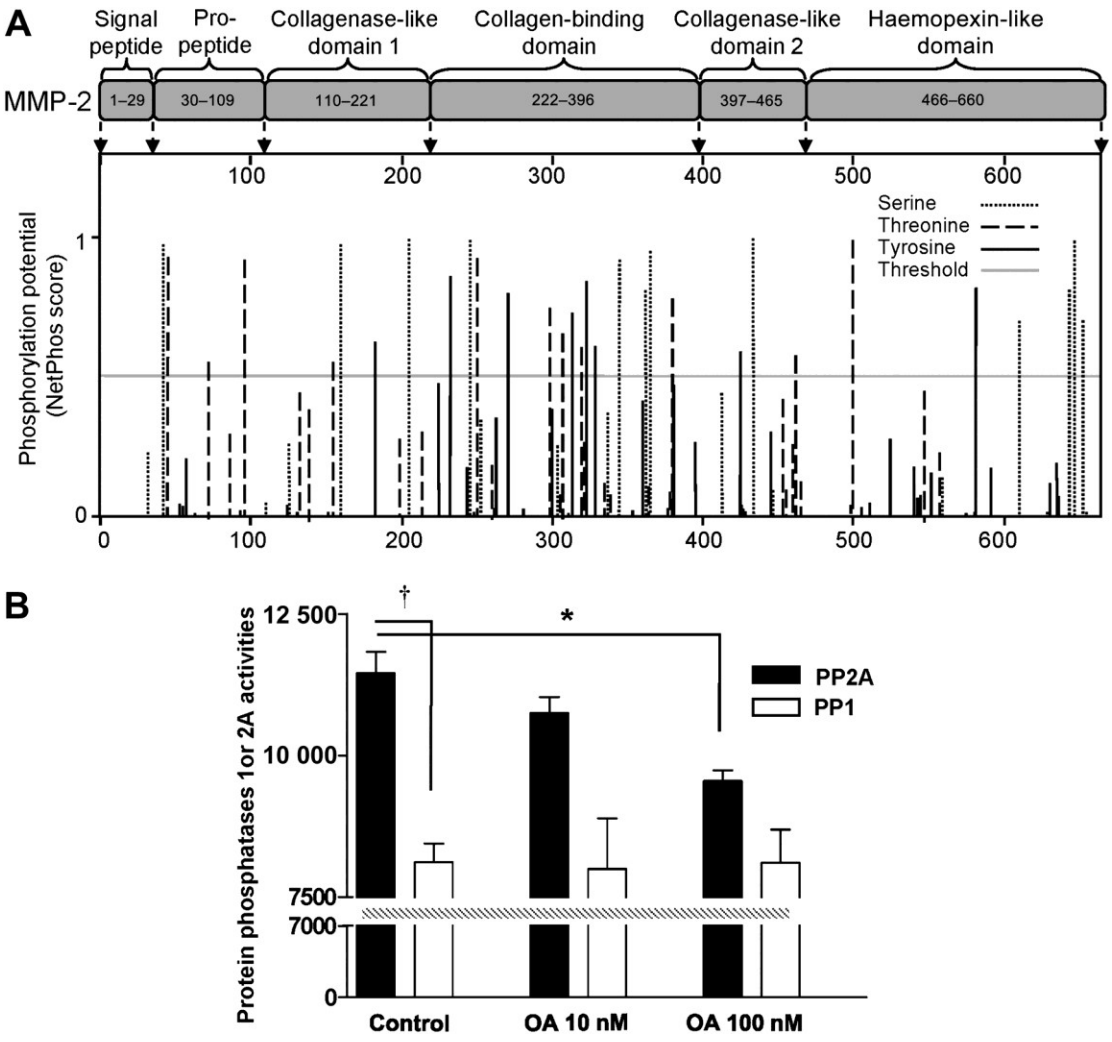
A
Signal peptide
Pro-peptide
Collagenase-like domain 1
Collagen-binding domain
Collagenase-like domain 2
Haemopexin-like domain
MMP-2
1–29
30–109
110–221
222–396
397–465
466–660
100
200
300
400
500
600
Serine
Threonine
Tyrosine
Threshold
Phosphorylation potential (NetPhos score)
1
0
0
100
200
300
400
500
600
B
†
*
12 500
10 000
7500
7000
0
PP2A
PP1
Protein phosphatases 1or 2A activities
Control
OA 10 nM
OA 100 nM

Figure 3

Matrix metalloproteinase 2 (MMP-2) activities and protein levels in coronary effluent and heart tissue. (A) Representative zymogram showing gelatinolytic activities in coronary effluent samples from perfused hearts collected at different time points (upper panel). The times given represent the end of the sampling period (see Methods). Densitometric analysis of specific activity of 72 kDa MMP-2 in coronary effluent samples (lower panel). (B) Representative zymograms (upper left panel) and western blots (upper right panel) showing gelatinolytic activities and MMP-2 protein in the heart tissue at the end of the perfusion, respectively. Densitometric analysis of specific activity of 72 and 62 kDa MMP-2 (lower left panel) or 72 kDa MMP-2 protein levels in the heart tissue (lower right panel). AE, aerobically perfused hearts; AE+OA, aerobically perfused hearts treated with 100 nM okadaic acid (OA); IR, ischaemia–reperfused hearts; IR+OA, ischaemia–reperfused hearts treated with 100 nM OA. *$p<0.05$ versus AE (analysis of variance, n=3 per group).

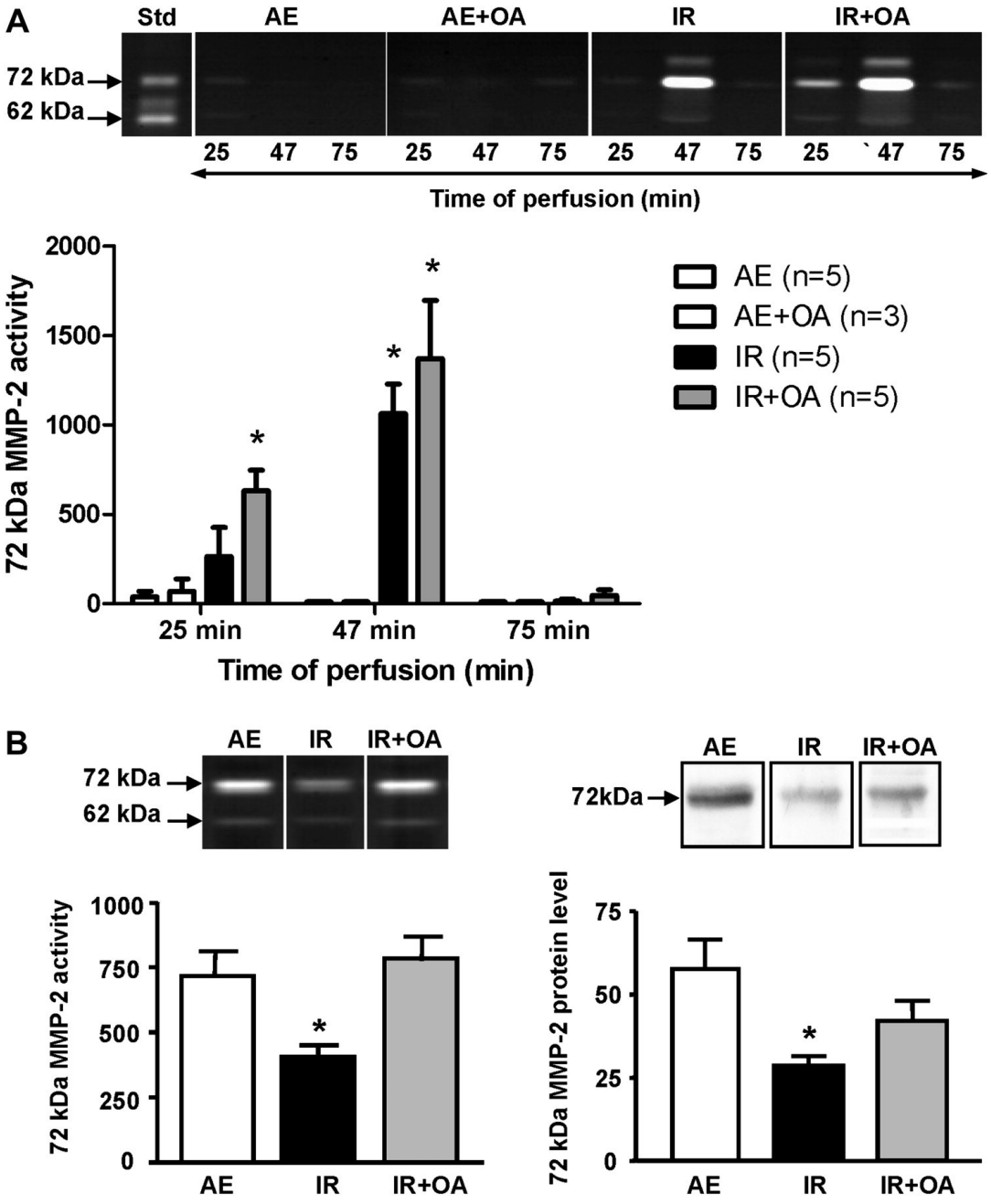
A
Std
AE
AE+OA
IR
IR+OA
72 kDa
62 kDa
25 47 75 25 47 75 25 47 75 25 ` 47 75
Time of perfusion (min)
72 kDa MMP-2 activity
2000
1500
1000
500
0
*
*
*
AE (n=5)
AE+OA (n=3)
IR (n=5)
IR+OA (n=5)
25 min
47 min
75 min
Time of perfusion (min)
B
AE
IR
IR+OA
72 kDa
62 kDa
72kDa
72 kDa MMP-2 activity
1000
750
500
250
0
72 kDa MMP-2 protein level
75
50
25
0
AE
IR
IR+OA

Figure 4

(A) Phosphorylation status of matrix metalloproteinase 2 (MMP-2) in heart tissue. Heart homogenates were immunoprecipitated with anti-phosphoserine antibody and then analysed for MMP-2 protein level by immunoblotting. IgG indicates immunoprecipitation using unrelated IgG as a negative control. r-MMP-2 indicates human recombinant MMP-2, which was immunoprecipitated with anti-phosphoserine antibody as a positive control. This experiment was repeated with different hearts from the same groups on two separate occasions and gave qualitatively similar results. AE, aerobically perfused hearts; IB, immunoblotting; IP, immunoprecipitation; IR, ischaemia–reperfused hearts; IR+OA, ischaemia–reperfused hearts treated with 100 nM okadaic acid (OA). (B) Effect of OA on troponin I (TnI) content in heart tissue. Representative TnI protein level in heart homogenates prepared at the end of perfusion as determined by western blotting (upper panel). Lower panel shows densitometric analysis of TnI content in the samples. AE, aerobically perfused hearts; IR, ischaemia–reperfused hearts; IR+OA, ischaemia–reperfused hearts treated with 100 nM OA. *$p<0.05$ versus AE (analysis of variance, n=5 per group)

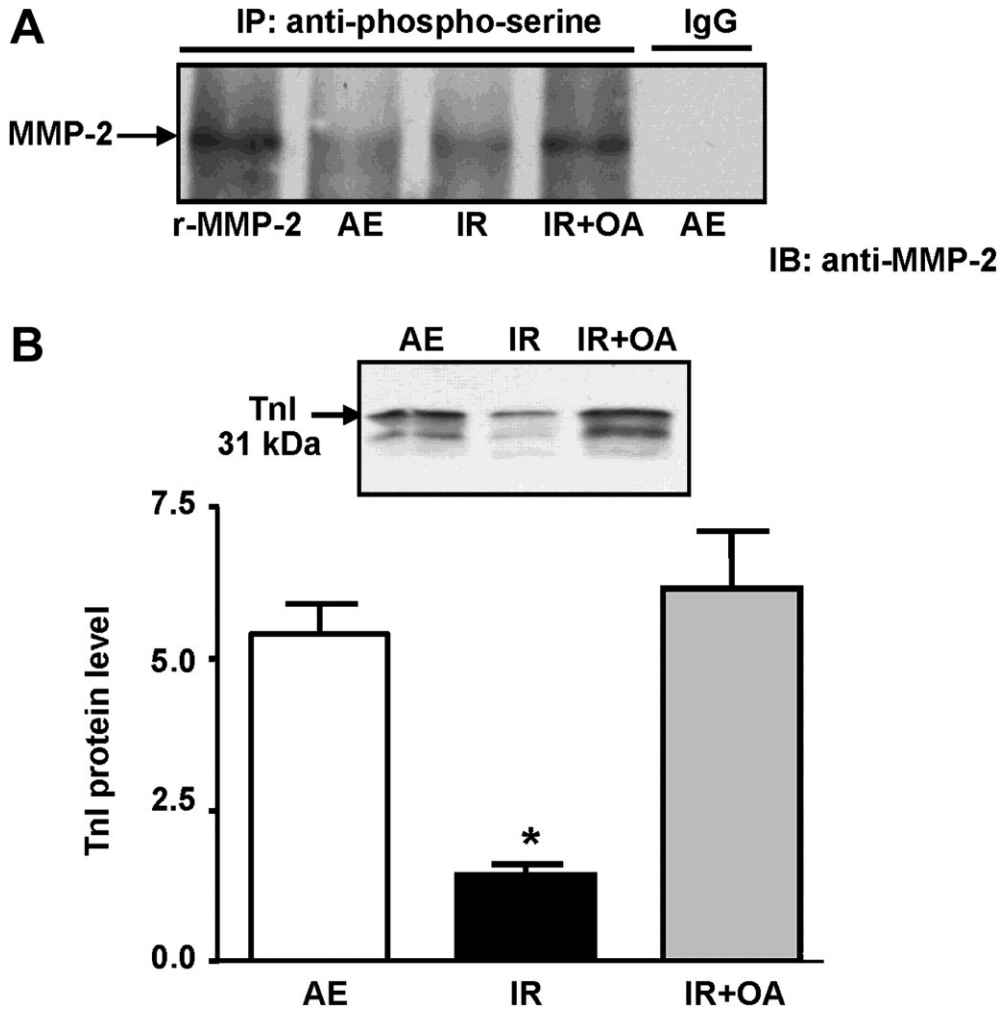
A
IP: anti-phospho-serine
IgG
MMP-2
r-MMP-2
AE
IR
IR+OA
AE
IB: anti-MMP-2
B
AE
IR
IR+OA
TnI
31 kDa
7.5
5.0
2.5
0.0
TnI protein level
*
AE
IR
IR+OA

References

1. Cheung PY, Sawicki G, Wozniak M, *et al*. Matrix metalloproteinase-2 contributes to ischemia–reperfusion injury in the heart. Circulation 2000;101:1833–9.

2. Wang W, Sawicki G, Schulz R . Peroxynitrite-induced myocardial injury is mediated through matrix metalloproteinase-2. Cardiovasc Res 2002;53:165–74.
3. Gao CQ, Sawicki G, Suarez-Pinzon WL, *et al*. Matrix metalloproteinase-2 mediates cytokine-induced myocardial contractile dysfunction. Cardiovasc Res 2003;57:426–33.

4. Schulz R. Intracellular targets of matrix metalloproteinase-2 in cardiac disease: rationale and therapeutic approaches. Annu Rev Pharmacol Toxicol 2007;47:211–42.

5. Nagase H, Visse R, Murphy G. Structure and function of matrix metalloproteinases and TIMPs. Cardiovasc Res 2006;69:562–73.

6. Wang W, Schulze CJ, Suarez-Pinzon WL, *et al*. Intracellular action of matrix metalloproteinase-2 accounts for acute myocardial ischemia and reperfusion injury.Circulation 2002;106:1543–9.

7. Sawicki G, Leon H, Sawicka J, *et al*. Degradation of myosin light chain in isolated rat hearts subjected to ischemia–reperfusion injury: a new intracellular target for matrix metalloproteinase-2. Circulation 2005;112:544–52.

8. Sung MM, Schulz CG, Wang W, *et al*. Matrix metalloproteinase-2 degrades the cytoskeletal protein alpha-actinin in peroxynitrite mediated myocardial injury. J Mol Cell Cardiol 2007;43:429–36.

9. Ali MA, Cho WJ, Hudson B, *et al*. Titin is a target of matrix metalloproteinase-2: implications in myocardial ischemia/reperfusion injury. Circulation 2010;122:2039–47.

10. Ishihara H, Martin BL, Brautigan DL, *et al*. Calyculin A and okadaic acid: inhibitors of protein phosphatase activity. Biochem Biophys Res Commun 1989;159:871–7.

11. Wera S, Hemmings BA. Serine/threonine protein phosphatases. Biochem J1995;311:17–29.

12. Dawson JF, Holmes CF. Molecular mechanisms underlying inhibition of protein phosphatases by marine toxins. Front Biosci 1999;4:D646–58.

13. Gupta RC, Neumann J, Watanabe AM, *et al*. Evidence for presence and hormonal regulation of protein phosphatase inhibitor-1 in ventricular cardiomyocyte. Am J Physiol1996;270:H1159–64.

14. Luss H, Klein-Wiele O, Boknik P, *et al*. Regional expression of protein phosphatase type 1 and 2A catalytic subunit isoforms in the human heart. J Mol Cell Cardiol2000;32:2349–59.

15. Sariahmetoglu M, Crawford BD, Leon H, *et al*. Regulation of matrix metalloproteinase-2 (MMP-2) activity by phosphorylation. FASEB J 2007;21:2486–95.

16. Nyalendo C, Michaud M, Beaulieu E, *et al*. Src-dependent phosphorylation of membrane type I matrix metalloproteinase on cytoplasmic tyrosine 573: role in endothelial and tumor cell migration. J Biol Chem 2007;282:15690–9.

17. Nyalendo C, Beaulieu E, Sartelet H, *et al*. Impaired tyrosine phosphorylation of membrane type 1-matrix metalloproteinase reduces tumor cell proliferation in three-dimensional matrices and abrogates tumor growth in mice. Carcinogenesis2008;29:1655–64.

18. Kobryn CE, Mandel LJ. Decreased protein phosphorylation induced by anoxia in proximal renal tubules. Am J Physiol 1994;267:C1073–9.

19. Blom N, Gammeltoft S, Brunak S. Sequence and structure-based prediction of eukaryotic protein phosphorylation sites. J Mol Biol 1999;294:1351–62.

20. Sawicki G, Salas E, Murat J, *et al*. Release of gelatinase A during platelet activation mediates aggregation. Nature 1997;386:616–19.

21. Laemmli UK. Cleavage of structural proteins during the assembly of the head of bacteriophage T4. Nature 1970;227:680–5.

22. Ferry G, Lonchampt M, Pennel L, *et al*. Activation of MMP-9 by neutrophil elastase in an in vivo model of acute lung injury. FEBS Lett 1997;402:111–15.

23. Bergman MR, Teerlink JR, Mahimkar R, *et al*. Cardiac matrix metalloproteinase-2 expression independently induces marked ventricular remodeling and systolic dysfunction. Am J Physiol Heart Circ Physiol 2007;292:H1847–60.

24. Fernandez JJ, Candenas ML, Souto ML, *et al*. Okadaic acid, useful tool for studying cellular processes. Curr Med Chem 2002;9:229–62.

25. Neumann J, Boknik P, Herzig S, *et al*. Evidence for physiological functions of protein phosphatases in the heart: evaluation with okadaic acid. Am J Physiol1993;265:H257–66.

26. Armstrong SC, Ganote CE. Effects of the protein phosphatase inhibitors okadaic acid and calyculin A on metabolically inhibited and ischaemic isolated myocytes. J Mol Cell Cardiol 1992;24:869–84.
27. Armstrong SC, Gao W, Lane JR, *et al*. Protein phosphatase inhibitors calyculin A and fostriecin protect rabbit cardiomyocytes in late ischemia. J Mol Cell Cardiol1998;30:61–73.
28. Armstrong SC, Hoover DB, Delacey MH, *et al*. Translocation of PKC, protein phosphatase inhibition and preconditioning of rabbit cardiomyocytes. J Mol Cell Cardiol1996;28:1479–92.
29. Fenton RA, Dickson EW, Dobson JG Jr.. Inhibition of phosphatase activity enhances preconditioning and limits cell death in the ischemic/reperfused aged rat heart. Life Sci2005;77:3375–88.
30. Weinbrenner C, Baines CP, Liu GS, *et al*. Fostriecin, an inhibitor of protein phosphatase 2A, limits myocardial infarct size even when administered after onset of ischemia.Circulation 1998;98:899–905.
31. Ingebritsen TS, Stewart AA, Cohen P. The protein phosphatases involved in cellular regulation. 6. Measurement of type-1 and type-2 protein phosphatases in extracts of mammalian tissues; an assessment of their physiological roles. Eur J Biochem1983;132:297–307.
32. Skrzypiec-Spring M, Grotthus B, Szelag A, *et al*. Isolated heart perfusion according to Langendorff – still viable in the new millennium. J Pharmacol Toxicol Methods2007;55:113–26.
33. Jordan JE, Zhao ZQ, Vinten-Johansen J. The role of neutrophils in myocardial ischemia–reperfusion injury. Cardiovasc Res 1999;43:860–78.

Bibliography

1. Organization WH. *WHO | Cardiovascular Diseases (CVDs)*. World Health Organization; 2015. http://www.who.int/mediacentre/factsheets/fs317/en/. Accessed July 14, 2015.

2. Noma A. ATP-regulated K+ channels in cardiac muscle. *Nature*. 1983;305(5930):147-148.

3. Ashcroft FM, Harrison DE, Ashcroft SJ. Glucose induces closure of single potassium channels in isolated rat pancreatic beta-cells. *Nature*. 1984;312(5993):446-448.

4. Inagaki N, Gonoi T, Clement 4th JP, et al. Reconstitution of IKATP: an inward rectifier subunit plus the sulfonylurea receptor. *Science*. 1995;270(5239):1166-1170.

5. Shyng S, Nichols CG. Octameric stoichiometry of the KATP channel complex. *J Gen Physiol*. 1997;110(6):655-664. http://www.pubmedcentral.nih.gov/articlerender.fcgi?artid=2229396&tool=pmcentrez&rendertype=abstract. Accessed June 20, 2015.

6. Aguilar-Bryan L, Clement JP, Gonzalez G, Kunjilwar K, Babenko A, Bryan J. Toward understanding the assembly and structure of KATP channels. *Physiol Rev*. 1998;78(1):227-245. http://www.ncbi.nlm.nih.gov/pubmed/9457174. Accessed June 20, 2015.

7. Aguilar-Bryan L, Nichols CG, Wechsler SW, Clement JP 4th, Boyd AE 3rd, González G, Herrera-Sosa H, Nguy K, Bryan J N DA. Cloning of the beta cell high-affinity sulfonylurea receptor: a regulator of insulin secretion. *Science*. 1995;268(5209):23-426.

8. Inagaki N, Gonoi T, Clement JP, et al. A family of sulfonylurea receptors determines the pharmacological properties of ATP-sensitive K+ channels. *Neuron*. 1996;16(5):1011-1017. http://www.ncbi.nlm.nih.gov/pubmed/8630239. Accessed June 20, 2015.

9. Isomoto S, Kondo C, Yamada M, et al. A novel sulfonylurea receptor forms with BIR (Kir6.2) a smooth muscle type ATP-sensitive K+ channel. *J Biol Chem*. 1996;271(40):24321-24324. http://www.ncbi.nlm.nih.gov/pubmed/8798681. Accessed June 20, 2015.

10. Chutkow WA, Simon MC, Le Beau MM, Burant CF. Cloning, tissue expression, and chromosomal localization of SUR2, the putative drug-binding subunit of cardiac, skeletal muscle, and vascular KATP channels. *Diabetes*. 1996;45(10):1439-1445.

11. Ashcroft FM, Gribble FM. Correlating structure and function in ATP-sensitive K+ channels. *Trends Neurosci*. 1998;21(7):288-294. http://www.ncbi.nlm.nih.gov/pubmed/9683320. Accessed June 20, 2015.

12. Miki T, Nagashima K, Seino S. The structure and function of the ATP-sensitive K+ channel in insulin-secreting pancreatic beta-cells. *J Mol Endocrinol*. 1999;22(2):113-123. http://www.ncbi.nlm.nih.gov/pubmed/10194514. Accessed June 20, 2015.

13. Babenko AP, Aguilar-Bryan L, Bryan J. A view of sur/KIR6.X, KATP channels. *Annu Rev Physiol*. 1998;60:667-687. doi:10.1146/annurev.physiol.60.1.667.

14. Aguilar-Bryan L, Nichols CG, Wechsler SW, et al. Cloning of the beta cell high-affinity sulfonylurea receptor: a regulator of insulin secretion. *Science*. 1995;268(5209):423-426. http://www.ncbi.nlm.nih.gov/pubmed/7716547. Accessed June 20, 2015.

15. Sakura H, Ammälä C, Smith PA, Gribble FM, Ashcroft FM. Cloning and functional expression of the cDNA encoding a novel ATP-sensitive potassium channel subunit expressed in pancreatic beta-cells, brain, heart and skeletal muscle. *FEBS Lett*. 1995;377(3):338-344. doi:10.1016/0014-5793(95)01369-5.

16. Liss B, Bruns R, Roeper J. Alternative sulfonylurea receptor expression defines metabolic sensitivity of K-ATP channels in dopaminergic midbrain neurons. *EMBO J*. 1999;18(4):833-846. doi:10.1093/emboj/18.4.833.

17. Karschin C, Ecke C, Ashcroft FM, Karschin A. Overlapping distribution of K(ATP) channel-forming Kir6.2 subunit and the sulfonylurea receptor SUR1 in rodent brain. *FEBS Lett*. 1997;401(1):59-64. http://www.ncbi.nlm.nih.gov/pubmed/9003806. Accessed June 20, 2015.

18. Babenko AP, Gonzalez G, Aguilar-Bryan L, Bryan J. Reconstituted human cardiac KATP channels: functional identity with the native channels from the sarcolemma of human ventricular cells. *Circ Res*. 1998;83(11):1132-1143. http://www.ncbi.nlm.nih.gov/pubmed/9831708. Accessed June 5, 2015.

19. Okuyama Y, Yamada M, Kondo C, et al. The effects of nucleotides and potassium channel openers on the SUR2A/Kir6.2 complex K+ channel expressed in a mammalian cell line, HEK293T cells. *Pflugers Arch*. 1998;435(5):595-603. http://www.ncbi.nlm.nih.gov/pubmed/9479011. Accessed June 20, 2015.

20. Yamada M, Isomoto S, Matsumoto S, et al. Sulphonylurea receptor 2B and Kir6.1 form a sulphonylurea-sensitive but ATP-insensitive K+ channel. *J Physiol*. 1997;499 (Pt 3:715-720. http://www.pubmedcentral.nih.gov/articlerender.fcgi?artid=1159289&tool=pmcentrez&rendertype=abstract. Accessed June 20, 2015.

21. Beech DJ, Zhang H, Nakao K, Bolton TB. K channel activation by nucleotide diphosphates and its inhibition by glibenclamide in vascular smooth muscle cells. *Br J Pharmacol*. 1993;110(2):573-582.

http://www.pubmedcentral.nih.gov/articlerender.fcgi?artid=2175936&tool=pmcentrez&rendertype=abstract. Accessed May 12, 2015.

22. Zhang HL, Bolton TB. Two types of ATP-sensitive potassium channels in rat portal vein smooth muscle cells. *Br J Pharmacol*. 1996;118(1):105-114. http://www.pubmedcentral.nih.gov/articlerender.fcgi?artid=1909472&tool=pmcentrez&rendertype=abstract. Accessed June 20, 2015.

23. Ashford ML, Sturgess NC, Trout NJ, Gardner NJ, Hales CN. Adenosine-5'-triphosphate-sensitive ion channels in neonatal rat cultured central neurones. *Pflugers Arch*. 1988;412(3):297-304. http://www.ncbi.nlm.nih.gov/pubmed/2460821. Accessed June 27, 2015.

24. Seino S. ATP-sensitive potassium channels: a model of heteromultimeric potassium channel/receptor assemblies. *Annu Rev Physiol*. 1999;61:337-362. doi:10.1146/annurev.physiol.61.1.337.

25. Bajgar R, Seetharaman S, Kowaltowski AJ, Garlid KD, Paucek P. Identification and properties of a novel intracellular (mitochondrial) ATP-sensitive potassium channel in brain. *J Biol Chem*. 2001;276(36):33369-33374. doi:10.1074/jbc.M103320200.

26. Flagg TP, Kurata HT, Masia R, et al. Differential structure of atrial and ventricular KATP: atrial KATP channels require SUR1. *Circ Res*. 2008;103(12):1458-1465. doi:10.1161/CIRCRESAHA.108.178186.

27. Schmid D, Stolzlechner M, Sorgner A, et al. An abundant, truncated human sulfonylurea receptor 1 splice variant has prodiabetic properties and impairs sulfonylurea action. *Cell Mol Life Sci*. 2012;69(1):129-148. doi:10.1007/s00018-011-0739-x.

28. Aguilar-Bryan L, Bryan J. Molecular biology of adenosine triphosphate-sensitive potassium channels. *Endocr Rev*. 1999;20(2):101-135.

29. Tarasov A, Dusonchet J, Ashcroft F. Metabolic Regulation of the Pancreatic Beta-Cell ATP-Sensitive K+ Channel: A Pas de Deux. *Diabetes*. 2004;53(Supplement 3):S113-S122. doi:10.2337/diabetes.53.suppl_3.S113.

30. Terzic a, Jahangir a, Kurachi Y. Cardiac ATP-sensitive K+ channels: regulation by intracellular nucleotides and K+ channel-opening drugs. *Am J Physiol*. 1995;269(Table 1):C525-C545.

31. Ashcroft FM, Kakei M. ATP-sensitive K+ channels in rat pancreatic beta-cells: modulation by ATP and Mg2+ ions. *J Physiol*. 1989;416:349-367. http://www.pubmedcentral.nih.gov/articlerender.fcgi?artid=1189219&tool=pmcentrez&rendertype=abstract. Accessed June 20, 2015.

32. Ingwall JS, Weiss RG. Is the failing heart energy starved? On using chemical energy to support cardiac function. *Circ Res*. 2004;95(2):135-145. doi:10.1161/01.RES.0000137170.41939.d9.

33. Cook DL, Satin LS, Ashford ML, Hales CN. ATP-sensitive K+ channels in pancreatic beta-cells. Spare-channel hypothesis. *Diabetes*. 1988;37(5):495-498. http://www.ncbi.nlm.nih.gov/pubmed/2452107. Accessed July 18, 2015.

34. Nichols CG, Lederer WJ. The regulation of ATP-sensitive K+ channel activity in intact and permeabilized rat ventricular myocytes. *J Physiol*. 1990;423:91-110.

35. Nichols CG, Shyng SL, Nestorowicz A, et al. Adenosine diphosphate as an intracellular regulator of insulin secretion. *Science*. 1996;272(5269):1785-1787. http://www.ncbi.nlm.nih.gov/pubmed/8650576. Accessed June 20, 2015.

36. Nilsson T, Schultz V, Berggren PO, Corkey BE, Tornheim K. Temporal patterns of changes in ATP/ADP ratio, glucose 6-phosphate and cytoplasmic free Ca2+ in glucose-stimulated pancreatic beta-cells. *Biochem J*. 1996;314 (Pt 1:91-94. http://www.pubmedcentral.nih.gov/articlerender.fcgi?artid=1217056&tool=pmcentrez&rendertype=abstract. Accessed June 20, 2015.

37. Lammens A, Schele A, Hopfner K-P. Structural biochemistry of ATP-driven dimerization and DNA-stimulated activation of SMC ATPases. *Curr Biol*. 2004;14(19):1778-1782. doi:10.1016/j.cub.2004.09.044.

38. Smith PC, Karpowich N, Millen L, et al. ATP binding to the motor domain from an ABC transporter drives formation of a nucleotide sandwich dimer. *Mol Cell*. 2002;10(1):139-149. http://www.pubmedcentral.nih.gov/articlerender.fcgi?artid=3516284&tool=pmcentrez&rendertype=abstract. Accessed April 29, 2015.

39. Ueda K, Komine J, Matsuo M, Seino S, Amachi T. Cooperative binding of ATP and MgADP in the sulfonylurea receptor is modulated by glibenclamide. *Proc Natl Acad Sci U S A*. 1999;96(4):1268-1272. http://www.pubmedcentral.nih.gov/articlerender.fcgi?artid=15452&tool=pmcentrez&rendertype=abstract. Accessed June 20, 2015.

40. Matsuo M, Tanabe K, Kioka N, Amachi T, Ueda K. Different binding properties and affinities for ATP and ADP among sulfonylurea receptor subtypes, SUR1, SUR2A, and SUR2B. *J Biol Chem*. 2000;275(37):28757-28763. doi:10.1074/jbc.M004818200.

41. Bienengraeber M, Alekseev AE, Abraham MR, et al. ATPase activity of the sulfonylurea receptor: a catalytic function for the KATP channel complex. *FASEB J*. 2000;14(13):1943-1952. doi:10.1096/fj.00-0027com.

42. De Wet H, Mikhailov M V, Fotinou C, et al. Studies of the ATPase activity of the ABC protein SUR1. *FEBS J*. 2007;274(14):3532-3544. doi:10.1111/j.1742-4658.2007.05879.x.

43. Zingman L V, Alekseev AE, Bienengraeber M, et al. Signaling in channel/enzyme multimers: ATPase transitions in SUR module gate ATP-sensitive K+ conductance. *Neuron*. 2001;31(2):233-245. http://www.ncbi.nlm.nih.gov/pubmed/11502255. Accessed June 20, 2015.

44. Matsuo M, Kimura Y, Ueda K. KATP channel interaction with adenine nucleotides. *J Mol Cell Cardiol*. 2005;38(6):907-916. doi:10.1016/j.yjmcc.2004.11.021.

45. Masia R, Nichols CG. Functional clustering of mutations in the dimer interface of the nucleotide binding folds of the sulfonylurea receptor. *J Biol Chem*. 2008;283(44):30322-30329. doi:10.1074/jbc.M804318200.

46. Masia R, Enkvetchakul D, Nichols CG. Differential nucleotide regulation of KATP channels by SUR1 and SUR2A. *J Mol Cell Cardiol*. 2005;39:491-501. doi:10.1016/j.yjmcc.2005.03.009.

47. Elvir-Mairena JR, Jovanovic A, Gomez LA, Alekseev AE, Terzic A. Reversal of the ATP-liganded state of ATP-sensitive K+ channels by adenylate kinase activity. *J Biol Chem*. 1996;271(50):31903-31908. doi:10.1074/jbc.271.50.31903.

48. Crawford RM, Ranki HJ, Botting CH, Budas GR, Jovanovic A. Creatine kinase is physically associated with the cardiac ATP-sensitive K+ channel in vivo. *FASEB J*. 2002;16(1):102-104. doi:10.1096/fj.01-0466fje.

49. Carrasco AJ, Dzeja PP, Alekseev AE, et al. Adenylate kinase phosphotransfer communicates cellular energetic signals to ATP-sensitive potassium channels. *Proc Natl Acad Sci U S A*. 2001;98(13):7623-7628. doi:10.1073/pnas.121038198.

50. Kubo S, Noda LH. Adenylate kinase of porcine heart. *Eur J Biochem*. 1974;48(2):325-331. http://www.ncbi.nlm.nih.gov/pubmed/4375035. Accessed June 20, 2015.

51. Kremen A. Informational aspects of Gibbs function output from nucleotide pools and of the adenylate kinase reaction. *J Theor Biol*. 1982;96(3):425-441. http://www.ncbi.nlm.nih.gov/pubmed/6289012. Accessed June 20, 2015.

52. Veuthey AL, Stucki J. The adenylate kinase reaction acts as a frequency filter towards fluctuations of ATP utilization in the cell. *Biophys Chem*. 1987;26(1):19-28. http://www.ncbi.nlm.nih.gov/pubmed/3036264. Accessed June 20, 2015.

53. Dzeja PP, Zeleznikar RJ, Goldberg ND. Adenylate kinase: kinetic behavior in intact cells indicates it is integral to multiple cellular processes. *Mol Cell Biochem*.

1998;184(1-2):169-182. http://www.ncbi.nlm.nih.gov/pubmed/9746320. Accessed June 20, 2015.

54. Zeleznikar RJ, Dzeja PP, Goldberg ND. Adenylate kinase-catalyzed phosphoryl transfer couples ATP utilization with its generation by glycolysis in intact muscle. *J Biol Chem*. 1995;270(13):7311-7319. http://www.ncbi.nlm.nih.gov/pubmed/7706272. Accessed June 20, 2015.

55. Saks VA, Khuchua ZA, Vasilyeva E V, Belikova OYu, Kuznetsov A V. Metabolic compartmentation and substrate channelling in muscle cells. Role of coupled creatine kinases in in vivo regulation of cellular respiration--a synthesis. *Mol Cell Biochem*. 133-134:155-192. http://www.ncbi.nlm.nih.gov/pubmed/7808453. Accessed June 20, 2015.

56. Larsson O, Ammälä C, Bokvist K, Fredholm B, Rorsman P. Stimulation of the KATP channel by ADP and diazoxide requires nucleotide hydrolysis in mouse pancreatic beta-cells. *J Physiol*. 1993;463:349-365. http://www.pubmedcentral.nih.gov/articlerender.fcgi?artid=1175347&tool=pmcentrez&rendertype=abstract. Accessed June 20, 2015.

57. Olson LK, Schroeder W, Robertson RP, Goldberg ND, Walseth TF. Suppression of adenylate kinase catalyzed phosphotransfer precedes and is associated with glucose-induced insulin secretion in intact HIT-T15 cells. *J Biol Chem*. 1996;271(28):16544-16552. http://www.ncbi.nlm.nih.gov/pubmed/8663240. Accessed June 20, 2015.

58. Weiss JN, Lamp ST. Cardiac ATP-sensitive K+ channels. Evidence for preferential regulation by glycolysis. *J Gen Physiol*. 1989;94(5):911-935. http://www.pubmedcentral.nih.gov/articlerender.fcgi?artid=2228974&tool=pmcentrez&rendertype=abstract. Accessed June 20, 2015.

59. Baukrowitz T, Schulte U, Oliver D, et al. PIP2 and PIP as determinants for ATP inhibition of KATP channels. *Science*. 1998;282(5391):1141-1144.

60. Fan Z, Makielski JC. Phosphoinositides Decrease Atp Sensitivity of the Cardiac Atp-Sensitive K+ Channel: A Molecular Probe for the Mechanism of Atp-Sensitive Inhibition. *J Gen Physiol*. 1999;114(2):251-270. doi:10.1085/jgp.114.2.251.

61. Okamura M, Kakei M, Ichinari K, et al. State-dependent modification of ATP-sensitive K+ channels by phosphatidylinositol 4,5-bisphosphate. *Am J Physiol Cell Physiol*. 2001;280(2):C303-C308. http://ajpcell.physiology.org/content/280/2/C303.abstract?ijkey=bf12428edd4b8da29ad70da624c386815f6ae7bd&keytype2=tf_ipsecsha. Accessed June 20, 2015.

62. Manning Fox JE, Nichols CG, Light PE. Activation of adenosine triphosphate-sensitive potassium channels by acyl coenzyme A esters involves multiple

phosphatidylinositol 4,5-bisphosphate-interacting residues. *Mol Endocrinol*. 2004;18(3):679-686. doi:10.1210/me.2003-0431.

63. Beguin P, Nagashima K, Nishimura M, Gonoi T, Seino S. PKA-mediated phosphorylation of the human K(ATP) channel: separate roles of Kir6.2 and SUR1 subunit phosphorylation. *EMBO J*. 1999;18(17):4722-4732. doi:10.1093/emboj/18.17.4722.

64. Lin YF, Jan YN, Jan LY. Regulation of ATP-sensitive potassium channel function by protein kinase A-mediated phosphorylation in transfected HEK293 cells. *EMBO J*. 2000;19(5):942-955. doi:10.1093/emboj/19.5.942.

65. Shi Y, Wu Z, Cui N, et al. PKA phosphorylation of SUR2B subunit underscores vascular KATP channel activation by beta-adrenergic receptors. *Am J Physiol Regul Integr Comp Physiol*. 2007;293(3):R1205-R1214. doi:10.1152/ajpregu.00337.2007.

66. Light PE, Bladen C, Winkfein RJ, Walsh MP, French RJ. Molecular basis of protein kinase C-induced activation of ATP-sensitive potassium channels. *Proc Natl Acad Sci U S A*. 2000;97(16):9058-9063. doi:10.1073/pnas.160068997.

67. Hayabuchi Y, Davies NW, Standen NB. Angiotensin II inhibits rat arterial KATP channels by inhibiting steady-state protein kinase A activity and activating protein kinase Ce. *J Physiol*. 2001;530(Pt 2):193-205. http://www.pubmedcentral.nih.gov/articlerender.fcgi?artid=2278407&tool=pmcentrez&rendertype=abstract. Accessed June 20, 2015.

68. Han J, Kim N, Kim E, Ho WK, Earm YE. Modulation of ATP-sensitive potassium channels by cGMP-dependent protein kinase in rabbit ventricular myocytes. *J Biol Chem*. 2001;276(25):22140-22147. doi:10.1074/jbc.M010103200.

69. Lazarenko R, Geisler J, Bayliss D, Larner J, Li C. D-chiro-inositol glycan stimulates insulin secretion in pancreatic β cells. *Mol Cell Endocrinol*. 2014;387(1-2):1-7. doi:10.1016/j.mce.2014.02.004.

70. Light PE, Allen BG, Walsh MP, French RJ. Regulation of adenosine triphosphate-sensitive potassium channels from rabbit ventricular myocytes by protein kinase C and type 2A protein phosphatase. *Biochemistry*. 1995;34(21):7252-7257. http://www.ncbi.nlm.nih.gov/pubmed/7766636. Accessed June 25, 2015.

71. Van Wagoner DR. Mechanosensitive gating of atrial ATP-sensitive potassium channels. *Circ Res*. 1993;72(5):973-983. http://www.ncbi.nlm.nih.gov/pubmed/8477531. Accessed June 20, 2015.

72. Van Wagoner DR, Lamorgese M. Ischemia potentiates the mechanosensitive modulation of atrial ATP-sensitive potassium channels. *Ann N Y Acad Sci*.

1994;723:392-395. http://www.ncbi.nlm.nih.gov/pubmed/8030893. Accessed June 20, 2015.

73. Saegusa N, Sato T, Saito T, Tamagawa M, Komuro I, Nakaya H. Kir6.2-deficient mice are susceptible to stimulated ANP secretion: K(ATP) channel acts as a negative feedback mechanism? *Cardiovasc Res*. 2005;67(1):60-68. doi:10.1016/j.cardiores.2005.03.011.

74. Shi L, Xu M, Liu J, et al. KATP channels are involved in regulatory volume decrease in rat cardiac myocytes. *Physiol Res*. 2009;58:645-652.

75. An D, Kewalramani G, Qi D, et al. beta-Agonist stimulation produces changes in cardiac AMPK and coronary lumen LPL only during increased workload. *Am J Physiol Metab*. 2005;288(6):E1120-E1127. doi:10.1152/ajpendo.00588.2004.

76. Mosca SM. Cardioprotective effects of stretch are mediated by activation of sarcolemmal, not mitochondrial, ATP-sensitive potassium channels. *Am J Physiol Circ Physiol*. 2007;293(2):H1007-H1012. doi:10.1152/ajpheart.00051.2007.

77. Ranki HJ, Budas GR, Crawford RM, Davies AM, Jovanović A. 17Beta-estradiol regulates expression of K(ATP) channels in heart-derived H9c2 cells. *J Am Coll Cardiol*. 2002;40(2):367-374. http://www.ncbi.nlm.nih.gov/pubmed/12106946. Accessed June 20, 2015.

78. Davies LM, Purves GI, Barrett-Jolley R, Dart C. Interaction with caveolin-1 modulates vascular ATP-sensitive potassium (KATP) channel activity. *J Physiol*. 2010;588:3255-3266. doi:10.1113/jphysiol.2010.194779.

79. Zhong G-Z, Li Y-B, Liu X-L, Guo L-S, Chen M, Yang X-C. Hydrogen sulfide opens the KATP channel on rat atrial and ventricular myocytes. *Cardiology*. 2010;115(2):120-126. doi:10.1159/000260073.

80. Li Y, Zhong G, Yang X, Liu X. [Effects of hydrogen sulfide on the K ATP current in isolated rat ventricular myocytes]. *Zhonghua Xin Xue Guan Bing Za Zhi*. 2009;37(5):445-448. http://www.ncbi.nlm.nih.gov/pubmed/19781223. Accessed June 21, 2015.

81. Zhao W, Zhang J, Lu Y, Wang R. The vasorelaxant effect of H(2)S as a novel endogenous gaseous K(ATP) channel opener. *EMBO J*. 2001;20(21):6008-6016. doi:10.1093/emboj/20.21.6008.

82. Cheng Y, Ndisang JF, Tang G, Cao K, Wang R. Hydrogen sulfide-induced relaxation of resistance mesenteric artery beds of rats. *Am J Physiol Heart Circ Physiol*. 2004;287(5):H2316-H2323. doi:10.1152/ajpheart.00331.2004.

83. Liang GH, Adebiyi A, Leo MD, McNally EM, Leffler CW, Jaggar JH. Hydrogen sulfide dilates cerebral arterioles by activating smooth muscle cell plasma membrane KATP channels. *Am J Physiol Heart Circ Physiol*. 2011;300(6):H2088-H2095. doi:10.1152/ajpheart.01290.2010.

84. Geng B, Yang J, Qi Y, et al. H2S generated by heart in rat and its effects on cardiac function. *Biochem Biophys Res Commun*. 2004;313(2):362-368. http://www.ncbi.nlm.nih.gov/pubmed/14684169. Accessed June 21, 2015.

85. Salloum FN. Hydrogen sulfide and cardioprotection - Mechanistic insights and clinical translatability. *Pharmacol Ther*. 2015. doi:10.1016/j.pharmthera.2015.04.004.

86. Zeldin DC. Epoxygenase pathways of arachidonic acid metabolism. *J Biol Chem*. 2001;276(39):36059-36062. doi:10.1074/jbc.R100030200.

87. Ye D, Zhou W, Lee H-C. Activation of rat mesenteric arterial KATP channels by 11,12-epoxyeicosatrienoic acid. *Am J Physiol Heart Circ Physiol*. 2005;288(1):H358-H364. doi:10.1152/ajpheart.00423.2004.

88. Batchu SN, Chaudhary KR, El-Sikhry H, et al. Role of PI3Kα and sarcolemmal ATP-sensitive potassium channels in epoxyeicosatrienoic acid mediated cardioprotection. *J Mol Cell Cardiol*. 2012;53(1):43-52. doi:10.1016/j.yjmcc.2012.04.008.

89. Qu Y-Y, Yuan M-Y, Liu Y, Xiao X-J, Zhu Y-L. The protective effect of epoxyeicosatrienoic acids on cerebral ischemia/reperfusion injury is associated with PI3K/Akt pathway and ATP-sensitive potassium channels. *Neurochem Res*. 2015;40(1):1-14. doi:10.1007/s11064-014-1456-2.

90. Davies NW. Modulation of ATP-sensitive K+ channels in skeletal muscle by intracellular protons. *Nature*. 1990;343(6256):375-377. doi:10.1038/343375a0.

91. Fan Z, Makielski JC. Intracellular H+ and Ca2+ modulation of trypsin-modified ATP-sensitive K+ channels in rabbit ventricular myocytes. *Circ Res*. 1993;72(3):715-722. http://www.ncbi.nlm.nih.gov/pubmed/8381726. Accessed July 17, 2015.

92. Fan Z, Tokuyama Y, Makielski JC. Modulation of ATP-sensitive K+ channels by internal acidification in insulin-secreting cells. *Am J Physiol*. 1994;267(4 Pt 1):C1036-C1044. http://www.ncbi.nlm.nih.gov/pubmed/7943266. Accessed July 17, 2015.

93. Han J, Kim N, Joo H, Kim E, Earm YE. ATP-sensitive K(+) channel activation by nitric oxide and protein kinase G in rabbit ventricular myocytes. *Am J Physiol Heart Circ Physiol*. 2002;283(4):H1545-H1554. doi:10.1152/ajpheart.01052.2001.

94. Baker JE, Contney SJ, Singh R, Kalyanaraman B, Gross GJ, Bosnjak ZJ. Nitric oxide activates the sarcolemmal K(ATP) channel in normoxic and chronically hypoxic

hearts by a cyclic GMP-dependent mechanism. *J Mol Cell Cardiol*. 2001;33(2):331-341. doi:10.1006/jmcc.2000.1305.

95. Kawano T, Zoga V, Kimura M, et al. Nitric oxide activates ATP-sensitive potassium channels in mammalian sensory neurons: action by direct S-nitrosylation. *Mol Pain*. 2009;5:12. doi:10.1186/1744-8069-5-12.

96. Trube G, Rorsman P, Ohno-Shosaku T. Opposite effects of tolbutamide and diazoxide on the ATP-dependent K+ channel in mouse pancreatic ?-cells. *Pfl*gers Arch Eur J Physiol*. 1986;407(5):493-499. doi:10.1007/BF00657506.

97. YANAGISAWA T, SATOH K, TAIRA N. Circumstantial evidence for increased potassium conductance of membrane of cardiac muscle by 2-nicotinamidoethyl nitrate (SG-75). *Jpn J Pharmacol*. 1979;29(5):687-694. doi:10.1254/jjp.29.687.

98. Henquin J-C, Meissner HP. Opposite effects of tolbutamide and diazoxide on 86Rb+ fluxes and membrane potential in pancreatic B cells. *Biochem Pharmacol*. 1982;31(7):1407-1415. doi:10.1016/0006-2952(82)90036-3.

99. Weir SW, Weston AH. The effects of BRL 34915 and nicorandil on electrical and mechanical activity and on 86Rb efflux in rat blood vessels. *Br J Pharmacol*. 1986;88(1):121-128. doi:10.1111/j.1476-5381.1986.tb09478.x.

100. Escande D, Thuringer D, Leguern S, Cavero I. The potassium channel opener cromakalim (BRL 34915) activates ATP-dependent K+ channels in isolated cardiac myocytes. *Biochem Biophys Res Commun*. 1988;154(2):620-625. http://www.ncbi.nlm.nih.gov/pubmed/2456760. Accessed June 20, 2015.

101. Arena JP, Kass RS. Activation of ATP-sensitive K channels in heart cells by pinacidil: dependence on ATP. *Am J Physiol*. 1989;257(6 Pt 2):H2092-H2096. http://www.ncbi.nlm.nih.gov/pubmed/2513734. Accessed June 20, 2015.

102. Ashcroft FM, Gribble FM. New windows on the mechanism of action of K(ATP) channel openers. *Trends Pharmacol Sci*. 2000;21(11):439-445.

103. Bienengraeber M, Olson TM, Selivanov VA, et al. ABCC9 mutations identified in human dilated cardiomyopathy disrupt catalytic KATP channel gating. *Nat Genet*. 2004;36(4):382-387. doi:10.1038/ng1329.

104. Garlid KD, Paucek P, Yarov-Yarovoy V, et al. Cardioprotective Effect of Diazoxide and Its Interaction With Mitochondrial ATP-Sensitive K+ Channels : Possible Mechanism of Cardioprotection. *Circ Res*. 1997;81(6):1072-1082. doi:10.1161/01.RES.81.6.1072.

105. O'Rourke B. Myocardial KATP Channels in Preconditioning. *Circ Res*. 2000;87(10):845-855. doi:10.1161/01.RES.87.10.845.

106. Suzuki M, Saito T, Sato T, et al. Cardioprotective effect of diazoxide is mediated by activation of sarcolemmal but not mitochondrial ATP-sensitive potassium channels in mice. *Circulation*. 2003;107(5):682-685.

107. Grover GJ, Garlid KD. ATP-Sensitive potassium channels: a review of their cardioprotective pharmacology. *J Mol Cell Cardiol*. 2000;32(4):677-695. doi:10.1006/jmcc.2000.1111.

108. Szewczyk A, Marbán E. Mitochondria: a new target for K channel openers? *Trends Pharmacol Sci*. 1999;20(4):157-161. http://www.ncbi.nlm.nih.gov/pubmed/10322501. Accessed June 21, 2015.

109. Kicińska A, D bska G, Kunz W, Szewczyk A. Mitochondrial potassium and chloride channels. *Acta Biochim Pol*. 2000;47(3):541-551. http://www.ncbi.nlm.nih.gov/pubmed/11310958. Accessed June 21, 2015.

110. Szewczyk A, Wojtczak L. Mitochondria as a pharmacological target. *Pharmacol Rev*. 2002;54(1):101-127. http://www.ncbi.nlm.nih.gov/pubmed/11870261. Accessed June 21, 2015.

111. Seharaseyon J, Ohler A, Sasaki N, et al. Molecular composition of mitochondrial ATP-sensitive potassium channels probed by viral Kir gene transfer. *J Mol Cell Cardiol*. 2000;32(11):1923-1930. http://www.ncbi.nlm.nih.gov/pubmed/11185581. Accessed June 21, 2015.

112. D'hahan N, Moreau C, Prost AL, et al. Pharmacological plasticity of cardiac ATP-sensitive potassium channels toward diazoxide revealed by ADP. *Proc Natl Acad Sci U S A*. 1999;96(21):12162-12167.

113. Matsuoka T, Matsushita K, Katayama Y, et al. C-Terminal Tails of Sulfonylurea Receptors Control ADP-Induced Activation and Diazoxide Modulation of ATP-Sensitive K+ Channels. *Circ Res*. 2000;87(10):873-880. doi:10.1161/01.RES.87.10.873.

114. Schwanstecher M, Sieverding C, Dörschner H, et al. Potassium channel openers require ATP to bind to and act through sulfonylurea receptors. *EMBO J*. 1998;17(19):5529-5535. doi:10.1093/emboj/17.19.5529.

115. Quayle JM, Bonev AD, Brayden JE, Nelson MT. Pharmacology of ATP-sensitive K+ currents in smooth muscle cells from rabbit mesenteric artery. *Am J Physiol*. 1995;269(5 Pt 1):C1112-C1118.

116. Matsushita K. Intramolecular Interaction of SUR2 Subtypes for Intracellular ADP-Induced Differential Control of KATP Channels. *Circ Res*. 2002;90(5):554-561. doi:10.1161/01.RES.0000012666.42782.30.

117. Dabrowski M, Ashcroft FM, Ashfield R, et al. The Novel Diazoxide Analog 3-Isopropylamino-7-Methoxy-4H-1,2,4-Benzothiadiazine 1,1-Dioxide Is a Selective Kir6.2/SUR1 Channel Opener. *Diabetes*. 2002;51(6):1896-1906. doi:10.2337/diabetes.51.6.1896.

118. I. C. Sulfonylureas and hypoglycemia. *Diabet Hypoglycemia*. 2009;2(3):1.

119. Jackson JE, Bressler R. Clinical pharmacology of sulphonylurea hypoglycaemic agents: part 1. *Drugs*. 1981;22(3):211-245. http://www.ncbi.nlm.nih.gov/pubmed/7021124. Accessed June 21, 2015.

120. Jackson JE, Bressler R. Clinical pharmacology of sulphonylurea hypoglycaemic agents: part 2. *Drugs*. 1981;22(4):295-320. http://www.ncbi.nlm.nih.gov/pubmed/7030708. Accessed June 21, 2015.

121. Sturgess NC, Ashford ML, Cook DL, Hales CN. The sulphonylurea receptor may be an ATP-sensitive potassium channel. *Lancet*. 1985;2(8453):474-475.

122. Seltzer HS. Efficacy and safety of oral hypoglycemic agents. *Annu Rev Med*. 1980;31:261-272. doi:10.1146/annurev.me.31.020180.001401.

123. Tal A. Oral hypoglycemic agents in the treatment of type II diabetes. *Am Fam Physician*. 1993;48(6):1089-1095. http://www.ncbi.nlm.nih.gov/pubmed/8237731. Accessed June 27, 2015.

124. Brady PA, Terzic A. The sulfonylurea controversy: more questions from the heart. *J Am Coll Cardiol*. 1998;31(5):950-956.

125. Winkler M, Stephan D, Bieger S, Kühner P, Wolff F, Quast U. Testing the bipartite model of the sulfonylurea receptor binding site: binding of A-, B-, and A + B-site ligands. *J Pharmacol Exp Ther*. 2007;322(2):701-708. doi:10.1124/jpet.107.123224.

126. Bryan J, Crane A, Vila-Carriles WH, Babenko AP, Aguilar-Bryan L. Insulin secretagogues, sulfonylurea receptors and K(ATP) channels. *Curr Pharm Des*. 2005;11(21):2699-2716. http://www.ncbi.nlm.nih.gov/pubmed/16101450. Accessed June 27, 2015.

127. Vila-Carriles WH, Zhao G, Bryan J. Defining a binding pocket for sulfonylureas in ATP-sensitive potassium channels. *FASEB J*. 2007;21(1):18-25. doi:10.1096/fj.06-6730hyp.

128. Babenko AP, Gonzalez G, Bryan J. Pharmaco-topology of sulfonylurea receptors. Separate domains of the regulatory subunits of K(ATP) channel isoforms are required for selective interaction with K(+) channel openers. *J Biol Chem*. 2000;275(2):717-720. http://www.ncbi.nlm.nih.gov/pubmed/10625598. Accessed June 27, 2015.

129. Gribble FM, Tucker SJ, Seino S, Ashcroft FM. Tissue specificity of sulfonylureas: studies on cloned cardiac and beta-cell K(ATP) channels. *Diabetes*. 1998;47(9):1412-1418. http://www.ncbi.nlm.nih.gov/pubmed/9726229. Accessed June 5, 2015.

130. Quast U, Stephan D, Bieger S, Russ U. The impact of ATP-sensitive K+ channel subtype selectivity of insulin secretagogues for the coronary vasculature and the myocardium. *Diabetes*. 2004;53 Suppl 3:S156-S164. http://www.ncbi.nlm.nih.gov/pubmed/15561904. Accessed June 27, 2015.

131. Manning Fox JE, Kanji HD, French RJ, Light PE. Cardioselectivity of the sulphonylurea HMR 1098: studies on native and recombinant cardiac and pancreatic K(ATP) channels. *Br J Pharmacol*. 2002;135(2):480-488. doi:10.1038/sj.bjp.0704455.

132. Zhang HX, Akrouh A, Kurata HT, Remedi MS, Lawton JS, Nichols CG. HMR 1098 is not an SUR isotype specific inhibitor of heterologous or sarcolemmal KATP channels. *J Mol Cell Cardiol*. 2011;50:552-560. doi:10.1016/j.yjmcc.2010.12.011.

133. Przyklenk K, Kloner RA, Yellon DM, eds. *Ischemic Preconditioning: The Concept of Endogenous Cardioprotection*. Boston, MA: Springer US; 1994. doi:10.1007/978-1-4615-2602-5.

134. LIU Y, SATO T, SEHARASEYON J, SZEWCZYK A, O'ROURKE B, MARBAN E. Mitochondrial ATP-Dependent Potassium Channels: Viable Candidate Effectors of Ischemic Preconditioninga. *Ann N Y Acad Sci*. 1999;874(1 HEART IN STRE):27-37. doi:10.1111/j.1749-6632.1999.tb09222.x.

135. Li X, Rapedius M, Baukrowitz T, et al. 5-Hydroxydecanoate and coenzyme A are inhibitors of native sarcolemmal KATP channels in inside-out patches. *Biochim Biophys Acta - Gen Subj*. 2010;1800(3):385-391. doi:10.1016/j.bbagen.2009.11.012.

136. Brana I, Tabernero J. Cardiotoxicity. *Ann Oncol*. 2010;21 Suppl 7(suppl_7):vii173-vii179. doi:10.1093/annonc/mdq295.

137. Albini A, Pennesi G, Donatelli F, Cammarota R, De Flora S, Noonan DM. Cardiotoxicity of anticancer drugs: the need for cardio-oncology and cardio-oncological prevention. *J Natl Cancer Inst*. 2010;102(1):14-25. doi:10.1093/jnci/djp440.

138. Meinert CL, Knatterud GL, Prout TE, Klimt CR. A study of the effects of hypoglycemic agents on vascular complications in patients with adult-onset diabetes. II. Mortality results. *Diabetes*. 1970;19:Suppl:789-830. http://www.ncbi.nlm.nih.gov/pubmed/4926376. Accessed June 21, 2015.

139. Seltzer HS. A summary of criticisms of the findings and conclusions of the University Group Diabetes Program (UGDP). *Diabetes*. 1972;21(9):976-979. http://www.ncbi.nlm.nih.gov/pubmed/5055722. Accessed June 21, 2015.

140. Schwartz TB, Meinert CL. The UGDP controversy: thirty-four years of contentious ambiguity laid to rest. *Perspect Biol Med*. 2004;47(4):564-574. http://www.ncbi.nlm.nih.gov/pubmed/15467178. Accessed June 21, 2015.

141. Ashcroft FM, Rorsman P. Electrophysiology of the pancreatic beta-cell. *Prog Biophys Mol Biol*. 1989;54(2):87-143. http://www.ncbi.nlm.nih.gov/pubmed/2484976. Accessed April 28, 2015.

142. Manuscript A. K ATP channels and cardiovascular disease : Suddenly a syndrome. *Circ Res*. 2014;112(7):1059-1072. doi:10.1161/CIRCRESAHA.112.300514.K.

143. Quayle JM, Nelson MT, Standen NB. ATP-sensitive and inwardly rectifying potassium channels in smooth muscle. *Physiol Rev*. 1997;77(4):1165-1232. http://www.ncbi.nlm.nih.gov/pubmed/9354814. Accessed June 21, 2015.

144. Abdelmoneim AS, Hasenbank SE, Seubert JM, Brocks DR, Light PE, Simpson SH. Variations in tissue selectivity amongst insulin secretagogues: a systematic review. *Diabetes Obes Metab*. 2012;14(2):130-138. doi:10.1111/j.1463-1326.2011.01496.x.

145. Klepzig H, Kober G, Matter C, et al. Sulfonylureas and ischaemic preconditioning; a double-blind, placebo-controlled evaluation of glimepiride and glibenclamide. *Eur Heart J*. 1999;20(6):439-446. http://www.ncbi.nlm.nih.gov/pubmed/10213347. Accessed June 21, 2015.

146. Samaha FF, Heineman FW, Ince C, Fleming J, Balaban RS. ATP-sensitive potassium channel is essential to maintain basal coronary vascular tone in vivo. *Am J Physiol*. 1992;262(5 Pt 1):C1220-C1227. http://www.ncbi.nlm.nih.gov/pubmed/1590361. Accessed June 21, 2015.

147. Imamura Y, Tomoike H, Narishige T, Takahashi T, Kasuya H, Takeshita A. Glibenclamide decreases basal coronary blood flow in anesthetized dogs. *Am J Physiol*. 1992;263(2 Pt 2):H399-H404. http://www.ncbi.nlm.nih.gov/pubmed/1510137. Accessed June 21, 2015.

148. Cole WC, McPherson CD, Sontag D. ATP-regulated K+ channels protect the myocardium against ischemia/reperfusion damage. *Circ Res*. 1991;69(3):571-581.

149. Toombs CF, Moore TL, Shebuski RJ. Limitation of infarct size in the rabbit by ischaemic preconditioning is reversible with glibenclamide. *Cardiovasc Res*. 1993;27(4):617-622. http://www.ncbi.nlm.nih.gov/pubmed/8324795. Accessed June 21, 2015.

150. Mitani A, Kinoshita K, Fukamachi K, et al. Effects of glibenclamide and nicorandil on cardiac function during ischemia and reperfusion in isolated perfused rat hearts. *Am J Physiol*. 1991;261(6 Pt 2):H1864-H1871. http://www.ncbi.nlm.nih.gov/pubmed/1836311. Accessed June 21, 2015.

151. Schulz R, Rose J, Heusch G. Involvement of activation of ATP-dependent potassium channels in ischemic preconditioning in swine. *Am J Physiol*. 1994;267(4 Pt 2):H1341-H1352. http://www.ncbi.nlm.nih.gov/pubmed/7943380. Accessed June 21, 2015.

152. Kristiansen SB, Løfgren B, Nielsen JM, et al. Comparison of two sulfonylureas with high and low myocardial K(ATP) channel affinity on myocardial infarct size and metabolism in a rat model of type 2 diabetes. *Diabetologia*. 2011;54(2):451-458. doi:10.1007/s00125-010-1970-y.

153. Tomai F, Crea F, Gaspardone A, et al. Ischemic preconditioning during coronary angioplasty is prevented by glibenclamide, a selective ATP-sensitive K+ channel blocker. *Circulation*. 1994;90(2):700-705. http://www.ncbi.nlm.nih.gov/pubmed/8044938. Accessed June 21, 2015.

154. Cleveland JC, Meldrum DR, Cain BS, Banerjee A, Harken AH. Oral sulfonylurea hypoglycemic agents prevent ischemic preconditioning in human myocardium. Two paradoxes revisited. *Circulation*. 1997;96(1):29-32. http://www.ncbi.nlm.nih.gov/pubmed/9236412. Accessed June 21, 2015.

155. Lang V, Light PE. The molecular mechanisms and pharmacotherapy of ATP-sensitive potassium channel gene mutations underlying neonatal diabetes. *Pharmgenomics Pers Med*. 2010;3:145-161. doi:10.2147/PGPM.S6969.

156. Tammaro P, Flanagan SE, Zadek B, et al. A Kir6.2 mutation causing severe functional effects in vitro produces neonatal diabetes without the expected neurological complications. *Diabetologia*. 2008;51(5):802-810. doi:10.1007/s00125-008-0923-1.

157. Reyes S, Park S, Johnson BD, Terzic A, Olson TM. KATP channel Kir6.2 E23K variant overrepresented in human heart failure is associated with impaired exercise stress response. *Hum Genet*. 2009;126(6):779-789. doi:10.1007/s00439-009-0731-9.

158. De Wet H, Rees MG, Shimomura K, et al. Increased ATPase activity produced by mutations at arginine-1380 in nucleotide-binding domain 2 of ABCC8 causes neonatal diabetes. *Proc Natl Acad Sci*. 2007;104(48):18988-18992. doi:10.1073/pnas.0707428104.

159. Riedel MJ, Steckley DC, Light PE. Current status of the E23K Kir6.2 polymorphism: implications for type-2 diabetes. *Hum Genet*. 2005;116(3):133-145. doi:10.1007/s00439-004-1216-5.

160. Gloyn AL, Weedon MN, Owen KR, et al. Large-scale association studies of variants in genes encoding the pancreatic beta-cell KATP channel subunits Kir6.2 (KCNJ11) and SUR1 (ABCC8) confirm that the KCNJ11 E23K variant is associated with type 2 diabetes. *Diabetes*. 2003;52(2):568-572. http://www.ncbi.nlm.nih.gov/pubmed/12540637. Accessed July 18, 2015.

161. Alsmadi O, Al-Rubeaan K, Wakil SM, et al. Genetic study of Saudi diabetes (GSSD): significant association of the KCNJ11 E23K polymorphism with type 2 diabetes. *Diabetes Metab Res Rev*. 2008;24(2):137-140. doi:10.1002/dmrr.777.

162. Palmer ND, Langefeld CD, Bryer-Ash M, Rotter JI, Taylor KD, Bowden DW. Association of the Kir6.2 E23K variant with reduced acute insulin response in African-Americans. *J Clin Endocrinol Metab*. 2008;93(12):4979-4983. doi:10.1210/jc.2008-0543.

163. Doi Y, Kubo M, Ninomiya T, et al. Impact of Kir6.2 E23K polymorphism on the development of type 2 diabetes in a general Japanese population: The Hisayama Study. *Diabetes*. 2007;56(11):2829-2833. doi:10.2337/db06-1709.

164. Zhou D, Zhang D, Liu Y, et al. The E23K variation in the KCNJ11 gene is associated with type 2 diabetes in Chinese and East Asian population. *J Hum Genet*. 2009;54(7):433-435. doi:10.1038/jhg.2009.54.

165. Florez JC, Burtt N, de Bakker PIW, et al. Haplotype Structure and Genotype-Phenotype Correlations of the Sulfonylurea Receptor and the Islet ATP-Sensitive Potassium Channel Gene Region. *Diabetes*. 2004;53(5):1360-1368. doi:10.2337/diabetes.53.5.1360.

166. Hamming KSC, Soliman D, Matemisz LC, et al. Coexpression of the type 2 diabetes susceptibility gene variants KCNJ11 E23K and ABCC8 S1369A alter the ATP and sulfonylurea sensitivities of the ATP-sensitive K(+) channel. *Diabetes*. 2009;58(10):2419-2424. doi:10.2337/db09-0143.

167. Fatehi M, Raja M, Carter C, Soliman D, Holt A, Light PE. The ATP-sensitive K(+) channel ABCC8 S1369A type 2 diabetes risk variant increases MgATPase activity. *Diabetes*. 2012;61(1):241-249. doi:10.2337/db11-0371.

168. Olson TM, Alekseev AE, Moreau C, et al. KATP channel mutation confers risk for vein of Marshall adrenergic atrial fibrillation. *Nat Clin Pract Cardiovasc Med*. 2007;4(2):110-116. doi:10.1038/ncpcardio0792.

169. Balana B, Dobrev D, Wettwer E, Christ T, Knaut M, Ravens U. Decreased ATP-sensitive K(+) current density during chronic human atrial fibrillation. *J Mol Cell Cardiol*. 2003;35(12):1399-1405. http://www.ncbi.nlm.nih.gov/pubmed/14654366. Accessed June 21, 2015.

170. Brundel BJJ., Van Gelder IC, Henning RH, et al. Alterations in potassium channel gene expression in atria of patients with persistent and paroxysmal atrial fibrillation: differential regulation of protein and mRNA levels for K+ channels. *J Am Coll Cardiol*. 2001;37(3):926-932. doi:10.1016/S0735-1097(00)01195-5.

171. Reyes S, Park S, Johnson BD, Terzic A, Olson TM. KATP channel Kir6.2 E23K variant overrepresented in human heart failure is associated with impaired exercise stress response. *Hum Genet*. 2009;126:779-789. doi:10.1007/s00439-009-0731-9.

172. Jovanović A, Jovanović S, Lorenz E, Terzic A. Recombinant cardiac ATP-sensitive K+ channel subunits confer resistance to chemical hypoxia-reoxygenation injury. *Circulation*. 1998;98(15):1548-1555. http://www.ncbi.nlm.nih.gov/pubmed/9769309. Accessed June 21, 2015.

173. Jovanovic A, Jovanovic S, Carrasco AJ, Terzic A. Acquired resistance of a mammalian cell line to hypoxia-reoxygenation through cotransfection of Kir6.2 and SUR1 clones. *Lab Invest*. 1998;78(9):1101-1107. http://www.ncbi.nlm.nih.gov/pubmed/9759654. Accessed June 21, 2015.

174. Jovanović N, Jovanović S, Jovanović A, Terzic A. Gene delivery of Kir6.2/SUR2A in conjunction with pinacidil handles intracellular Ca2+ homeostasis under metabolic stress. *FASEB J*. 1999;13(8):923-929. http://www.ncbi.nlm.nih.gov/pubmed/10224235. Accessed June 21, 2015.

175. Nichols CG, Ripoll C, Lederer WJ. ATP-sensitive potassium channel modulation of the guinea pig ventricular action potential and contraction. *Circ Res*. 1991;68:280-287. doi:10.1161/01.RES.68.1.280.

176. Suzuki M, Li RA, Miki T, et al. Functional roles of cardiac and vascular ATP-sensitive potassium channels clarified by Kir6.2-knockout mice. *Circ Res*. 2001;88(6):570-577. http://www.ncbi.nlm.nih.gov/pubmed/11282890. Accessed June 21, 2015.

177. Lederer WJ, Nichols CG, Smith GL. The mechanism of early contractile failure of isolated rat ventricular myocytes subjected to complete metabolic inhibition. *J Physiol*. 1989;413:329-349. http://www.pubmedcentral.nih.gov/articlerender.fcgi?artid=1189104&tool=pmcentrez&rendertype=abstract. Accessed June 21, 2015.

178. Venkatesh N, Lamp ST, Weiss JN. Sulfonylureas, ATP-sensitive K+ channels, and cellular K+ loss during hypoxia, ischemia, and metabolic inhibition in mammalian ventricle. *Circ Res*. 1991;69(3):623-637. http://www.ncbi.nlm.nih.gov/pubmed/1908355. Accessed June 21, 2015.

179. Flagg TP, Enkvetchakul D, Koster JC, Nichols CG. Muscle KATP channels: recent insights to energy sensing and myoprotection. *Physiol Rev*. 2010;90:799-829. doi:10.1152/physrev.00027.2009.

180. Suzuki M, Sasaki N, Miki T, et al. Role of sarcolemmal K(ATP) channels in cardioprotection against ischemia/reperfusion injury in mice. *J Clin Invest*. 2002;109(4):509-516. doi:10.1172/JCI14270.

181. Zingman L V, Hodgson DM, Bast PH, et al. Kir6.2 is required for adaptation to stress. *Proc Natl Acad Sci U S A*. 2002;99(20):13278-13283. doi:10.1073/pnas.212315199.

182. Gumina RJ, O'Cochlain DF, Kurtz CE, et al. KATP channel knockout worsens myocardial calcium stress load in vivo and impairs recovery in stunned heart. *Am J Physiol Heart Circ Physiol*. 2007;292:H1706-H1713. doi:10.1152/ajpheart.01305.2006.

183. Wolleben CD, Sanguinetti MC, Siegl PK. Influence of ATP-sensitive potassium channel modulators on ischemia-induced fibrillation in isolated rat hearts. *J Mol Cell Cardiol*. 1989;21(8):783-788.

184. Kantor PF, Coetzee WA, Carmeliet EE, Dennis SC, Opie LH. Reduction of ischemic K+ loss and arrhythmias in rat hearts. Effect of glibenclamide, a sulfonylurea. *Circ Res*. 1990;66(2):478-485. http://www.ncbi.nlm.nih.gov/pubmed/2105170. Accessed June 27, 2015.

185. Zhang HL, Li YS, Fu SX, Yang XP. Effects of glibenclamide and tolbutamide on ischemia- and ouabain-induced arrhythmias and membrane potentials of ventricular myocardium from rat and guinea pig. *Zhongguo Yao Li Xue Bao*. 1991;12(5):398-402. http://www.ncbi.nlm.nih.gov/pubmed/1819892. Accessed June 27, 2015.

186. Tosaki A, Szerdahelyi P, Engelman RM, Das DK. Potassium channel openers and blockers: do they possess proarrhythmic or antiarrhythmic activity in ischemic and reperfused rat hearts? *J Pharmacol Exp Ther*. 1993;267(3):1355-1362. http://www.ncbi.nlm.nih.gov/pubmed/8263798. Accessed June 27, 2015.

187. Dhein S, Pejman P, Krüsemann K. Effects of the I(K.ATP) blockers glibenclamide and HMR1883 on cardiac electrophysiology during ischemia and reperfusion. *Eur J Pharmacol*. 2000;398(2):273-284. http://www.ncbi.nlm.nih.gov/pubmed/10854840. Accessed June 27, 2015.

188. Leprán I, Baczkó I, Varró A, Papp JG. ATP-sensitive potassium channel modulators: both pinacidil and glibenclamide produce antiarrhythmic activity during acute myocardial infarction in conscious rats. *J Pharmacol Exp Ther*. 1996;277(3):1215-1220. http://www.ncbi.nlm.nih.gov/pubmed/8667181. Accessed June 27, 2015.

189. Baczkó I, Leprán I, Papp JG. KATP channel modulators increase survival rate during coronary occlusion-reperfusion in anaesthetized rats. *Eur J Pharmacol*. 1997;324(1):77-83. http://www.ncbi.nlm.nih.gov/pubmed/9137916. Accessed June 27, 2015.

190. Billman GE, Avendano CE, Halliwill JR, Burroughs JM. The effects of the ATP-dependent potassium channel antagonist, glyburide, on coronary blood flow and susceptibility to ventricular fibrillation in unanesthetized dogs. *J Cardiovasc*

Pharmacol. 1993;21(2):197-204. http://www.ncbi.nlm.nih.gov/pubmed/7679152. Accessed June 27, 2015.

191. Billman GE, Englert HC, Schölkens BA. HMR 1883, a novel cardioselective inhibitor of the ATP-sensitive potassium channel. Part II: effects on susceptibility to ventricular fibrillation induced by myocardial ischemia in conscious dogs. *J Pharmacol Exp Ther*. 1998;286(3):1465-1473. http://www.ncbi.nlm.nih.gov/pubmed/9732412. Accessed June 27, 2015.

192. El-Reyani NE, Bozdogan O, Baczkó I, Leprán I, Papp JG. Comparison of the efficacy of glibenclamide and glimepiride in reperfusion-induced arrhythmias in rats. *Eur J Pharmacol*. 1999;365(2-3):187-192. http://www.ncbi.nlm.nih.gov/pubmed/9988102. Accessed June 27, 2015.

193. Billman GE, Houle MS, Englert HC, Gögelein H. Effects of a novel cardioselective ATP-sensitive potassium channel antagonist, 1-[[5-[2-(5-chloro-o-anisamido)ethyl]-beta-methoxyethoxyphenyl]sulfonyl]-3-methylthiourea, sodium salt (HMR 1402), on susceptibility to ventricular fibrillation induced by myoc. *J Pharmacol Exp Ther*. 2004;309(1):182-192. doi:10.1124/jpet.103.061416.

194. Vajda S, Baczkó I, Leprán I. Selective cardiac plasma-membrane K(ATP) channel inhibition is defibrillatory and improves survival during acute myocardial ischemia and reperfusion. *Eur J Pharmacol*. 2007;577(1-3):115-123. doi:10.1016/j.ejphar.2007.08.016.

195. Gonca E, Bozdogan O. Both mitochondrial KATP channel opening and sarcolemmal KATP channel blockage confer protection against ischemia/reperfusion-induced arrhythmia in anesthetized male rats. *J Cardiovasc Pharmacol Ther*. 2010;15(4):403-411. doi:10.1177/1074248410372925.

196. Cacciapuoti F, Spiezia R, Bianchi U, Lama D, D'Avino M, Varricchio M. Effectiveness of glibenclamide on myocardial ischemic ventricular arrhythmias in non-insulin-dependent diabetes mellitus. *Am J Cardiol*. 1991;67(9):843-847. http://www.ncbi.nlm.nih.gov/pubmed/1707221. Accessed June 27, 2015.

197. Lomuscio A, Vergani D, Marano L, Castagnone M, Fiorentini C. Effects of glibenclamide on ventricular fibrillation in non-insulin-dependent diabetics with acute myocardial infarction. *Coron Artery Dis*. 1994;5(9):767-771. http://www.ncbi.nlm.nih.gov/pubmed/7858767. Accessed June 27, 2015.

198. Davis TM, Parsons RW, Broadhurst RJ, Hobbs MS, Jamrozik K. Arrhythmias and mortality after myocardial infarction in diabetic patients. Relationship to diabetes treatment. *Diabetes Care*. 1998;21(4):637-640. http://www.ncbi.nlm.nih.gov/pubmed/9571356. Accessed June 27, 2015.

199. Friedel HA, Brogden RN. Pinacidil. A review of its pharmacodynamic and pharmacokinetic properties, and therapeutic potential in the treatment of hypertension. *Drugs*. 1990;39(6):929-967. http://www.ncbi.nlm.nih.gov/pubmed/2196168. Accessed June 27, 2015.

200. Remme CA, Wilde AA. KATP channel openers, myocardial ischemia, and arrhythmias--should the electrophysiologist worry? *Cardiovasc Drugs Ther*. 2000;14(1):17-22. http://www.ncbi.nlm.nih.gov/pubmed/10755196. Accessed June 27, 2015.

201. Ueda H, Hayashi T, Tsumura K, Yoshimaru K, Nakayama Y, Yoshikawa J. Intravenous nicorandil can reduce QT dispersion and prevent bradyarrhythmia during percutaneous transluminal coronary angioplasty of the right coronary artery. *J Cardiovasc Pharmacol Ther*. 2004;9(3):179-184. http://www.ncbi.nlm.nih.gov/pubmed/15378138. Accessed June 27, 2015.

202. Ueda H, Nakayama Y, Tsumura K, Yoshimaru K, Hayashi T, Yoshikawa J. Intravenous nicorandil can reduce the occurrence of ventricular fibrillation and QT dispersion in patients with successful coronary angioplasty in acute myocardial infarction. *Can J Cardiol*. 2004;20(6):625-629. http://www.ncbi.nlm.nih.gov/pubmed/15152293. Accessed June 27, 2015.

203. Spinelli W, Sorota S, Siegal M, Hoffman BF. Antiarrhythmic actions of the ATP-regulated K+ current activated by pinacidil. *Circ Res*. 1991;68(4):1127-1137.

204. Carlsson L, Abrahamsson C, Drews L, Duker G. Antiarrhythmic effects of potassium channel openers in rhythm abnormalities related to delayed repolarization. *Circulation*. 1992;85(4):1491-1500. http://www.ncbi.nlm.nih.gov/pubmed/1555289. Accessed June 27, 2015.

205. Vegh A, Györgyi K, Papp JG, Sakai K, Parratt JR. Nicorandil suppressed ventricular arrhythmias in a canine model of myocardial ischaemia. *Eur J Pharmacol*. 1996;305(1-3):163-168. http://www.ncbi.nlm.nih.gov/pubmed/8813547. Accessed June 27, 2015.

206. Bao L, Hadjiolova K, Coetzee WA, Rindler MJ. Endosomal KATP channels as a reservoir after myocardial ischemia: a role for SUR2 subunits. *Am J Physiol Heart Circ Physiol*. 2011;300(1):H262-H270. doi:10.1152/ajpheart.00857.2010.

207. Du Q, Jovanović S, Clelland A, et al. Overexpression of SUR2A generates a cardiac phenotype resistant to ischemia. *FASEB J*. 2006;20(8):1131-1141. doi:10.1096/fj.05-5483com.

208. Li RA, Leppo M, Miki T, Seino S, Marbán E. Molecular basis of electrocardiographic ST-segment elevation. *Circ Res*. 2000;87(10):837-839. http://www.ncbi.nlm.nih.gov/pubmed/11073877. Accessed June 12, 2015.

209. Baczkó I, Giles WR, Light PE. Pharmacological activation of plasma-membrane KATP channels reduces reoxygenation-induced Ca(2+) overload in cardiac myocytes via modulation of the diastolic membrane potential. *Br J Pharmacol*. 2004;141(6):1059-1067. doi:10.1038/sj.bjp.0705702.

210. Baczko I, Jones L, McGuigan CF, et al. Plasma membrane KATP channel-mediated cardioprotection involves posthypoxic reductions in calcium overload and contractile dysfunction: mechanistic insights into cardioplegia. *FASEB J*. 2005;19(8):980-982. doi:10.1096/fj.04-3008fje.

211. McPherson CD, Pierce GN, Cole WC. Ischemic cardioprotection by ATP-sensitive K+ channels involves high-energy phosphate preservation. *Am J Physiol*. 1993;265(5 Pt 2):H1809-H1818.

212. Frasier CR, Moore RL, Brown DA. Exercise-induced cardiac preconditioning: how exercise protects your achy-breaky heart. *J Appl Physiol*. 2011;111(3):905-915. doi:10.1152/japplphysiol.00004.2011.

213. Zingman L V., Zhu Z, Sierra A, et al. Exercise-induced expression of cardiac ATP-sensitive potassium channels promotes action potential shortening and energy conservation. *J Mol Cell Cardiol*. 2011;51(1):72-81. doi:10.1016/j.yjmcc.2011.03.010.

214. Tong X, Porter LM, Liu G, et al. Consequences of cardiac myocyte-specific ablation of KATP channels in transgenic mice expressing dominant negative Kir6 subunits. *Am J Physiol Heart Circ Physiol*. 2006;291(2):H543-H551. doi:10.1152/ajpheart.00051.2006.

215. Murry CE, Jennings RB, Reimer KA. Preconditioning with ischemia: a delay of lethal cell injury in ischemic myocardium. *Circulation*. 1986;74(5):1124-1136.

216. Gumina RJ, Pucar D, Bast P, et al. Knockout of Kir6.2 negates ischemic preconditioning-induced protection of myocardial energetics. *Am J Physiol Circ Physiol*. 2003;284(6):H2106-H2113. doi:10.1152/ajpheart.00057.2003.

217. Zordoky BNM, Robertson IM, Dyck JRB. Preclinical and clinical evidence for the role of resveratrol in the treatment of cardiovascular diseases. *Biochim Biophys Acta*. 2015;1852(6):1155-1177. doi:10.1016/j.bbadis.2014.10.016.

218. Du RH, Dai T, Cao WJ, Lu M, Ding JH, Hu G. Kir6.2-containing ATP-sensitive K(+) channel is required for cardioprotection of resveratrol in mice. *Cardiovasc Diabetol*. 2014;13(1):35. doi:10.1186/1475-2840-13-35.

219. Hwang J-T, Kwon DY, Park OJ, Kim MS. Resveratrol protects ROS-induced cell death by activating AMPK in H9c2 cardiac muscle cells. *Genes Nutr*. 2008;2(4):323-326. doi:10.1007/s12263-007-0069-7.

220. Chan AY, Dolinsky VW, Soltys CL, et al. Resveratrol inhibits cardiac hypertrophy via AMP-activated protein kinase and Akt. *J Biol Chem*. 2008;283(35):24194-24201. doi:10.1074/jbc.M802869200.

221. Gu XS, Wang ZB, Ye Z, et al. Resveratrol, an activator of SIRT1, upregulates AMPK and improves cardiac function in heart failure. *Genet Mol Res*. 2014;13(1):323-335. doi:10.4238/2014.January.17.17.

222. Um J-H, Park S-J, Kang H, et al. AMP-activated protein kinase-deficient mice are resistant to the metabolic effects of resveratrol. *Diabetes*. 2010;59(3):554-563. doi:10.2337/db09-0482.

223. Stanley WC, Chandler MP. Energy metabolism in the normal and failing heart: potential for therapeutic interventions. *Heart Fail Rev*. 2002;7(2):115-130.

224. Neubauer S. The failing heart--an engine out of fuel. *N Engl J Med*. 2007;356(11):1140-1151. doi:10.1056/NEJMra063052.

225. Gibbs CL. Cardiac energetics. *Physiol Rev*. 1978;58(1):174-254. http://www.ncbi.nlm.nih.gov/pubmed/146205. Accessed June 24, 2015.

226. Stanley WC, Lopaschuk GD, Hall JL, McCormack JG. Regulation of myocardial carbohydrate metabolism under normal and ischaemic conditions. Potential for pharmacological interventions. *Cardiovasc Res*. 1997;33(2):243-257. http://www.ncbi.nlm.nih.gov/pubmed/9074687. Accessed June 24, 2015.

227. Wisneski JA, Stanley WC, Neese RA, Gertz EW. Effects of acute hyperglycemia on myocardial glycolytic activity in humans. *J Clin Invest*. 1990;85(5):1648-1656. doi:10.1172/JCI114616.

228. Gertz EW, Wisneski JA, Stanley WC, Neese RA. Myocardial substrate utilization during exercise in humans. Dual carbon-labeled carbohydrate isotope experiments. *J Clin Invest*. 1988;82(6):2017-2025. doi:10.1172/JCI113822.

229. Jain SS, Chabowski A, Snook LA, et al. Additive effects of insulin and muscle contraction on fatty acid transport and fatty acid transporters, FAT/CD36, FABPpm, FATP1, 4 and 6. *FEBS Lett*. 2009;583(13):2294-2300. doi:10.1016/j.febslet.2009.06.020.

230. Schwenk RW, Luiken JJFP, Bonen A, Glatz JFC. Regulation of sarcolemmal glucose and fatty acid transporters in cardiac disease. *Cardiovasc Res*. 2008;79(2):249-258. doi:10.1093/cvr/cvn116.

231. Schwenk RW, Holloway GP, Luiken JJFP, Bonen A, Glatz JFC. Fatty acid transport across the cell membrane: regulation by fatty acid transporters. *Prostaglandins Leukot Essent Fatty Acids*. 82(4-6):149-154. doi:10.1016/j.plefa.2010.02.029.

232. Angin Y, Steinbusch LKM, Simons PJ, et al. CD36 inhibition prevents lipid accumulation and contractile dysfunction in rat cardiomyocytes. *Biochem J*. 2012;448(1):43-53. doi:10.1042/BJ20120060.

233. Heather LC, Pates KM, Atherton HJ, et al. Differential translocation of the fatty acid transporter, FAT/CD36, and the glucose transporter, GLUT4, coordinates changes in cardiac substrate metabolism during ischemia and reperfusion. *Circ Heart Fail*. 2013;6(5):1058-1066. doi:10.1161/CIRCHEARTFAILURE.112.000342.

234. Glatz JFC, Luiken JJFP, Bonen A. Membrane fatty acid transporters as regulators of lipid metabolism: implications for metabolic disease. *Physiol Rev*. 2010;90(1):367-417. doi:10.1152/physrev.00003.2009.

235. Kienesberger PC, Pulinilkunnil T, Nagendran J, Dyck JRB. Myocardial triacylglycerol metabolism. *J Mol Cell Cardiol*. 2013;55:101-110. doi:10.1016/j.yjmcc.2012.06.018.

236. Quiroga AD, Lehner R. Liver triacylglycerol lipases. *Biochim Biophys Acta*. 2012;1821(5):762-769. doi:10.1016/j.bbalip.2011.09.007.

237. Lopaschuk GD, Ussher JR, Folmes CDL, Jaswal JS, Stanley WC. Myocardial fatty acid metabolism in health and disease. *Physiol Rev*. 2010;90(1):207-258. doi:10.1152/physrev.00015.2009.

238. Keung W, Ussher JR, Jaswal JS, et al. Inhibition of carnitine palmitoyltransferase-1 activity alleviates insulin resistance in diet-induced obese mice. *Diabetes*. 2013;62(3):711-720. doi:10.2337/db12-0259.

239. He L, Kim T, Long Q, et al. Carnitine palmitoyltransferase-1b deficiency aggravates pressure overload-induced cardiac hypertrophy caused by lipotoxicity. *Circulation*. 2012;126(14):1705-1716. doi:10.1161/CIRCULATIONAHA.111.075978.

240. Saddik M, Gamble J, Witters LA, Lopaschuk GD. Acetyl-CoA carboxylase regulation of fatty acid oxidation in the heart. *J Biol Chem*. 1993;268(34):25836-25845. http://www.ncbi.nlm.nih.gov/pubmed/7902355. Accessed June 24, 2015.

241. Dyck JRB, Cheng J-F, Stanley WC, et al. Malonyl coenzyme a decarboxylase inhibition protects the ischemic heart by inhibiting fatty acid oxidation and stimulating glucose oxidation. *Circ Res*. 2004;94(9):e78-e84. doi:10.1161/01.RES.0000129255.19569.8f.

242. Dyck JR, Barr AJ, Barr RL, Kolattukudy PE, Lopaschuk GD. Characterization of cardiac malonyl-CoA decarboxylase and its putative role in regulating fatty acid oxidation. *Am J Physiol*. 1998;275(6 Pt 2):H2122-H2129. http://www.ncbi.nlm.nih.gov/pubmed/9843812. Accessed June 24, 2015.

243. Dyck JRB, Lopaschuk GD. AMPK alterations in cardiac physiology and pathology: enemy or ally? *J Physiol*. 2006;574(Pt 1):95-112. doi:10.1113/jphysiol.2006.109389.

244. Hardie DG. Regulation of fatty acid and cholesterol metabolism by the AMP-activated protein kinase. *Biochim Biophys Acta*. 1992;1123(3):231-238. http://www.ncbi.nlm.nih.gov/pubmed/1536860. Accessed June 24, 2015.

245. Hardie DG, Hawley SA. AMP-activated protein kinase: the energy charge hypothesis revisited. *BioEssays*. 2001;23(12):1112-1119. doi:10.1002/bies.10009.

246. Neely JR, Morgan HE. Relationship between carbohydrate and lipid metabolism and the energy balance of heart muscle. *Annu Rev Physiol*. 1974;36:413-459. doi:10.1146/annurev.ph.36.030174.002213; 10.1146/annurev.ph.36.030174.002213.

247. Hardie DG. Regulation of fatty acid synthesis via phosphorylation of acetyl-CoA carboxylase. *Prog Lipid Res*. 1989;28(2):117-146. http://www.ncbi.nlm.nih.gov/pubmed/2575259. Accessed June 24, 2015.

248. Huss JM, Kelly DP. Nuclear receptor signaling and cardiac energetics. *Circ Res*. 2004;95(6):568-578. doi:10.1161/01.RES.0000141774.29937.e3.

249. Finck BN, Lehman JJ, Leone TC, et al. The cardiac phenotype induced by PPARα overexpression mimics that caused by diabetes mellitus. *J Clin Invest*. 2002;109(1):121-130. doi:10.1172/JCI14080.

250. Patti ME, Butte AJ, Crunkhorn S, et al. Coordinated reduction of genes of oxidative metabolism in humans with insulin resistance and diabetes: Potential role of PGC1 and NRF1. *Proc Natl Acad Sci U S A*. 2003;100(14):8466-8471. doi:10.1073/pnas.1032913100.

251. Campbell FM, Kozak R, Wagner A, et al. A role for peroxisome proliferator-activated receptor alpha (PPARalpha) in the control of cardiac malonyl-CoA levels: reduced fatty acid oxidation rates and increased glucose oxidation rates in the hearts of mice lacking PPARalpha are associated with hig. *J Biol Chem*. 2002;277(6):4098-4103. doi:10.1074/jbc.M106054200.

252. Liu C, Lin JD. PGC-1 coactivators in the control of energy metabolism. *Acta Biochim Biophys Sin (Shanghai)*. 2011;43(4):248-257. doi:10.1093/abbs/gmr007.

253. Scarpulla RC. Metabolic control of mitochondrial biogenesis through the PGC-1 family regulatory network. *Biochim Biophys Acta*. 2011;1813(7):1269-1278. doi:10.1016/j.bbamcr.2010.09.019.

254. Nagendran J, Waller TJ, Dyck JRB. AMPK signalling and the control of substrate use in the heart. *Mol Cell Endocrinol*. 2013;366(2):180-193. doi:10.1016/j.mce.2012.06.015.

255. Lehman JJ, Barger PM, Kovacs A, Saffitz JE, Medeiros DM, Kelly DP. Peroxisome proliferator-activated receptor gamma coactivator-1 promotes cardiac mitochondrial biogenesis. *J Clin Invest*. 2000;106(7):847-856. doi:10.1172/JCI10268.

256. Yang J, Holman GD. Long-term metformin treatment stimulates cardiomyocyte glucose transport through an AMP-activated protein kinase-dependent reduction in GLUT4 endocytosis. *Endocrinology*. 2006;147(6):2728-2736. doi:10.1210/en.2005-1433.

257. Chiu L-L, Tsai Y-L, Lee W-C, et al. Acute effect of exercise-hypoxia challenge on GLUT4 protein expression in rat cardiac muscle. *High Alt Med Biol*. 2005;6(3):256-262. doi:10.1089/ham.2005.6.256.

258. Ralphe JC, Nau PN, Mascio CE, Segar JL, Scholz TD. Regulation of myocardial glucose transporters GLUT1 and GLUT4 in chronically anemic fetal lambs. *Pediatr Res*. 2005;58(4):713-718. doi:10.1203/01.PDR.0000180546.42475.69.

259. Calvani M, Reda E, Arrigoni-Martelli E. Regulation by carnitine of myocardial fatty acid and carbohydrate metabolism under normal and pathological conditions. *Basic Res Cardiol*. 2000;95(2):75-83. http://www.ncbi.nlm.nih.gov/pubmed/10826498. Accessed June 24, 2015.

260. Stanley WC, Recchia FA, Lopaschuk GD. Myocardial substrate metabolism in the normal and failing heart. *Physiol Rev*. 2005;85(3):1093-1129. doi:10.1152/physrev.00006.2004.

261. GARLAND PB, RANDLE PJ, NEWSHOLME EA. CITRATE AS AN INTERMEDIARY IN THE INHIBITION OF PHOSPHOFRUCTOKINASE IN RAT HEART MUSCLE BY FATTY ACIDS, KETONE BODIES, PYRUVATE, DIABETES, AND STARVATION. *Nature*. 1963;200:169-170. http://www.ncbi.nlm.nih.gov/pubmed/14073034. Accessed June 24, 2015.

262. Minchenko O, Opentanova I, Caro J. Hypoxic regulation of the 6-phosphofructo-2-kinase/fructose-2,6-bisphosphatase gene family (PFKFB-1-4) expression in vivo. *FEBS Lett*. 2003;554(3):264-270. http://www.ncbi.nlm.nih.gov/pubmed/14623077. Accessed June 24, 2015.

263. Mor I, Cheung EC, Vousden KH. Control of glycolysis through regulation of PFK1: old friends and recent additions. *Cold Spring Harb Symp Quant Biol*. 2011;76:211-216. doi:10.1101/sqb.2011.76.010868.

264. Rovira J, Irimia JM, Guerrero M, Cadefau JA, Cussó R. Upregulation of heart PFK-2/FBPase-2 isozyme in skeletal muscle after persistent contraction. *Pflugers Arch*. 2012;463(4):603-613. doi:10.1007/s00424-011-1068-5.

265. Werner JC, Sicard RE. Lactate metabolism of isolated, perfused fetal, and newborn pig hearts. *Pediatr Res*. 1987;22(5):552-556. doi:10.1203/00006450-198711000-00016.

266. Hafstad AD, Khalid AM, How O-J, Larsen TS, Aasum E. Glucose and insulin improve cardiac efficiency and postischemic functional recovery in perfused hearts from type 2 diabetic (db/db) mice. *Am J Physiol Endocrinol Metab*. 2007;292(5):E1288-E1294. doi:10.1152/ajpendo.00504.2006.

267. Buchanan J, Mazumder PK, Hu P, et al. Reduced cardiac efficiency and altered substrate metabolism precedes the onset of hyperglycemia and contractile dysfunction in two mouse models of insulin resistance and obesity. *Endocrinology*. 2005;146(12):5341-5349. doi:10.1210/en.2005-0938.

268. Ussher JR, Wang W, Gandhi M, et al. Stimulation of glucose oxidation protects against acute myocardial infarction and reperfusion injury. *Cardiovasc Res*. 2012;94(2):359-369. doi:10.1093/cvr/cvs129.

269. Zhang L, Ussher JR, Oka T, Cadete VJJ, Wagg C, Lopaschuk GD. Cardiac diacylglycerol accumulation in high fat-fed mice is associated with impaired insulin-stimulated glucose oxidation. *Cardiovasc Res*. 2011;89(1):148-156. doi:10.1093/cvr/cvq266.

270. Herzig S, Raemy E, Montessuit S, et al. Identification and functional expression of the mitochondrial pyruvate carrier. *Science*. 2012;337(6090):93-96. doi:10.1126/science.1218530.

271. Bricker DK, Taylor EB, Schell JC, et al. A mitochondrial pyruvate carrier required for pyruvate uptake in yeast, Drosophila, and humans. *Science*. 2012;337(6090):96-100. doi:10.1126/science.1218099.

272. Divakaruni AS, Murphy AN. Cell biology. A mitochondrial mystery, solved. *Science*. 2012;337(6090):41-43. doi:10.1126/science.1225601.

273. Strumiło S. Short-term regulation of the mammalian pyruvate dehydrogenase complex. *Acta Biochim Pol*. 2005;52(4):759-764. http://www.ncbi.nlm.nih.gov/pubmed/16025163. Accessed June 24, 2015.

274. Sharma N, Okere IC, Brunengraber DZ, et al. Regulation of pyruvate dehydrogenase activity and citric acid cycle intermediates during high cardiac power generation. *J Physiol*. 2005;562(Pt 2):593-603. doi:10.1113/jphysiol.2004.075713.

275. Gey U, Czupalla C, Hoflack B, Rödel G, Krause-Buchholz U. Yeast pyruvate dehydrogenase complex is regulated by a concerted activity of two kinases and two phosphatases. *J Biol Chem*. 2008;283(15):9759-9767. doi:10.1074/jbc.M708779200.

276. RANDLE PJ, GARLAND PB, HALES CN, NEWSHOLME EA. The glucose fatty-acid cycle. Its role in insulin sensitivity and the metabolic disturbances of diabetes mellitus. *Lancet*. 1963;1(7285):785-789. http://www.ncbi.nlm.nih.gov/pubmed/13990765. Accessed January 18, 2015.

277. Depre C, Vanoverschelde JL, Taegtmeyer H. Glucose for the heart. *Circulation*. 1999;99(4):578-588. http://www.ncbi.nlm.nih.gov/pubmed/9927407. Accessed June 24, 2015.

278. Taegtmeyer H, Hems R, Krebs HA. Utilization of energy-providing substrates in the isolated working rat heart. *Biochem J*. 1980;186(3):701-711. http://www.pubmedcentral.nih.gov/articlerender.fcgi?artid=1161705&tool=pmcentrez&rendertype=abstract. Accessed June 24, 2015.

279. Das DK, Engelman RM, Rousou JA, Breyer RH. Aerobic vs anaerobic metabolism during ischemia in heart muscle. *Ann Chir Gynaecol*. 1987;76(1):68-76. http://www.ncbi.nlm.nih.gov/pubmed/3592561. Accessed June 27, 2015.

280. Bolli R, Marban E. Molecular and cellular mechanisms of myocardial stunning. *Physiol Rev*. 1999;79(2):609-634.

281. Renlund DG, Lakatta EG, Mellits ED, Gerstenblith G. Calcium-dependent enhancement of myocardial diastolic tone and energy utilization dissociates systolic work and oxygen consumption during low sodium perfusion. *Circ Res*. 1985;57(6):876-888. http://www.ncbi.nlm.nih.gov/pubmed/4064261. Accessed June 27, 2015.

282. Piwnica-Worms D, Jacob R, Horres CR, Lieberman M. Na/H exchange in cultured chick heart cells. pHi regulation. *J Gen Physiol*. 1985;85(1):43-64. http://www.pubmedcentral.nih.gov/articlerender.fcgi?artid=2215810&tool=pmcentrez&rendertype=abstract. Accessed June 27, 2015.

283. Lazdunski M, Frelin C, Vigne P. The sodium/hydrogen exchange system in cardiac cells: its biochemical and pharmacological properties and its role in regulating internal concentrations of sodium and internal pH. *J Mol Cell Cardiol*. 1985;17(11):1029-1042. http://www.ncbi.nlm.nih.gov/pubmed/3001319. Accessed June 27, 2015.

284. Bers DM, Barry WH, Despa S. Intracellular Na+ regulation in cardiac myocytes. *Cardiovasc Res*. 2003;57(4):897-912. http://www.ncbi.nlm.nih.gov/pubmed/12650868. Accessed June 27, 2015.

285. Van Echteld CJ, Kirkels JH, Eijgelshoven MH, van der Meer P, Ruigrok TJ. Intracellular sodium during ischemia and calcium-free perfusion: a 23Na NMR study. *J Mol Cell Cardiol*. 1991;23(3):297-307. http://www.ncbi.nlm.nih.gov/pubmed/1880814. Accessed June 27, 2015.

286. Ferrari R, Ceconi C, Curello S, et al. Oxygen-mediated myocardial damage during ischaemia and reperfusion: role of the cellular defences against oxygen toxicity. *J Mol Cell Cardiol*. 1985;17(10):937-945. http://www.ncbi.nlm.nih.gov/pubmed/4068039. Accessed June 27, 2015.

287. Steenbergen C, Murphy E, Levy L, London RE. Elevation in cytosolic free calcium concentration early in myocardial ischemia in perfused rat heart. *Circ Res*. 1987;60(5):700-707. http://www.ncbi.nlm.nih.gov/pubmed/3109761. Accessed June 27, 2015.

288. Stone D, Darley-Usmar V, Smith DR, O'Leary V. Hypoxia-reoxygenation induced increase in cellular Ca2+ in myocytes and perfused hearts: the role of mitochondria. *J Mol Cell Cardiol*. 1989;21(10):963-973. http://www.ncbi.nlm.nih.gov/pubmed/2479760. Accessed June 27, 2015.

289. Marban E, Koretsune Y, Corretti M, Chacko VP, Kusuoka H. Calcium and its role in myocardial cell injury during ischemia and reperfusion. *Circulation*. 1989;80(6 Suppl):IV17-IV22. http://www.ncbi.nlm.nih.gov/pubmed/2513146. Accessed June 27, 2015.

290. Verhoeven AJ, Woods A, Brennan CH, et al. The AMP-activated protein kinase gene is highly expressed in rat skeletal muscle. Alternative splicing and tissue distribution of the mRNA. *Eur J Biochem*. 1995;228(2):236-243. http://www.ncbi.nlm.nih.gov/pubmed/7705334. Accessed June 21, 2015.

291. Beg ZH, Allmann DW, Gibson DM. Modulation of 3-hydroxy-3-methylglutaryl coenzyme A reductase activity with cAMP and wth protein fractions of rat liver cytosol. *Biochem Biophys Res Commun*. 1973;54(4):1362-1369. http://www.ncbi.nlm.nih.gov/pubmed/4356818. Accessed June 21, 2015.

292. Carlson CA, Kim KH. Regulation of hepatic acetyl coenzyme A carboxylase by phosphorylation and dephosphorylation. *J Biol Chem*. 1973;248(1):378-380. http://www.ncbi.nlm.nih.gov/pubmed/4692841. Accessed June 21, 2015.

293. Hardie DG, Hawley SA, Scott JW. AMP-activated protein kinase--development of the energy sensor concept. *J Physiol*. 2006;574(Pt 1):7-15. doi:10.1113/jphysiol.2006.108944.

294. Hawley SA, Davison M, Woods A, et al. Characterization of the AMP-activated protein kinase kinase from rat liver and identification of threonine 172 as the major site at which it phosphorylates AMP-activated protein kinase. *J Biol Chem*. 1996;271(44):27879-27887. http://www.ncbi.nlm.nih.gov/pubmed/8910387. Accessed May 12, 2015.

295. Hardie DG, Salt IP, Hawley SA, Davies SP. AMP-activated protein kinase: an ultrasensitive system for monitoring cellular energy charge. *Biochem J*. 1999;338 (Pt

3:717-722. http://www.pubmedcentral.nih.gov/articlerender.fcgi?artid=1220108&tool=pmcentrez&rendertype=abstract. Accessed June 21, 2015.

296. Frederich M, Balschi JA. The relationship between AMP-activated protein kinase activity and AMP concentration in the isolated perfused rat heart. *J Biol Chem*. 2002;277(3):1928-1932. doi:10.1074/jbc.M107128200.

297. Xiao B, Sanders MJ, Underwood E, et al. Structure of mammalian AMPK and its regulation by ADP. *Nature*. 2011;472(7342):230-233. doi:10.1038/nature09932.

298. Oakhill JS, Steel R, Chen Z-P, et al. AMPK Is a Direct Adenylate Charge-Regulated Protein Kinase. *Science (80-)*. 2011;332(6036):1433-1435. doi:10.1126/science.1200094.

299. Sakamoto K, McCarthy A, Smith D, et al. Deficiency of LKB1 in skeletal muscle prevents AMPK activation and glucose uptake during contraction. *EMBO J*. 2005;24(10):1810-1820. doi:10.1038/sj.emboj.7600667.

300. Hurley RL, Anderson KA, Franzone JM, Kemp BE, Means AR, Witters LA. The Ca2+/calmodulin-dependent protein kinase kinases are AMP-activated protein kinase kinases. *J Biol Chem*. 2005;280(32):29060-29066. doi:10.1074/jbc.M503824200.

301. Shaw RJ, Kosmatka M, Bardeesy N, et al. The tumor suppressor LKB1 kinase directly activates AMP-activated kinase and regulates apoptosis in response to energy stress. *Proc Natl Acad Sci U S A*. 2004;101(10):3329-3335. doi:10.1073/pnas.0308061100.

302. Woods A, Johnstone SR, Dickerson K, et al. LKB1 is the upstream kinase in the AMP-activated protein kinase cascade. *Curr Biol*. 2003;13(22):2004-2008. http://www.ncbi.nlm.nih.gov/pubmed/14614828. Accessed June 21, 2015.

303. Hawley SA, Boudeau J, Reid JL, et al. Complexes between the LKB1 tumor suppressor, STRAD alpha/beta and MO25 alpha/beta are upstream kinases in the AMP-activated protein kinase cascade. *J Biol*. 2003;2(4):28. doi:10.1186/1475-4924-2-28.

304. Woods A, Dickerson K, Heath R, et al. Ca2+/calmodulin-dependent protein kinase kinase-beta acts upstream of AMP-activated protein kinase in mammalian cells. *Cell Metab*. 2005;2(1):21-33. doi:10.1016/j.cmet.2005.06.005.

305. Momcilovic M, Hong S-P, Carlson M. Mammalian TAK1 activates Snf1 protein kinase in yeast and phosphorylates AMP-activated protein kinase in vitro. *J Biol Chem*. 2006;281(35):25336-25343. doi:10.1074/jbc.M604399200.

306. Hawley SA, Pan DA, Mustard KJ, et al. Calmodulin-dependent protein kinase kinase-beta is an alternative upstream kinase for AMP-activated protein kinase. *Cell Metab*. 2005;2(1):9-19. doi:10.1016/j.cmet.2005.05.009.

307. Xie M, Zhang D, Dyck JRB, et al. A pivotal role for endogenous TGF-beta-activated kinase-1 in the LKB1/AMP-activated protein kinase energy-sensor pathway. *Proc Natl Acad Sci U S A*. 2006;103(46):17378-17383. doi:10.1073/pnas.0604708103.

308. Davies SP, Helps NR, Cohen PT, Hardie DG. 5'-AMP inhibits dephosphorylation, as well as promoting phosphorylation, of the AMP-activated protein kinase. Studies using bacterially expressed human protein phosphatase-2C alpha and native bovine protein phosphatase-2AC. *FEBS Lett*. 1995;377(3):421-425. doi:10.1016/0014-5793(95)01368-7.

309. Luiken JJFP, Coort SLM, Willems J, et al. Contraction-induced fatty acid translocase/CD36 translocation in rat cardiac myocytes is mediated through AMP-activated protein kinase signaling. *Diabetes*. 2003;52(7):1627-1634. http://www.ncbi.nlm.nih.gov/pubmed/12829625. Accessed June 22, 2015.

310. Dyck JR, Kudo N, Barr AJ, Davies SP, Hardie DG, Lopaschuk GD. Phosphorylation control of cardiac acetyl-CoA carboxylase by cAMP-dependent protein kinase and 5'-AMP activated protein kinase. *Eur J Biochem*. 1999;262(1):184-190. http://www.ncbi.nlm.nih.gov/pubmed/10231380. Accessed June 22, 2015.

311. Davies SP, Sim AT, Hardie DG. Location and function of three sites phosphorylated on rat acetyl-CoA carboxylase by the AMP-activated protein kinase. *Eur J Biochem*. 1990;187(1):183-190. http://www.ncbi.nlm.nih.gov/pubmed/1967580. Accessed June 22, 2015.

312. Ha J, Daniel S, Broyles SS, Kim KH. Critical phosphorylation sites for acetyl-CoA carboxylase activity. *J Biol Chem*. 1994;269(35):22162-22168. http://www.ncbi.nlm.nih.gov/pubmed/7915280. Accessed June 22, 2015.

313. Jaswal JS, Gandhi M, Finegan BA, Dyck JRB, Clanachan AS. Effects of adenosine on myocardial glucose and palmitate metabolism after transient ischemia: role of 5'-AMP-activated protein kinase. *Am J Physiol Heart Circ Physiol*. 2006;291(4):H1883-H1892. doi:10.1152/ajpheart.01147.2005.

314. Zordoky BNM, Nagendran J, Pulinilkunnil T, et al. AMPK-dependent inhibitory phosphorylation of ACC is not essential for maintaining myocardial fatty acid oxidation. *Circ Res*. 2014;115(5):518-524. doi:10.1161/CIRCRESAHA.115.304538.

315. Saha AK, Schwarsin AJ, Roduit R, et al. Activation of malonyl-CoA decarboxylase in rat skeletal muscle by contraction and the AMP-activated protein kinase activator 5-aminoimidazole-4-carboxamide-1-beta -D-ribofuranoside. *J Biol Chem*. 2000;275(32):24279-24283. doi:10.1074/jbc.C000291200.

316. Sambandam N, Steinmetz M, Chu A, Altarejos JY, Dyck JRB, Lopaschuk GD. Malonyl-CoA decarboxylase (MCD) is differentially regulated in subcellular compartments by 5'AMP-activated protein kinase (AMPK). Studies using H9c2 cells overexpressing MCD and AMPK by adenoviral gene transfer technique. *Eur J Biochem*. 2004;271(13):2831-2840. doi:10.1111/j.1432-1033.2004.04218.x.

317. Mu J, Brozinick Jr JT, Valladares O, Bucan M, Birnbaum MJ. A role for AMP-activated protein kinase in contraction- and hypoxia-regulated glucose transport in skeletal muscle. *Mol Cell*. 2001;7(5):1085-1094.

318. Russell RR, Bergeron R, Shulman GI, Young LH. Translocation of myocardial GLUT-4 and increased glucose uptake through activation of AMPK by AICAR. *Am J Physiol*. 1999;277(2 Pt 2):H643-H649. http://www.ncbi.nlm.nih.gov/pubmed/10444490. Accessed June 22, 2015.

319. Yang J, Holman GD. Insulin and contraction stimulate exocytosis, but increased AMP-activated protein kinase activity resulting from oxidative metabolism stress slows endocytosis of GLUT4 in cardiomyocytes. *J Biol Chem*. 2005;280(6):4070-4078. doi:10.1074/jbc.M410213200.

320. Omar MA, Fraser H, Clanachan AS. Ischemia-induced activation of AMPK does not increase glucose uptake in glycogen-replete isolated working rat hearts. *Am J Physiol Heart Circ Physiol*. 2008;294(3):H1266-H1273. doi:10.1152/ajpheart.01087.2007.

321. Marsin AS, Bertrand L, Rider MH, et al. Phosphorylation and activation of heart PFK-2 by AMPK has a role in the stimulation of glycolysis during ischaemia. *Curr Biol*. 2000;10(20):1247-1255. http://www.ncbi.nlm.nih.gov/pubmed/11069105. Accessed June 22, 2015.

322. Kudo N, Barr AJ, Barr RL, Desai S, Lopaschuk GD. High rates of fatty acid oxidation during reperfusion of ischemic hearts are associated with a decrease in malonyl-CoA levels due to an increase in 5'-AMP-activated protein kinase inhibition of acetyl-CoA carboxylase. *J Biol Chem*. 1995;270(29):17513-17520. http://www.ncbi.nlm.nih.gov/pubmed/7615556. Accessed June 22, 2015.

323. Russell RR, Li J, Coven DL, et al. AMP-activated protein kinase mediates ischemic glucose uptake and prevents postischemic cardiac dysfunction, apoptosis, and injury. *J Clin Invest*. 2004;114(4):495-503. doi:10.1172/JCI19297.

324. Kudo N, Gillespie JG, Kung L, et al. Characterization of 5'AMP-activated protein kinase activity in the heart and its role in inhibiting acetyl-CoA carboxylase during reperfusion following ischemia. *Biochim Biophys Acta*. 1996;1301(1-2):67-75. http://www.ncbi.nlm.nih.gov/pubmed/8652652. Accessed June 22, 2015.

325. Kim AS, Miller EJ, Wright TM, et al. A small molecule AMPK activator protects the heart against ischemia-reperfusion injury. *J Mol Cell Cardiol*. 2011;51(1):24-32. doi:10.1016/j.yjmcc.2011.03.003.

326. Paiva MA, Rutter-Locher Z, Gonçalves LM, et al. Enhancing AMPK activation during ischemia protects the diabetic heart against reperfusion injury. *Am J Physiol Heart Circ Physiol*. 2011;300(6):H2123-H2134. doi:10.1152/ajpheart.00707.2010.

327. Xing Y, Musi N, Fujii N, et al. Glucose metabolism and energy homeostasis in mouse hearts overexpressing dominant negative alpha2 subunit of AMP-activated protein kinase. *J Biol Chem*. 2003;278(31):28372-28377. doi:10.1074/jbc.M303521200.

328. Shibata R, Sato K, Pimentel DR, et al. Adiponectin protects against myocardial ischemia-reperfusion injury through AMPK- and COX-2-dependent mechanisms. *Nat Med*. 2005;11(10):1096-1103. doi:10.1038/nm1295.

329. Tsuchida A, Yang XM, Burckhartt B, Mullane KM, Cohen M V, Downey JM. Acadesine extends the window of protection afforded by ischaemic preconditioning. *Cardiovasc Res*. 1994;28(3):379-383. http://www.ncbi.nlm.nih.gov/pubmed/8174159. Accessed June 22, 2015.

330. Calvert JW, Gundewar S, Jha S, et al. Acute metformin therapy confers cardioprotection against myocardial infarction via AMPK-eNOS-mediated signaling. *Diabetes*. 2008;57(3):696-705. doi:10.2337/db07-1098.

331. Shinmura K, Tamaki K, Saito K, Nakano Y, Tobe T, Bolli R. Cardioprotective effects of short-term caloric restriction are mediated by adiponectin via activation of AMP-activated protein kinase. *Circulation*. 2007;116(24):2809-2817. doi:10.1161/CIRCULATIONAHA.107.725697.

332. Hao J, Kim HS, Choi W, Ha TS, Ahn HY, Kim CH. Mechanical Stretch-Induced Protection against Myocardial Ischemia-Reperfusion Injury Involves AMP-Activated Protein Kinase. *Korean J Physiol Pharmacol*. 2010;14(1):1-9. doi:10.4196/kjpp.2010.14.1.1.

333. Folmes CDL, Wagg CS, Shen M, Clanachan AS, Tian R, Lopaschuk GD. Suppression of 5'-AMP-activated protein kinase activity does not impair recovery of contractile function during reperfusion of ischemic hearts. *Am J Physiol Heart Circ Physiol*. 2009;297(1):H313-H321. doi:10.1152/ajpheart.01298.2008.

334. Yoshida H, Bao L, Kefaloyianni E, et al. AMP-activated protein kinase connects cellular energy metabolism to KATP channel function. *J Mol Cell Cardiol*. 2012;52(2):410-418. doi:10.1016/j.yjmcc.2011.08.013.

335. Lim A, Park SH, Sohn JW, et al. Glucose deprivation regulates KATP channel trafficking via AMP-activated protein kinase in pancreatic beta-cells. *Diabetes*. 2009;58(12):2813-2819. doi:10.2337/db09-0600.

336. Chen P-C, Kryukova YN, Shyng S-L. Leptin regulates KATP channel trafficking in pancreatic β-cells by a signaling mechanism involving AMP-activated protein kinase (AMPK) and cAMP-dependent protein kinase (PKA). *J Biol Chem*. 2013;288(47):34098-34109. doi:10.1074/jbc.M113.516880.

337. Park S-H, Ho W-K, Jeon J-H. AMPK regulates K(ATP) channel trafficking via PTEN inhibition in leptin-treated pancreatic β-cells. *Biochem Biophys Res Commun*. 2013;440(4):539-544. doi:10.1016/j.bbrc.2013.09.099.

338. Caspi L, Wang PYT, Lam TKT. A balance of lipid-sensing mechanisms in the brain and liver. *Cell Metab*. 2007;6(2):99-104. doi:10.1016/j.cmet.2007.07.005.

339. Coll AP, Farooqi IS, O'Rahilly S. The hormonal control of food intake. *Cell*. 2007;129(2):251-262. doi:10.1016/j.cell.2007.04.001.

340. Gelling RW, Morton GJ, Morrison CD, et al. Insulin action in the brain contributes to glucose lowering during insulin treatment of diabetes. *Cell Metab*. 2006;3(1):67-73. doi:10.1016/j.cmet.2005.11.013.

341. Obici S, Zhang BB, Karkanias G, Rossetti L. Hypothalamic insulin signaling is required for inhibition of glucose production. *Nat Med*. 2002;8(12):1376-1382. doi:10.1038/nm1202-798.

342. Schwartz MW, Porte D. Diabetes, obesity, and the brain. *Science*. 2005;307(5708):375-379. doi:10.1126/science.1104344.

343. Wang PYT, Caspi L, Lam CKL, et al. Upper intestinal lipids trigger a gut-brain-liver axis to regulate glucose production. *Nature*. 2008;452(7190):1012-1016. doi:10.1038/nature06852.

344. Pocai A, Lam TKT, Gutierrez-Juarez R, et al. Hypothalamic K(ATP) channels control hepatic glucose production. *Nature*. 2005;434(7036):1026-1031. doi:10.1038/nature03439.

345. Lam TKT, Gutierrez-Juarez R, Pocai A, Rossetti L. Regulation of blood glucose by hypothalamic pyruvate metabolism. *Science*. 2005;309(5736):943-947. doi:10.1126/science.1112085.

346. Ross R, Wang PYT, Chari M, et al. Hypothalamic protein kinase C regulates glucose production. *Diabetes*. 2008;57(8):2061-2065. doi:10.2337/db08-0206.

347. Abraham MA, Yue JTY, LaPierre MP, et al. Hypothalamic glucagon signals through the KATP channels to regulate glucose production. *Mol Metab*. 2014;3(2):202-208. doi:10.1016/j.molmet.2013.11.007.

348. Dubinsky WP, Mayorga-Wark O, Schultz SG. Colocalization of glycolytic enzyme activity and KATP channels in basolateral membrane of Necturus enterocytes. *Am J Physiol*. 1998;275(6 Pt 1):C1653-C1659. http://www.ncbi.nlm.nih.gov/pubmed/9843727. Accessed June 22, 2015.

349. Dhar-Chowdhury P, Harrell MD, Han SY, et al. The glycolytic enzymes, glyceraldehyde-3-phosphate dehydrogenase, triose-phosphate isomerase, and pyruvate kinase are components of the K(ATP) channel macromolecular complex and regulate its function. *J Biol Chem*. 2005;280(46):38464-38470. doi:10.1074/jbc.M508744200.

350. Jovanović S, Du Q, Crawford RM, Budas GR, Stagljar I, Jovanović A. Glyceraldehyde 3-phosphate dehydrogenase serves as an accessory protein of the cardiac sarcolemmal K(ATP) channel. *EMBO Rep*. 2005;6(9):848-852. doi:10.1038/sj.embor.7400489.

351. Hong M, Kefaloyianni E, Bao L, et al. Cardiac ATP-sensitive K+ channel associates with the glycolytic enzyme complex. *FASEB J*. 2011;25(7):2456-2467. doi:10.1096/fj.10-176669; 10.1096/fj.10-176669.

352. Minokoshi Y, Alquier T, Furukawa N, et al. AMP-kinase regulates food intake by responding to hormonal and nutrient signals in the hypothalamus. *Nature*. 2004;428(6982):569-574. doi:10.1038/nature02440.

353. Alekseev AE, Reyes S, Yamada S, et al. Sarcolemmal ATP-sensitive K(+) channels control energy expenditure determining body weight. *Cell Metab*. 2010;11(1):58-69. doi:10.1016/j.cmet.2009.11.009.

354. Fahrenbach JP, Stoller D, Kim G, et al. Abcc9 is required for the transition to oxidative metabolism in the newborn heart. *FASEB J*. 2014;28:2804-2815. doi:10.1096/fj.13-244459.

355. Kovacic S, Soltys C-LM, Barr AJ, Shiojima I, Walsh K, Dyck JRB. Akt activity negatively regulates phosphorylation of AMP-activated protein kinase in the heart. *J Biol Chem*. 2003;278(41):39422-39427. doi:10.1074/jbc.M305371200.

356. Shimoni Y, Severson D, Giles W. Thyroid status and diabetes modulate regional differences in potassium currents in rat ventricle. *J Physiol*. 1995;488 (Pt 3:673-688. http://www.ncbi.nlm.nih.gov/pubmed/8576857. Accessed July 3, 2015.

357. Latour MG, Alquier T, Oseid E, et al. GPR40 is necessary but not sufficient for fatty acid stimulation of insulin secretion in vivo. *Diabetes*. 2007;56(4):1087-1094. doi:10.2337/db06-1532.

358. Kin T, Shapiro J. Surgical aspects of human islet isolation. *Islets*. 2014;2(5):265-273. doi:10.4161/isl.2.5.13019.

359. Kienesberger PC, Pulinilkunnil T, Sung MMY, et al. Myocardial ATGL overexpression decreases the reliance on fatty acid oxidation and protects against pressure overload-induced cardiac dysfunction. *Mol Cell Biol*. 2012;32(4):740-750. doi:10.1128/MCB.06470-11.

360. Riedel MJ, Light PE. Saturated and cis/trans unsaturated acyl CoA esters differentially regulate wild-type and polymorphic beta-cell ATP-sensitive K+ channels. *Diabetes*. 2005;54(7):2070-2079. http://www.ncbi.nlm.nih.gov/pubmed/15983208. Accessed July 20, 2015.

361. Riedel MJ, Boora P, Steckley D, de Vries G, Light PE. Kir6.2 polymorphisms sensitize beta-cell ATP-sensitive potassium channels to activation by acyl CoAs: a possible cellular mechanism for increased susceptibility to type 2 diabetes? *Diabetes*. 2003;52(10):2630-2635. http://www.ncbi.nlm.nih.gov/pubmed/14514649. Accessed July 20, 2015.

362. Fatehi M, Carter CRJ, Youssef N, Hunter BE, Holt A, Light PE. Molecular determinants of ATP-sensitive potassium channel MgATPase activity: diabetes risk variants and diazoxide sensitivity. *Biosci Rep*. 2015. doi:10.1042/BSR20150143.

363. Miki T, Nagashima K, Tashiro F, et al. Defective insulin secretion and enhanced insulin action in KATP channel-deficient mice. *Proc Natl Acad Sci U S A*. 1998;95(18):10402-10406.

364. Bell RM, Mocanu MM, Yellon DM. Retrograde heart perfusion: the Langendorff technique of isolated heart perfusion. *J Mol Cell Cardiol*. 2011;50(6):940-950. doi:10.1016/j.yjmcc.2011.02.018.

365. Lopaschuk GD, Hansen CA, Neely JR. Fatty acid metabolism in hearts containing elevated levels of CoA. *Am J Physiol*. 1986;250(3 Pt 2):H351-H359. http://www.ncbi.nlm.nih.gov/pubmed/3953832. Accessed July 20, 2015.

366. Barr RL, Lopaschuk GD. Direct measurement of energy metabolism in the isolated working rat heart. *J Pharmacol Toxicol Methods*. 1997;38(1):11-17. http://www.ncbi.nlm.nih.gov/pubmed/9339411. Accessed July 22, 2015.

367. Saddik M, Lopaschuk GD. Myocardial triglyceride turnover and contribution to energy substrate utilization in isolated working rat hearts. *J Biol Chem*. 1991;266(13):8162-8170. http://www.ncbi.nlm.nih.gov/pubmed/1902472. Accessed July 20, 2015.

368. Robitaille R, Tremblay JP. Non-uniform responses to Ca2+ along the frog neuromuscular junction: effects on the probability of spontaneous and evoked

transmitter release. *Neuroscience*. 1991;40(2):571-585. http://www.ncbi.nlm.nih.gov/pubmed/1674115. Accessed July 20, 2015.

369. Kantor PF, Lopaschuk GD OL. Heart physiology and pathophysiology. In: Sperelakis N, Kurachi Y, Terzic A CM, ed. *Heart Physiology and Pathophysiology.* Fourth edi. San Diego Calif: Academic Press; 2001:543-569.

370. Holloway GP, Gurd BJ, Snook LA, Lally J, Bonen A. Compensatory increases in nuclear PGC1alpha protein are primarily associated with subsarcolemmal mitochondrial adaptations in ZDF rats. *Diabetes*. 2010;59(4):819-828. doi:10.2337/db09-1519.

371. Yang Z-W, Chen J-K, Ni M, et al. Role of Kir6.2 subunits of ATP-sensitive potassium channels in endotoxemia-induced cardiac dysfunction. *Cardiovasc Diabetol*. 2013;12:75. doi:10.1186/1475-2840-12-75.

372. Nichols CG, Lederer WJ. Adenosine triphosphate-sensitive potassium channels in the cardiovascular system. *Am J Physiol*. 1991;261:H1675-H1686.

373. Marinovic J, Ljubkovic M, Stadnicka A, Bosnjak ZJ, Bienengraeber M. Role of sarcolemmal ATP-sensitive potassium channel in oxidative stress-induced apoptosis: mitochondrial connection. *Am J Physiol Circ Physiol*. 2008;294(3):H1317-H1325. doi:10.1152/ajpheart.00840.2007; 10.1152/ajpheart.00840.2007.

374. Liu H, Zhang HY, Zhu X, Shao Z, Yao Z. Preconditioning blocks cardiocyte apoptosis: role of K ATP channels and PKC-ε. *Am J Physiol - Hear Circ Physiol*. 2002;282(4):H1380-H1386. doi:10.1152/ajpheart.00348.2001.

375. Quindry JC, Miller L, McGinnis G, et al. Ischemia reperfusion injury, KATP channels, and exercise-induced cardioprotection against apoptosis. *J Appl Physiol*. 2012;113(3):498-506. doi:10.1152/japplphysiol.00957.2011.

376. Gross GJ, Auchampach JA. Blockade of ATP-sensitive potassium channels prevents myocardial preconditioning in dogs. *Circ Res*. 1992;70(2):223-233.

377. Suzuki M, Saito T, Sato T, et al. Cardioprotective effect of diazoxide is mediated by activation of sarcolemmal but not mitochondrial ATP-sensitive potassium channels in mice. *Circulation*. 2003;107(5):682-685. http://www.ncbi.nlm.nih.gov/pubmed/12578868. Accessed June 20, 2015.

378. Nichols CG. KATP channels as molecular sensors of cellular metabolism. *Nature*. 2006;440(7083):470-476. doi:10.1038/nature04711.

379. Bienengraeber M, Alekseev AE, Abraham MR, et al. ATPase activity of the sulfonylurea receptor: a catalytic function for the KATP channel complex. *FASEB J.* 2000;14(13):1943-1952. doi:10.1096/fj.00-0027com.

380. Opie LH. Metabolism of the heart in health and disease. I. *Am Heart J*. 1968;76(5):685-698.

381. Opie LH. Metabolism of the heart in health and disease. II. *Am Heart J*. 1969;77(1):100-122 contd.

382. Jaswal JS, Keung W, Wang W, Ussher JR, Lopaschuk GD. Targeting fatty acid and carbohydrate oxidation--a novel therapeutic intervention in the ischemic and failing heart. *Biochim Biophys Acta*. 2011;1813(7):1333-1350. doi:10.1016/j.bbamcr.2011.01.015; 10.1016/j.bbamcr.2011.01.015.

383. Zlatkovic J, Arrell DK, Kane GC, Miki T, Seino S, Terzic A. Proteomic profiling of KATP channel-deficient hypertensive heart maps risk for maladaptive cardiomyopathic outcome. *Proteomics*. 2009;9(5):1314-1325. doi:10.1002/pmic.200800718.

384. Hardie DG, Ross FA, Hawley SA. AMPK: a nutrient and energy sensor that maintains energy homeostasis. *Nat Rev cell Biol*. 2012;13(4):251-262. doi:10.1038/nrm3311; 10.1038/nrm3311.

385. Ji L, Zhang X, Liu W, et al. AMPK-regulated and Akt-dependent enhancement of glucose uptake is essential in ischemic preconditioning-alleviated reperfusion injury. *PLoS One*. 2013;8(7):e69910. doi:10.1371/journal.pone.0069910.

386. Yoshida H, Bao L, Kefaloyianni E, et al. AMP-activated protein kinase connects cellular energy metabolism to KATP channel function. *J Mol Cell Cardiol*. 2012;52(2):410-418. doi:10.1016/j.yjmcc.2011.08.013.

387. Krippeit-Drews P, Bäcker M, Düfer M, Drews G. Phosphocreatine as a determinant of K(ATP) channel activity in pancreatic beta-cells. *Pflugers Arch*. 2003;445(5):556-562. doi:10.1007/s00424-002-0975-x.

388. Miki T, Nagashima K, Tashiro F, et al. Defective insulin secretion and enhanced insulin action in KATP channel-deficient mice. *Proc Natl Acad Sci U S A*. 1998;95(September):10402-10406. doi:10.1073/pnas.95.18.10402.

389. Masoud WGT, Ussher JR, Wang W, et al. Failing mouse hearts utilize energy inefficiently and benefit from improved coupling of glycolysis and glucose oxidation. *Cardiovasc Res*. 2014;101(1):30-38. doi:10.1093/cvr/cvt216.

390. Barr RL, Lopaschuk GD. Methodology for measuring in vitro/ex vivo cardiac energy metabolism. *J Pharmacol Toxicol Methods*. 2000;43(2):141-152.

391. Gandhi M, Finegan BA, Clanachan AS. Role of glucose metabolism in the recovery of postischemic LV mechanical function: effects of insulin and other metabolic

modulators. *Am J Physiol Circ Physiol*. 2008;294(6):H2576-H2586. doi:10.1152/ajpheart.00942.2007; 10.1152/ajpheart.00942.2007.

392. Samovski D, Su X, Xu Y, Abumrad NA, Stahl PD. Insulin and AMPK regulate FA translocase/CD36 plasma membrane recruitment in cardiomyocytes via Rab GAP AS160 and Rab8a Rab GTPase. *J Lipid Res*. 2012;53(4):709-717. doi:10.1194/jlr.M023424.

393. Jäger S, Handschin C, St-Pierre J, Spiegelman BM. AMP-activated protein kinase (AMPK) action in skeletal muscle via direct phosphorylation of PGC-1alpha. *Proc Natl Acad Sci U S A*. 2007;104(29):12017-12022. doi:10.1073/pnas.0705070104.

394. Grover GJ, D'Alonzo AJ, Parham CS, Darbenzio RB. Cardioprotection with the KATP opener cromakalim is not correlated with ischemic myocardial action potential duration. *J Cardiovasc Pharmacol*. 1995;26(1):145-152.

395. Lou P-H, Zhang L, Lucchinetti E, et al. Infarct-remodelled hearts with limited oxidative capacity boost fatty acid oxidation after conditioning against ischaemia/reperfusion injury. *Cardiovasc Res*. 2012;97(2):251-261. doi:10.1093/cvr/cvs323.

396. Nagendran J, Pulinilkunnil T, Kienesberger PC, et al. Cardiomyocyte-specific ablation of CD36 improves post-ischemic functional recovery. *J Mol Cell Cardiol*. 2013;63:180-188. doi:10.1016/j.yjmcc.2013.07.020; 10.1016/j.yjmcc.2013.07.020.

397. Kantor PF, Lucien A, Kozak R, Lopaschuk GD. The antianginal drug trimetazidine shifts cardiac energy metabolism from fatty acid oxidation to glucose oxidation by inhibiting mitochondrial long-chain 3-ketoacyl coenzyme A thiolase. *Circ Res*. 2000;86(5):580-588.

398. Fragasso G, Perseghin G, De Cobelli F, et al. Effects of metabolic modulation by trimetazidine on left ventricular function and phosphocreatine/adenosine triphosphate ratio in patients with heart failure. *Eur Heart J*. 2006;27(8):942-948. doi:10.1093/eurheartj/ehi816.

399. Sossalla S, Wagner S, Rasenack ECL, et al. Ranolazine improves diastolic dysfunction in isolated myocardium from failing human hearts--role of late sodium current and intracellular ion accumulation. *J Mol Cell Cardiol*. 2008;45(1):32-43. doi:10.1016/j.yjmcc.2008.03.006.

400. Sabbah HN, Chandler MP, Mishima T, et al. Ranolazine, a partial fatty acid oxidation (pFOX) inhibitor, improves left ventricular function in dogs with chronic heart failure. *J Card Fail*. 2002;8(6):416-422. doi:10.1054/jcaf.2002.129232.

401. Chandler MP, Stanley WC, Morita H, et al. Short-term treatment with ranolazine improves mechanical efficiency in dogs with chronic heart failure. *Circ Res*.

2002;91(4):278-280. http://www.ncbi.nlm.nih.gov/pubmed/12193459. Accessed June 30, 2015.

402. Fragasso G, Palloshi A, Puccetti P, et al. A randomized clinical trial of trimetazidine, a partial free fatty acid oxidation inhibitor, in patients with heart failure. *J Am Coll Cardiol*. 2006;48(5):992-998. doi:10.1016/j.jacc.2006.03.060.

403. Sukhodub A, Jovanović S, Du Q, et al. AMP-activated protein kinase mediates preconditioning in cardiomyocytes by regulating activity and trafficking of sarcolemmal ATP-sensitive K(+) channels. *J Cell Physiol*. 2007;210(1):224-236. doi:10.1002/jcp.20862.

404. Bergeron R, Ren JM, Cadman KS, et al. Chronic activation of AMP kinase results in NRF-1 activation and mitochondrial biogenesis. *Am J Physiol Metab*. 2001;281(6):E1340-E1346.

405. Jager S, Handschin C, St-Pierre J, Spiegelman BM. AMP-activated protein kinase (AMPK) action in skeletal muscle via direct phosphorylation of PGC-1alpha. *Proc Natl Acad Sci U S A*. 2007;104(29):12017-12022. doi:10.1073/pnas.0705070104.

406. Wu Z, Puigserver P, Andersson U, et al. Mechanisms controlling mitochondrial biogenesis and respiration through the thermogenic coactivator PGC-1. *Cell*. 1999;98(1):115-124. doi:10.1016/S0092-8674(00)80611-X.

407. Hu X, Xu X, Huang Y, et al. Disruption of sarcolemmal ATP-sensitive potassium channel activity impairs the cardiac response to systolic overload. *Circ Res*. 2008;103(9):1009-1017. doi:10.1161/CIRCRESAHA.107.170795.

408. Barger PM, Kelly DP. PPAR signaling in the control of cardiac energy metabolism. *Trends Cardiovasc Med*. 2000;10(6):238-245.

409. Kersten S, Seydoux J, Peters JM, Gonzalez FJ, Desvergne B, Wahli W. Peroxisome proliferator-activated receptor alpha mediates the adaptive response to fasting. *J Clin Invest*. 1999;103(11):1489-1498. doi:10.1172/JCI6223.

410. Habets DDJ, Coumans WA, El Hasnaoui M, et al. Crucial role for LKB1 to AMPKalpha2 axis in the regulation of CD36-mediated long-chain fatty acid uptake into cardiomyocytes. *Biochim Biophys Acta*. 2009;1791(3):212-219. doi:10.1016/j.bbalip.2008.12.009.

411. Holm C, Kirchgessner TG, Svenson KL, et al. Hormone-sensitive lipase: sequence, expression, and chromosomal localization to 19 cent-q13.3. *Science*. 1988;241(4872):1503-1506. http://www.ncbi.nlm.nih.gov/pubmed/3420405. Accessed June 28, 2015.

412. Liu Q, Gauthier M-S, Sun L, Ruderman N, Lodish H. Activation of AMP-activated protein kinase signaling pathway by adiponectin and insulin in mouse adipocytes: requirement of acyl-CoA synthetases FATP1 and Acsl1 and association with an elevation in AMP/ATP ratio. *FASEB J*. 2010;24(11):4229-4239. doi:10.1096/fj.10-159723.

413. Yue T, Bao W, Jucker BM, et al. Activation of peroxisome proliferator-activated receptor-alpha protects the heart from ischemia/reperfusion injury. *Circulation*. 2003;108(19):2393-2399. doi:10.1161/01.CIR.0000093187.42015.6C.

414. Bulhak AA, Jung C, Ostenson C-G, Lundberg JO, Sjöquist P-O, Pernow J. PPAR-alpha activation protects the type 2 diabetic myocardium against ischemia-reperfusion injury: involvement of the PI3-Kinase/Akt and NO pathway. *Am J Physiol Heart Circ Physiol*. 2009;296(3):H719-H727. doi:10.1152/ajpheart.00394.2008.

415. Xu Y, Lu L, Greyson C, et al. The PPAR-alpha activator fenofibrate fails to provide myocardial protection in ischemia and reperfusion in pigs. *Am J Physiol Circ Physiol*. 2006;290(5):H1798-H1807. doi:10.1152/ajpheart.00631.2005.

416. Dewald O, Sharma S, Adrogue J, et al. Downregulation of peroxisome proliferator-activated receptor-alpha gene expression in a mouse model of ischemic cardiomyopathy is dependent on reactive oxygen species and prevents lipotoxicity. *Circulation*. 2005;112(3):407-415. doi:10.1161/CIRCULATIONAHA.105.536318.

417. Embi N, Rylatt DB, Cohen P. Glycogen synthase kinase-3 from rabbit skeletal muscle. Separation from cyclic-AMP-dependent protein kinase and phosphorylase kinase. *Eur J Biochem*. 1980;107(2):519-527.

418. Omar MA, Wang L, Clanachan AS. Cardioprotection by GSK-3 inhibition: role of enhanced glycogen synthesis and attenuation of calcium overload. *Cardiovasc Res*. 2010;86(3):478-486. doi:10.1093/cvr/cvp421; 10.1093/cvr/cvp421.

419. Ashcroft FM. Adenosine 5'-triphosphate-sensitive potassium channels. *Annu Rev Neurosci*. 1988;11:97-118. doi:10.1146/annurev.ne.11.030188.000525.

420. Flagg TP, Kurata HT, Masia R, et al. Differential structure of atrial and ventricular KATP: atrial KATP channels require SUR1. *Circ Res*. 2008;103(12):1458-1465. doi:10.1161/CIRCRESAHA.108.178186.

421. Antcliff JF, Haider S, Proks P, Sansom MSP, Ashcroft FM. Functional analysis of a structural model of the ATP-binding site of the KATP channel Kir6.2 subunit. *EMBO J*. 2005;24(2):229-239. doi:10.1038/sj.emboj.7600487.

422. Higgins CF, Linton KJ. The ATP switch model for ABC transporters. *Nat Struct Mol Biol*. 2004;11(10):918-926. doi:10.1038/nsmb836.

423. Moreau C, Prost A-L, Dérand R, Vivaudou M. SUR, ABC proteins targeted by KATP channel openers. *J Mol Cell Cardiol*. 2005;38(6):951-963. doi:10.1016/j.yjmcc.2004.11.030.

424. Abdallah Y, Wolf C, Meuter K, Piper HM, Reusch HP, Ladilov Y. Preconditioning with diazoxide prevents reoxygenation-induced rigor-type hypercontracture. *J Mol Cell Cardiol*. 2010;48(1):270-276. doi:10.1016/j.yjmcc.2009.04.013.

425. Law JK-Y, Yeung C-K, Yiu K-L, Rudd JA, Ingebrandt S, Chan M. A study of the relationship between pharmacologic preconditioning and adenosine triphosphate-sensitive potassium (KATP) channels on cultured cardiomyocytes using the microelectrode array. *J Cardiovasc Pharmacol*. 2010;56:60-68. doi:10.1097/FJC.0b013e3181e0bab6.

426. Arrell DK, Elliott ST, Kane LA, et al. Proteomic analysis of pharmacological preconditioning: novel protein targets converge to mitochondrial metabolism pathways. *Circ Res*. 2006;99(7):706-714. doi:10.1161/01.RES.0000243995.74395.f8.

427. Pain T, Yang XM, Critz SD, et al. Opening of mitochondrial K(ATP) channels triggers the preconditioned state by generating free radicals. *Circ Res*. 2000;87(6):460-466. http://www.ncbi.nlm.nih.gov/pubmed/10988237. Accessed July 3, 2015.

428. González G, Zaldívar D, Carrillo E, Hernández A, García M, Sánchez J. Pharmacological preconditioning by diazoxide downregulates cardiac L-type Ca(2+) channels. *Br J Pharmacol*. 2010;161(5):1172-1185. doi:10.1111/j.1476-5381.2010.00960.x.

429. Wojtovich AP, Urciuoli WR, Chatterjee S, Fisher AB, Nehrke K, Brookes PS. Kir6.2 is not the mitochondrial KATP channel but is required for cardioprotection by ischemic preconditioning. *Am J Physiol Heart Circ Physiol*. 2013;304:H1439-H1445. doi:10.1152/ajpheart.00972.2012.

430. Zhang H, Flagg TP, Nichols CG. Cardiac sarcolemmal KATP channels: Latest twists in a questing tale! *J Mol Cell Cardiol*. 2010;48(1):71-75. doi:10.1016/j.yjmcc.2009.07.002.

431. Xue Y, Xie N, Cao L, Zhao X, Jiang H, Chi Z. Diazoxide preconditioning against seizure-induced oxidative injury is via the PI3K/Akt pathway in epileptic rat. *Neurosci Lett*. 2011;495(2):130-134. doi:10.1016/j.neulet.2011.03.054.

432. Wang Y, Ahmad N, Kudo M, Ashraf M. Contribution of Akt and endothelial nitric oxide synthase to diazoxide-induced late preconditioning. *Am J Physiol Heart Circ Physiol*. 2004;287(3):H1125-H1131. doi:10.1152/ajpheart.00183.2004.

433. Hausenloy DJ, Tsang A, Yellon DM. The reperfusion injury salvage kinase pathway: a common target for both ischemic preconditioning and postconditioning. *Trends Cardiovasc Med*. 2005;15(2):69-75. doi:10.1016/j.tcm.2005.03.001.

434. Trapp S, Tucker SJ, Ashcroft FM. Activation and inhibition of K-ATP currents by guanine nucleotides is mediated by different channel subunits. *Proc Natl Acad Sci U S A*. 1997;94(16):8872-8877. http://www.pubmedcentral.nih.gov/articlerender.fcgi?artid=23175&tool=pmcentrez&rendertype=abstract. Accessed July 2, 2015.

435. Gribble FM. The essential role of the Walker A motifs of SUR1 in K-ATP channel activation by Mg-ADP and diazoxide. *EMBO J*. 1997;16(6):1145-1152. doi:10.1093/emboj/16.6.1145.

436. Bokvist K, Ammälä C, Ashcroft FM, Berggren PO, Larsson O, Rorsman P. Separate processes mediate nucleotide-induced inhibition and stimulation of the ATP-regulated K(+)-channels in mouse pancreatic beta-cells. *Proc Biol Sci*. 1991;243(1307):139-144. doi:10.1098/rspb.1991.0022.

437. Pearson ER, Flechtner I, Njølstad PR, et al. Switching from Insulin to Oral Sulfonylureas in Patients with Diabetes Due to Kir6.2 Mutations. *N Engl J Med*. 2006;355(5):467-477. doi:10.1056/NEJMoa061759.

438. Kolic J, Spigelman AF, Plummer G, et al. Distinct and opposing roles for the phosphatidylinositol 3-OH kinase catalytic subunits p110α and p110β in the regulation of insulin secretion from rodent and human beta cells. *Diabetologia*. 2013;56(6):1339-1349. doi:10.1007/s00125-013-2882-4.

439. Kim MS, Kewalramani G, Puthanveetil P, et al. Acute diabetes moderates trafficking of cardiac lipoprotein lipase through p38 mitogen-activated protein kinase-dependent actin cytoskeleton organization. *Diabetes*. 2008;57(1):64-76. doi:10.2337/db07-0832.

440. Leclerc GM, Leclerc GJ, Fu G, Barredo JC. AMPK-induced activation of Akt by AICAR is mediated by IGF-1R dependent and independent mechanisms in acute lymphoblastic leukemia. *J Mol Signal*. 2010;5:15. doi:10.1186/1750-2187-5-15.

441. Sutherland C, Leighton IA, Cohen P. Inactivation of glycogen synthase kinase-3 beta by phosphorylation: new kinase connections in insulin and growth-factor signalling. *Biochem J*. 1993;296 (Pt 1:15-19. http://www.pubmedcentral.nih.gov/articlerender.fcgi?artid=1137648&tool=pmcentrez&rendertype=abstract. Accessed July 2, 2015.

442. Delcommenne M, Tan C, Gray V, Rue L, Woodgett J, Dedhar S. Phosphoinositide-3-OH kinase-dependent regulation of glycogen synthase kinase 3 and protein kinase B/AKT by the integrin-linked kinase. *Proc Natl Acad Sci U S A*. 1998;95(19):11211-11216.

http://www.pubmedcentral.nih.gov/articlerender.fcgi?artid=21621&tool=pmcentrez&rendertype=abstract. Accessed June 18, 2015.

443. Hay N, Sonenberg N. Upstream and downstream of mTOR. *Genes Dev*. 2004;18(16):1926-1945. doi:10.1101/gad.1212704.

444. Fooks HM, Martin ACR, Woolfson DN, Sessions R., Hutchinson EG. Amino Acid Pairing Preferences in Parallel β-Sheets in Proteins. *J Mol Biol*. 2006;356(1):32-44. doi:10.1016/j.jmb.2005.11.008.

445. De Wet H, Fotinou C, Amad N, Dreger M, Ashcroft FM. The ATPase activities of sulfonylurea receptor 2A and sulfonylurea receptor 2B are influenced by the C-terminal 42 amino acids. *FEBS J*. 2010;277(12):2654-2662. doi:10.1111/j.1742-464X.2010.07675.x.

446. Alekseev AE, Hodgson DM, Karger AB, Park S, Zingman L V, Terzic A. ATP-sensitive K+ channel channel/enzyme multimer: metabolic gating in the heart. *J Mol Cell Cardiol*. 2005;38(6):895-905. doi:10.1016/j.yjmcc.2005.02.022.

447. Senior AE, Gadsby DC. ATP hydrolysis cycles and mechanism in P-glycoprotein and CFTR. *Semin Cancer Biol*. 1997;8(3):143-150. doi:10.1006/scbi.1997.0065.

448. Wang X. Novel pharmacological preconditioning with diazoxide attenuates myocardial stunning in coronary artery bypass grafting. *Eur J Cardio-Thoracic Surg*. 2003;24(6):967-973. doi:10.1016/S1010-7940(03)00438-X.

449. Cohen M V, Baines CP, Downey JM. Ischemic preconditioning: from adenosine receptor to KATP channel. *Annu Rev Physiol*. 2000;62:79-109. doi:10.1146/annurev.physiol.62.1.79.

450. Gross GJ, Fryer RM. Sarcolemmal versus mitochondrial ATP-sensitive K+ channels and myocardial preconditioning. *Circ Res*. 1999;84(9):973-979. http://www.ncbi.nlm.nih.gov/pubmed/10325234. Accessed July 4, 2015.

451. Coetzee WA. Multiplicity of effectors of the cardioprotective agent, diazoxide. *Pharmacol Ther*. 2013;140(2):167-175. doi:10.1016/j.pharmthera.2013.06.007.

452. Kim M-Y, Kim MJ, Yoon IS, et al. Diazoxide acts more as a PKC-epsilon activator, and indirectly activates the mitochondrial K(ATP) channel conferring cardioprotection against hypoxic injury. *Br J Pharmacol*. 2006;149(8):1059-1070. doi:10.1038/sj.bjp.0706922.

453. Light PE, Bladen C, Winkfein RJ, Walsh MP, French RJ. Molecular basis of protein kinase C-induced activation of ATP-sensitive potassium channels. *Proc Natl Acad Sci U S A*. 2000;97(16):9058-9063. doi:10.1073/pnas.160068997.

454. Ping P, Zhang J, Pierce WM, Bolli R. Functional Proteomic Analysis of Protein Kinase C Signaling Complexes in the Normal Heart and During Cardioprotection. *Circ Res*. 2001;88(1):59-62. doi:10.1161/01.RES.88.1.59.

455. Zhou H-Z, Karliner JS, Gray MO. Moderate alcohol consumption induces sustained cardiac protection by activating PKC-epsilon and Akt. *Am J Physiol Heart Circ Physiol*. 2002;283(1):H165-H174. doi:10.1152/ajpheart.00408.2001.

456. Matsui T, Tao J, del Monte F, et al. Akt Activation Preserves Cardiac Function and Prevents Injury After Transient Cardiac Ischemia In Vivo. *Circulation*. 2001;104(3):330-335. doi:10.1161/01.CIR.104.3.330.

457. Cross DA, Alessi DR, Cohen P, Andjelkovich M, Hemmings BA. Inhibition of glycogen synthase kinase-3 by insulin mediated by protein kinase B. *Nature*. 1995;378(6559):785-789. doi:10.1038/378785a0.

458. Ugi S, Imamura T, Maegawa H, et al. Protein Phosphatase 2A Negatively Regulates Insulin's Metabolic Signaling Pathway by Inhibiting Akt (Protein Kinase B) Activity in 3T3-L1 Adipocytes. *Mol Cell Biol*. 2004;24(19):8778-8789. doi:10.1128/MCB.24.19.8778-8789.2004.

459. Hanley PJ, Mickel M, Löffler M, Brandt U, Daut J. K(ATP) channel-independent targets of diazoxide and 5-hydroxydecanoate in the heart. *J Physiol*. 2002;542(Pt 3):735-741. http://www.pubmedcentral.nih.gov/articlerender.fcgi?artid=2290447&tool=pmcentrez&rendertype=abstract. Accessed July 7, 2015.

460. Hanley PJ, Daut J. K(ATP) channels and preconditioning: a re-examination of the role of mitochondrial K(ATP) channels and an overview of alternative mechanisms. *J Mol Cell Cardiol*. 2005;39(1):17-50. doi:10.1016/j.yjmcc.2005.04.002.

461. Kopustinskiene DM, Toleikis A, Saris N-EL. Adenine nucleotide translocase mediates the K(ATP)-channel-openers-induced proton and potassium flux to the mitochondrial matrix. *J Bioenerg Biomembr*. 2003;35(2):141-148. http://www.ncbi.nlm.nih.gov/pubmed/12887012. Accessed July 7, 2015.

462. Liu B, Zhu X, Chen C-L, et al. Opening of the mitoKATP channel and decoupling of mitochondrial complex II and III contribute to the suppression of myocardial reperfusion hyperoxygenation. *Mol Cell Biochem*. 2010;337(1-2):25-38. doi:10.1007/s11010-009-0283-2.

463. Villareal DT, Koster JC, Robertson H, et al. Kir6.2 variant E23K increases ATP-sensitive K+ channel activity and is associated with impaired insulin release and enhanced insulin sensitivity in adults with normal glucose tolerance. *Diabetes*. 2009;58(8):1869-1878. doi:10.2337/db09-0025.

464. Glukhov A V., Flagg TP, Fedorov V V., Efimov IR, Nichols CG. Differential KATP channel pharmacology in intact mouse heart. *J Mol Cell Cardiol*. 2010;48:152-160. doi:10.1016/j.yjmcc.2009.08.026.

465. Liu Y, Ren G, O'Rourke B, Marbán E, Seharaseyon J. Pharmacological comparison of native mitochondrial K(ATP) channels with molecularly defined surface K(ATP) channels. *Mol Pharmacol*. 2001;59(2):225-230. http://www.ncbi.nlm.nih.gov/pubmed/11160857. Accessed July 2, 2015.

466. Segel I. *Enzyme Kinetics. Behavior and Analysis of Rapid Equilibrium and Steady-State Enzyme Systems*. (Herries DG, ed.). John Wiley & Sons; 1975. doi:10.1016/0307-4412(76)90018-2.

467. Loo TW, Clarke DM. Rapid purification of human P-glycoprotein mutants expressed transiently in HEK 293 cells by nickel-chelate chromatography and characterization of their drug-stimulated ATPase activities. *J Biol Chem*. 1995;270(37):21449-21452. http://www.ncbi.nlm.nih.gov/pubmed/7665554. Accessed May 23, 2015.

468. Tombline G, Bartholomew L, Gimi K, Tyndall GA, Senior AE. Synergy between conserved ABC signature Ser residues in P-glycoprotein catalysis. *J Biol Chem*. 2004;279(7):5363-5373. doi:10.1074/jbc.M311964200.

469. Ovize M, Kloner RA, Przyklenk K. Stretch preconditions canine myocardium. *Am J Physiol*. 1994;266(1 Pt 2):H137-H146. http://www.ncbi.nlm.nih.gov/pubmed/8304494. Accessed July 9, 2015.

470. Nakagawa C, Asayama J, Katamura M, et al. Myocardial stretch induced by increased left ventricular diastolic pressure preconditions isolated perfused hearts of normotensive and spontaneously hypertensive rats. *Basic Res Cardiol*. 1997;92(6):410-416. http://www.ncbi.nlm.nih.gov/pubmed/9464865. Accessed July 9, 2015.

471. Smith MA, Moylan JS, Reid MB. Mechanical signal transduction in glucose transport of murine extensor digitorum longus (EDL) muscle. *FASEB J*. 2007;21(6):A1355 - d - 1356. http://www.fasebj.org/cgi/content/meeting_abstract/21/6/A1355-d. Accessed July 7, 2015.

472. Rubin LJ, Magliola L, Feng X, Jones AW, Hale CC. Metabolic activation of AMP kinase in vascular smooth muscle. *J Appl Physiol*. 2005;98(1):296-306. doi:10.1152/japplphysiol.00075.2004.

473. Organization WH. *WHO | WHO Model Lists of Essential Medicines*. World Health Organization; 2015. http://www.who.int/medicines/publications/essentialmedicines/en/. Accessed July 10, 2015.

474. Thulé PM, Umpierrez G. Sulfonylureas: a new look at old therapy. *Curr Diab Rep*. 2014;14(4):473. doi:10.1007/s11892-014-0473-5.

475. Brown GR, Foubister AJ. Receptor binding sites of hypoglycemic sulfonylureas and related [(acylamino)alkyl]benzoic acids. *J Med Chem*. 1984;27(1):79-81. http://www.ncbi.nlm.nih.gov/pubmed/6361256. Accessed July 11, 2015.

476. Johnson JA, Simpson SH, Toth EL, Majumdar SR. Reduced cardiovascular morbidity and mortality associated with metformin use in subjects with Type 2 diabetes. *Diabet Med*. 2005;22(4):497-502. doi:10.1111/j.1464-5491.2005.01448.x.

477. Neumann D, Schlattner U, Wallimann T. A molecular approach to the concerted action of kinases involved in energy homoeostasis. *Biochem Soc Trans*. 2001;31(1):169. doi:10.1042/BST0310169.

478. Dolinsky VW, Chan AYM, Robillard Frayne I, Light PE, Des Rosiers C, Dyck JRB. Resveratrol prevents the prohypertrophic effects of oxidative stress on LKB1. *Circulation*. 2009;119(12):1643-1652. doi:10.1161/CIRCULATIONAHA.108.787440.

479. Ikeda Y, Sato K, Pimentel DR, et al. Cardiac-specific deletion of LKB1 leads to hypertrophy and dysfunction. *J Biol Chem*. 2009;284(51):35839-35849. doi:10.1074/jbc.M109.057273.

480. Shaw RJ. LKB1 and AMP-activated protein kinase control of mTOR signalling and growth. *Acta Physiol (Oxf)*. 2009;196(1):65-80. doi:10.1111/j.1748-1716.2009.01972.x.

481. Gögelein H, Ruetten H, Albus U, Englert HC, Busch AE. Effects of the cardioselective KATP channel blocker HMR 1098 on cardiac function in isolated perfused working rat hearts and in anesthetized rats during ischemia and reperfusion. *Naunyn Schmiedebergs Arch Pharmacol*. 2001;364(1):33-41. http://www.ncbi.nlm.nih.gov/pubmed/11485036. Accessed July 12, 2015.

482. Ye Y, Lin Y, Perez-Polo JR, Birnbaum Y. Oral glyburide, but not glimepiride, blocks the infarct-size limiting effects of pioglitazone. *Cardiovasc Drugs Ther*. 2008;22(6):429-436. doi:10.1007/s10557-008-6138-3.

483. Maddock HL, Siedlecka SM, Yellon DM. Myocardial protection from either ischaemic preconditioning or nicorandil is not blocked by gliclazide. *Cardiovasc Drugs Ther*. 2004;18(2):113-119. doi:10.1023/B:CARD.0000029028.75316.5e.

484. Abdelmoneim AS, Eurich DT, Gamble JM, et al. Risk of acute coronary events associated with glyburide compared with gliclazide use in patients with type 2 diabetes: a nested case-control study. *Diabetes Obes Metab*. 2014;16(1):22-29. doi:10.1111/dom.12173.

485. Gratia S, Kay L, Potenza L, et al. Inhibition of AMPK signalling by doxorubicin: at the crossroads of the cardiac responses to energetic, oxidative, and genotoxic stress. *Cardiovasc Res*. 2012;95(3):290-299. doi:10.1093/cvr/cvs134.

486. Zingman L V, Alekseev a E, Hodgson-Zingman DM, Terzic a. ATP-sensitive potassium channels: metabolic sensing and cardioprotection. *J Appl Physiol*. 2007;103:1888-1893. doi:10.1152/japplphysiol.00747.2007.

487. Yokota R, Tanaka M, Yamasaki K, et al. Blockade of ATP-sensitive K+ channels attenuates preconditioning effect on myocardial metabolism in swine: myocardial metabolism and ATP-sensitive K+ channels. *Int J Cardiol*. 1998;67(3):225-236. http://www.ncbi.nlm.nih.gov/pubmed/9894703. Accessed July 10, 2015.

488. Kamigaki M, Ichihara K, Abiko Y. Enhancement of Ischemic Myocardial Metabolic Derangement by Glibenclamide. *Jpn J Pharmacol*. 1994;65(2):121-129. doi:10.1254/jjp.65.121.

489. Powers SK, Murlasits Z, Wu M, Kavazis AN. Ischemia-reperfusion-induced cardiac injury: a brief review. *Med Sci Sports Exerc*. 2007;39(9):1529-1536. doi:10.1249/mss.0b013e3180d099c1.

490. Pasdois P, Beauvoit B, Costa ADT, et al. Sarcoplasmic ATP-sensitive potassium channel blocker HMR1098 protects the ischemic heart: implication of calcium, complex I, reactive oxygen species and mitochondrial ATP-sensitive potassium channel. *J Mol Cell Cardiol*. 2007;42(3):631-642. doi:10.1016/j.yjmcc.2006.12.014.

491. Oldenburg O, Yang X-M, Krieg T, et al. P1075 opens mitochondrial K(ATP) channels and generates reactive oxygen species resulting in cardioprotection of rabbit hearts. *J Mol Cell Cardiol*. 2003;35(9):1035-1042. http://www.ncbi.nlm.nih.gov/pubmed/12967626. Accessed July 10, 2015.

492. Carreira RS, Lee P, Gottlieb RA. Mitochondrial therapeutics for cardioprotection. *Curr Pharm Des*. 2011;17(20):2017-2035. http://www.pubmedcentral.nih.gov/articlerender.fcgi?artid=3765248&tool=pmcentrez&rendertype=abstract. Accessed July 13, 2015.

493. Rainbow RD, Norman RI, Hudman D, Davies NW, Standen NB. Reduced effectiveness of HMR 1098 in blocking cardiac sarcolemmal K(ATP) channels during metabolic stress. *J Mol Cell Cardiol*. 2005;39(4):637-646. doi:10.1016/j.yjmcc.2005.06.017.

494. Cook GA. The hypoglycemic sulfonylureas glyburide and tolbutamide inhibit fatty acid oxidation by inhibiting carnitine palmitoyltransferase. *J Biol Chem*. 1987;262(11):4968-4972. http://www.ncbi.nlm.nih.gov/pubmed/3104327. Accessed July 10, 2015.

495. Ford WR, Lopaschuk GD, Schulz R, Clanachan AS. K(ATP)-channel activation: effects on myocardial recovery from ischaemia and role in the cardioprotective response to adenosine A1-receptor stimulation. *Br J Pharmacol*. 1998;124(4):639-646. doi:10.1038/sj.bjp.0701872.

496. Matsui T, Nagoshi T, Hong E-G, et al. Effects of chronic Akt activation on glucose uptake in the heart. *Am J Physiol Endocrinol Metab*. 2006;290(5):E789-E797. doi:10.1152/ajpendo.00564.2004.

497. Statistics - Heart and Stroke Foundation of Canada. http://www.heartandstroke.com/site/c.ikIQLcMWJtE/b.3483991/k.34A8/Statistics.htm#references. Accessed July 14, 2015.

498. Opie LH. Metabolism of the heart in health and disease. I. *Am Heart J*. 1968;76(5):685-698. http://www.ncbi.nlm.nih.gov/pubmed/4235250. Accessed June 28, 2015.

499. Opie LH. Metabolism of the heart in health and disease. II. *Am Heart J*. 1969;77(1):100-122 contd. http://www.ncbi.nlm.nih.gov/pubmed/4882561. Accessed June 28, 2015.

500. Suga H. Ventricular energetics. *Physiol Rev*. 1990;70(2):247-277. http://physrev.physiology.org/content/70/2/247.abstract. Accessed July 17, 2015.

501. Bienengraeber M, Alekseev a E, Abraham MR, et al. ATPase activity of the sulfonylurea receptor: a catalytic function for the KATP channel complex. *FASEB J*. 2000;14:1943-1952. doi:10.1096/fj.00-0027com.

502. Selivanov VA, Alekseev AE, Hodgson DM, Dzeja PP, Terzic A. Nucleotide-gated KATP channels integrated with creatine and adenylate kinases: amplification, tuning and sensing of energetic signals in the compartmentalized cellular environment. *Mol Cell Biochem*. 256-257(1-2):243-256. http://www.pubmedcentral.nih.gov/articlerender.fcgi?artid=2760266&tool=pmcentrez&rendertype=abstract. Accessed July 16, 2015.

503. Dzeja PP, Terzic A. Phosphotransfer reactions in the regulation of ATP-sensitive K+ channels. *FASEB J*. 1998;12(7):523-529. http://www.ncbi.nlm.nih.gov/pubmed/9576479. Accessed July 16, 2015.

504. Sambandam N, Lopaschuk GD. AMP-activated protein kinase (AMPK) control of fatty acid and glucose metabolism in the ischemic heart. *Prog Lipid Res*. 2003;42(3):238-256. http://www.ncbi.nlm.nih.gov/pubmed/12689619. Accessed July 16, 2015.

505. O'Keefe JH, McCallister BD, Blackstone EH. Sulfonylurea drugs and cardiovascular mortality. *J Am Coll Cardiol*. 1999;34(3):958. http://www.ncbi.nlm.nih.gov/pubmed/10483986. Accessed July 10, 2015.

506. Bell DSH. Do sulfonylurea drugs increase the risk of cardiac events? *CMAJ*. 2006;174(2):185-186. doi:10.1503/cmaj.051237.

507. Gross GJ, Auchampach JA. Blockade of ATP-sensitive potassium channels prevents myocardial preconditioning in dogs. *Circ Res*. 1992;70(2):223-233. http://www.ncbi.nlm.nih.gov/pubmed/1310443. Accessed July 10, 2015.

508. Ashcroft FM, Gribble FM. Tissue-specific effects of sulfonylureas: lessons from studies of cloned K(ATP) channels. *J Diabetes Complications*. 14(4):192-196. http://www.ncbi.nlm.nih.gov/pubmed/11004427. Accessed June 5, 2015.

509. Hardie DG. Role of AMP-activated protein kinase in the metabolic syndrome and in heart disease. *FEBS Lett*. 2008;582(1):81-89. doi:10.1016/j.febslet.2007.11.018.

510. Ruderman NB, Xu XJ, Nelson L, et al. AMPK and SIRT1: a long-standing partnership? *Am J Physiol Endocrinol Metab*. 2010;298(4):E751-E760. doi:10.1152/ajpendo.00745.2009.

511. Johnson JA, Simpson SH, Toth EL, Majumdar SR. Reduced cardiovascular morbidity and mortality associated with metformin use in subjects with Type 2 diabetes. *Diabet Med*. 2005;22(4):497-502. doi:10.1111/j.1464-5491.2005.01448.x.

512. Sillars B, Davis WA, Hirsch IB, Davis TME. Sulphonylurea-metformin combination therapy, cardiovascular disease and all-cause mortality: the Fremantle Diabetes Study. *Diabetes Obes Metab*. 2010;12(9):757-765. doi:10.1111/j.1463-1326.2010.01230.x.

513. Jabůrek M, Yarov-Yarovoy V, Paucek P, Garlid KD. State-dependent inhibition of the mitochondrial KATP channel by glyburide and 5-hydroxydecanoate. *J Biol Chem*. 1998;273(22):13578-13582. http://www.ncbi.nlm.nih.gov/pubmed/9593694. Accessed July 16, 2015.

514. Szewczyk A, Czyz A, Nałecz MJ. ATP-regulated potassium channel blocker, glibenclamide, uncouples mitochondria. *Pol J Pharmacol*. 49(1):49-52. http://www.ncbi.nlm.nih.gov/pubmed/9431552. Accessed July 15, 2015.

515. White CW, Rashed HM, Patel TB. Sulfonylureas inhibit metabolic flux through rat liver pyruvate carboxylase reaction. *J Pharmacol Exp Ther*. 1988;246(3):971-974. http://www.ncbi.nlm.nih.gov/pubmed/3138409. Accessed July 16, 2015.

516. Duda M, Konior A, Klemenska E, Beresewicz A. Preconditioning protects endothelium by preventing ET-1-induced activation of NADPH oxidase and xanthine

oxidase in post-ischemic heart. *J Mol Cell Cardiol*. 2007;42(2):400-410. doi:10.1016/j.yjmcc.2006.10.014.

517. Terzic A, Dzeja PP, Holmuhamedov EL. Mitochondrial K(ATP) channels: probing molecular identity and pharmacology. *J Mol Cell Cardiol*. 2000;32(11):1911-1915. doi:10.1006/jmcc.2000.1256.

518. Zhang J, Xie Z, Dong Y, Wang S, Liu C, Zou M-H. Identification of nitric oxide as an endogenous activator of the AMP-activated protein kinase in vascular endothelial cells. *J Biol Chem*. 2008;283(41):27452-27461. doi:10.1074/jbc.M802578200.

519. Malester B, Tong X, Ghiu I, et al. Transgenic expression of a dominant negative K(ATP) channel subunit in the mouse endothelium: effects on coronary flow and endothelin-1 secretion. *FASEB J*. 2007;21:2162-2172. doi:10.1096/fj.06-7821com.

520. Pountney DJ, Sun ZQ, Porter LM, et al. Is the molecular composition of K(ATP) channels more complex than originally thought? *J Mol Cell Cardiol*. 2001;33(8):1541-1546. doi:10.1006/jmcc.2001.1407.

521. Agah R, Frenkel PA, French BA, Michael LH, Overbeek PA, Schneider MD. Gene recombination in postmitotic cells. Targeted expression of Cre recombinase provokes cardiac-restricted, site-specific rearrangement in adult ventricular muscle in vivo. *J Clin Invest*. 1997;100(1):169-179. doi:10.1172/JCI119509.

522. Ponce de León V, Mérillat A-M, Tesson L, Anegón I, Hummler E. Generation of TALEN-mediated GRdim knock-in rats by homologous recombination. *PLoS One*. 2014;9(2):e88146. doi:10.1371/journal.pone.0088146.

523. Davies B, Davies G, Preece C, Puliyadi R, Szumska D, Bhattacharya S. Site specific mutation of the Zic2 locus by microinjection of TALEN mRNA in mouse CD1, C3H and C57BL/6J oocytes. *PLoS One*. 2013;8(3):e60216. doi:10.1371/journal.pone.0060216.

524. Donahoe SM, Stewart GC, McCabe CH, et al. Diabetes and mortality following acute coronary syndromes. *JAMA*. 2007;298(7):765-775. doi:10.1001/jama.298.7.765.

525. Lee T-M, Chou T-F. Impairment of myocardial protection in type 2 diabetic patients. *J Clin Endocrinol Metab*. 2003;88(2):531-537. doi:10.1210/jc.2002-020904.

526. Meier JJ. Is impairment of ischaemic preconditioning by sulfonylurea drugs clinically important? *Heart*. 2004;90(1):9-12. doi:10.1136/heart.90.1.9.

527. Chen Z-C, Cheng Y-Z, Chen L-J, Cheng K-C, Li Y-X, Cheng J-T. Increase of ATP-sensitive potassium (KATP) channels in the heart of type-1 diabetic rats. *Cardiovasc Diabetol*. 2012;11(1):8. doi:10.1186/1475-2840-11-8.

528. Bayeva M, Sawicki KT, Ardehali H. Taking diabetes to heart--deregulation of myocardial lipid metabolism in diabetic cardiomyopathy. *J Am Heart Assoc*. 2013;2(6):e000433. doi:10.1161/JAHA.113.000433.

529. Nishino N, Tamori Y, Kasuga M. Insulin efficiently stores triglycerides in adipocytes by inhibiting lipolysis and repressing PGC-1alpha induction. *Kobe J Med Sci*. 2007;53(3):99-106. http://www.ncbi.nlm.nih.gov/pubmed/17684441. Accessed July 2, 2015.

530. Belke DD, Larsen TS, Gibbs EM, Severson DL. Altered metabolism causes cardiac dysfunction in perfused hearts from diabetic (db/db) mice. *Am J Physiol Endocrinol Metab*. 2000;279(5):E1104-E1113. http://ajpendo.physiology.org/content/279/5/E1104.abstract?ijkey=381408a43946df7688b49bc9f4e82619f040f96c&keytype2=tf_ipsecsha. Accessed July 17, 2015.

531. Schwenk RW, Luiken JJFP, Bonen A, Glatz JFC. Regulation of sarcolemmal glucose and fatty acid transporters in cardiac disease. *Cardiovasc Res*. 2008;79(2):249-258. doi:10.1093/cvr/cvn116.

532. Hausenloy DJ, Yellon DM. New directions for protecting the heart against ischaemia-reperfusion injury: targeting the Reperfusion Injury Salvage Kinase (RISK)-pathway. *Cardiovasc Res*. 2004;61(3):448-460. doi:10.1016/j.cardiores.2003.09.024.

533. Huang C, Yitzhaki S, Perry CN, et al. Autophagy induced by ischemic preconditioning is essential for cardioprotection. *J Cardiovasc Transl Res*. 2010;3(4):365-373. doi:10.1007/s12265-010-9189-3.

534. Inoki K, Kim J, Guan KL. AMPK and mTOR in cellular energy homeostasis and drug targets. *Annu Rev Pharmacol Toxicol*. 2011;52:381-400. doi:10.1146/annurev-pharmtox-010611-134537.

535. Diaz-Troya S, Perez-Perez ME, Florencio FJ, Crespo JL. The role of TOR in autophagy regulation from yeast to plants and mammals. *Autophagy*. 2008;4(7):851-865.

536. Ravikumar B, Vacher C, Berger Z, et al. Inhibition of mTOR induces autophagy and reduces toxicity of polyglutamine expansions in fly and mouse models of Huntington disease. *Nat Genet*. 2004;36(6):585-595. doi:10.1038/ng1362.

537. Xie Z, Klionsky DJ. Autophagosome formation: core machinery and adaptations. *Nat Cell Biol*. 2007;9(10):1102-1109. doi:10.1038/ncb1007-1102.

538. Mizushima N, Yamamoto A, Matsui M, Yoshimori T, Ohsumi Y. In vivo analysis of autophagy in response to nutrient starvation using transgenic mice expressing a fluorescent autophagosome marker. *Mol Biol Cell*. 2004;15(3):1101-1111. doi:10.1091/mbc.E03-09-0704.

539. Samokhvalov V, Alsaleh N, El-Sikhry HE, et al. Epoxyeicosatrienoic acids protect cardiac cells during starvation by modulating an autophagic response. *Cell Death Dis*. 2013;4:e885. doi:10.1038/cddis.2013.418.

540. Franchini KG, Torsoni AS, Soares PHA, Saad MJA. Early Activation of the Multicomponent Signaling Complex Associated With Focal Adhesion Kinase Induced by Pressure Overload in the Rat Heart. *Circ Res*. 2000;87(7):558-565. doi:10.1161/01.RES.87.7.558.

541. Xiao L, Gong L-L, Yuan D, et al. Protein phosphatase-1 regulates Akt1 signal transduction pathway to control gene expression, cell survival and differentiation. *Cell Death Differ*. 2010;17(9):1448-1462. doi:10.1038/cdd.2010.16.